THE

LONDON, EDINBURGH, AND DUBLIN

PHILOSOPHICAL MAGAZINE

AND

JOURNAL OF SCIENCE.

[SEVENTH SERIES.]

SUPPLEMENT, FEBRUARY 1933.

XXXII. *On the Ignition of Explosive Gaseous Mixtures by Small Flames.* By JOHN M. HOLM, *B.Sc., Ph.D., Carnegie Senior Research Scholar in the University of Glasgow* *.

INTRODUCTION.

THE following communication is an extension of the work on the above subject reported in a previous paper [1]. It is primarily concerned with the measurement of the limiting diameter of tube or aperture in a thin plate which will just allow the flame of an explosive mixture to propagate. Previous measurements have shown that this limiting diameter is independent of the thermal conductivity of the material forming the tube and, under certain conditions, of that of the thin plate.

An approximate formula, which has been developed on the assumption that the flame is extinguished by the cooling effect of the unburnt gas in contact with its nearly hemispherical surface, indicates that the limiting diameter, d, is given by

$$d = \frac{4\bar{k}(T_i - T_0)}{v(Q - \bar{C}_p(T_f - T_0))}, \quad \ldots \quad (1)$$

where $\bar{k}$ is the average thermal conductivity of the gaseous mixture between T_0, the room temperature, and T_i, the

* Communicated by Professor E. Taylor Jones, D.Sc.

temperature of the surface of the hemispherical flame. v is the limiting value to which the velocity of propagation tends as the tube diameter tends to the limiting value. Q is the amount of heat evolved when one c.c. of the gaseous mixture at temperature T_0 and atmospheric pressure is burnt at constant pressure, and $\bar{C}_p$ is the mean specific heat of the products of combustion between T_0 and T_f, the average temperature of the burnt gases escaping through the plane surface of the hemisphere.

It was assumed that $\bar{k}$ could be calculated from a simple formula expressing the thermal conductivity as a linear function of the temperature, but a more accurate value is probably obtained by employing the result derived from Sutherland's viscosity formula [2], *i. e.*,

$$k = \frac{k_0(273+C)\theta^{3/2}}{(\theta+C)273^{3/2}} = \frac{A\theta^{3/2}}{\theta+C}, \quad . \quad . \quad . \quad . \quad (2)$$

where k is the thermal conductivity at θ° absolute, k_0 its value at 0° C., and C a constant.

Let $\theta_0 = 273+T_0$ and $\theta_1 = 273+T_i$; then, by substituting $\theta = C\psi^2$, we have

$$\bar{k}(\theta_1-\theta_0) = \int_{\theta_0}^{\theta_1} k\,d\theta = 2AC^{3/2}\left[\frac{\psi^3}{3} - \psi + \tan^{-1}\psi\right]_{\psi_0}^{\psi_1}. \quad (3)$$

The values of $\bar{k}$, calculated by means of equation (3) for several gases over various temperature ranges, are given in Table I., the values of k_0 and C being obtained from Kaye and Laby's tables [3]. They are generally slightly lower than those calculated from the linear formula.

If we assume that the thermal conductivity of a gaseous mixture can be calculated from those of its components by means of the formula

$$k = \frac{c_1}{100}k_1 + \frac{c_2}{100}k_2 + , \quad . \quad . \quad . \quad . \quad (4)$$

where c_1, c_2, etc. are the percentage concentrations (by volume) of the component gases whose thermal conductivities are k_1, k_2, etc., we find that for the 9·5 per cent. methane-air mixture the average thermal conductivity over the range 18° to 750° C. is ·0001116. The corresponding value previously used was ·0001248.

This new value of $\bar{k}$ reduces the calculated limiting diameter for that mixture from 1·37 to 1·23 mm. The actual experimental value is 3·80 mm., with an error of 2·5 per cent

In equation (1) T_i is the temperature of the curved surface of the hemispherical flame and has been called the ignition temperature of the mixture. It does not follow, however, that T_i is the ignition temperature as determined in the usual manner. Thus, if there is a time lag between the attainment of the temperature T_i and the appearance of flame in the mixture, then the actual flame surface will not coincide with the isothermal surface given by T_i = constant. This is because the mixture is flowing through that surface with a finite velocity. The existence of such a time lag appears to be probable from the experimental work of various authors [4].

TABLE I.

Mean Thermal Conductivities over the range 18° C. to T_i.

Gas.	k_0.	C.	T_i.	$\overline{k}$.
Air	·0000583	125	570° C.	·0000989
Air	·0000583	125	600	·0001006
Air	·0000583	125	750	·0001084
Air	·0000583	125	1665	·0001491
Methane	·0000703	200	750	·0001413
Methane.....	·0000703	200	1665	·0002010
Hydrogen	·0003790	94	600	·0006305
Neon	·0000106	45	750	·0000176
Argon	·0000378	138	750	·0000715
Helium	·0003310	33	750	·0005391
Carbon dioxide ...	·0000329	545	750	·0000823

It is fairly obvious that T_i is the rapid ignition temperature, which might be defined as the ignition temperature for which the time lag was small compared with $\frac{d}{v}$, d being the limiting diameter for the mixture and v the limiting value to which the velocity of propagation tends as the tube diameter is reduced to d. To take a concrete example, for a 9·5 per cent. methane-air mixture the value of $\frac{d}{v}$ is about ·027 second, so that T_i would have to be the ignition temperature having a time lag of the order of 1 millisecond.

From the experimental work of N. S. Walls, R. V. Wheeler, W. Rintoul, and A. G. White[5] it would appear that the time lag on ignition of a 9·5 per cent. methane-air mixture by flames of temperature about 1600° C. was of the order of 3 milliseconds. J. W. McDavid's results[6] also indicate that the rapid ignition temperature of methane-air mixtures is greater than 1000° C. Thus it seems probable that the value of T_i in the formula is considerably higher than that previously assumed for this mixture, namely, 750° C., which is the ignition temperature with a lag of about half a second[7].

This suggests that in equation (1) T_i may be practically equal to T_f. Assuming that this is the case, the value of T_i which will give d equal to 3·80 mm. for a 9·5 per cent. methane-air mixture has been found by successive approximation to be 1665° C.

It is well known that the flame of an explosive mixture will fail to propagate in a given vessel if the pressure of the mixture is reduced below a certain limiting value. The limiting pressure depends on the nature of the combustible gas, the amount of it present in the mixture, and on the dimensions of the explosion vessel.

Using methane-air mixtures W. Mason and R. V. Wheeler[7] have determined the limiting pressures for vertically downward propagation in a tube 2 cm. in diameter. The results show that as the pressure of the mixture is reduced from atmospheric, the range of inflammability is continually narrowed, till at pressures less than 120 mm. of mercury no methane-air mixture is capable of giving flame propagation. The curve showing the variation of this limiting pressure with the concentration of methane in the mixture is very similar to that already obtained for the variation with concentration of the limiting diameter for flame propagation along tubes (see curves PQR and DEF respectively in Graph I.). The minimum on the former curve occurs at 9·1 per cent. of methane, the value of the minimum limiting pressure being about 120 mm., while the minimum on the latter occurs at 9·43 per cent. *, the value of the minimum limiting diameter being 3·80 mm.

The similarity between these two curves, *i. e.*, between the curve showing the variation of the limiting pressure for flame propagation along a tube of fixed diameter and that

* Corrected for the presence of 2·03 per cent. of water vapour in the mixture, *i. e.*, by multiplying the percentage concentration of methane by ·9797. This is the only curve to which this correction has been applied.

showing the variation with concentration of the limiting diameter for flame propagation along tubes for the same combustible gas at atmospheric pressure, can be explained in a simple manner from the above theory for limiting diameters.

Graph I.

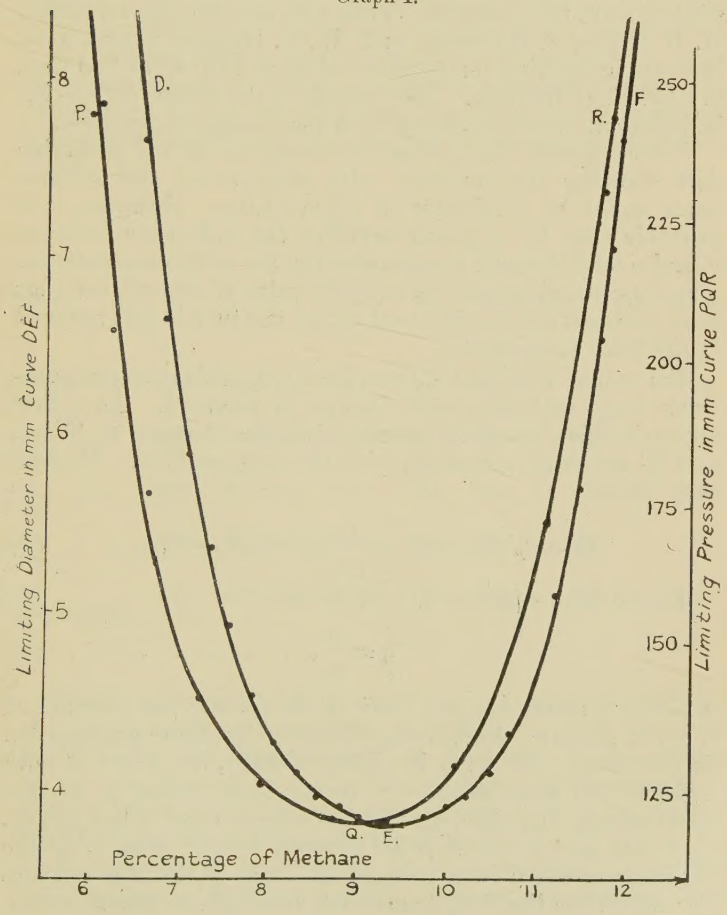

In equation (1) the symbols refer to the values of the constants at atmospheric pressure, p_0, and room temperature T_0. Let d', $\overline{k}'$, T_i', etc. be their values for the same mixture at a pressure of p mm. of mercury and temperature T_0. We shall examine, as far as possible, the manner in which these constants change with pressure.

One of the most successful deductions from the kinetic theory of gases indicates that the thermal conductivity of a gas is independent of the pressure. This has been found to be true experimentally down to pressures of about 1 mm. Hence $\bar{k}'$ is equal to $\bar{k}$ if T_i' is equal to T_i.

The ignition temperature of various gases appear to change slightly with the pressure. Thus with methane-air mixtures, H. B. Dixon, J. Harwood, and W. F. Higgins [8] record an increase in ignition temperature of from 746° C. at 760 mm. to 815° C. at 100 mm. The change in the value of $(T_i - T_0)$ is, however, small compared with the change in pressure.

Unfortunately there does not seem to be any available data showing the variation with pressure of the uniform flame speed of a mixture in a given tube. However, it is probable that for a given mixture the difference between v' and v will be small compared with the difference between p and p_0, for, although the calorific value of the mixture has been reduced, the specific heat of the mixture is also reduced in the same proportion.

The values of Q' and $\bar{C}_p'$ are, however, subject to comparatively large variations with change in pressure. As a first approximation we shall assume that the changes in T_i', v', and T_f' are small compared with the changes in p. We can then write

$$Q' - \bar{C}_p'(T_f' - T_0) = \frac{p}{p_0}(Q - \bar{C}_p(T_f - T_0)). \quad . \quad . \quad (5)$$

Hence from equation (1) we have

$$\frac{d}{d'} = \frac{p}{p_0}, \quad . \quad . \quad . \quad . \quad . \quad . \quad . \quad . \quad (6)$$

which expresses the fact that if we reduce the pressure of a given mixture the limiting diameter for flame propagation is increased. So far p is quite arbitrary, but d and d' both refer to the same mixture ; we can thus choose p so that the limiting diameter, d', will have some fixed value, say d_0. Let this new value of p be denoted by p' ; then p' is the limiting pressure in a tube of diameter d_0 for the mixture for which the limiting diameter at atmospheric pressure is d. Equation (6) thus becomes

$$p' = \frac{p_0}{d_0} d. \quad . \quad . \quad . \quad . \quad . \quad . \quad . \quad . \quad (7)$$

Hence the curve showing the variation of p' with concentration will be exactly similar to that showing the variation of d with concentration.

From equation (7) we find that the minimum limiting pressure for flame propagation with methane-air mixtures in a tube 2 cm. in diameter should be 144 mm., and should occur at a concentration of 9·43 per cent. of methane. The actual experimental value of this limiting pressure at 9·43 per cent. is 121 mm. By introducing the values of T_i', v', and T_f', a correction could be applied to equation (7) which would probably give better agreement with the observations.

On making similar calculations for hydrogen-air and ethyl ether-air mixtures further evidence is obtained to show that the formula for the limiting diameter is substantially correct. The results and values used for the constants are detailed in Table II.

TABLE II.

Mixture.	T_i.	$\bar{k}$.	v.	Q.	T_f.	$\bar{C}_p(T_f - T_0)$.	$d_{calc.}$	$d_{exp.}$
	° C.				° C.		mm.	mm.
$CH_4+2O_2+7{\cdot}52N_2$	750	·0001116	14·0	·844	1670	·654	1·23	3·80
$CH_4+2O_2+7{\cdot}52A$	750	·0000851	28·7	·844	1665	·535	·28	2·12
$CH_4+2O_2+7{\cdot}52N_2$	1665	·0001541	14·0	·844	1665	·653	3·80	3·80
$2H_2+O_2+3{\cdot}76N_2$	600	·0002699	67·1	·847	1900	·699	·63	·93
$(C_2H_5)_2O+4(O_2+3{\cdot}76N_2)$	570	·0000988	17·3	·812	1500	·690	1·04	2·69

When equation (11) [1] is applied as previously to calculate the percentage concentration of hydrogen, c', at the usual lower limit of inflammability we find that if the average flame temperature is only the ignition temperature, *i. e.*, 600° C., then c' is 6·96 per cent., while if it is as high as 1900° C. the value of c' is 23·7 per cent.

The average of eight values of c' for vertically downward propagation is 9·23 per cent. [9]. Hence the average flame temperature at the usual lower limit of inflammability lies between 600 and 1900° C., and by successive approximation we find that if T_f is equal to 790° C. then c' is equal to 9·23 per cent. (see Table III.).

It is interesting to note that the value of c' for vertically upward propagation is only about 4·15 per cent. [9], which means that the average flame temperature at that limit is less

than the accepted ignition temperature. It would appear that there is only sufficient heat in the mixture to raise the average temperature of the products of combustion to 365° C. Attention has already been drawn to this point by A. G. White [10], and an explanation of the phenomenon, based on the greater rate of diffusion of hydrogen compared with that of oxygen, given by F. Goldmann [11].

It has been found experimentally that the minimum limiting diameter for propagation along tubes filled with ethyl ether-air mixtures occurs at a concentration of 5·13 per cent. of ether by volume, and has the value of 2·69 mm. The theoretical mixture for complete combustion contains

Table III.

T_f.	$\bar{C}_p(T_f - T_0)$.	c'.	Remarks.
° C.		Per cent.	
1900	·5909 + ·003669 c	23·67	Approx. flame temp.
790	·2294 + ·003788 c	9·23	Lt. for vert. downward propagation.
600	·1720 + ·003931 c	6·96	Normal ignition temp.
365	·1018 + ·004125 c	4·15	Lt. for vert. upward propagation.

3·38 per cent. of ether, while if the carbon is only burnt to carbon dioxide the theoretical mixture is

$$(C_2H_5)_2O + 4(O_2 + 3{\cdot}76N_2) = 4CO + 5H_2O + 15{\cdot}04N_2, \quad (8)$$

or 4·99 per cent. of ether.

Assuming that the reaction in the flame takes place according to equation (8), the values of the constants in Table II. have been used to calculate the limiting diameter. Several workers [12] have recorded a value for the ignition temperature of ether-air mixtures as low as 185° C. This, however, is probably the ignition temperature with a very considerable lag, and gives a result for the limiting diameter which is much too low (·126 mm.).

Experimental Work.

Variation of Velocity of Flame Propagation with Tube Diameter.

In the theory given in the Introduction [1] it has been assumed that, at the limiting diameter for propagation, the

small hemispherical flame burning at the top of the tube goes out abruptly when the velocity of the mixture is slightly less than the limiting value to which the velocity of propagation tends at the limiting diameter.

Let v' be the velocity of the mixture which is just great enough to maintain a self-supporting flame at the top of the tube for diameters less than the limiting diameter, and let v'' be the velocity of the mixture which is just great enough to prevent the hemispherical flame from travelling down the tube for diameters greater than the limiting diameter. Thus it has been assumed that v' and v'' tend to the same limit, namely v, at the limiting diameter for propagation. If this is not the case, then v in equation (1) must be taken as the value of v' at the limiting diameter.

To test this point the apparatus previously described[1] has been used. The method of determining v' was as follows:—Having made up a mixture of known composition in the gas container, the rate of flow was adjusted so that a self-supporting flame was just able to burn at the top of the tube, and the time taken for 500 c.c. of the mixture to flow through the tube measured by a stop-watch. This time was of the order of 300 seconds. The rate of flow was then slightly reduced so that it was just impossible to maintain a self-supporting flame at the top of the tube, and the time again noted for 500 c.c. to flow. Knowing the tube diameter, the mean of these two times was used to calculate v'. The two times usually differed by about 7 per cent. A similar procedure was followed in determining v''.

Measurements were also made of the greatest rate of flow which would allow any type of flame to burn at the top of the tube, the flame being carried upward by the flow for higher velocities. Usually 1000 c.c. of the mixture was used in making these determinations. The type of flame which formed corresponded either to (*a*) or (*b*) in plate i. [1].

The values of v' and v'' for a 9·5 per cent. methane-air mixture are shown in Graph II. by the curves AB and BC. It is clear that v' and v'' both tend to the same value at the limiting diameter, which is represented by the abscissa of DB. This was also found to be true for an 8·5 per cent. methane-air mixture.

In Graph II. the curve AE shows the variation with diameter of the greatest velocity of the mixture which will permit a flame to burn at the top of the tube. The diameter corresponding to the point A is the limiting diameter determined by Method IV. p. 41 [1].

On plotting the actual rate of flow, *i. e.*, $\pi r^2 v''$, against the

diameter it is found that for the curve BC the graph is practically a straight line. Hence for diameters slightly

Graph II.

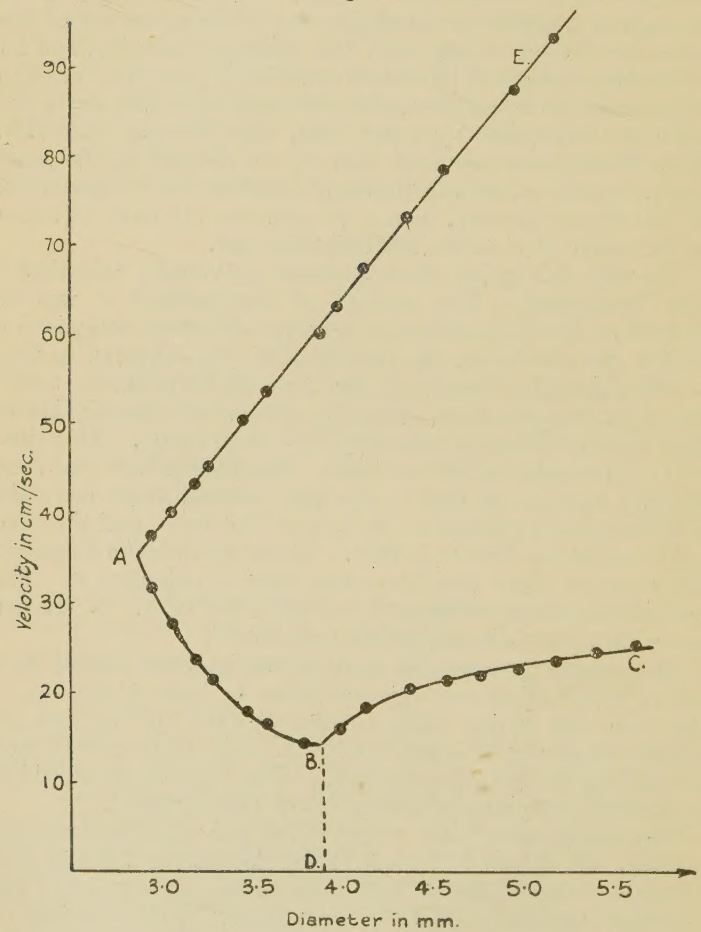

greater than the limiting diameter the velocity of propagation can be represented by

$$v'' = \frac{A}{r} - \frac{B}{r^2}, \quad . \quad . \quad . \quad . \quad . \quad . \quad (9)$$

where A and B are constant for a given mixture. Values of A and B for three mixtures are contained in Table IV.

This equation holds for values of r up to about one-and-a-half times the limiting radius for propagation.

In the case of a 5·0 per cent. ether-air mixture v' and v'' do not tend to the same value at the limiting diameter. This is shown clearly in Graph III., in which the rate of flow is plotted against the tube diameter. The velocities corresponding to the points B and B′ at the limiting diameter are 17·3 and 21·8 cm./sec.

Another interesting point connected with Graph III. is that the rate of flow remains practically constant over a considerable portion of AB. This means that the amount of heat produced in the limiting self-supporting flame remains practically constant as the diameter of the tube below it is reduced—a result which is in agreement with the theory. Along BF the limiting flame was practically hemispherical, but along FA it tended to change first to the

TABLE IV.

Mixture.	A.	B.	v.
	cm.²/sec.	cm.³/sec.	cm./sec.
9·5 per cent. methane-air ...	14·90	2·34	14·0
8·5 per cent. methane-air ...	13·82	2·30	13·2
5·0 per cent. ether-air	14·47	1·55	17·3

flat disk type, and finally becoming slightly conical at A. These flames, having relatively less efficient cooling surfaces, can exist with smaller rates of heat-supply, as is indicated by the decrease in the rate of flow along FA.

Hydrogen-Air Mixtures.

Employing the apparatus and methods previously described [1] the limiting diameters for propagation along tubes and for ignition through circular apertures in thin plates have been determined for hydrogen-air mixtures *. It was not necessary to use Method II., page 37 [1], as it was possible to maintain a self-supporting flame burning at the top of the tube or above the aperture in the thin plate down to a concentration of 13·5 per cent. of hydrogen.

* The hydrogen was supplied by the British Oxygen Company, Manchester, and stated to contain less than ½ per cent. of impurities.

The hydrogen-air mixtures have been characterized by the violence of the resulting explosion and the small value of the limiting diameter over a large part of the explosive range. The main results were very similar to those described in detail for the coal-gas-air mixtures. The work was carried out in a totally dark room, as the hydrogen

Graph III.

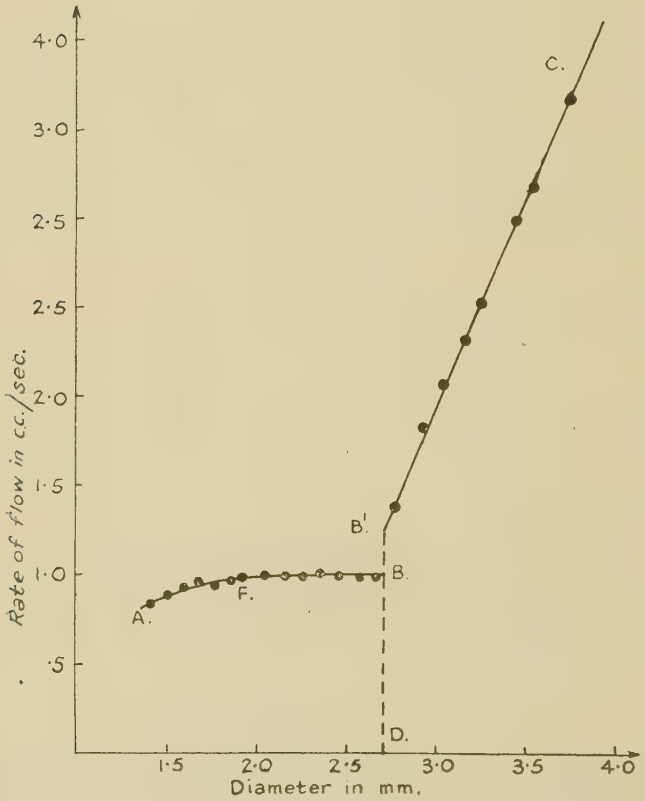

flames were very pale blue in colour and almost non-luminous.

The behaviour of the flames in propagating down the tubes was simpler than that of the methane-air mixtures, as they did not go into vibration in the lower half of the tube. Thus, if the diameter of the tube was great enough to allow propagation to take place, the flame, travelling

steadily down the tube, produced ignition of the rest of the mixture in the explosion tube AB. This was true for all three sets of tubes, *i.e.*, copper and glass A and B, and held for all mixtures examined, *i.e.*, from 13·5 to 65 per cent. of hydrogen. The coal-gas-air mixtures behaved in a similar manner over the most explosive part of the range.

The phenomenon of flame separation was observed with mixtures containing more than 56 per cent. of hydrogen, the flame which travelled down the tube being of a deep purple colour, while that remaining at the top was normal, almost non-luminous hydrogen-air flame.

With concentrations greater than 45 per cent. the almost spherical flame burning under the apertures in the thin plates was obtained. The time during which it was possible to keep this flame burning under the plate without producing general ignition was remarkably long. By allowing a 50 per cent. mixture to escape very slowly in the explosion tube AB it was possible to maintain this almost spherical flame for nearly 6 minutes under a 1·05 mm. hole in a mica plate without producing general ignition. As before, it was possible by opening the needle valve slowly to cause this flame to rise up through the hole and give a disk flame burning as previously above the plate.

These spherical flames under the plates did not vibrate at an audible frequency, but with mixtures containing more than 45 per cent. of hydrogen if the diameter of the tube was less than the limiting value for propagation the small flame burning at the top of the tube emitted a high-pitched sound just before going out.

Results.

Copper Foil.—The curves ABC and BG in Graph IV. show the variation of the limiting diameters obtained by Methods I. and III. for concentrations between 13·5 and 65 per cent. of hydrogen. The minimum diameter is only ·80 mm. and occurs at 35 per cent. This minimum diameter is only ·444 of that for coal-gas-air mixtures and ·231 of that for methane-air mixtures.

Mica Plates.—From 13·5 to 28 per cent. the limiting diameters for circular apertures in mica sheets were about 5 per cent. less than the corresponding ones for copper foil. For concentrations between 28 and 42 per cent. it was not possible to use the mica plates, as they were damaged by the force of the explosion. Occasionally the circular disk of mica inside the clamp-ring was blown right out of the plate.

This is rather remarkable, as the lower end of the explosion tube just dipped under a water surface. For concentrations greater than 42 per cent. the ease with which the edges

Graph IV.

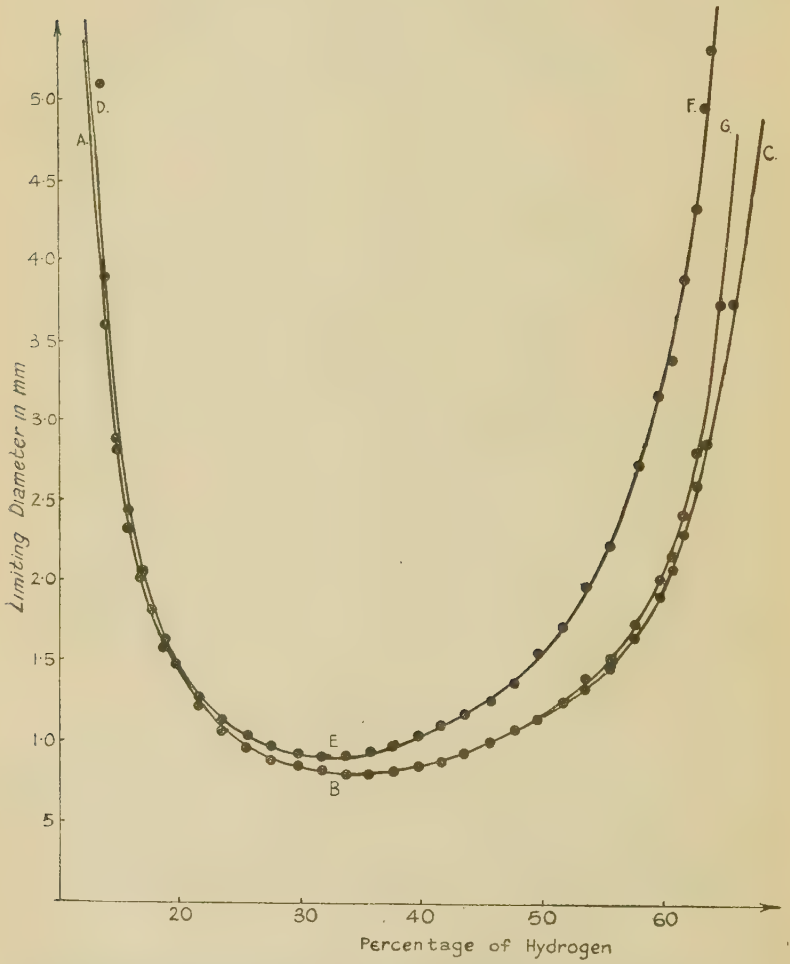

of the apertures became red hot rendered it difficult to determine the limiting diameters exactly.

Tubes.—As with every other gas examined the limiting diameters for propagation along copper and glass tubes were identical over the entire explosion range. The curve

marked DEF in Graph IV. shows the results. It differs from those already obtained as it rises more quickly to the left of the minimum than to the right. The minimum diameter is ·90 mm. and occurs at a concentration of 33 per cent. of hydrogen.

It is interesting to note that Mallard and Le Chatelier [13] found that the flame of a 30 per cent. hydrogen-air mixture just failed to propagate along a tube the diameter of which was ·9 mm. From the graph we find that the limiting diameter for this concentration is ·93 mm., with an error of $\pm$·023 mm.

The observations of W. A. Haward and T. Otagawa[14] show that the maximum uniform flame speed with hydrogen-air mixtures in a 2·5 cm. tube is obtained with a 38·6 per cent. mixture. Thus the minimum on the curves occurs at a concentration which is, within the experimental error, the mean between the concentration for theoretically complete combustion and that giving the maximum flame speed.

Ethyl Ether-Air Mixtures.

Since the theory indicates that mixtures having low ignition temperatures should have correspondingly small limiting diameters it was decided to determine the limiting diameters for ethyl ether-vapour-air mixtures. In some circumstances the ignition temperature of these mixtures appears to be as low as 185° C. [12], but, as has been already mentioned, this is probably not the ignition temperature specified in equation (1). Measurements by the concentric tube method give the ignition temperature of ethyl ether-air mixtures as 570° C. [15].

As ether is soluble in water and also in most liquids, the mixture could not be made up as previously over water in the glass container. A satisfactory method was devised by utilizing a strong rectangular copper vessel, the volume of which was about 4·8 litres. By an arrangement of tubes and stop-cocks this container could be connected to either a Hyvac pump and exhausted, or to a foot-pump and air compressed into it, or could be connected to two drying bottles partly filled with ethyl ether. The pressure inside the container could be read on a large mercury manometer.

The method of making up the mixture was as follows :—

(1) The container was exhausted by the vacuum-pump down to a pressure of less than 1 mm. of mercury, to eliminate traces of the previous mixture.

(2) Air was admitted to the container till the pressure was (p_0-h) cm. of mercury, p_o being the atmospheric pressure and h about 20 cm.

(3) The container was then connected to the ether saturators and air drawn through the two bottles till the pressure inside was again atmospheric.

(4) Air was forced into the container by the foot-pump till the pressure was (p_o+h') cm., h' being usually 80·0 cm.

The percentage of ether vapour in the mixture was calculated from

$$c=\frac{100p_sh}{p_o(p_o+h')}, \quad . \quad . \quad . \quad . \quad . \quad (10)$$

where p_s is the saturation vapour pressure of ether at the temperature of that in the second saturator. The temperature of this ether was kept fairly constant by immersing the bottle in a water-bath. During process (3) the temperature of this bath never changed by more than ·05° C.

In order to determine p_s two barometer tubes were constructed and mounted side by side. By admitting a little ether to the top of one of the columns the difference between the level of the mercury in the two tubes gave the saturation vapour pressure of ether at the room temperature. The temperature was read on a Cassella alcohol thermometer graduated in fifths of a degree Centigrade.

By means of this apparatus it was found that the vapour pressure, p_s, could be represented by

$$p_s=11{\cdot}73+1{\cdot}666\,\mathrm{T}\text{ cm. of mercury} \quad . \quad . \quad (11)$$

over the range from 14 to 17° C., T being the temperature in degrees Centigrade. This equation was used to calculate p_s for equation (10), T being taken as the temperature of the water-bath.

From the values of p_s at 0°, 10°, and 20° C. given in Kaye and Laby's Tables [16] the values of the constants in the Kirchhoff-Rankine-Dupré vapour pressure formula have been calculated, giving

$$\log_{10}p_s=27{\cdot}534-\frac{2345{\cdot}7}{\theta}-6{\cdot}8448\log_{10}\theta, \quad . \quad (12)$$

θ being the absolute temperature.

This equation gives $p_s=35{\cdot}81$ cm. and $\frac{\partial p_s}{\partial\theta}=1{\cdot}60$ cm./° C. at 15° C., while equation (11) gives $p_s=36{\cdot}73$ cm. and

$\frac{\partial p_s}{\partial \theta} = 1{\cdot}666$ cm./°C. at 15° C. The difference between the two values of p_s amounts to 2·54 per cent.

It soon became evident that the limiting diameters were very sensitive to small changes in the concentration of the ether, and on account of this it was difficult to obtain absolutely consistent results.

On drawing off the mixture from the top of the container, which was only 27·3 cm. high, it was found that as the mixture was used the concentration of the ether appeared to increase steadily; thus, for concentrations less than 5·1 per cent. the limiting diameters tended to decrease as the mixture was used, while for greater concentrations they tended to increase. This was interpreted as indicating that the concentration of the ether at the bottom of the container was slightly greater than at the top.

To prove that the ether tended to settle in the lower part of the container two outlets were taken, one from the top and the other from the bottom, and connected to the needle valve, so that by turning two stop-cocks the mixture could either be drawn off from the top or bottom of the container. On making up a mixture of average concentration about 3·70 per cent., and allowing it to stand for 15 hours, it was found that the limiting diameters for the upper and lower fractions were 4·05 and 3·52 mm. respectively. From Graph V. we see that these diameters correspond to concentrations of 3·61 and 3·85 per cent. When used within half an hour of being made up a mixture of the same average concentration gave limiting diameters of 4·05 and 3·68 mm. for the upper and lower fractions. The limiting diameters for the upper and lower fractions of an average 6·65 per cent. mixture half an hour after being made up were 4·05 and 4·66 mm., corresponding to concentrations of 6·55 and 6·74 per cent.

This effect was eliminated by turning the container on its side, so that its vertical height was only 11·3 cm., and by taking an outlet from its centre. The mixtures were allowed to stand for about 15 minutes before being used.

It should be explained that with the ether-air mixtures the lower end of the explosion tube AB just dipped under a mercury surface instead of a water surface as previously.

The phenomena, which have already been detailed for other combustible gases, were also observed with ethyl ether-air mixtures, flame separation taking place with concentrations greater than 6·25 per cent., and the almost spherical flame burning under the plates with concentrations

greater than 6·5 per cent. This spherical flame did not expand to a diameter much greater than that of the hole above it, and did not burn for any length of time under the plate, usually about $\frac{1}{2}$ and never more than 5 seconds. This made it difficult to decide whether ignition was taking place immediately, *i.e.*, in less than $\frac{1}{5}$ second, or by the almost spherical flame expanding and giving very slightly delayed ignition. The diameter which has been determined for ignition through holes in thin plates for concentrations of 6·25 per cent. and greater is the smallest diameter through which ignition can be obtained when the rate of flow is slowly reduced from that giving a hemispherical flame above the plate. It corresponds to the smallest limiting diameter in table i., p. 40 [1].

Except for concentrations between 5·0 and 6·5 per cent. the flame, travelling down the tube which just gave propagation, produced ignition of the rest of the mixture in the explosion tube AB. This applied to all three sets of tubes. Between these limits the diameter of tube necessary to produce ignition of the mixture in AB was greater than that for propagation alone, as with these mixtures the flame went into vibration in the lower half of the tube.

Results.

Circular Apertures in Thin Plates.—Curve ABC in Graph V. shows the variation of the limiting diameter for copper foil obtained by Method I. for concentrations between 3·0 and 6·0 per cent. of ether, the minimum diameter being 2·50 mm. at a concentration of 5·13 per cent. This minimum diameter is intermediate in value between those for coal-gas and methane-air mixtures, as was also the violence of the explosion. The limiting diameters for the mica plates were about 5 per cent. less than the corresponding ones for copper foil between 3·0 and 6·0 per cent. tubes.

The equality of the limiting diameters for propagation along copper and glass tubes was again verified for mixtures containing between 3·0 and 7·0 per cent. of ether. The minimum diameter on this curve, *i.e.*, DEF Graph V., is 2·69 mm., and occurs at 5·13 per cent. This curve can be represented by the same experimental equation as has been previously used, *i.e.*,

$$d = d_0 + \alpha(c - c_0)(e^{\beta(c-c_0)} - 1), \quad . \quad . \quad . \quad (13)$$

where d is the limiting diameter at concentration c, (c_0, d_0) the coordinates of the minimum, and α and β constants

chosen to fit the curve. The values of α and β are given in Table V.

Effect of Diluting Gases.

In the theory given to explain the failure of flames to travel along tubes of small diameter it has been assumed

Graph V.

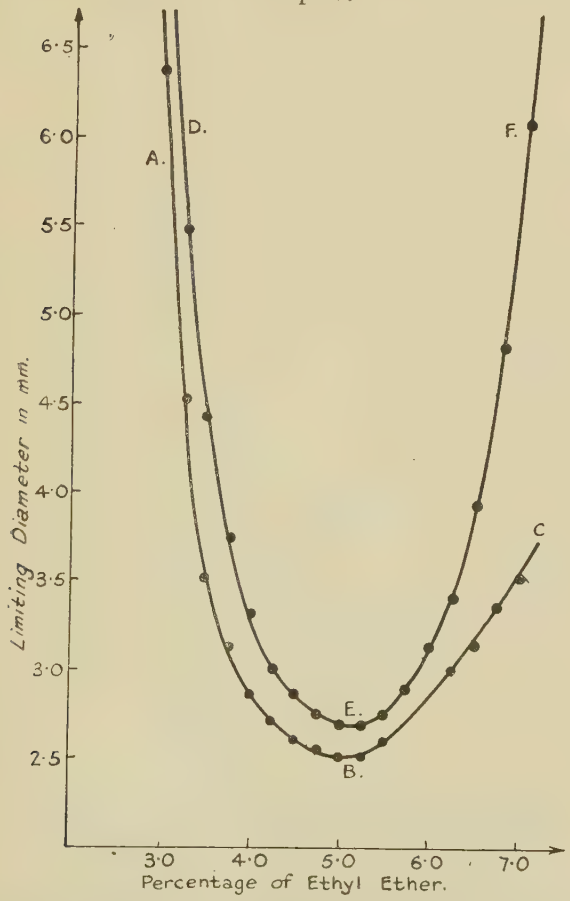

that the extinction of the flame is controlled by the thermal properties of the gaseous mixture, the thermal conductivity and the specific heat being two of the principal terms. It is thus necessary to show experimentally that the limiting diameters for propagation change with these terms in a manner which could be predicted from the theory.

The hypothesis can be tested by studying the effect of various diluting gases ; for example, if all the nitrogen of the air in the mixture were replaced by an equal volume of another inert, diatomic gas of different thermal conductivity, the effect of a change in the average thermal conductivity of the mixture could be ascertained. Unfortunately Providence has not supplied us with such a gas. However, by taking two fresh sets of observations, one in which the nitrogen of the mixture is replaced by argon,

TABLE V.

Curve.	c_0.	d_0.	Range.	α.	β.
	Per cent.	mm.	Per cent.	mm.	
DE Graph IV....	33·0	·90	15·0 $\leq c \leq$ 33·0	*·031843	*·22978
EF Graph IV....	33·0	·90	33·0 $\leq c \leq$ 63·0	*·098510	*·11820
DE Graph V. ...	5·125	2·69	2·75 $\leq c \leq$ 5·125	·24257	1·0479
EF Graph V. ...	5·125	2·69	5·125 $\leq c \leq$ 7·00	·29313	1·0491
A′B′ Graph VIII.	9·75	4·00	6·75 $\leq c \leq$ 9·75	·10872	·83234
DE′ Graph IX....	9·75	4·00	6·75 $\leq c \leq$ 9·75	·10872	·83234
B′C′ Graph VIII.	9·75	4·00	9·75 $\leq c \leq$ 12·75	·10872	·83234
AB″ Graph VIII.	9·75	3·72	6·75 $\leq c \leq$ 9·75	·17798	·65192
B″C′ Graph VIII.	9·75	3·72	9·75 $\leq c \leq$ 12·75	·20207	·65929
AB Graph VIII.	9·88	3·46	6·38 $\leq c \leq$ 9·88	·22330	·57800
BC Graph VIII.	9·88	3·46	9·88 $\leq c \leq$ 13·25	·05868	1·0390
E′F′ Graph IX....	9·75	4·00	9·75 $\leq c \leq$ 12·50	·21168	·75710
DE Graph IX....	9·63	3·80	6·38 $\leq c \leq$ 9·63	·23260	·65800
EF Graph IX....	9·63	3·80	9·63 $\leq c <$ 12·50	·15530	·89740
EF′ Graph IX....	9·75	3·82	9·75 $\leq c \leq$ 12·25	·24895	·72778

* Equation (4), p. 52 (1).

and another in which it is replaced by helium, the result of a change in the thermal conductivity of the mixture could be found. Since both gases are monatomic, they have identical molecular heats, but their average thermal conductivities between 18 and 750° C. are in the ratio of 1 : 7·5 (see Table I.).

The first set of observations with argon * as the diluting

* Obtained from the British Oxygen Company, Wembley, and stated to contain ·6 per cent. of nitrogen and ·4 per cent. of oxygen as impurities.

gas instead of nitrogen in methane-air mixtures has been obtained, and is shown by curve D′E′F′, Graph VI. The corresponding results for propagation along tubes with methane-air mixtures is shown by curve DEF. On account

Graph VI.

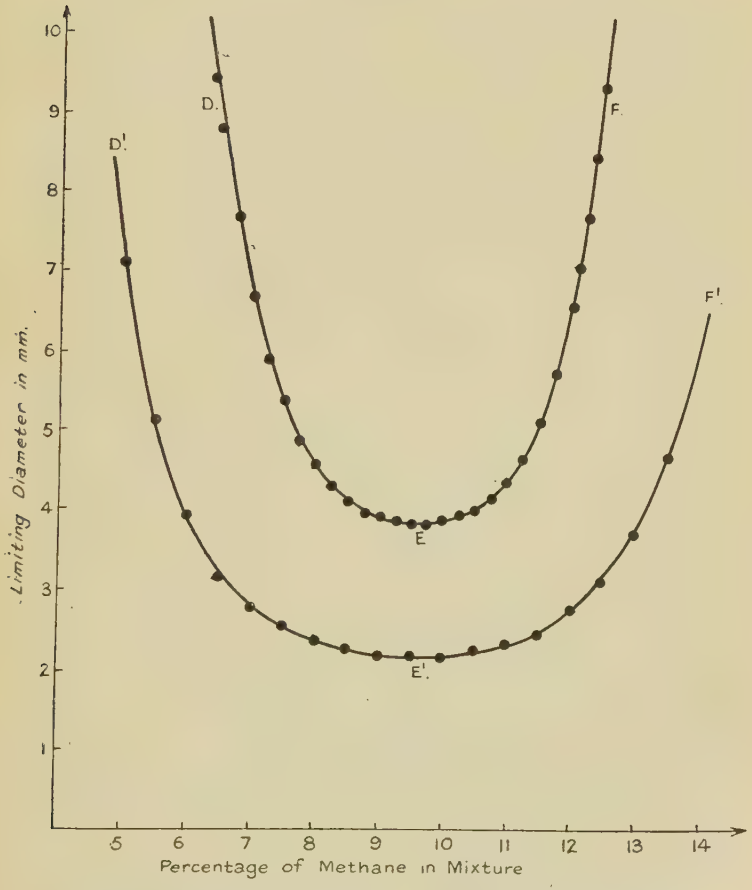

of the high cost of helium in this country it has unfortunately not been found possible to obtain the second set of observations.

The results show that the effect of this substitution is to decrease the limiting diameters for propagation down tubes, the reduction in diameter at the minimum being from 3·80 to 2·12 mm. The minima on the two curves occur at the

same concentration, *i. e.*, about 9·63 per cent. of methane. This decrease in the limiting diameter is partly due to the reduction in the average thermal conductivity of the mixture and partly to the reduction in the specific heat. The reduction in thermal conductivity has been calculated to be about 24 per cent., while the reduction in specific heat is about 18 per cent. From equation (1) it is evident that both of these reductions tend to decrease the limiting diameter.

Measurements of v' for tubes of diameter slightly less than the limiting value for the 9·5 per cent. mixture indicate that v in equation (1) is about 28·7 cm./sec. In this connexion the observations of H. F. Coward and B. E. Hess [17] are interesting; they show that when the nitrogen of the air in a 9·5 per cent. methane-air mixture is replaced by argon, the uniform flame speed in a horizontal tube 2·5 cm. in diameter is increased by 2·67 times. The ratio of the two corresponding values of v is 2·05.

It is to be expected that the flame temperatures for the methane-oxygen-argon mixtures will be higher than those for the corresponding methane-air mixtures, but, assuming them to be the same, the value of d calculated from equation (1) for the 9·5 per cent. mixture has been found to be ·28 mm., or about ·23 times the calculated value for the methane-air mixture (see Table II.). The experimental value for the methane-oxygen-argon mixture is about ·56 times that for the corresponding methane-air mixture. This discrepancy could be reduced by assuming a higher value for T_f in equation (1).

From Graph VI. we see that the range of inflammability has been extended by replacing the nitrogen of the mixture by argon, the lower limiting concentration for a tube 8·78 mm. in diameter being reduced from about 6·50 to 4·75 per cent., *i. e.*, a decrease of 1·75 per cent. From the nature of the curves it is probable that the difference in the limiting concentrations in tubes of greater diameter, say 2 or 3 cm., would be less than this.

On applying equation (11), p. 27 [1] to calculate the percentage of methane, c', in the methane-oxygen-argon mixture at the usual lower limit of inflammability, we find that, assuming T_f to be 1425° C., *i. e.*, the calculated flame temperature at the usual lower limit of inflammability of methane-air mixtures,

$$\overline{C}_p(T_f - T_0) = ·3231 + ·01470c,$$

giving $$c' = 4·36 \text{ per cent.},$$

which represents a decrease of 1·3 per cent. from the corresponding concentration for methane-air mixtures. This is confirmed by the results of H. F. Coward and B. E. Hess [17], which indicate that the concentration of methane at the usual lower limit of inflammability for this oxygen-argon atmosphere is about 4·40 per cent.

When the nitrogen of the air in methane-air mixtures was replaced by an equal volume of carbon dioxide it was found that not even the 9·5 per cent. mixture was inflammable in the tube 2 cm. in diameter. This is contrary to the results of J. Roskowski [18], who found that methane was inflammable in this atmosphere, the limits of inflammability in a closed globe of 35 c.c. capacity being 8·9 and 11·7 per cent., but is in agreement with those of H. F. Coward and Jones [19], which show that for the mixture $CH_4 + 2O_2 + nCO_2$ the maximum value of n which will give a mixture inflammable in a tube 1·9 cm. in diameter is about 6·4. For a 9·5 per cent. mixture with the previous atmosphere the value of n is 7·52. It has been found that the value of n which would give a mixture having a limiting diameter of 3·80 mm. was 4·1.

The effect of the substitution is to increase the specific heat of the mixture, since carbon dioxide, being a triatomic molecule, has a considerably higher specific heat than nitrogen. As carbon dioxide is fairly soluble in water, the mixtures were made up by the method already described for the ether-air mixtures.

By employing a more explosive mixture, such as is formed by mixing coal gas with air, it is possible to replace all the nitrogen of the mixture by carbon dioxide and still obtain an inflammable mixture. The effect of this substitution is shown in Graph VII., and it may be seen that the limiting diameters are considerably increased and the range of inflammability decreased. The minimum diameter is increased from 1·80 to 5·53 mm., the concentration of coal-gas at the minima being the same, namely 20·5 per cent.

Partitions in a Vertical Tube.

All the above results have been obtained with small stationary flames formed by the explosive mixture burning as it escapes slowly into the atmosphere from the top of a tube, or through a circular aperture in a thin plate. It was decided to investigate the conditions under which a large flame travelling with its full velocity of uniform propagation could be extinguished by a partition erected across the tube along which the tube was travelling.

In this new method the stationary explosive mixture was contained in a vertical glass tube 40 cm. long and 2 cm. in diameter. At a distance of 25 cm. from the top the tube was divided, so that various types of partitions could be introduced to separate the upper part of the tube from the

Graph VII.

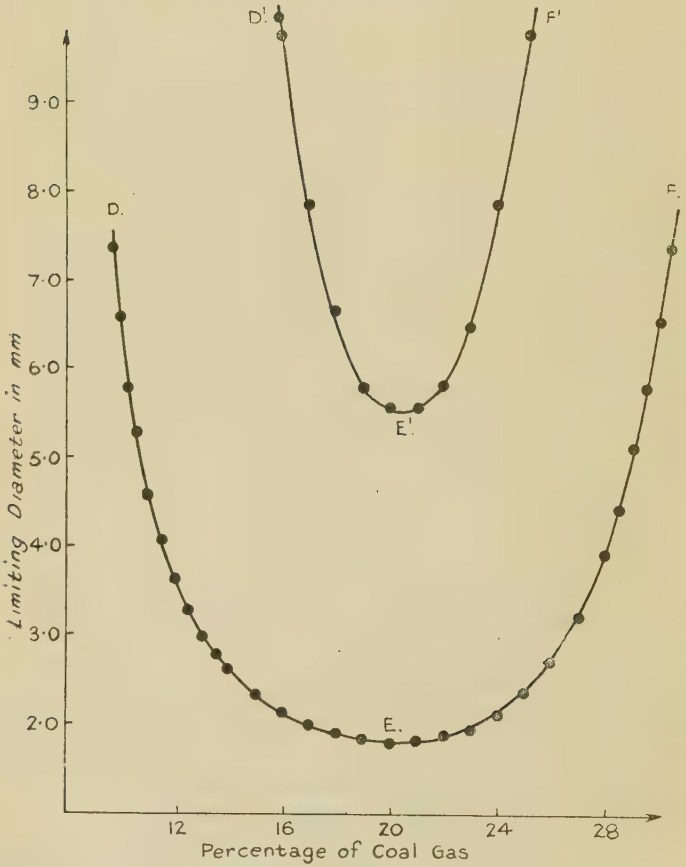

lower. This was effected by adding above the explosion tube AB (fig. 2, p. 35 [1]) another glass tube, 25 cm. in length and 2 cm. in diameter, having brass flanges similar to PQ attached to either end. The partition, such as a single circular hole in a thin plate or a piece of wire gauze, was inserted between PQ and the lower flange of the 25 cm.

tube, and the arrangement made rigid by clamping these two flanges together. In the case of metal gauzes, felt disks, having concentric holes 2 cm. in diameter, were used to make the joint gas-tight. Having filled both tubes with the explosive mixture, the upper tube was closed by a glass disk resting against the surface of the top flange.

When the mixture was ignited by sliding this glass disk off the flange and swinging a large flame horizontally across the top of the tube, the flame, travelling for 25 cm. down the tube, had practically attained its maximum velocity when it reached the partition. The size of the aperture or apertures in the partition was then varied till this large, rapidly moving flame just failed to ignite the remainder of the mixture in the lower part of the tube.

The experiments have been carried out with methane-air mixtures, using as partitions either a single or a series of nine circular holes in copper foil or thin sheets of mica, short lengths of copper or glass tubing, or gauzes made of either iron-wire or cotton-threads.

The results obtained by this new method for partitions consisting of single circular holes in copper foil and thin sheets of mica are shown in Graph VIII. by curve A′B′C′, which is exactly symmetrical about the minimum at 9·75 per cent. Over the *entire* explosive range the limiting diameters for the copper and mica partitions were identical. By comparing A′B′C′ with ABC, which is the curve for single apertures in copper foil obtained by the previous method, it may be seen that the new limiting diameters are greater, a result which is rather difficult to explain satisfactorily. It was found that if the tube on the lower side of the partition was reduced in length from 15 cm. to 6 cm. that the limiting diameters over part of the explosive range was reduced (see curve AB″C′, Graph VIII.).

The corresponding results for partitions consisting of short tubes are shown in Graph IX. The lengths of the tubes were ten times their internal diameter and they were inserted into the upper end of AB (fig. 2 [1]) by means of a rubber stopper, so that their top end was 1·5 cm. above the surface of PQ. As before, there was no difference between the results for copper and glass tubes. DEF is the curve obtained by the previous method for propagation down tubes, while DE′F′ is the corresponding curve for the new method. The curves A′B′ (Graph VIII.) and DE′ (Graph IX.) are identical, so that over this part of the explosive range the effectiveness of a single hole in a thin plate in extinguishing the flame is equal to that of a short

tube and is independent of the material of which the thin plate or tube is made. When the lower part of the tube, *i. e.*, AB, was reduced in length to 6 cm. the curve obtained

Graph VIII.

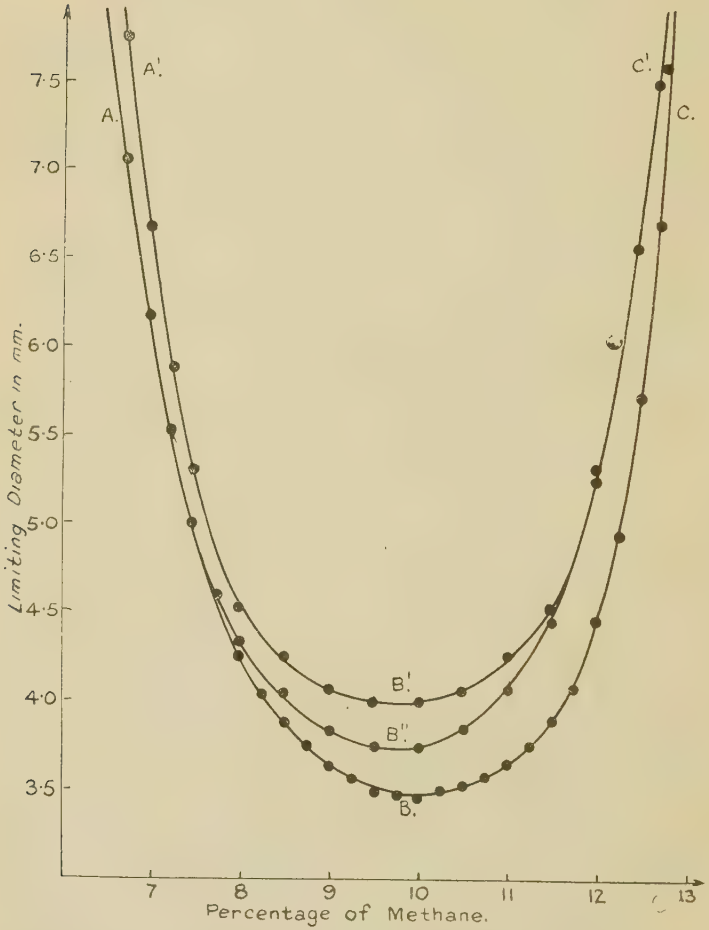

coincided with DEF'—that is, over the greater part of the range the diameter was the same as that given for propagation down tubes.

The minima on all these curves occur at the same concentration within the experimental error, *i. e.*, 9·75 per cent. of methane. The graphs may be represented by

equation (13) and the appropriate values of the constants are given in Table V.

The next type of partition investigated consisted of thin sheets of copper or mica, perforated by nine holes of equal

Graph IX.

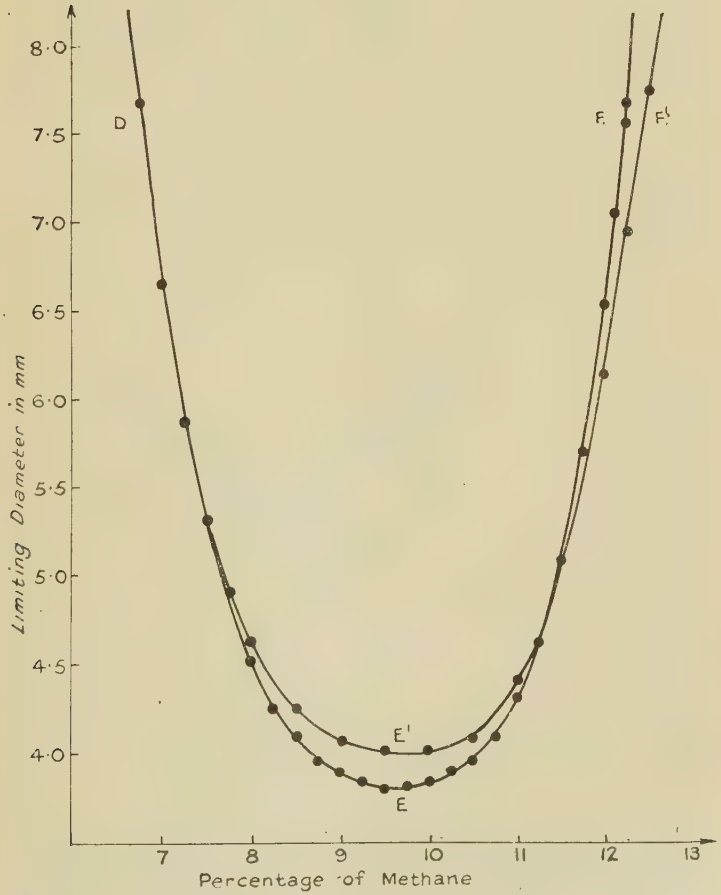

diameter arranged in three rows of three, so as to lie as symmetrically as possible inside a square whose side was 1·53 cm. The nine-hole gratings were first secured by the ring and clamps to close the upper end of the explosion tube AB, and the limiting diameter of the holes which would just give ignition by Method I. (p. 37 [1]) determined.

These diameters are shown by curve GHI (Graph X.) for the copper foil gratings. For concentrations less than 9·75 per cent. of methane the results for the mica gratings coincided with GH, but the combined heating effect of the small flames for greater concentrations damaged the gratings and prevented consistent results from being obtained. Curve ABC shows the corresponding results given by Method I. for single circular apertures in copper foil. The reduction in limiting diameter necessary when

Graph X.

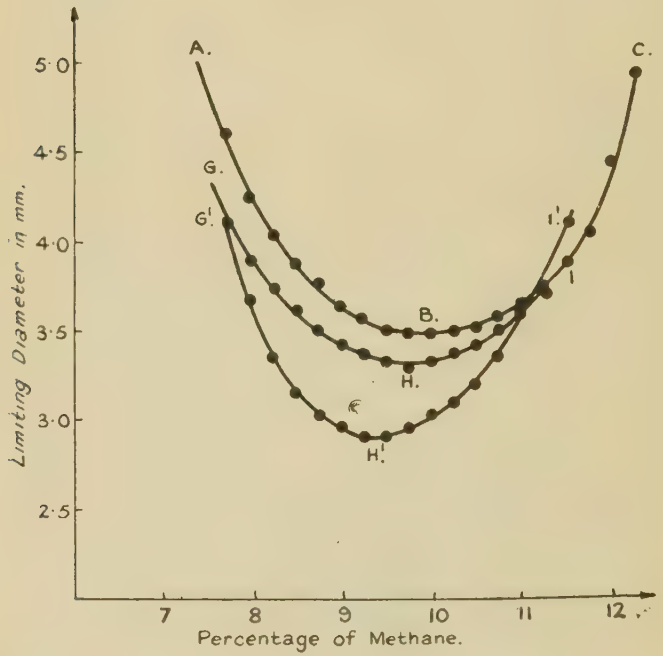

employing the nine-hole gratings instead of a single hole is readily explained, since the presence of the eight small hemispherical flames surrounding the central flame will reduce the cooling effect, and so necessitate a smaller diameter for extinction.

When the gratings were mounted as partitions at 25 cm. from the top of the 40 cm. tube it was found that the results for the copper and mica gratings were identical over the range examined, 8·75 to 11·25 per cent. of methane. The new limiting diameters were generally less

than those given by Method I., and the minimum on the curve appeared to occur at a slightly lower concentration, *i.e.*, about 9·38 instead of 9·75 per cent. (see curve G′H′I′, Graph X.).

Similar results have been obtained for partitions consisting of pieces of iron-wire gauze or cotton-net normally used for window curtains. Over the most explosive part of the methane-air range, 8·5 to 11·5 per cent., it appeared to be immaterial whether the gauze was made of iron wire or cotton thread, the size of the mesh and the diameter of the wire or cotton thread being the important factors. For example, with a 9·5 per cent. methane-air mixture the flame could just be prevented from igniting the remainder of the mixture in the lower tube by an iron gauze, the meshes of which were squares with 2·72 mm. sides, the diameter of the wire being ·46 mm., or by a cotton gauze having square meshes with 2·65 mm sides and thread of thickness about ·5 mm.

Discussion.

It should be pointed out that the flames in all these experiments, with tubes, single holes in thin plates, and nine-hole gratings, cannot be left burning indefinitely at the top of the tube or above the thin plate independently of the rate of flow of the mixture, or of the thermal conductivity of the tube or thin plate without ultimately producing propagation or ignition. This is due to the heating up of the material by the flame, which allows the flame to travel through a smaller aperture than normally. From equation (1) we see that if T_0 increases then the limiting diameter is reduced. It is obvious that d must tend to zero as the temperature of the tube or thin plate tends to the ignition temperature of the mixture, T_i.

It is only when the rate of flow is such that the under surface of the flame is approximately hemispherical that the temperature of the material remains sensibly at room temperature, no matter how long the flame is allowed to burn or of what material the tube or thin plate is made. In Method I. the rate of flow was such that when the escaping gas was lit the flame which formed was of the flat disk type shown at (*c*) (pl. i.[1]). The rate of flow was then quickly adjusted so as to give the hemispherical type of flame shown at (*d*), the disk flame only being allowed to remain for a few seconds.

The time during which a disk flame could be kept burning without affecting the limiting diameter depended on the thermal conductivity of the material and on the amount

of the combustible gas present in the mixture. It was less for mica and glass than for copper, and decreased as the concentration of the mixture approached the usual upper limit of inflammability. For single apertures in thin plates it was of the order of 10 seconds for the mica and 10 minutes for copper for mixtures containing less than 9 per cent. of methane.

The experiments may be interpreted in the following manner :—Suppose we have a partition across a tube which is filled with a *stationary* explosive mixture, and that the diameter of the tube is greater than the limiting value for propagation with that mixture. If the mixture is ignited at an open end of the tube the flame will travel along till it comes to the partition, where it will either be extinguished in a few seconds or will propagate through and continue along the tube. Under these circumstances the effectiveness of the partition in preventing propagation will be determined primarily by the size and spacing of its orifices, the thermal conductivity of its material being comparatively unimportant.

If, however, the mixture is flowing along the tube toward the open end with a velocity which is greater than a certain minimum and less than the normal flame velocity along the tube, then, when the flame reaches the partition it will either propagate through or will continue to burn on the side of the partition nearer the open end of the tube. Under these conditions it is not primarily a question of extinguishing the flame *immediately*, but one of conducting the total heat of the flame away, so as to prevent the partition being ultimately heated to the ignition temperature of the mixture, or to a temperature at which the flame is able to propagate through its orifices. Hence the effectiveness of the partition in *ultimately* preventing propagation will depend on its thermal conductivity as well as on the size and spacing of its orifices.

The minimum rate of flow referred to above is the limiting rate of flow which is just sufficient to ensure that the surfaces of the small flames facing the orifices will be approximately hemispherical. If this minimum rate is not exceeded then the effectiveness of the partition is still primarily determined by the size and spacing of its orifices.

Summary.

The previous theory of the failure of the flames of explosive gaseous mixtures to travel along narrow tubes has been developed, and a definite connexion established between the limiting diameter for flame propagation at constant pressure

and the limiting pressure for flame propagation in a tube of fixed diameter. The experimental part of the paper describes the measurement of the variation of the velocity of flame propagation with tube diameter, for diameters near the limiting value, the determination of the limiting diameters for hydrogen-air and ethyl ether-air mixtures, the effect of inert diluents on the limiting diameters, and the results of experiments on the extinction of a rapidly moving flame by various types of partitions erected across the tube along which the flame is travelling.

The work confirms the hypothesis that the extinction of the flame is due to the cooling effect of the unburnt gas in contact with its external flame surface, the limiting diameters being controlled by the thermal properties of the gaseous mixture.

In conclusion, the writer again wishes to express his indebtedness to Professor Taylor Jones for his helpful advice and encouragement. The experimental part of the investigation was performed in the Research Laboratories of the Natural Philosophy Department of the University of Glasgow.

References.

(1) J. M. Holm, Phil. Mag. ser. 7, xiv. p. 18 (1932).
(2) W. Sutherland, Phil. Mag. xxxvi. p. 507 (1893).
(3) G. W. C. Kaye and T. H. Laby, 'Physical and Chemical Constants,' 1932 ed., p. 157.
(4) W. A. Bone and D. T. A. Townend, 'Flame and Combustion in Gases,' 1927 ed., pp. 65–68.
(5) Safety in Mines Research Board, Paper no. 24.
(6) J. W. McDavid, Trans. Chem. Soc. cxi. p. 1003 (1917).
(7) W. Mason and R. V. Wheeler, Trans. Chem. Soc. ciii. p. 45 (1918.)
(8) H. B. Dixon, J. Harwood, and W. F. Higgins, Trans. Faraday Soc. xxii. p. 272 (1926).
(9) *Vide* (4) above, p. 487.
(10) A. G. White, Trans. Chem. Soc. cxxv. p. 2387 (1924).
(11) F. Goldmann, *Zeit. phys. Chem.* B 5, p. 307 (1929).
(12) A. G. White and T. W. Price, Trans. Chem. Soc. cxv. p. 1462 (1919),
(13) Mallard and Le Chatelier, *Compt. Rend.* xciii. p. 145 (1881).
(14) W. A. Haward and T. Otagawa, Trans. Chem. Soc. cix. p. 83 (1916).
(15) *Vide* (4) above, p. 483.
(16) *Vide* (3) above, p. 45.
(17) H. F. Coward and B. E. Hess, Trans. Faraday Soc. xxii. p. 305 (1926).
(18) J. Roszkowski, *Journ. Gasbeleuchtung*, xxxiii. pp. 491 *et seq.* (1890).
(19) H. F. Coward and G. W. Jones, Bureau of Mines, Bulletin 279, p. 57.

Glasgow.
28th October, 1932.

XXXIII. *The Oscillation of Fluid in a Moving Tank.* *By* Prof. G. E. Pavlenko *.

1. LET us take an open tank of an arbitrary form partly filled with some fluid, and performing a certain periodic motion of an arbitrary character, *i. e.*, consisting of translation as well as of a rotating motion in the vertical plane (fig. 1). This motion will result in the oscillation of the fluid contained in the tank, followed by the deformation of the surface of this fluid.

Such phenomena take place on ships having fluid cargoes, *e. g.*, on tankers and on ships provided with ballast or fuel tanks and being in the rough sea.

Fig. 1.

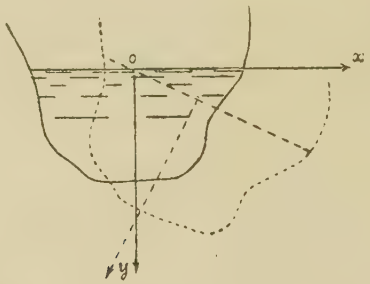

The motion of the tank in the vertical plane.

Let us assume that the motion of the tank is given, *i. e.*, that all the successive positions and speeds are known.

2. The motion of a fluid may be obtained as the result of superposition of two motions: (1) of the translation, which is identical with the motion that would be performed by a fluid as a solid fixed to the tank, and (2) of the relative motion, representing the motion of a fluid kinematically possible in the case of a fixed tank.

Evidently the translation is given in the conditions of the problem, and only the relative motion is to be determined.

In their most general form the equations of such a motion will be

$$\xi = x + \xi_1(x, y, t) + \xi_2(x, y, t),$$
$$\eta = y + \eta_1(x, y, t) + \eta_2(x, y, t),$$

* Communicated by the Author.

where x and y are the original coordinates of a particle of fluid corresponding to the state of rest, whilst ξ and η will be the coordinates of the displaced particle. By the sign "1" is denoted the displacement of a particle from its original position as the result of translation, and by the sign "2" the displacement caused by the relative motion.

3. As the translation is known, we may exclude it from our examination by modifying the conditions of our problem in the following way. Let us assume that the tank is fixed whilst the fluid is performing a certain motion under the action of periodically changing extraneous forces, which will consist of (1) the force of gravity, varying in direction, and (2) of the forces of inertia. These forces are known, and may be introduced as the function of the coordinates of particles of time.

In such a problem the general equations of motion must assume the form

$$\xi = x + \xi_2(x, y, t)$$
$$\eta = y + \eta_2(x, y, t).$$

4. Let us investigate the motion that a fluid may have in an actually fixed tank in the case of absence of any external forces, except the force of gravity, that is constant in value and direction. We shall denote this motion as free motion, to distinguish it from those types of motion which take place under the action of periodical external influences, and will be called forced motion. Of all the possible forms of free motion we shall consider the peculiar cases of simple harmonic oscillations of a fluid, *i. e.*, of such oscillations where all the particles perform the oscillating motion simultaneously according to the sinusoidal law, having a common period and a common phase for all the particles.

In order to observe the changes in the amplitude of oscillations let us agree to determine it by the amplitude of oscillations of one particle, no matter which, say with the original coordinates x_0 and y_0.

Let us assume the amplitude of this particle (or one of its components parallel to the axis, ξ or η) to be equal to a. Then the amplitude components of each particle parallel to the coordinate axes will be Aa and Ba, where A and B are the different numbers for different particles. Such a motion may be determined by the equations

$$\xi = x + A(x, y)a \sin(\sigma t + \alpha),$$
$$\eta = y + B(x, y)a \sin(\sigma t + \alpha),$$

or, denoting by q the function of time only equal to $a \sin(\sigma t + \alpha)$, and by A and B the functions only of the coordinates of the particles,

$$\xi = x + Aq$$
$$\eta = y + Bq.$$

5. The velocity component parallel to the coordinate axes :

$$v_x = A(x, y) a\sigma \cos(\sigma t + \alpha) = Aq',$$
$$v_y = B(x, y) a\sigma \cos(\sigma t + \alpha) = Bq'.$$

The kinetic energy of motion of all the mass of water,

$$V = \tfrac{1}{2}\int_0 (v_x^2 + v_y^2) dm = \tfrac{1}{2} a^2\sigma^2 \cos^2(\sigma t + d) \int_0 (A^2 + B^2) dm,$$

where dm is the mass of a particle. Knowing that in the cases of extreme deviations, corresponding to $t = \frac{\pi(n+\frac{1}{2}) - \alpha}{\sigma}$, all the kinetic energy is transferred into the potential one, and that in the mean positions, *i. e.*, when $t = \frac{\pi n - \alpha}{\sigma}$, all the potential energy is transformed into the kinetic one, and that the full energy presents a constant value, independent of time, we may write at once the expression of the potential energy :

$$U = \tfrac{1}{2} a^2\sigma^2 \sin^2(\sigma t + \alpha) \int_0 (A^2 + B^2) dm,$$

or briefly,

$$V = \tfrac{1}{2} M q'^2, \qquad U = \tfrac{1}{2}\sigma^2 M q^2,$$

where

$$M = \int_0 (A^2 + B^2) dm.$$

6. Let us now introduce into our problem the given extraneous forces which we shall express as the function of time and of coordinates of the fluid particles.

Applying the method of small oscillations, we may take in this expression the original coordinates of particles, neglecting the influence which the displacement of particles will have on the magnitude of the extraneous forces acting on them.

To a certain particle with the coordinates x and y of the mass dm will be applied the force having the components

$$X(x, y) \sin \omega t \, dm \quad \text{and} \quad Y(x, y) \sin \omega t \, dm.$$

During the interval of time dt each particle will perform displacements along the axes of coordinates $v_x \, dt$ and $v_y \, dt$,

and the work of external forces expanded for this purpose will be

$$(Xv_x\,dt + Yv_y\,dt)\sin\omega t\,dm,$$

and the same for all the mass of fluid :

$$\int_0 (Xv_x\,dt + Yv_y dt)\sin\omega t dm = q'\sin\omega t\ dt \int_0 (AX + BY)dm$$

$$= Qq'\sin\omega t\,dt,$$

where $$Q = \int_0 (AX + BY)dm.$$

7. The increase of the full energy of motion during the interval of time dt is equal to the work of external forces during the same interval of time :

$$\frac{\partial(V+U)}{\partial t}dt = Qq'\sin\omega t \quad \text{or} \quad Mq'q'' + \sigma^2 Mq'q$$

$$= Qq'\sin\omega t\ \ q'' + \sigma^2 q = \frac{Q}{M}\sin\omega t.$$

The same result may be obtained by means of Lagrange's equation in the second form, considering q as the generalized coordinate of motion of a fluid.

Hence

$$q = \frac{\frac{Q}{M}}{1-\left(\frac{\omega}{\sigma}\right)^2}\sin\omega t \quad \text{and} \quad a = \frac{\frac{Q}{M}}{1-\left(\frac{\omega}{\sigma}\right)^2}.$$

Whatever the period of free oscillation of this particular form of motion expressed by the function M may be, the forced oscillations of this form will have the period equal to the period of external forces, the phase common with the phase of these forces and the amplitude determined according to the formula obtained.

8. The question of determining the free or the forced motions of a fluid in a tank may be, therefore, reduced to the finding of such functions as A and B, that would satisfy the conditions of paragraph 4. The form of these functions depends on the dimensions and form of the tank. Considering as different only these functions, not one of which can be obtained by means of a linear transformation from any other, *i. e.*, between which there is no dependence of type,

$$c_1A_1 + c_2A_2 + \ldots + c_nA_n = 0 \quad \text{or} \quad c_1B_1 + c_2B_2 + \ldots + c_nB_n = 0,$$

we must come to the conclusion that if, according to the conditions of the problem, such functions really exist, the quantity of the different corresponding numbers σ_i, and consequently of the different factors q_i, must be equal to the number of degrees of freedom. This fact, together with the possibility of existence of oscillations, corresponding to the form of every pair of functions A_i and B_i independently from others, allows us to attribute to the values q_i the sense of the normal coordinates of the system. In the general case the number of degrees of freedom, and consequently the number of normal coordinates determined by characteristic numbers σ_i is equal to infinity.

Using the principle of superposition of normal coordinates, we may express every possible motion of a fluid in a tank, in the case of absence of external forces, variable in time, by the equations

$$\xi = x + \sum_{i=1}^{i=\infty} A_i q_i$$

$$\eta = y + \sum_{i=1}^{i=\infty} B_i q_i,$$

where $q_i = a_i \sin(\sigma_i t + \alpha_i)$; a_i and α_i are constant, and are determined by the original conditions.

9. Under the action of a periodic external force, determined in Cartesian coordinates as the values X and V, and in q_i coordinates as the values Q_i, the fluid will perform a periodic motion with the period of the external force ; the form of this motion may be represented by the superposition of motions in each separate coordinate.

In order that every possible motion of the given system could be not only formally, but also physically, represented by equations of this type, it is necessary that the series of these functions A_i and B_i should be conjugate and present a full and close system.

10. The number of these functions, which we shall call fundamental functions, may be considered as finite in certain particular cases. For example, if the tank containing a fluid consists of a couple of vertical tubes of small cross-sections connected with each other, it would be appropriate in some practical questions to neglect the deformation of the surface in every tube and to examine only the modification of the mean height of levels. The problem having such conditions deals with the system with one degree of freedom.

Likewise three tubes connected with each other may be considered as a system with two degrees of freedom.

The number of degrees of freedom is infinite in all the cases where the area of free surface is so great that the change of its shape is taken into consideration.

We may find the fundamental functions in every particular case by solving the general equations of hydromechanics and applying the boundary conditions on the walls of the tank and on the free surface. For the most part all the fundamental functions may be represented by a common expression, including the characteristic number, that can assume a series of definite values. In other cases the system of fundamental functions may be subdivided into groups, each of which will possess this property.

11. As an illustration let us consider the most important, in the applied sense, case of a tank having the shape of a rectangular parallelepiped and moving in the plane parallel to one of its side-walls. As the motion of the fluid is caused by the alteration of extraneous forces and pressures on the surface of walls, and depends very little on the forces of friction, we may count that this motion scarcely differs from that which an ideal fluid would have in the same external conditions, and we shall assume that the velocities of motion have the potential expressed by

$$\phi(x, y, t).$$

12. In order to find the velocity potential in a particular case, satisfying the conditions of periodicity of paragraph 4, and corresponding to the characteristic number σ, we may write

$$\phi(x, y, t) = \tau(x, y) \sin(\sigma t + \alpha).$$

As the velocity potential must satisfy the Laplace equation, it must be satisfied by the function τ, *i. e.*,

$$\frac{\partial^2 \tau}{\partial x^2} + \frac{\partial^2 \tau}{\partial y^2} = 0.$$

Let us look for the solution of this equation in the form

$$\tau(x, y) = f_1(x) f_2(y).$$

After substitution we have

$$-\frac{1}{f}\frac{\partial^2 f_1}{\partial x^2} = \frac{1}{f_2}\frac{\partial^2 f_2}{\partial y^2}.$$

As the functions in both parts of the equation depend on the different variables x and y independent of each other, the equality means that each of these parts must be equal to

the same constant number. According to the character of the problem we consider this number as a positive and denote it by κ^2, whence we have two equations

$$\frac{\partial^2 f_1}{\partial x^2} + \kappa^2 f_1 = 0,$$

$$\frac{\partial^2 f_2}{\partial y_2} - \kappa^2 f_2 = 0.$$

Hence $$f_1(x) = b \sin(\kappa x + \beta)$$

$$f_2(y) = ce^{\kappa y} + de^{-\kappa y},$$

where b, c, d and β are arbitrary constants.

Thus the expression of the potential in our case will be

$$\phi(x, y, t) = (ge^{\kappa y} + he^{-\kappa y}) \sin(\kappa x + \beta) \sin(\sigma t + \alpha).$$

Fig. 2.

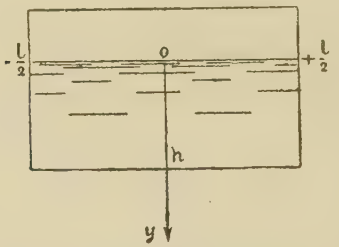

The tank of rectangular form.

13. Let us submit this expression to the boundary conditions on the surface of the bottom and walls of the tank; for that purpose let us suppose its dimensions and the position of the coordinate axes to be such as shown on fig. 2.

The boundary conditions will assume the form

$$(1) \qquad \frac{\partial \phi}{\partial y_{y=h}} = 0,$$

$$(2) \qquad \frac{\partial \phi}{\partial x_{x=\frac{l}{2}}} = 0,$$

$$(3) \qquad \frac{\partial \phi}{\partial x_{x=-\frac{l}{2}}} = 0.$$

The first condition gives

$$ge^{\kappa h} - he^{-\kappa h} = 0,$$

whence $$g=\frac{m}{2}e^{-\kappa h}\,; \qquad h=\frac{m}{2}e^{\kappa h},$$

where m is an arbitrary constant.

The second condition gives

$$\cos\left(\kappa\frac{l}{2}+\beta\right)=0,$$

whence $$\beta=-\kappa\frac{l}{2}+\pi(n_1+\tfrac{1}{2}),$$

where n_1 is an integer.

The third condition gives

$$\cos\left(-\kappa\frac{l}{2}+\beta\right)=0,$$

whence $$\beta=\kappa\frac{l}{2}+\pi(n_2+\tfrac{1}{2}),$$

where n_2 is an integer.

Combining the second and the third conditions we obtain

$$\kappa=\frac{n_3\pi}{l},$$

where $$n_3=n_1-n_2, \text{ and } \beta=n_4\frac{\pi}{2},$$

where $$n_4=n_1+n_2+1.$$

After this the velocity potential takes the form

$$\phi=m\cosh\kappa(y-h)\left\{\begin{matrix}\sin\\ \cos\end{matrix}\right\}\kappa x.\sin(\sigma t-\alpha),$$

where κ with $\sin\kappa x$ may assume only odd values :

$$\frac{\pi}{l}, \quad \frac{3\pi}{l}, \quad \frac{5\pi}{l} \text{ etc.},$$

and with $\cos\kappa x$ only even ones :

$$\frac{2\pi}{l}, \frac{4\pi}{l}, \text{ etc.}$$

14. The last boundary condition is—the pressures upon the free surface of water must be constant. Expressing the form of the surface by the equation

$$y=\eta_0(x, t),$$

and denoting the pressure by $p(x, y, t)$, we may write this condition in the form

$$p(x, \eta_0, t)=\text{const.}$$

The equation of the free surface may be obtained from the velocity potential according to the condition

$$\frac{\partial \phi}{\partial y_{y=0}} = \frac{\partial \eta_0}{\partial t},$$

which is correct to the limits of the assumption of small motions.

Applying this condition, we get

$$\eta_0 = a \left\{ \begin{matrix} \sin \\ \cos \end{matrix} \right\} \kappa x \cos(\sigma t + \alpha),$$

where

$$a = \frac{m\kappa}{\sigma} \sinh \kappa h.$$

The possible forms of oscillation of the surface with the first four values are shown in fig. 3.

Fig. 3.

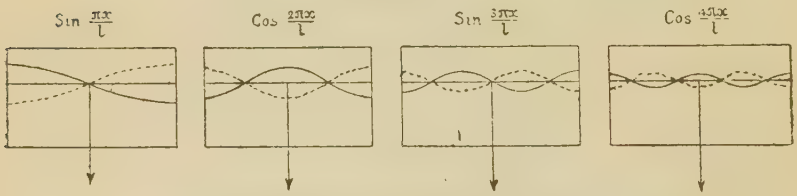

Different types of free fluid oscillation in a rectangular tank.

Now the velocity potential may be written in the form

$$\phi = a \frac{\sigma}{\kappa} \frac{\cosh \kappa(y-h)}{\sinh \kappa h} \left\{ \begin{matrix} \sin \\ \cos \end{matrix} \right\} \kappa x \sin(\sigma t + \alpha).$$

Here a is the amplitude of a point of the free surface at the wall of the tank ; we shall identify this point with that mentioned in paragraph 4, which determines the amplitude of oscillations of the fluid.

In order to apply the boundary condition, let us write the Lagrange's integral, connecting the pressures with the form of motion of the fluid and presenting the result of integration of the principal equation of hydromechanics, provided there exists the velocity potential

$$U - P - \frac{v^2}{2} = \frac{\partial \phi}{\partial t} + f(t),$$

where U is the potential function of the extraneous forces, P

is the function of pressures connected with the pressure by dependence,

$$\frac{dp}{\rho} = d\mathrm{P},$$

where ρ is the specific mass (density), v is the velocity of a particle of the fluid, $f(t)$ is an arbitrary function of time, constant with regard to coordinates; we may assume this function equal to zero, without restricting the degree of generality, as we may count it to be included in the velocity potential.

As of all the external forces only the force of gravity is acting, we may write

$$\mathrm{U} = gy.$$

Further, we assume that the fluid is homogenous and incompressible; consequently

$$\mathrm{P} = \frac{p}{\rho}.$$

Owing to the small velocity of motion, we neglect the term $\frac{v^2}{2}$ as a small value of the higher order, comparing with all the other terms, and finally we have

$$p = \rho g y - \rho \frac{\partial \phi}{\partial t}.$$

Let us apply the condition of the constancy of pressures on the surface

$$p(x, \eta_0, t) = a\rho g \left\{ \begin{matrix} \sin \\ \cos \end{matrix} \right\} \kappa x \cos(\sigma t + \alpha)$$

$$- a\rho \frac{\sigma^2}{\kappa} \coth \kappa h \left\{ \begin{matrix} \sin \\ \cos \end{matrix} \right\} \kappa x \cos(\sigma t + \alpha) = \text{const.}$$

This condition may be fulfilled for every x and every t provided

$$\sigma^2 = \kappa g \tanh \kappa h.$$

Thus, to the series of values κ determined according to paragraph 13 corresponds a series of characteristic numbers σ:

$$\sigma = \sqrt{\frac{n\pi \tanh \frac{n\pi h}{l}}{l}},$$

where $n = 1, 2, 3,$ etc.

15. Let us form the expression of the components parallel to the coordinate axes :

$$v_x = \frac{\partial \phi}{\partial x} = a\sigma \frac{\cosh \kappa(y-h)}{\sinh \kappa h} \left\{ \begin{matrix} +\cos \\ -\sin \end{matrix} \right\} \kappa x \sin(\sigma t + \alpha),$$

$$v_y = \frac{\partial \phi}{\partial y} = a\sigma \frac{\sinh \kappa(y-h)}{\sinh \kappa h} \left\{ \begin{matrix} \sin \\ \cos \end{matrix} \right\} \kappa x \sin(\sigma t + \alpha).$$

Comparing these expressions with the general expressions, obtained in paragraph 5, we find the fundamental functions

$$A(x, y) = \frac{\cosh \kappa(y-h) \left\{ \begin{matrix} +\cos \\ -\sin \end{matrix} \right\} \kappa x}{\sinh \kappa h};$$

$$B(x, y) = \frac{\sinh \kappa(y-h) \left\{ \begin{matrix} \sin \\ \cos \end{matrix} \right\} \kappa x}{\sinh \kappa h}.$$

For an infinite series of values κ we get a system of fundamental functions which is evidently conjugate, complete and close for the given volume.

16. In order to find the velocity potential of an arbitrary motion of a fluid that is not subject to the influence of external forces varying with time, it is necessary to set an original condition for a certain moment, e. g., $t = 0$. Besides, it is sufficient to know these conditions only for the free surface of a fluid.

Let these conditions be

$$\eta_0(x, 0) = f(x); \quad \frac{\partial}{\partial t} \eta_0(x, 0) = f'(x).$$

We may present each of the functions f and f' as the sum of two functions f_1 and f_2, one of which is odd and the other even, using for this purpose the following method

$$\frac{f(x) - f(-x)}{2} = f_1(x); \quad \frac{f(x) + f(-x)}{2} = f_2(x),$$

where evidently $f_1(x) + f_2(x) = f(x)$, and also for $f'(x)$.

Let us develop the odd functions in Fourier's series by sin * and the even functions by cos † :

* The possibility of such development of an arbitrary odd function may be shown in the following way :—

Let us transport the origin into the point $x_0 = \frac{l}{2}$; then

$$x = x - \frac{l}{2}, \quad f_0(x) = f_1\left(x_1 - \frac{l}{2}\right) = \psi(x).$$

$$f_1(x)=\sum_{i=1}^{i=\infty} a_i \sin\frac{2(i-\frac{1}{2})\pi x}{l},\quad f_2(x)=\sum_{i=1}^{i=\infty} b_i \cos\frac{2i\pi x}{l};$$

$$f_1'(x)=\sum_{i=1}^{i=\infty} a_i' \sin\frac{2(i-\frac{1}{2})\pi x}{l},\quad f_2'(x)=\sum_{i=1}^{i=\infty} b_i' \cos\frac{2i\pi x}{l}.$$

We have the right to regard this function to be periodic with the period $2l$, and even in respect to x; then

$$\psi(x_1)=\sum_{j=1}^{j=\infty} c_j \cos\frac{j\pi x_1}{l}.$$

But according to the condition the function is odd; consequently

$$f_1(x)=-f_1(-x) \quad \text{or} \quad f_1\left(x_1-\frac{l}{2}\right)=-f_1\left(\frac{l}{2}-x_1\right).$$

Hence $$\psi(x_1)=-\psi(x_1+l).$$

Besides, there must be place for every j:

$$c_j \cos\frac{j\pi x_1}{l}=-c_j \cos\frac{j\pi(-x_1+l)}{l}.$$

For the odd j this equation becomes an identity with every c; for the even ones it may be possible only with $c_j=0$.

Consequently

$$\psi(x_1)=\sum_{j=1,3,5\ldots} c_j \cos\frac{j\pi x_1}{l}=f_1\left(x_1-\frac{l}{2}\right).$$

Substituting now $x_1=x+\frac{l}{2}$, we get:

$$f_1(x)=\sum_{j=1,3,5\ldots} c_j \cos\left(\frac{\pi j x}{l}+\frac{\pi j}{2}\right)=\sum_{i=1}^{i=\infty} a_i \sin\frac{2(i-\frac{1}{2})\pi x}{l}.$$

† (P. 370.) The absence of the first (constant) terms of development may be explained by the constancy of volume of the fluid. As

$$\int_{-\frac{l}{2}}^{+\frac{l}{2}} f(x)\,dx=0 \quad \text{and} \quad \int_{-\frac{l}{2}}^{+\frac{l}{2}} f(-x)\,dx=0,$$

therefore

$$\int_{-\frac{l}{2}}^{+\frac{l}{2}} f'(x)\,dx=0 \quad \text{and} \quad \int_{-\frac{l}{2}}^{+\frac{l}{2}} f'(-x)\,dx=0;$$

whence

$$a_0=\frac{1}{l}\int_{-\frac{l}{2}}^{+\frac{l}{2}} f'(x)\,dx=\frac{1}{2l}\int_{-\frac{l}{2}}^{+\frac{l}{2}} [f(x)-f(-x)]\,dx=0,$$

and in a similar way

$$b_0=a_0'=b_0'=0.$$

The equation of the free surface will be

$$\eta_0(x,t)=\sum_{i=1}^{i=\infty}\left(a\ \sin\frac{2(i-\frac{1}{2})\pi x}{l}+b_i\cos\frac{2i\pi x}{l}\right)\cos\sigma_i t$$
$$+\sum_{i=1}^{i=\infty}\left(\frac{a_i'}{\sigma_i}\sin\frac{2(i-\frac{1}{2})\pi x}{l}+\frac{b_i'}{\sigma_i}\cos\frac{2i\pi x}{l}\right)\sin\sigma_i t.$$

17. Let us now pass to the case of a tank, performing an oscillating motion. In the general case this motion may be given by the equation of translation of a certain point and by one equation of rotation round this point. Let this point be the origin $x=0$, $y=0$, and the required equations be

$$\xi_1=\xi_0\sin\omega t,$$
$$\eta_1=\eta_0\sin\omega t,$$
$$\theta=\theta_0\sin\omega t.$$

For the abridgement of calculations we choose a common phase for all the items of motion of the tank; a more general case of different phases does not introduce any additional difficulties.

The translation of any particle of fluid will be determined by the equations

$$\xi=x+\xi_0\sin\omega t-y\theta_0\sin\omega t,$$
$$\eta=y+\eta_0\sin\omega t+x\theta_0\sin\omega t.$$

The velocities of these particles:

$$v_x=\xi_0\omega\cos\omega t-y\theta_0\omega\cos\omega t,$$
$$v_y=\eta\,\omega\cos\omega t+x\theta_0\omega\cos\omega t.$$

Accelerations:

$$v_x'=-\xi_0\omega^2\sin\omega t+y\theta_0\omega^2\sin\omega t,$$
$$v_y'=-\eta_0\omega^2\sin\omega t-x\theta_0\omega^2\sin\omega t.$$

Forces of inertia:

$$-v_x'\,dm=(\xi_0-y\theta_0)\omega^2\sin\omega t\,dm,$$
$$-v_y'\,dm=(\eta_0+x\theta_0)\omega^2\sin\omega t\,dm.$$

The alteration of direction of the force of gravity at the inclination will be taken into account by the introduction of a periodic component parallel to the axis x:

$$g\,dm\,\theta_0\sin\omega t.$$

Thus the amplitude components of accelerations of the forces, acting on a particle of fluid (see paragraph 6) will be

$$X(x, y) = (\xi_0\omega^2 - y\theta_0\omega^2 + g\theta_0),$$
$$Y(x, y) = (\eta_0 + x\theta_0)\omega^2.$$

18. In order to solve the problem of forced motions of a fluid, we must form (1) the integral M (paragraph 5) and (2) the integral Q (paragraph 6):

$$M\int_0(A^2 + B^2)dm = \rho\int_0^h\int_{-\frac{l}{2}}^{+\frac{l}{2}}(A^2 + B^2)\,dx\,dy.$$

We substitute the values A and B from paragraph 15:

$$M = \frac{\rho}{\sinh^2\kappa h}\int_0^h\int_{-\frac{l}{2}}^{+\frac{l}{2}}\Big[\cosh^2\kappa(y-h)\left\{\begin{matrix}\cos^2\\ \sin^2\end{matrix}\right\}\kappa x + \sinh^2\kappa(y-h)\left\{\begin{matrix}\sin^2\\ \cos^2\end{matrix}\right\}\kappa x\Big]dx\,dy = \frac{\rho l}{2\kappa\tanh\kappa h},$$

$$Q = \int(AX + BY)dm = \rho\int_0^h\int_{-\frac{l}{2}}^{+\frac{l}{2}}(AX + BY)\,dx\,dy$$

$$= \frac{\rho}{\sin\kappa h}\int_0^h\int_{-\frac{l}{2}}^{+\frac{l}{2}}\Big[\xi_0\omega^2 + g\theta_0 - y\theta_0\omega^2)\cosh\kappa(y-h)\left\{\begin{matrix}+\cos\\ -\sin\end{matrix}\right\}\kappa x + (\eta_0 + x\theta_0)\omega^2\sinh\kappa(y-h)\left\{\begin{matrix}\sin\\ \cos\end{matrix}\right\}\kappa x\Big]dx\,dy$$

$$= \frac{2\rho\sin\frac{\kappa l}{2}}{\kappa^2}\Big[\xi_0\omega^2 + g\theta_0 + \frac{\theta_0\omega^2}{\kappa}\frac{\cosh\kappa h - 1}{\sinh\kappa h}\Big],$$

whence

$$\frac{Q}{M}\frac{4\tanh\kappa h\sin\frac{\kappa l}{2}}{\kappa l}\Big[\xi_0\omega^2 + g\theta_0 + \frac{\theta_0\omega^2}{\kappa}\frac{\cosh\kappa h - 1}{\sinh\kappa h}\Big].$$

The interesting consequence of the expression obtained is that the integral Q will be equal to zero at the values of trigonometric functions written below. It follows from this that oscillating motions (and consequently all kinds of motion) of tank are unable to cause motions of fluid of

symmetrical form. Thus the form of motion sought for will consist only of such principal motions for which

$$\kappa = \frac{\pi}{l}, \frac{3\pi}{l}, \frac{5\pi}{l}, \text{ etc.}$$

19. The motion of fluid in a tank caused by the oscillating motion of the latter is determined by the periodic alteration in the form of surface :

$$\eta_0(x,t) = \sum_{i=1,3,5} \frac{4\tanh\frac{i\pi h}{l}\sin\frac{i\pi}{2}}{i\pi\left(1-\frac{\omega^2}{\sigma_i^2}\right)}\left[\xi_0\omega^2 + g\theta_0 + \frac{\theta_0\omega^2 l}{i\pi}\frac{\cosh\frac{i\pi h}{l}-1}{\sinh\frac{i\pi h}{l}}\right]\sin\frac{i\pi x}{l}\sin\omega t,$$

where $$\sigma_i^2 = \frac{i\pi g}{l}\tanh\frac{i\pi h}{l}.$$

In the particular case when the motion of the tank is purely translative (without inclination), with the horizontal amplitude component equal to ξ_0 (the vertical component is of no influence), the expression assumes a simpler form ;

$$\eta_0(x,t) = \sum_{i=1,3,5\ldots} \frac{4\xi_0\omega^2\tanh\frac{i\pi h}{l}\sin\frac{i\pi}{2}\sin\frac{i\pi x}{l}}{i\pi\left(1-\frac{\omega^2}{\sigma_i^2}\right)}\sin\omega t.$$

20. The solution obtained for the case of the oscillating motion of a tank may be extended to the case of any motion. As an illustration let us take the following practical problem : the motion of a starting locomotive, containing an oil-tank, is determined by the expression $\xi(t)$.

Let us put this expression in the form

$$\xi(t) = \int_0^\infty \xi_0(\omega)\sin\omega t\, d\omega.$$

The motion of the fluid surface in the tank will be determined by the equation

$$\eta_0(x,t) = \sum_{i=1,3,5\ldots} \frac{4\tanh\frac{i\pi h}{l}\sin\frac{i\pi}{2}}{i\pi}\sin\frac{i\pi x}{l}\int_0^\infty \frac{\xi_0(\omega)\omega^2}{1-\frac{\omega^2}{\sigma_i^2}}\sin\omega t\, d\omega.$$

XXXIV. *Spectral Composition of an X-Ray Radiation determined from its Filtration Curve.* *By* Ludwik Silberstein, *Ph.D.**

IT is well known that the radiation emitted by any of the usual types of X-ray tube is complex, non-homogeneous —that is to say, it consists of a continuous spectrum† which, under ordinary technical circumstances, stretches from 0·1 or a few tenths up to 1·2 or 1·3 A. The direct experimental determination of the composition of, or the spectral distribution of, intensity within, such radiation samples is very laborious and beset with a number of technical difficulties; so much so that up to the present but a very few X-ray samples have actually been thus analyzed.

On the other hand, the so-called absorption curve or *filtration curve* of an X-ray radiation sample can be determined with ease, and a huge number of such "curves," representing the total transmitted intensity as a function of the thickness of the filter (*e. g.*, aluminium or copper), is now available.

Under these circumstances the problem of determining theoretically the spectral composition from the filtration curve naturally suggests itself.

It is the purpose of the present paper to give in general an approximate, and for a wide class of sub-cases a rigorous, method of solving it, and to explain these methods on some concrete examples.

The problem in hand can be accurately stated as follows:—

A sample of X-radiation, from a given tube operated under a given set of conditions, is being filtered through a number of foils of a substance, as, *e. g.*, aluminium or copper, of different thicknesses x. The absorption coefficient of the filter (for quasi-monochromatic rays) is an empirically determined function of the wave-length, $\mu=\mu(\lambda)$. The total intensity $I(x)$ of the transmitted radiation, as fraction of the incident one, has been measured for a set of different thicknesses x, and thus the "filtration curve" of the sample, I plotted against x, has been constructed. Such being the case, it is required to determine the spectral composition of that radiation sample, *i. e.*, the specific intensity I_λ as a function of the wave-length, $I_\lambda=f(\lambda)$, within the incident radiation.

* Communication no. 506 from the Kodak Research Laboratories.

† With or without the superposition of a proper line spectrum.

The attenuation factor for quasi-homogeneous radiation of wave-length ranging from λ to $\lambda+d\lambda$ being $e^{-\mu(\lambda)x}$, and the partial incident intensity within these λ-limits being $f(\lambda)d\lambda$, we have

$$\int_0^\infty e^{-\mu(\lambda)x} f(\lambda)d\lambda = I(x). \quad . \quad . \quad . \quad . \quad (1)$$

Since, moreover, $I(x)$, as stated above, stands for the *ratio* of the transmitted to the incident intensity, $I(0)=1$, so that

$$\int_0^\infty f(\lambda)d\lambda = 1. \quad . \quad . \quad . \quad . \quad . \quad . \quad (2)$$

In the absence of any information as to the actual wave-length extension of the radiation sample, the extreme values, 0 and ∞, have been taken for the limits of the integral. In practice this interval will be considerably reduced.

The problem, thus formulated, is:

Given $I(x)$ and $\mu(\lambda)$ as functions of x and of λ, find the unknown function $I_\lambda \equiv f(\lambda)$. In other words, solve the *integral equation*, (1), of what is termed "the first kind," with $I(x)$ as the given, $f(\lambda)$ as the unknown function, and $e^{-\mu(\lambda)\cdot x}$ as the "kernel," a given function of the two independent variables x and λ*.

Instead of the wave-length λ we may introduce the absorption coefficient μ of the filter as integration variable. For brevity put

$$f(\lambda)\frac{d\lambda}{d\mu} \equiv \frac{f(\lambda)}{\mu'} = \phi(\mu), \quad . \quad . \quad . \quad . \quad (3)$$

and denote $\mu(0)$ by μ_0. Then, since to all purposes $\mu(\infty)=\infty$, equation (1) will become

$$\int_{\mu_0}^\infty e^{-x\mu}\phi(\mu)d\mu = I(x), \quad . \quad . \quad . \quad . \quad (1a)$$

an integral equation for the unknown function $\phi(\mu)$ with a simplified kernel, which is now symmetrical in the two independent variables x, μ.

A rigorous solution of this equation or the equivalent one, (1), for any given function $I(x)$ is out of the question. The usual methods developed in the theory of linear integral

* $\mu=\mu(\lambda)$ being, at any rate, known *graphically* as function of the wave-length, with sufficient accuracy for Al and Cu at least.

equations * would, in the best of cases, lead to an exceedingly clumsy form of solution, which in practice would be scarcely of any value.

Under these circumstances I have in a first paper on this subject ('Journal of the Optical Society of America,' xxii. May 1932) contented myself with an approximate algebraic method of solving this problem. Since all details concerning such solutions are given in that paper it will be enough to review here this part of the investigation but very briefly, and then pass on to a description of the rigorous (and not unhandy) solution of the problem for the case of a *particular form of* $I(x)$, a form, that is, which has since turned out to represent faithfully enough the actual filtration curves of many X-ray samples.

I. *Approximate Solution of Integral Equation.*

Using the form (1) of the equation, suppose $\lambda = a$ up to b to be the whole wave-length interval in which perceptible radiation intensities may at all be expected, so that

$$\int_a^b e^{-\mu(\lambda)x} f(\lambda) d\lambda = I(x).$$

For a the well-known quantum limit, determined by $hc/\lambda_m = Ve$, *i. e.*,

$$\lambda_m = \frac{12{\cdot}34}{V},$$

in Angström units (V being the voltage applied to the tube in kilovolts), can be taken. As to b, the upper limit, all practical cases will be amply covered by setting $b = 1{\cdot}3$ Å. at the utmost. Now the total interval $b - a$ being divided into a number n of equal parts $\Delta\lambda$ and $\lambda_1, \ldots . \lambda_n$ being the mid-points of these parts, the integral equation can be replaced approximately by

$$\Delta\lambda \cdot \sum_{i=1}^{n} e^{-\mu(\lambda_i)x} f(\lambda_i) = I(x).$$

To determine the n unknowns $f(\lambda_i)$, which henceforth may be denoted by f_i, one has but to write down n such linear equations belonging to a set of n different thicknesses $x_\kappa (\kappa = 1, 2, \ldots n)$ of the filter, all of these of course for one

* As a matter of fact these methods have been largely constructed for the integral equations of "the second kind," *i. e.*, of the type $f(x) - \sigma \int k(x, y) f(y) dy = F(x)$, where σ is a parameter, whereas not much attention has been paid to the equations of the first kind.

and the same set of λ's. Thus, and omitting the common factor $\Delta\lambda$ (so that f will represent the radiant intensity contained within the interval $\lambda_i \mp \frac{1}{2}\Delta\lambda$), the set of equations will become, with $\mu(\lambda_i)=\mu_i$,

$$e^{-\mu_1 x_\kappa} f_1 + e^{-\mu_2 x_\kappa} f_2 + \ldots + e^{-\mu_n x_\kappa} f_n = I_\kappa,$$

$\kappa = 1, 2, \ldots n.$

The selection of the thicknesses, which is in wide limits unhampered, can be suited to the actual circumstances of the case under investigation. Since the absorption coefficient μ increases very rapidly with λ, the coefficients of the unknown f_i's will rapidly decrease in passing from lower to higher suffixes i. In order, then, to give the longer waves contained in the radiation a chance to assert themselves at all in our system of equations some of the thicknesses at least must be chosen possibly small. The most important among them will clearly be $x=0$ itself, corresponding to the absence of a filter. Let this stand for x_1. Then $I_1 = I(0) = 1$ will be the total incident intensity. The value of x_2 will be taken as small as is feasible, and the remaining x_κ increasingly greater. (The particular choice $x_3 = 2x_2$, $x_4 = 3x_2$, etc., offering some computational advantages, will be mentioned presently.) Ultimately the system of n equations for as many "ordinates" f_i of the required spectral curve becomes

$$\left.\begin{aligned} f_1 + f_2 + \ldots\ldots + f_n &= I_1 = 1, \\ e^{-\mu_1 x_2} f_1 + e^{-\mu_2 x_2} f_2 + \ldots + e^{-\mu_n x_2} f_n &= I_2, \\ \cdot\ \cdot\ \cdot

The technicalities of the computation are described in the paper quoted above. Here it will be enough to quote some results relating to the case of $n=3$, namely, for the particular selection of the set of thicknesses

$$x_1=0, \quad \text{any } x_2, \quad x_3=2x_2. \quad . \quad . \quad . \quad . \quad (6)$$

With the abbreviations

$$a=e^{-\mu_1 x_2}, \quad b=e^{-\mu_2 x_2}, \quad c=e^{-\mu_3 x_2}$$

the determinant of the system assumes the Cauchy form

$$D=\begin{vmatrix} a' & b' & c' \\ a^2 & b^2 & c^2 \end{vmatrix}=(a-b)(b-c)(c-a).$$

Its nine minors are readily found to be

$D_{11}=-bc(b-c)$, $D_{21}=-ca(c-a)$, etc., by cycl. perm.

$D_{12}=b^2-c^2$, etc.

$D_{13}=c-b$, etc.

Thus the expressions (5′) for the three spectral ordinates are simplified down to

$$\left.\begin{aligned} f_1&=\frac{c-b}{D}\{bcI_1-(b+c)I_2+I_3\},\\ f_2&=\frac{a-c}{D}\{caI_1-(c+a)I_2+I_3\},\\ f_3&=\frac{b-a}{D}\{abI_1-(a+b)I_2+I_3\}, \end{aligned}\right\} \quad . \quad . \quad . \quad (7)$$

with $D=(a-b)(b-c)(c-a)$, as above. These solutions hold whenever $x_3=2x_2$, and, of course, for any triad of wave-lengths, λ_1, λ_2, λ_3.

For the sake of illustration of the method the last set of formulæ has been applied to the radiations emitted at various potentials by two X-ray tubes, a *Metalix* and a *Media*, for which Al-filtration curves have been determined experimentally by T. C. Neeff (*Fortschritte a. d. Gebiet d. Röntgenstrahlen*, xli. p. 414, 1930).

As thicknesses were chosen

$$x_1=0, \quad x_2=0{\cdot}1, \quad x_3=0{\cdot}2 \text{ cm.},$$

and as wave-lengths

$$\lambda_1=0{\cdot}3, \quad \lambda_2=0{\cdot}7, \quad \lambda=1{\cdot}1 \text{ Å.U.},$$

covering a total interval from 0·1 to 1·3 Å.

Inserting the corresponding values of the absorption coefficient of aluminium, one finds

$$a=0{\cdot}866, \quad b=0{\cdot}259, \quad c=0{\cdot}0045,$$

so that the formulæ (7) become

$$\left.\begin{aligned} f_1&=0{\cdot}0022\,I_1-0{\cdot}505\,I_2+1{\cdot}912\,I_3,\\ f_2&=-0{\cdot}0252\,I_1+5{\cdot}630\,I_2+6{\cdot}465\,I_3,\\ f_3&=1{\cdot}023\,I_1-5{\cdot}125\,I_2+4{\cdot}553\,I_3. \end{aligned}\right\} \quad . \quad (7\,a)$$

These formulæ can now be applied to the spectral analysis of *any* X-ray sample for which the ratios of the total intensities transmitted through foils of 1 and 2 mm. aluminium to the original total intensity have been experimentally determined (filtration data).

For the *Metalix* tube, with $I_1=1$, the data derived from Neeffs's paper are, at four different potentials V,

$V_{(\text{kv.})}$.	I_2.	I_3.
30	0·0624	0·0210
50	0·0868	0·0339
70	$0{\cdot}121_6$	0·0590
100	$0{\cdot}179_7$	0·0931

The substitution of these numbers for the I_κ in (7 *a*) gives the following result. The wave-lengths λ are in Å. In the last column the position λ_q of the quantum limit of the continuous spectrum is inserted.

$f(\lambda)$ for Metalix.

V/λ.	0·3.	0·7.	1·1.	λ_q.
30.....	·011	·190	·799	0·41
50.....	·023	·244	·733	0·25
70.....	·054	·278	·668	0·18
100.....	·089	·385	·526	0·12

Similarly the filtration data for the *Media* tube, which or the same four potentials are

$$I_2=0{\cdot}128_0, \quad 0{\cdot}211_0, \quad 0{\cdot}296_9, \quad 0{\cdot}362_3,$$
$$I_3=0{\cdot}0532, \quad 0{\cdot}0958, \quad 0{\cdot}157_1, \quad 0{\cdot}225_5,$$

give, after substitution in (7 *a*), the following table for the spectral intensity distribution in the radiation from this tube :—

$f(\lambda)$ for Media.

V/λ.	0·3.	0·7.	1·1.
30	·040	·350	·610
50	·079	·542	·379
70	·153	·629	·218
100	·251	·554	·195

Since $I_1 = 1$ by convention, so that $f_1 + f_2 + f_3 = 1$, each of these $f_i = f(\lambda_i)$ expresses *the fraction* of the whole intensity contained within the corresponding wave-length interval. The first interval ranges from 0·1 to 0·5 Å., and contains therefore in each of the four cases (corresponding to the four different voltages) the theoretical quantum limit λ_q of the continuous X-ray spectrum. The fraction f_1 of the total intensity is then actually to be attributed to the interval extending from λ_q to 0·5 Å., while the remaining two numbers, f_2, f_3, call for no such qualification except that some slight part of f_3 may in reality be spread beyond 1·3 Å. Thus, *e. g.*, at 70 kv. 5 per cent. of the intensity is contained in the case of Metalix, between 0·18 and 0·5 Å., 78 per cent. between 0·5 and 0·9, and 67 per cent. is spread over the interval reaching from 0·9 to 1·3 Å. (and possibly beyond). Both sets of results, for the two tubes, seem to be quite satisfactory, exhibiting a steady and marked shifting of the intensity from longer to shorter waves, in brief a "hardening" of the X-ray radiation with increasing potential, as might well be expected. The values of $f(0{\cdot}3)$ are also wholly consistent with the quantum limits of the spectra.

A comparison of the two tables would show that the radiation emitted by the tube Media is, at each potential, markedly harder than that from Metalix.

At any rate these two sets of results are regular and self-consistent enough to inspire a fair degree of confidence in the "*Al*, 3-*analyzer*," a brief reference name for the analyzing set of formulæ (7*a*), implying three wave-lengths and Al as filter. This set of formulæ, therefore, ought to be reliably applicable to any other samples of X-ray radiation.

It may be mentioned here that an analogous Cu, 3-analyzer built up on the pattern of the formulæ(7) for the same λ_1,

λ_2, λ_3 and thicknesses x_1, x_2, $x_3 = 0$, 0·005, and 0·01 cm., being applied to a number of copper-filtration curves obtained by L. S. Taylor ('Radiology,' xvi. p. 302, March 1931), has also yielded acceptable results for the spectral distribution of intensity. But aluminium as analyzing filter turned out to be decidedly preferable to copper, since the latter leads to much greater coefficients in the final formulæ, and puts therefore a higher claim on the precision of the I_κ-data.

An example of an Al, 4-analyzer and its application to the radiations emitted by the Media tube at four different potentials will be found in the writer's paper quoted above. Here it may suffice to say that the four-ordinate spectral table thus arrived at corroborates substantially the composition of these X-ray samples found by means of the Al, 3-analyzer and tabulated above.

The same paper contains also a discussion of the probable errors of the f_i-values as brought about by the inaccuracy of the filtration data I_κ.

There also a slight modification of the method, adapted to plots of half-value layers against the thickness of a pre-filter, is developed and illustrated by nine numerical examples (with four $f(\lambda)$ each, *loc. cit.* pp. 277 *et seq.*). The method thus modified offers, under certain circumstances, some practical advantages.

II. *Rigorous Solution of Integral Equation for a Wide Class of Filtration Curves, yielding Complete Spectral Curves.*

Let us now return to the integral equation (1*a*) for $\phi(\mu) = f(\lambda) : \frac{d\mu}{d\lambda}$ as the unknown function of the absorption coefficient μ of the filter, and through it of the wave-length λ. This equation can be slightly simplified by substituting, for the lower limit of the integral, *zero* instead of μ_0, for which there is a good justification. In fact, for aluminium, *e. g.*, the observed absorption coefficient is already for $\lambda = 0{\cdot}017$ Å. a little less than 0·16 per cm., so that at any rate $\mu_0 = \mu(0) < 0{\cdot}16$, and possibly smaller, and therefore practically negligible in comparison with all μ-values, from $\lambda = 0{\cdot}2$ onwards. For $\lambda = 0{\cdot}2$ and 0·3, $\mu = 0{\cdot}83$ and 1·43 respectively.

With this simplification the equation for $\phi(\mu)$ becomes

$$\int_0^\infty e^{-x\mu}\phi(\mu)d\mu = I(x), \qquad \ldots \quad (8)$$

to hold for all positive values of x, including zero, for which by convention $I(0)=1$, so that

$$\int_0^\infty \phi(\mu)d\mu=1. \quad . \quad . \quad . \quad . \quad . \quad (8a)$$

A *general* solution, *i.e.*, for *any* given function $I(x)$ (representing the filtration properties of the X-ray sample), even of this somewhat simplified integral equation, (8), is, as has been mentioned before, out of the question. In fact, although exactly the same transformation

$$T\phi=\int_0^\infty e^{-xu}\phi(u)du,$$

has already been introduced by Laplace * as an aid to solving some differential equations, and has been attacked extensively by Abel, Murphy, Lord Kelvin, Borel, Pincherle, and other mathematicians, the inverse transformation T^{-1}, leading from $T\phi$ (*i. e.*, our $I(x)$) to ϕ, which would at once solve the X-ray problem, is far from being known in a convenient, nay in any form.

It so happens, however, that most and possibly all of the observed filtration curves (with either Al or Cu as filter) available at the present time can be represented, generally with a fair and in some cases with great accuracy, by an empirical formula which the writer constructed in 1931 upon the data for Metalix and Media radiations (with Al-filter), mentioned before, and for a set of radiations (with Cu as filter) investigated by L. S. Taylor ('Radiology,' xvi. March 1931), for the practical use in these laboratories, namely, by the two-parametric formula

$$\log I(x)=-Ax-B\sqrt{x} \quad . \quad . \quad . \quad . \quad (9')$$

or

$$I(x)=e^{-Ax-B\sqrt{x}}, \quad . \quad . \quad . \quad . \quad . \quad (9)$$

where A, B are constant coefficients whose numerical values vary from tube to tube and depend upon the applied voltage. Thus, *e. g.*, the Al-filtration data for the Metalix tube, obtained by Neeff, are well represented by (9) with

$$A=0 \quad \text{and} \quad B=2{\cdot}68,\ 2{\cdot}37,\ 2{\cdot}03,\ 1{\cdot}64\ \text{mm.}^{-1/2};$$

for the potentials

$$V=30,\ 50,\ 70,\ 100\ \text{kv.}$$

* It is generally known as the *Laplace transformation*. In our case $T\phi$ is the given function $I(x)$.

respectively, and those for the tube Media by the same formula with the coefficients

	$A=0{\cdot}320,$	$0{\cdot}212,$	$0{\cdot}092,$
	$B=1{\cdot}19,$	$0{\cdot}97_2,$	$0{\cdot}89_6,$
for	$V=50,$	$70,$	100 kv.,

and somewhat less closely, but still satisfactorily, with $A=-0{\cdot}014$, $B=2{\cdot}05$ at the potential 30 kv. It seems very likely that the filtration curves of all radiation samples emitted by the usual X-ray tubes can be represented with sufficient accuracy by the formula (9), and some even, as, *e. g.*, those for Metalix and for a great number of filtration curves obtained more recently by Dr. H. T. Meyer (*Strahlentherapie*, xxxviii. p. 329, 1930) for a therapeutic AEG tube of type T III., by its reduced form $I(x)=e^{-B\sqrt{x}}$, *i. e.*, with $A=0$.

With the form (9) of the function $I(x)$ our integral equation (8) becomes

$$\int_0^\infty e^{-x\mu}\phi(\mu)d\mu=e^{-Ax-B\sqrt{x}}. \quad . \quad . \quad . \quad (10)$$

Now, having exchanged several letters with Prof. Harry Batemann (Pasadena), first about the general integral equation (8) and then about its sub-case (10), which practically covers the whole field of interest, I have learned from him that a rigorous solution of the latter equation can be immediately derived from a certain integral evaluated by Laplace.

This integral, itself perhaps not widely known, may be derived here as follows. Start from the well-known result

$$\int_0^\infty e^{-z^2}dz=\tfrac{1}{2}\sqrt{\pi}.$$

Substitute

$$z=u-\frac{p}{u}, \qquad dz=du+\frac{pdu}{u^2}$$

(where $p=$ const.); then

$$\tfrac{1}{2}\sqrt{\pi}=\int_{\sqrt{p}}^\infty e^{-(u-p/u)^2}du+p\int_{\sqrt{p}}^\infty e^{-(u-p/u)^2}\frac{du}{u^2}.$$

Now the second integral is, with $p/u=s$,

$$-\int_{\sqrt{p}}^0 e^{-\left(\frac{p}{s}-s\right)^2}ds=\int_0^{\sqrt{p}} e^{-\left(\frac{p}{s}-s\right)^2}ds=\int_0^{\sqrt{p}} e^{-\left(\frac{p}{u}-u\right)^2}du,$$

and therefore

$$\tfrac{1}{2}\sqrt{\pi}=\int_0^\infty e^{-(u-p/u)^2}du=e^{2p}\int_0^\infty e^{-u^2-p^2/u^2}du.$$

Here write pq instead of p, so that

$$\frac{1}{2}\frac{\sqrt{\pi}}{q}e^{-2pq}=-\int_0^\infty e^{-\left(q^2\frac{2u^2}{q^2}+\frac{p^2}{u^2/q^2}\right)}\frac{du}{q};$$

and finally, with u/q replaced throughout by u,

$$\int_0^\infty e^{-\frac{p^2}{u^2}-q^2u^2}du=\frac{\sqrt{\pi}}{2q}e^{-2pq}. \quad . \quad . \quad . \quad (L)$$

This is the required *Laplace integral*, which is easily seen to contain the solution of our X-ray problem as reduced to the integral equation (10).

In fact, substitute

$$u=\frac{1}{\sqrt{\mu-A}}, \qquad p^2=x, \qquad q^2=\tfrac{1}{4}B^2. \quad . \quad (11)$$

Then $du=-\frac{1}{2}\frac{d\mu}{(\mu-A)^{3/2}}$ and to $u=0$, $u=\infty$ will correspond $\mu=\infty$ and $\mu=A$ respectively, so that (L) will become

$$-\int_\infty^A e^{-x(\mu-A)-B^2/4(\mu-A)}\frac{d\mu}{2(\mu-A)^{3/2}}=\frac{\sqrt{\pi}}{B}e^{-B\sqrt{x}}$$

or

$$\int_A^\infty e^{-x\mu}\left\{\frac{B}{2\sqrt{\pi}}e^{-\frac{B^2}{4(\mu-A)}}.(\mu-A)^{-3/2}\right\}d\mu=e^{-Ax-B\sqrt{x}}.$$

A comparison of this result with (10) shows directly that our integral equation (10) is satisfied by

$$\left.\begin{aligned}&\phi(\mu)=0 \quad \text{for } \mu\leqq A,\\ &\phi(\mu)=\frac{B}{2\sqrt{\pi}}(\mu-A)^{-3/2}.e^{-B^2/4(\mu-A)} \quad \text{for } \mu\geqq A,\end{aligned}\right\}, \quad (12)$$

the two branches of this function $\phi(\mu)$ attaching themselves to each other continuously at $\mu=A$.

Thus (12) is *a solution* of the integral equation (10), and since it has been proved by Lerch (*Acta Mathematica*, xxvii. 1903) that the equation

$$\int_0^\infty e^{-x\mu}g(\mu)d\mu=0, \qquad x>0,$$

has no continuous solution differing from the trivial one, $g = const. = 0$, the function (12) is *the only* (*continuous*) *solution* of our problem.

It remains to pass from $\phi(\mu)$ to the specific intensity, or ordinate of the spectral curve, $I_\lambda = f(\lambda)$. The relation between these two functions is given by (3), so that

$$f(\lambda) = \phi(\mu)\mu' = \phi(\mu)\frac{d\mu}{d\lambda} \quad . \quad . \quad . \quad . \quad . \quad (13)$$

Ultimately, therefore, (12) *with* (13) *give the complete spectral curve of an X-ray sample whose filtration curve is of the form* (9), and which is thus characterized by the two coefficients A and B.

Let λ_A be the wave-length to which corresponds $\mu = A$. Then, by (13) and (12), the complete spectral curve is

$$\left.\begin{aligned} f(\lambda) &= 0, \qquad \text{for } \lambda \leqq \lambda_A, \\ f(\lambda) &= \frac{B}{2\sqrt{\pi}} \frac{e^{-B^2/4(\mu - A)}}{(\mu - A)^{3/2}} \frac{d\mu}{d\lambda}, \qquad \text{for } \lambda \geqq \lambda_A. \end{aligned}\right\} \quad (14)$$

(N.B.—If A is negative, μ is necessarily greater than A, being by its physical meaning essentially positive. In this case no real λ_A exists, and the second of (14) holds for all wave-lengths from $\lambda = 0$ onwards.)

The widely used cube-formula, $\mu = \alpha + \beta\lambda^3$, represents the absorption coefficient itself rather roughly, but it may be accurate enough for evaluating the derivative $d\mu/d\lambda$ appearing in (14). Thus, and setting $\alpha = 0$ (since we have already adopted the approximate equality $\mu_0 = 0$),

$$\frac{d\mu}{d\lambda} = 3\beta\lambda^2 = 3\beta^{1/3}\mu^{2/3}.$$

Hence, and after using the abbreviation

$$C = \frac{3\beta^{1/3}}{2\sqrt{\pi}} \quad . \quad . \quad . \quad . \quad . \quad . \quad (15)$$

for a constant factor which depends only on β, and therefore on the nature of *the filter* alone, the equation of the spectral curve becomes, for $\lambda \geqq \lambda_A$,

$$f(\lambda) = CB \frac{\mu^{2/3}}{(\mu - A)^{3/2}} e^{-\frac{B^2}{4(\mu - A)}}, \qquad \mu = \mu(\lambda), \qquad (16)$$

and $f(\lambda) = 0$ for $\lambda \leqq \lambda_A$. It will be kept in mind that the total intensity of the radiation has been here taken as unity, $\int_0^\infty f(\lambda)d\lambda = 1$. As to the absorption coefficient μ itself, it is

convenient and more accurate not to eliminate it once and for all by means of the cube-formula, but to leave it as it stands, and to substitute for it ultimately, in numerical results, the observed or closely interpolated values corresponding to any λ-value which is of interest. It will be kept in mind that $B\sqrt{x}$ is a pure number, so that B^2 is a reciprocal length. So also are μ and A, so that $B^2/(\mu-A)$ appearing in the exponential is a pure number, as it should be.

The general properties of the spectral curve (16) can be easily studied. The curve sets in with $f=0$ for $\mu=A$, *i. e.*, at the wave-length λ_A (provided that A is not negative). It is here tangential to the λ-axis; in fact, the derivative of f with respect to λ is, apart from the constant factor BC,

$$f'(\lambda)=\{\tfrac{2}{3}\mu^{-1/3}(\mu-A)^{-3/2}-\tfrac{3}{2}\mu^{2/3}(\mu-A)^{-5/2} + \frac{B^2}{4}\mu^{2/3}(\mu-A)^{-7/2}\}e^{-\frac{B^2}{4(\mu-A)}}\frac{du}{d\lambda},$$

and this vanishes for $\mu=A$, *i. e.*, for $\lambda=\lambda_A$.

This derivative vanishes once more, at a wave-length λ_m say, where $f(\lambda)$ attains a maximum. To evaluate λ_m, or the corresponding absorption coefficient μ_m of the filter, it is preferable to use the relation (13), which gives

$$f'(\lambda)=\phi(\mu)\mu''+\phi'(\mu)\mu'^2, \qquad \mu'=d\mu/d\lambda.$$

This vanishes for

$$\frac{\phi'(\mu)}{\phi(\mu)}=-\frac{\mu''}{\mu'^2}$$

or

$$\frac{d}{d\mu}\log\phi(\mu)=\frac{d}{d\lambda}\left(\frac{1}{\mu'}\right).$$

Thus, if we again assume $\mu=\beta\lambda^3$,

$$\frac{d}{d\mu}\log\phi(\mu)=-\frac{2}{3\mu},$$

i. e., after a simple computation based on (12),

$$\frac{3}{2}\frac{1}{\mu_m-A}-\frac{B^2}{4(\mu_m-A)^2}=\frac{2}{3\mu_m}$$

or

$$\mu_m^2-(\tfrac{1}{5}A+\tfrac{3}{10}B^2)\mu_m=\tfrac{4}{5}A^2, \quad . \quad . \quad . \quad (17)$$

a quadratic for μ_m. The root of this equation with negatively taken radical would manifestly give a negative absorption

coefficient μ_m, which is absurd. We are thus left with the unique solution

$$\mu_m = \tfrac{1}{10}\{A + \tfrac{3}{2}B^2 + \sqrt{(A + \tfrac{3}{2}B^2)^2 + 80A^2}\}. \quad . \quad (18)$$

It is not difficult to verify that this value of μ gives a genuine *maximum* of $f(\lambda)$, so that the corresponding wave-length λ_m marks the position of the peak of the spectral curve. This salient feature of the spectral curve is thus expressed directly in terms of the two coefficients A, B characterizing, through the filtration curve, the X-ray sample which was to be analyzed.

If, for instance, as in the case of the radiations from the Metalix tube, the coefficient A *vanishes*, so that the equation (9) of the filtration curve reduces to

$$I(x) = e^{-B\sqrt{x}}, \quad . \quad . \quad . \quad . \quad . \quad . \quad (9a)$$

then the equation of the corresponding spectral curve (16) becomes, from $\lambda = 0$ onwards, replacing the total emitted intensity $I(0) = I_0$,

$$f(\lambda) = I_0 CB\mu^{-5/6} e^{-\frac{B^2}{4\mu}}; \quad \mu = \mu(\lambda). \quad . \quad . \quad (16a)$$

It will be remembered that this, as also the more general form (16), is based on the assumption $\alpha = 0$, so that $\mu(0) = 0$. This spectral curve sets in at $\lambda = 0$, tangentially to the λ-axis. Rigorously such a situation would disagree somewhat with the known fact that the continuous X-ray spectrum ends rather abruptly at the quantum limit $\lambda_q = 12{\cdot}34/V$. Practically, however, there is scarcely a disagreement, for the initial ascent of our spectral curve (16 a) is so slow that, even at the potential $V = 100$ kv. (when $\lambda_q = 0{\cdot}12$ Å.) the ordinate $f(\lambda)$ for $\lambda = 0{\cdot}1$ bears to the maximum ordinate a ratio of the order of one-millionth, and can thus to all intents and purposes be neglected.

For greater λ the slope of the curve (16 a) increases rather rapidly, the curve soon becomes very steep, and by (18) reaches a *maximum* at a wave-length to which corresponds the absorption coefficient (of the filter)

$$\mu_m = \tfrac{3}{10}B^2. \quad . \quad . \quad . \quad . \quad . \quad . \quad (18a)$$

This is a very direct and simple relation between a prominent feature of the spectral curve (position of peak) of an X-ray sample and the unique coefficient B in its filtration curve $I(x) = e^{-B\sqrt{x}}$.

To give a practical application of the formulæ (18 a) and (16 a) let us consider the radiations emitted at various potentials by the *Metalix* tube. For the Al-filtration

curves of these radiations the coefficient A, as has already been mentioned, vanishes, and the coefficient B has, in mm.$^{-1/2}$, at the voltages 30, 50, 70, and 100 kv., the values 2·68, 2·37, 2·03, and 1·64—that is to say, in cm.$^{-1/2}$

$$B_{30}=8{\cdot}47, \quad B_{50}=7{\cdot}49, \quad B_{70}=6{\cdot}42, \quad B_{100}=5{\cdot}19,$$

decreasing throughout the set with increasing voltage (X-rays getting steadily "harder").

Thus, and since μ increases with λ, we see in the first place by formula (18a) that the peak of the spectral curve of the Metalix radiation is displaced with increasing potential towards shorter waves. According to this formula the maximum specific intensity $f(\lambda)$ in these four radiation samples occurs at the wave-lengths corresponding respectively to the following values of the absorption coefficient of aluminium :—

$$\mu_m=21{\cdot}55, \quad 16{\cdot}85, \quad 12{\cdot}36, \text{ and } 8{\cdot}07 \text{ cm.}^{-1},$$

i. e. (by a sufficiently accurate interpolation from the table of observed μ-values given in Compton's book on 'X-rays and Electrons'), at the wave-lengths

$$\lambda_m=0{\cdot}816, \quad 0{\cdot}755, \quad 0{\cdot}676, \text{ and } 0{\cdot}590 \text{ Å.},$$

for $V=30$, 50, 70, and 100 kv.

Incidentally we may note that these $\lambda_{max.}$ are nearly enough represented by a linear function of V, namely, by $\lambda_m=0{\cdot}910-0{\cdot}00326\,V$, where V is taken in kilovolts.

The knowledge of the values of the coefficient B for Metalix enables us to construct at once, by (16a), the complete spectral curve for each of the four X-ray samples emitted by this tube. In fact, that formula contains, apart from the variable μ, only the coefficients B and C. The numerical value of the latter, which is a factor common to all ordinates $f(\lambda)$ and to all curves, corresponding to different potentials, is immaterial so far as the relative specific intensities (or relative "ordinates") are concerned; but if one wishes to read from the area of the f, λ-graph under any part of the spectral curve the fraction of the total intensity contained within the corresponding wave-length interval, one has to evaluate numerically the coefficient C, *i. e.*, by (15), $\frac{3}{2\sqrt{\pi}}\beta^{1\cdot3}$. Now for aluminium the values of β or $\Delta\mu:\Delta(\lambda^3)$, derived from the pairs of observed μ-values for $\lambda=0{\cdot}3$, $0{\cdot}4$, and for $\lambda=0{\cdot}4$, $0{\cdot}5$, are

$$37{\cdot}9 \text{ and } 38{\cdot}1 \text{ cm.}^{-1}/(\text{Å.})^3$$

respectively. Thus, taking

$$\beta = 38 \text{ cm.}^{-1}(\text{Å.})^{-3} = 38 \cdot 10^{24} \text{ cm.}^{-4},$$

we have

$$C = \frac{3}{2\sqrt{\pi}} \beta^{1/3} = 2 \cdot 845 \cdot 10^8 \text{ cm.}^{-4/3}. \quad . \quad . \quad (19)$$

If this value, as it stands, be substituted in (16*a*), $f(\lambda)d\lambda$ will correctly express the intensity contained between λ and $\lambda + d\lambda$, giving $\int_0^\infty f(\lambda)d\lambda = 1$, provided λ is expressed in centimetres. If λ is taken in Ångströms while μ is still expressed in reciprocal centimetres the factor 10^8 has to be dropped. With this understanding, then, the equation (16*a*) becomes

$$f(\lambda) = 2 \cdot 845 \, I_0 B \mu^{-5/6} e^{-B^2/4\mu}. \quad . \quad . \quad (16b)$$

The total intensities I_0 of the X-rays emitted by Metalix at $V = 30$, 50, 70, 100 kv., as given by Neeff, in arbitrary units, are 2·29, 5·70, 10·20, 16·75, or if the intensity for $V = 100$ kv. is taken as unity,

$$I_0 = 0 \cdot 137, \quad 0 \cdot 340, \quad 0 \cdot 609, \quad 1 \cdot 000$$

respectively. Thus, and with the values of B_{30} etc., B_{100} quoted a moment ago, the last formula gives ultimately the following equations for the spectral curves of the radiations emitted by the Metalix tube at the four different potentials:—

$$f(\lambda) = 3 \cdot 30 \mu^{-5/6} . 10^{-7 \cdot 80/\mu} \quad (30 \text{ kv.}),$$

$$f(\lambda) = 7 \cdot 25 \mu^{-5/6} . 10^{-6 \cdot 09/\mu} \quad (50 \text{ kv.}),$$

$$f(\lambda) = 11 \cdot 12 \mu^{-5/6} . 10^{-4 \cdot 47/\mu} \quad (70 \text{ kv.}),$$

$$f(\lambda) = 14 \cdot 75 \mu^{-5/6} . 10^{-2 \cdot 92/\mu} \quad (100 \text{ kv.}).$$

Each of these equations holds for all wave-lengths, from $\lambda = 0$ onward, and, as said before, $\mu = \mu(\lambda)$ is the absorption coefficient of aluminium in cm.$^{-1}$.

The four spectral curves represented by these equations are drawn in fig. 1, with λ as abscissa and $f(\lambda)$ as ordinate, the ratios of the ordinates of the several curves, corresponding to any given wave-length, are correctly represented, from the lowest curve, corresponding to a potential of 30 kv. up to the highest, for 100 kv. Thus the area under any portion of any one of these curves gives directly the correct fraction of the total radiant intensity contained within the corresponding λ-interval.

Let us now return to the more general equation (16) of the spectral curve corresponding to a filtration curve in which both the coefficients, A and B, assert themselves. Re-instating the total emitted intensity $I_0 = \int_0^\infty f(\lambda)d\lambda$ as factor, and using for Al the value (19) of the coefficient C, we now have the required spectral-curve equation

$$f(\lambda) = 2{\cdot}85 I_0 B \mu^{2/3} (\mu - A)^{-3/2} e^{-\frac{B^2}{4(\mu - A)}}, \quad . \quad (20)$$

Fig. 1.

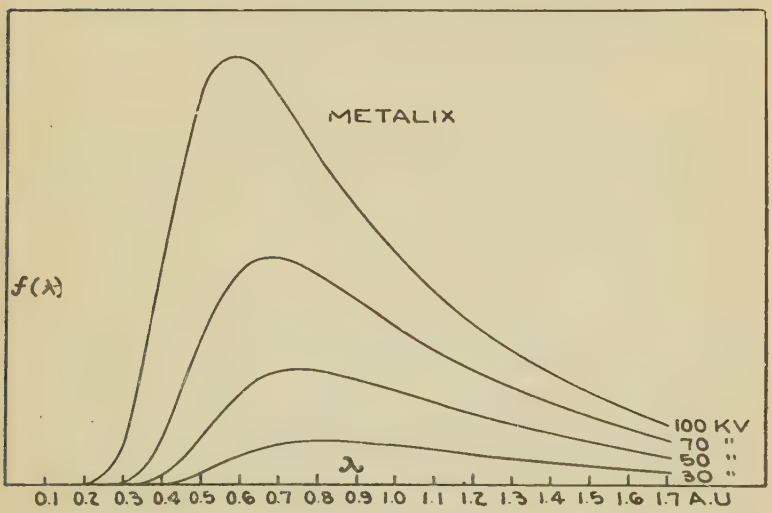

valid for $\mu \geqq A$, and $f(\lambda) = 0$ for $0 \leqq \mu \leqq A$. Here μ is to be taken in reciprocal centimetres and λ in Å. The values of I_0, A, and B being known for a sample of X-rays whose filtration curve is of the form (9), the equation (20) gives the complete *spectral curve* of that radiation sample. The position of the *maximum* ordinate of this spectral curve is determined by the value (18) of μ_m, expressed in terms of A and B alone.

For the sake of illustration let us consider the three samples of radiation emitted by the tube *Media* at $V = 50$, 70, and 100 kv.

These radiations, when filtered through aluminium, show a behaviour which is very closely represented by the

formula (9) with the following values of the coefficients A, B:—

	V.	A.	B.
(*Media*)	50 kv.	3·20 cm.$^{-1}$	3·76 cm.$^{-1/2}$
	70	2·12	3·07
	100	0·92	2·83

(21)

It will be enough to compute and to draw the spectral curve (20) only for one of these X-ray samples, say of that for $V=100$ kv., and to give the initial points (λ_A) and the positions of the peaks (λ_m) for all three samples.

By (20), with $I_0=1$, and by the last line of (21), the equation of the spectral curve for $V=100$ kv. is

$$f(\lambda)=8{\cdot}07\mu^{2/3}(\mu-0{\cdot}92)^{-3/2}e^{-\frac{2{\cdot}003}{\mu-0{\cdot}92}}, \quad . \quad (20\,a)$$

valid for $\mu\geqq 0{\cdot}92$, and $f(\lambda)=0$ for $\mu\leqq 0{\cdot}92$. The wave-length to which corresponds the absorption coefficient $\mu=A=0{\cdot}92$ (*i. e.*, with the density of aluminium $\rho=2{\cdot}70$, the mass-absorption coefficient $A/\rho=0{\cdot}341$) is

$$\lambda_A=0{\cdot}230\ \text{Å}.$$

(It may be mentioned here that the quantum limit is $\lambda_q=0{\cdot}123$ Å.) For $\lambda=0{\cdot}250$ the absorption coefficient is very nearly $\mu=1$ (namely, $0{\cdot}370\times 2{\cdot}70$), so that, by the formula (20 a), $f(\lambda)=4{\cdot}8.10^{-9}$, which is practically evanescent in comparison with $f_{\text{max.}}$, amounting to over two whole units. For $\lambda=0{\cdot}300$ we have $\mu=1{\cdot}434$ and, by (20 a), $f(\lambda)=0{\cdot}567$, which already is a considerable value. Further, $f(0{\cdot}350)=1{\cdot}83$, while by (18), with $A=0{\cdot}92$, $B=2{\cdot}83$ as in (21), the maximum intensity is reached for

$$\mu=\mu_m=2{\cdot}831\ \text{cm}^{-1}, \text{ or } \mu/\rho=1{\cdot}05,$$

which corresponds to the wave-length

$$\lambda_m=0{\cdot}400.$$

The value of this maximum is, by (20 a),

$$f(\lambda_m)=2{\cdot}14.$$

Beyond this peak the curve descends rather slowly. Thus, *e.g.*, $f(0{\cdot}500)=1{\cdot}72$, $f(0{\cdot}600)=1{\cdot}23$, and so on. A graphical representation of a sufficient branch of the spectral function (20 a) is given in figure 2. So far the analysis of the X-rays emitted by Media at 100 kv.

The positions of the maxima (λ_m) and of the starting-points (λ_A) of the spectral curves of the three samples of radiation emitted by Media are collected in the following table :—

$V=50$,	70,	100 kv.
$\mu_m=6{\cdot}207$,	$4{\cdot}131$,	$2{\cdot}831$ cm^{-1}.
$\lambda_m=0{\cdot}540$,	$0{\cdot}463$,	$0{\cdot}400$ Å.
$\lambda_A=0{\cdot}417$,	$0{\cdot}353$,	0 230 Å.

There is thus a steady and marked shifting of the starting-point and of the peak of the spectral curve, with increasing potential, towards smaller wave-lengths.

These numerical details ought to give a sufficient idea of the spectral intensity distribution in the contemplated X-ray

Fig. 2.

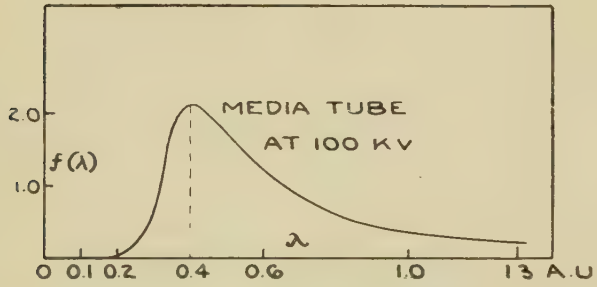

samples and to serve as a good illustration of the proposed method of spectral analysis of such radiations.

Supplement.

Effect of non-vanishing μ_0.—In what precedes we have assumed, for the sake of simplicity, that μ_0, *i. e.*, μ for $\lambda=0$, is evanescent. Some reason for this assumption is, no doubt, afforded by the circumstance that, *e. g.*, for aluminium the mass-absorption coefficient for $\lambda=0{\cdot}017$ Å. (as given in Compton's book already quoted) is as low as $\mu/\rho=0{\cdot}058$, and therefore $\mu=0{\cdot}157$, almost five times smaller than for $\lambda=0{\cdot}2$, while the interval of principal interest extends from $0{\cdot}2$ onwards.

Yet, as there is no serious difficulty in taking account of the possibly non-vanishing value of μ_0, the more general solution of the problem in hand may be supplied here.

If μ_0 is not disregarded, the original integral equation $\int_0^\infty e^{-x\mu} f(\lambda) d\lambda = I(x)$ becomes

$$\int_{\mu_0}^\infty e^{-x\mu} \phi(\mu) d\mu = I(x),$$

where, as before, $f(\lambda) = \phi(\mu) d\mu/d\lambda$, or writing $\mu' = \mu - \mu_0$,

$$\int_0^\infty e^{-x\mu'} \phi(\mu' + \mu_0) d\mu' = e^{x\mu_0} I(x).$$

Here the right-hand member is still a given function of x alone.

Thus, if again

$$I(x) = I_0 e^{-Ax - B\sqrt{x}},$$

the integral equation becomes

$$\int_0^\infty e^{-x\mu'} \phi(\mu' + \mu_0) d\mu' = I_0 \cdot e^{-(A-\mu_0)x - B\sqrt{x}},$$

and in much the same way as before its solution is found to be

$$\phi(\mu' + \mu_0) = \phi(\mu) = \frac{I_0 B}{2\sqrt{\pi}} [\mu' - (A - \mu_0)]^{-3/2} e^{-\frac{B^2}{4[\mu' - (A-\mu_0)]}}$$

for $\mu' \geqq A - \mu_0$, *i. e.*,

$$\phi(\mu) = \frac{I_0 B}{2\sqrt{\pi}} (\mu - A)^{-3/2} e^{-\frac{B^2}{4(\mu - A)}} \quad \text{for } \mu \geqq A,$$

and $$\phi(\mu) = 0 \text{ for } \mu \leqq A,$$

exactly as with $\mu_0 = 0$. Only $f(\lambda)$ will be modified, through $d\mu/d\lambda$. We shall now have

$$\mu = \mu_0 + \beta\lambda^3,$$

whence

$$\frac{d\mu}{d\lambda} = 3\beta\lambda^2 = 3\beta^{1/3}(\mu - \mu_0)^{2/3},$$

so that ultimately the equation of the spectral curve will become

$$f(\lambda) = CI_0 B \cdot (\mu - A)^{-3/2} (\mu - \mu_0)^{2/3} e^{-\frac{B^2}{4(\mu - A)}}, \qquad \mu \geqq A$$

(and $f(\lambda) = 0$ for $\mu \leqq A$), where C has its previous meaning.

Rochester, N.Y.
June 27, 1932.

XXXV. *The Electrical Conductivity of Aqueous Solutions of Sodium and Potassium Hydroxides and the Limiting Mobility of the Hydroxyl Ion at 25°.* *By* George Harold Jeffery, *B.Sc.(Lond.)*, *A.I.C.*, *and* Arthur Israel Vogel, *D.Sc.(Lond.)*, *D.I.C.*, *F.I.C.**.

NO trustworthy conductivity measurements extending to high dilutions of aqueous solutions of alkali hydroxides are available in the literature. The present research was undertaken to fill this gap and also in order to evaluate the limiting mobility of the hydroxyl ion.

Earlier work, most of which must be regarded as approximate, was carried out chiefly at 18°, and includes that of Ostwald (J. pr. Chem. xxxiii. p. 352, 1886; xxxv. p. 112, 1887), Bredig (*Z. physikal. Chem.* xiii. p. 289, 1894), Winkelblech (*ibid.* xxvi. p. 428, 1901), Foster (Physical Review, viii. p. 257, 1899), Loomis (*Ann. Physik.* lx. p. 547, 1897), Calvert (*Z. physikal. Chem.* xxxviii. p.530, 1901), Jones (Am. Chem. J. xxvi. p. 428, 1901), Bousfield and Lowry (Phil. Trans. cciv. p. 292, 1905), Noyes (Publ. Carnegie Inst. no. 63, p. 262, 1907), Heydweiller (*Ann. Physik.* xlviii. p. 681, 1915), Frary and Nietz (J. Amer. Chem. Soc. xxxvii. p. 2263, 1915), and Raikes, Yorke, and Ewart (J. Chem. Soc. p. 630, 1926). Randall and Scalione (J. Amer. Chem. Soc. xlix. p. 1486, 1927), have carried out measurements with the alkali hydroxides at 25° with equilibrium water in a Jena glass conductivity cell, but make no reference to the very important water correction, and it would seem that their figures are uncorrected for solvent conductivity.

The water correction for strong bases has been discussed by several authors (Kendall, J. Amer. Chem. Soc. xxxviii. pp. 1480, 2460, 1916; Washburn, *ibid.* xl. p. 190, 1918; Wynne-Jones, J. Phys. Chem. xxxi. p. 1647, 1927), but apart from a general agreement that it is relatively large and positive the quantitative aspect has been omitted. The exact mode of application of the water correction on the assumption that the only impurity is carbonic acid has been considered by Remy (*Z. Elektrochem.* xxxi. p. 88, 1925), Laue (*Z. anorgan. Chem.*

* Communicated by the Authors.

clxv. p. 305, 1927), and by Kolthoff (Rec. trav. chim. xlviii. p. 664, 1929). Kolhoff's method forms the basis of that used in the present paper owing to its simplicity and comparatively few assumptions.

New determinations have been made of the conductivities at 25° of sodium and potassium hydroxides in Pyrex cells of the Hartley and Barrett type (J. Chem Soc. ciii. p. 789, 1913) *. Two distinct methods of preparation for the stock solutions of each alkali hydroxide (see Experimental) have been employed. The results are indicated in figs. 1 and 2. Briefly the correction for solvent conductivity consisted in calculating the total concentration of the carbonic acid from the specific conductivity of the water used, and then computing its influence on the specific conductivity of the alkali hydroxide solution; the results thus obtained are designated "corrected." It will be observed that the "uncorrected" results pass through a maximum at about 0·0005 N and that the maximum disappears after the application of the water correction. The experimental figures of Randall and Scalione (*loc. cit.*) are also indicated.

Evidence in support of the view that carbonic acid is the main impurity in conductivity water has been obtained by carrying out two runs for sodium hydroxide, prepared by the electrolysis method, with two grades of water differing considerably in conductivity, viz., with specific conductivities of 0·465 (obtained by using equilibrium water in the boiler, Vogel and Jeffery, J. Chem. Soc. p. 1204, 1931) and 1·13 gemmho respectively. The results are collected in Table I., in which is appended for purposes of comparison, the corresponding conductivites, Λ_c interp., interpolated from the conductivity concentration curve obtained with equilibrium water. They are also indicated in fig. 1. Above 0·0005 N the agreement is satisfactory, and hence only the results above this concentration have been employed for extrapolation purposes. Similar evidence has previously been obtained by Wynne-Jones (J. Chem. Soc. p. 630, 1926),

* Independent experiments showed that the change in conductivity of the most concentrated solutions (0·008—0·01 N) did not exceed 0·1 per cent. when left in the Pyrex conductivity cell for 14 hours, a period very much in excess of the time taken for a complete series of measurements.

Fig. 1.

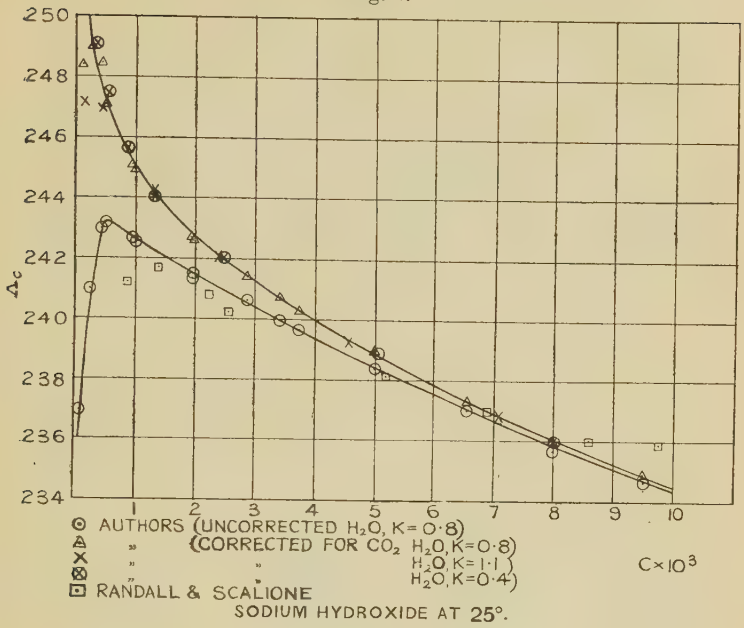
250
248
246
244
242
240
238
236
234
Λ_c
1 2 3 4 5 6 7 8 9 10
AUTHORS (UNCORRECTED H_2O, K= 0·8)
" (CORRECTED FOR CO_2 H_2O, K=0·8)
" " H_2O, K= 1·1)
" " H_2O, K=0·4)
RANDALL & SCALIONE
C×10³
SODIUM HYDROXIDE AT 25°.

Fig. 2.

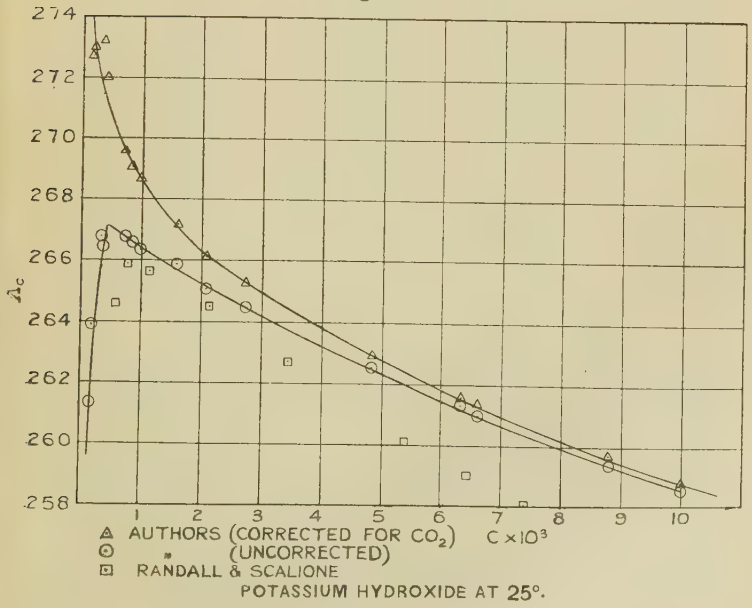
274
272
270
268
266
264
262
260
258
Λ_c
1 2 3 4 5 6 7 8 9 10
AUTHORS (CORRECTED FOR CO_2)
" (UNCORRECTED)
RANDALL & SCALIONE
C×10³
POTASSIUM HYDROXIDE AT 25°.

who found that by applying a correction based on the assumption that the conductivity of the water was due to carbon dioxide (no details are given), to Raike, Yorke, and Ewart's results (*loc. cit.*) for a run on sodium hydroxide at 18° with water of 0·599 gemmho purity, the resulting figures were in close agreement with those obtained with ultra-pure conductivity water (ca. 0·08–0·09 gemmho).

The conductivity at infinite dilution for the present authors' "corrected" results above 0·0005 N has been determined by means of the formula

$$\Lambda_0^n = \Lambda + BC^n,$$

Table I.

NaOH. $C \times 10^4$.	Run 3. Λ_c obs.	Cell V. Λ_c corr.	$\kappa = 1{\cdot}13$ gemmho. Λ_c interp.
1·462	216·1	247·2	250·0
4·624	237·2	247·0	247·2
8·606	239·92	245·48	245·42
12·56	240·34	244·21	244·26
24·27	239·92	242·03	242·02
45·70	238·16	239·25	239·27
71·06	236·08	236·81	236·82
	Run 4.	Cell S.	$\kappa = 0{\cdot}465$ gemmho.
3·306	246·9	249·0	248·1
5·462	245·7	246·5	246·8
8·686	244·52	245·61	245·41
13·00	243·24	244·01	244·11
25·10	241·65	242·05	241·93
50·80	238·70	238·85	238·78
79·66	235·86	235·98	236·06

the method of Ferguson and Vogel (this Journal, l. p. 971, 1925) as modified by us (J. Chem. Soc. p. 405, 1932) being employed. We find :—

for NaOH $\Lambda_0^n = \Lambda_c + 58{\cdot}00\ C^{0{\cdot}180}$ leading to $\Lambda_0^n = 216{\cdot}51$;
for KOH $\Lambda_0^n = \Lambda_c + 57{\cdot}80\ C^{0{\cdot}178}$ leading to $\Lambda_0^n = 285{\cdot}46$

Both equations hold over the range 5 to 40–50 $\times 10^{-4}$ N. The very low values of "n" are noteworthy. Extra-

polation has also been carried out by the square root formula

$$\Lambda_0^s = \Lambda_c + x\mathrm{C}^{0\cdot5},$$

with the following results :

NaOH $\Lambda_0^s = \Lambda_c + 177\cdot7\ \mathrm{C}^{0\cdot5}$ leading to $\Lambda_0^s = 250\cdot8$;
KOH $\Lambda_0^s = \Lambda_c + 178\cdot4\ \mathrm{C}^{0\cdot5}$ leading to $\Lambda_0^s = 274\cdot4$.

The corresponding values of x calc., computed from the Debye-Hückel-Onsager equation (compare Jeffery and Vogel, J. Chem. Soc. p. 405, 1932) and of $\Delta = 100$ (x obs.$-x$ calc.)/x calc. are 117·1, + 51·2 and 122·4, +45·8 respectively. These very large deviations from the complete dissociation theory, coupled with the limited range of validity of this formula (see Experimental) render this method of extrapolation of little value in the present instance. Raikes, Yorke, and Ewart (J. Chem. Soc. p. 630, 1926) used the square root formula over the range N/100 to N/30, which is almost completely outside the range of its legitimate applicability. Randall and Scalione (*loc. cit.*) employed the approximate method of Randall (J. Amer. Chem. Soc. xxxviii. p. 788, 1916) for extrapolation ; in view of their use of the data of Parker (*ibid.* xlv. p. 2017, 1923) and of Bray and Hunt (*ibid.* xxxiii. p. 781, 1911), which have been shown to be appreciably in error (Jeffery and Vogel, J. Chem. Soc. p. 403, 1932), too much significance cannot be attached to their computations which led to values of Λ_0 of 243·9 and 266·8 for sodium and potassium hydroxides respectively at 25°.

The most probable value for the limiting kation transport number of potassium chloride at 25°, deduced from the results of MacInnes and Dole (J. Amer. Chem. Soc. liii. p. 1357, 1931) and of Longsworth (*ibid.* liv. p. 2741, 1932) is 0·490. The limiting mobilities of the sodium and potassium ions based on this transport number are 49·8 and 73·4 respectively (Jeffery and Vogel, J. Chem. Soc. p. 1722, 1931), and hence the limiting mobility of the hydroxyl ion at 25° is $261\cdot5 - 49\cdot8 = 211\cdot7$ as deduced from our sodium hydroxide measurements, and $285\cdot5 - 73\cdot4 = 212\cdot1$ as deduced from the potassium hydroxide determinations. This gives a mean value of 211·9 with a maximum variation from the mean of $\pm$ 0·1 per cent.

Experimental.

Conductivity Water.—This was prepared as described by Vogel and Jeffery (J. Chem. Soc. p. 1201, 1931).

Preparation of Materials and Solutions.

Sodium Hydroxide. Specimen 1.—Cornog's method (J. Amer. Chem. Soc. xliii. p. 2573, 1921) was modified as follows : a portion was cut from the middle of a large block of Kahlbaum's purest sodium and placed under pure sodium dried xylene. A piece weighing about 0·5 gram was cut from the middle of this, the cutting and the weighing operations being performed under the xylene. The sodium—no attempt was made to remove the adhering xylene—was dropped in small pieces into a large Pyrex weighing bottle containing equilibrium water saturated with ether and also covered with a layer about 2 cm. deep of the same freshly distilled A. R. ether (the latter precaution is essential if stable colourless solutions are to be obtained). The sodium always retained its bright surface. When all the sodium had reacted the aqueous layer was transferred by means of a Pyrex glass siphon into a clean Pyrex weighing bottle, and the dissolved ether removed by boiling on an electric hot plate. A soda-lime guard tube was attached whilst the liquid was cooling down. This stock solution was analysed by titration against approximately N/20 hydrochloric acid with phenol phthalein as indicator. The hydrochloric acid was estimated by titrating with baryta solution which had been standardized against pure potassium hydrogen phthalate. Independent analyses agreed to within 0·1 per cent. Carefully calibrated pipettes and burettes were used throughout.

Specimen 2.—This was prepared from Kahlbaum's purest sodium chloride by electrolysis (see Britton, 'Hydrogen Ions,' p. 190, 1929). A 2 cm. layer of purified redistilled mercury was carefully covered with about 100 c.c. of a saturated solution of sodium chloride in conductivity water in a 250 c.c. pear-shaped separating funnel. The electrodes consisted of two Pyrex tubes containing sealed-in platinum wires, one of which was completely immersed in the mercury (kathode) whilst the other dipped into the solution (anode). A current

of 0·5 amp. from a series of accumulators was passed for about 45 minutes, the mercury layer was then cautiously run off through the very short funnel stem into about 100 c.c. of equilibrium water in a Pyrex weighing bottle. Interaction between the sodium amalgam and the water was allowed to proceed for 12 hours, ingress of carbon dioxide being prevented by a soda-lime guard tube. The aqueous solution was then decanted into another Pyrex weighing bottle. This formed a new stock solution, and its strength was estimated as above.

Potassium Hydroxide. Specimen 1.—Prepared from Kahlbaum's purest potassium chloride by the electrolysis method.

Specimen 2.—Prepared from Kahlbaum's purest potassium, which was "free from sodium, lithium, cæsium, rubidium and all heavy metals . . . it is practically 100 per cent. pure potassium" (Kahlbaum's report) by the ether method.

The stock solutions were prepared the evening before the actual run was carried out, so that the time of standing in contact with Pyrex glass was reduced to a minimum.

Measurement of Conductivity.—The technique was similar to that previously described (Jeffrey and Vogel, J. Chem. Soc. p. 1723, 1931). Successive additions of weighed amounts of stock solution were made from a Pyrex weight pipette to a known weight of conductivity water in a Hartley cell, immersed in an electrically controlled thermostat at $25 \pm 0{\cdot}01°$ C., a current of carbon dioxide free air being passed through the cell during the addition, and the resistance was determined after each addition. The Pyrex Hartley cells S and V (J. Chem. Soc. p. 1724, 1931) were employed for the runs and a small Kohlrausch cell for the conductivity water which was outside the range of the other cells. The cell constants were : S, $0{\cdot}03422_8$; V, $0{\cdot}002781_5$, and the Kohlrausch cell, 0·2390. These were frequently determined during the course of the work by the authors' method (J. Chem. Soc. p. 1719, 1931), but no appreciable variation could be detected. A determination by Parker and Parker's method (J. Amer. Chem. Soc. xlvi. p. 312, 1924) with 0·01 N potassium chloride prepared with equilibrium water gave values agreeing within 0·05 per cent.

Solvent Correction.—This involves two series of calculations: (*a*) computation of the *total* concentration of carbon dioxide, assuming that this is the only impurity, from the specific conductivity of the water employed (compare Laue, *Z. anorg. Chem.* clxv. p. 305, 1927), and (*b*) determination of the extent of its interaction with the alkali hydroxide (compare Kolthoff, Rec. trav. chim. xlviii. p. 664, 1929).

(*a*). For carbonic acid, we have

$$K_1 = \frac{[H^+]\,[HCO_3^-]}{[H_2CO_3 + CO_2]} \quad . \quad . \quad . \quad . \quad . \quad (1)$$

$$K_2 = \frac{[H^+]\,[CO_3^{--}]}{[HCO_3^-]} \quad . \quad . \quad . \quad . \quad . \quad (2)$$

where K_1 and K_2 are the classical primary and secondary dissociation constants respectively. Also let the ionic product of water

$$= K_w = [H^+]\,[OH^-] \quad . \quad . \quad . \quad . \quad (3)$$

Assume, in the first place, that $[CO_3^{--}]$ in conductivity water is so small that it may be neglected—it can readily be shown that the error thus introduced is negligibly small—and hence only the hydrogen and the hydrogen carbonate ions contribute to the conductivity.

If κ_w = specific conductivity of the water used, then

$$\kappa_w \times 1000 = \lambda H\,[H^+] + \lambda HCO_3\,[HCO_3^-],$$

where λH and λHCO_3 are the limiting mobilities of the hydrogen and hydrogen carbonate ions respectively.

Now

$$[H^+] = [HCO_3^-]$$

hence

$$[HCO_3^-] = [H^+] = \frac{\kappa_w \times 1000}{\lambda H + \lambda HCO_3} \quad . \quad . \quad . \quad . \quad (4)$$

From equation (1)

$$[H_2CO_3 + CO_2] = \frac{[HCO_3^-]^2}{K_1} = \frac{[H^+]^2}{K_1} \quad . \quad (5)$$

Hence total concentration of carbon dioxide, etc.

$$\Sigma CO_2 = [HCO_3^-] + [H_2CO_3 + CO_2],$$

which may be computed from equations (4) and (5).

The mobility of the bicarbonate ion was obtained by extrapolating to Λ_0 from Kendall's data for sodium bicarbonate (J. Amer. Chem. Soc. xxxviii. p. 1486, 1916) by the "n" formula. The results are expressed by the equation

$$\Lambda_0 = \Lambda_c + 186{\cdot}6\ C^{0{\cdot}624},$$

leading to $\Lambda_0 = 96{\cdot}7$ and hence

$$\lambda HCO_3 = 46{\cdot}9\ (\lambda Na = 49{\cdot}8).\lambda H$$

was taken as 348·0 (J. Chem. Soc. p. 1722, 1931). Kendall's value of $K_1 = 3{\cdot}50 \times 10^{-7}$ based on $\Lambda_0 = 393{\cdot}4$ was employed in all the calculations *.

(*b*) Let $\Sigma CO_2 = b$, and original concentration of base, BOH, expressed in molarities, $= a$, i. e., $\Sigma B = a$.

Assume ΣCO_2 reacts completely as carbonate: owing to hydrolysis of the carbonate ions, part is transferred

* The exact value for $\Lambda_0 = 348{\cdot}0 + 46{\cdot}9 = 394{\cdot}9$, and leads to the following values for K_1 with Kendall's experimental results (*loc. cit.*).

v.	Λ.	$K_1 \times 10^7$.
36·4	1·403	3·47
51·3	1·659	3·45
72·8	1·977	3·46
102·4	2·341	3·45
145·5	2·820	3·53
	Mean	3·47

The use of the more accurate figure has very little influence on the results.

into bicarbonate. The hydrolysis of the bicarbonate ion is small and may be neglected. We have

$$H_2CO_3 + 2BOH = B_2CO_3 + 2H_2O.$$

$$B_2CO_3 \rightleftharpoons 2B^+ + CO_3^{--}$$

$$CO_3^{--} + H_2O \rightleftharpoons HCO_3^- + OH^-.$$

It is further assumed that in dilute solutions the dissociation of the electrolyte is complete.

Then

$$[OH^-] = a - 2[CO_3^{--}] - [HCO_3^-]. \quad . \quad . \quad . \quad (6)$$

$$[CO_3^{--}] = b - [HCO_3^-] \quad . \quad . \quad . \quad . \quad . \quad . \quad . \quad (7)$$

From (6) and (7)

$$[OH^-] = a - 2b - [HCO_3^-].$$

Now

$$\frac{[OH^-]\,[HCO_3^-]}{[CO_3^{--}]} = \frac{[OH^-]\,[HCO_3^-]}{b - [HCO_3^-]} = \frac{K_w}{K_2} \quad . \quad . \quad (8)$$

Combining (7) and (8), one obtains

$$(a - 2b + [HCO_3^-]) = \frac{K_w}{K_2}(b - [HCO_3^-]), \quad . \quad . \quad (9)$$

or

$$[HCO_3^-]^2 + \left(a - 2b + \frac{K_w}{K_2}\right)[HCO_3^-] - \frac{K_w}{K_2}b = 0. \quad (10)$$

From the quadratic equation (10) $[HCO_3^-]$ may be calculated and thence $[CO_3^{--}]$ and $[OH^-]$ from equations (7) and (8) respectively.

If the specific conductivity actually measured is κ obs., then

$$1000\,\kappa \text{ obs.} = a\lambda B + [OH^-]\lambda OH + 2[CO_3^{--}]\lambda CO_3 + [HCO_3^{--}]\lambda HCO_3,$$

where λ OH etc. refer to the limiting mobilities of the respective ions. If the water contained no carbonic acid, the true specific conductivity of the solution, κ true, would be

$$1000\,\kappa \text{ true} = a(\lambda B + \lambda OH).$$

The correction $\Delta\kappa$ to be added to the observed value, κ obs., is therefore

$$1000\ \Delta\kappa = (a - [OH^-])\lambda OH - 2[CO_3^{--}]\lambda CO_3 - [HCO_3^-]\lambda HCO_3 \quad . \quad . \quad . \quad (11)$$

For the calculations $\lambda B = \lambda Na$ or $\lambda K = 49{\cdot}8$ or $73{\cdot}4$ respectively (J. p. 1722, 1931); λCO_3 assumed equal to $2\lambda HCO_3 = 93{\cdot}8$ (compare Vogel, J. Chem. Soc. p. 1485, 1929; Chandler, J. Amer. Chem. Soc. xxx. p. 694, 1908); $K_2 = 4{\cdot}1 \times 10^{-11}$ (mean result derived by Seyler and Lloyd, J. iii. p. 138, 1917, and Walker, Bray, and Johnston, J. Amer. Chem. Soc. xlix. p. 1246, 1927); and $K_w = 9{\cdot}9 \times 10^{-15}$ (Roberts, *ibid.* lii. p. 3877, 1930). The activity coefficients have in all cases been taken as unity. An approximate value for the limiting mobility of the hydroxyl ion was deduced by calculating Λ_o from the uncorrected results at concentrations above 0·0005 N. The results were

$$NaOH\ \Lambda_0 = \Lambda_c + 465{\cdot}9\ C^{0{\cdot}824} = 244{\cdot}3.$$

$$KOH\ \Lambda_0 = \Lambda_c + 417{\cdot}9\ C^{0{\cdot}809} = 268{\cdot}0,$$

giving a preliminary value for λOH of 194·5.

Calculation of the Concentrations.—All the concentrations are expressed g.-mols. per litre of solution and were computed as described in J. Chem. Soc. p. 1723, 1931.

Results.—The following tables give the experimental values of the equivalent conductivity, Λ_c obs., and also Λ_c corr., the same figures after application of the solvent correction, at the various concentrations C, expressed in g.-mols. per litre. The letters S and V refer to the Pyrex Hartley cell employed. The mean values of Λ_0^n, evaluated from the equation

$$\Lambda_0^n = \Lambda_c + BC^n,$$

the values of the constants of which are given, are included at the head of the tables. The corresponding figures for the square root relation $\Lambda_0^n = \Lambda_c + xC^{0{\cdot}5}$ are also given; Λ_c calc. was obtained by the use of these constants, and its difference from Λ_c obs. is shown in the column headed "Diff."; κ is the specific conductivity

of the water used expressed in gemmhos, and M is the molecular weight.

Sodium Hydroxide at 25°. (M=40·01.)

$\Lambda_0^n = \Lambda_c + 58{\cdot}00\ C.^{0{\cdot}180}$. $\Lambda_0^n = 261{\cdot}51$.

$\Lambda_0^s = \Lambda_c + 177{\cdot}7\ C.^{0{\cdot}5}$. $\Lambda_0^s = 250{\cdot}8$

Series.	κ.	$C \times 10^4$.	Λ_c obs.	Λ_c corr.	Δ_c calc. Diff.	Λ_0^n*.
1 (V) ...	0·793	0·945	236·9	248·4	—	—
First		4·462	243·0	248·5	—	—
specimen.		9·668	242·71	245·12	245·21 −0·09	261·65
		19·65	241·40	242·73	242·93 −0·20	261·57
		34·24	239·91	240·69	240·40 +0·29	261·51
		50·06	238·41	238·89	(238·38) + 0·51	261·29
		65·31	236·98	237·55	—	(260·45)
2 (S)	0·715	2·756	241·0	248·3	—	—
Second ..		5·295	243·20	248·52	(246·71) + 0·41	(261·98)
specimen.		9·901	242·62	245·00	245·21 − 0·21	261·65
		19·66	241·52	242·62	242·92 − 0·30	261·47
		28·68	240·61	241·39	241·29 + 0·10	261·56
		37·52	239·65	240·25	239·91 + 0·34	261·28
		80·11	235·70	235·99	—	(260·11)
		95·12	234·65	234·89	—	(259·87)
3 (V) ...	1·13	1·462	216·1	247·2	—	—
		4·624	237·2	247·0	—	—
		8·606	239·92	245·48	245·53 − 0·05	261·72
		12·56	240·34	244·21	244·50 − 0·29	261·69
		24·27	239·92	242·03	242·05 − 0·02	262·60
		45·70	238·16	239·25	(238·70) + 0·55	261·19
		71·06	236·08	236·81	—	(260·56)
4 (S)	0·465	3·306	246·9	249·0	—	—
		5·462	245·7	246·5	246·65 + 0·15	(262·47)
		8·686	244·52	245·61	245·56 + 0·15	261·87
		13·00	243·24	244·01	244·39 − 0·28	261·50
		50·80	238·70	238·85	—	261·20
		79·66	235·86	235·98	—	(260·22)

* The values in parenthesis were not employed in the calculations.

Potassium Hydroxide at 25°. (M=56·11.)

$\Lambda_0^n = \Lambda_c + 57{\cdot}80\ C^{0{\cdot}178}$. $\Lambda_0^n = 285{\cdot}46$

$\Lambda_c^s = \Lambda_c + 178{\cdot}4\ C^{0{\cdot}5}$. $\Lambda_0^s = 274{\cdot}4$

Series.	κ.	$C \times 10^4$.	Λ_c obs.	Λ_c corr.	Λ_c calc. Diff.	Λ_0^n *.
1 (S)	0·638	1·524	261·4	272·7	—	—
First		3·536	266·8	273·2	—	—
specimen.		7·297	266·80	269·61	269·58+0·03	285·59
		10·06	266·42	268·70	268·75 − 0·05	285·62
		21·15	265·10	266·16	266·20 − 0·04	285·46
		48·47	262·51	262·89	261·98 + 0·91	285·24
		63·44	261·30	261·58	—	(285·89)
		99·95	258·60	258·80	—	(284·20)
2 (V) ...	0·717	1·816	263·9	273·0	—	—
Second		3·513	266·50	272·02	—	—
specimen.		8·648	266·61	269·05	269·16 − 0·11	285·52
		16·10	265·90	267·24	267·25 − 0·01	285·54
		27·52	264·51	265·30	265·04 + 0·26	285·54
		65·59	261·02	261·35	259·96 + 1·36	(284·97)
		87·95	259·42	259·67	—	(284·56)

Δ_c at Round Concentrations.—The values of the equivalent conductivity at round concentrations are given below. Interpolation was carried out on a large scale Δ_c−C graph drawn with a flexible spline.

$C \times 10^4$.	NaOH.	KOH.
5·0	247·00	270·57
10·0	244·95	268·62
20·0	242·73	266·41
30·0	241·25	264·99
40·0	239·96	263·83
50·0	238·84	262·76
60·0	237·85	261·82
70·0	236·90	260·98
80·0	236·06	260·22
90·0	235·26	259·53
100·0	234·53	258·90

* The values in parenthesis were not employed in the calculations.

Note.—The use of the preliminary value $\lambda OH=194{\cdot}5$ instead of the more correct figure 211·8 in applying the solvent correction affects only the values at very low concentrations; the magnitude of the differences for all the runs is evident from the following table, which gives Λ_c corr. with $\lambda OH=194{\cdot}5$ and Λ_c' corr. with $\lambda OH=211{\cdot}8$.

Sodium Hydroxide.

$C\times10^4$.	Λ_c corr.	Λ_c' corr.
0·945	248·4	249·0
4·462	248·52	248·74
9·668	245·12	245·24
2·756	248·50	248·85
5·295	247·11	247·31
9·901	245·00	245·12

Potassium Hydroxide.

1·524	272·7	273·2
3·536	273·22	273·53
7·297	269·62	269·76
10·06	268·70	268·81
1·816	273·0	273·5
3·513	272·02	272·47
8·648	269·05	269·19

At higher concentrations there is no change. This does not affect the magnitudes of the constants in the "n" or the square root formula or the corresponding mean values of Λ_0. A slight change in the values of Λ^c at round concentration is necessary.

$C\times10^4$.	NaOH.	KOH.
5·0	247·19	270·77
10·0	245·05	268·70

The authors express their indebtedness to Imperial Chemical Industries, to the Royal Society (A. I. V.), and to the Chemical Society (G. H. J.) for grants which have helped to defray the cost of the research.

Woolwich Polytechnic, London, S.E. 18.
University College, Southampton.

XXXVI. *On the Propagation of a Lightning Discharge through the Atmosphere.* *By* E. C. Halliday, *M.Sc., Ph.D., Lecturer in Physics, University of the Witwatersrand* *.

[Plates IX.–XI.]

Introduction.

An electrical discharge through a gas occupies a measurable time for its propagation. The dielectric between the two charges which are being neutralized breaks down at some point, forming an ionized conducting path, and this break-down continues progressively through the dielectric until the two charges are joined by a conducting path, whereupon a flow of electricity neutralizes them. The manner in which this progressive break-down takes place has been discussed by G. C. Simpson [1], N. E. Dorsey [2], and others. The nature of a spark between spark-balls has been investigated photographically by a number of observers, the most interesting method of attack being that of E. O. Lawrence and F. G. Dunnington, who used a "Kerr" cell to determine the stage in the progress of the spark at which the photograph was to be taken [3]. A lightning flash takes place under rather different conditions from those which obtain in an experiment conducted in the laboratory. The discharge can hardly be counted as a discharge between electrodes for the cloud is not a conductor, and the electrode effects of negative brush and positive streamer need not necessarily take place at the cloud. Above the ground, and extending for some distance up towards the cloud, there is a space-charge due to point-discharge on a large scale from the surface of the earth (from tree-tops, telegraph poles, and other pointed conductors), under the influence of the field produced by the cloud [4]. This may very well produce, at some point between the ground and the cloud, a region of potential gradient higher than that observed at the ground-level. Such a result of point-discharge has been discussed by Schonland and Allibone, who have described experiments which show that one effect is to produce, in the flash, branching towards the positive instead of towards the negative charge [5]. Thus it is not a necessary hypothesis that the manner of propagation of a lightning flash is the same as that of a spark-discharge. In an experimental attack upon the problem the difficulty is encountered that the stage in the formation of

* Communicated by Dr. B. F. J. Schonland, Cape Town.

the flash at which observation is to be made cannot be selected as it can be in the laboratory. A method has been devised by C. V. Boys by which a record of the progress of a flash of lightning can be recorded, and he has published one such record [6], [7]. This paper describes the results of observations on lightning flashes made by the same method.

Experimental Method.

The apparatus devised by C. V. Boys for recording the progress of a lightning flash is briefly as follows. A pair of 6-inch focus lenses were mounted on a brass disk so as to be on a diameter of the disk, on opposite sides of and equidistant from the centre. The disk could be rotated by a geared crank in front of an 8×10-inch photographic plate at any speed up to 2400 r.p.m. The action of the apparatus is as follows. Assuming that the initial break-down of the dielectric occurs just under the base of the cloud and that thereafter it progresses towards the ground, and assuming that the rotating lenses at the commencement of the break-down are vertically above each other and rotating in a clockwise direction, a distortion of the resultant images takes place. In the upper image the starting-point continues luminous during the whole time of the propagation of the flash and is therefore carried to the right. The point where the flash ends is luminous for the shortest time and suffers no distortion. The resultant image consists of a sharp edge showing the outlines of the flash, but drawn into a blurred ribbon to the right-hand side, the broadest part of the ribbon being at the point where the flash commenced. In the lower image the opposite process takes place. Now, if we consider the sharp edges of the two images, we find that in the top image the part of the flash last to become luminous is carried to the right, while in the lower image it is carried to the left. Thus by the distortion of the images the direction of propagation can be deduced. In the case where the two lenses are in a horizontal line at the commencement of the flash a different distortion takes place. The left-hand image, produced by a lens moving upwards, will show the following effect. The upper point, where break-down commences, will be carried upwards a distance d. The lower point, where the flash ends, will be a distance d above the place it would have occupied if there had been no movement of the lens. As a result the length of the image is not altered, but the upper end of it shows a blurring owing to the motion. As for the right-hand image where the lens is moving downwards, the starting-point will be carried downwards a distance

d, while the lower point where the flash ends will be a distance *d* below the place where it would have been without lens movement. The starting-point leaves a trail of length *d* behind it, and thus the image has been lengthened by an amount *d* by the movement of the lens. In this case the direction of propagation is revealed by a difference in the lengths of the two images of the same flash. Where the left-hand image is shorter than the right-hand image direction of propagation is downwards, and where the opposite is true the direction is upwards.

Fig. 3.

During the winter of 1931, at the suggestion of Dr. B. F. J. Schonland, of the University of Cape Town, a camera with rotating lenses was constructed in the workshop of the Physics Department, University of the Witwatersrand (Pl. IX. fig. 1). A whole plate camera-body was mounted on a large baseboard. In front of it two brass uprights with bearings at their upper ends held a horizontal shaft directed normally at the centre of the focussing screen of the camera. A brass plate on the end of the shaft carried two 5 cm. focus lenses with iris stops giving a maximum aperture of f. 2·7, 3·7 cm. on each side of the centre of the

Fig. 5.

Flash II. A.

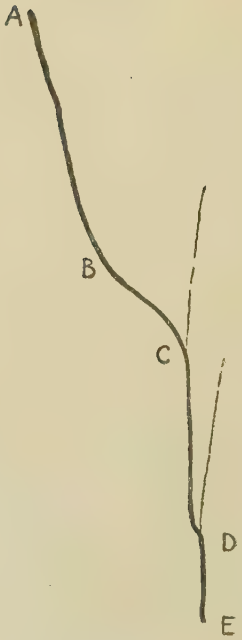

Flash II. B.

disk. The shaft was rotated by a small 220 volt electric motor, and speeds a little higher than 1500 r.p.m. could be attained. During the storm season of 1931–1932 attempts were made to secure photographs of lightning flashes, although not many storms suitable for photography occurred. On the 16th February three photographs were taken of flashes in a storm 16 kms. away. The photographs themselves are

Fig. 7.

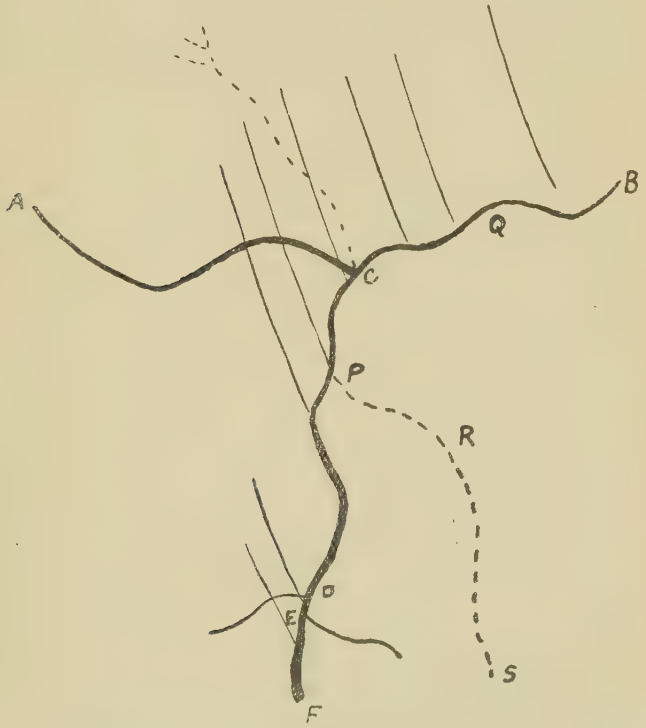

shown in figs. 2 and 4 (Pl. X.) and figs. 6 and 6 *a* (Pl. XI.), and explanatory diagrams of the left-hand image in each case are given in figs. 3, 5, and 7. The three flashes themselves will be referred to as I., II., and III. The rotation in each case is clockwise.

Results of Measurements.

On each of the three plates the photograph was taken with the lenses approximately in the horizontal line so that the method of measuring the change in length of the images could be employed.

Flash I., shown in fig. 2 (Pl. X.) and fig. 3, consists of three separate discharges, all taking place in an interval of less than ·01 sec. The top image of the last flash was obscured by one of the lens supports. The important images are those showing the first flash, and they are almost in a horizontal line. The images were measured with the micrometer microscope of the Yale University, through the kindness of Dr. Alden. Points of reference were chosen wherever a fork joined the main flash and where there were marked kinks in the flash. These points were marked A, B, C, D, E, F, G, H. Several sets of readings of the points of reference were made with the microscope travelling along

Table I. (see fig. 3).

Section of flash.	Observer.	Left-hand image.	Right-hand image.	L.H.I.–R.H.I.	Per cent. change of length.
		mm.	mm.	mm.	
A–B...	i.	1·38	1·20	+·18	+15
B–C...	i.	·35	·33	+·02	+ 6
A–C...	ii.	1·73	1·38	+·35	+25
C–D...	i.	·43	·38	+·05	+13
	ii.	·43	·43	0	0
D–E...	i.	1·31	1·33	−·02	− 1·5
	ii.	1·38	1·48	−·10	− 7
E–F...	i.	1·10	·84	+·26	+31
	ii.	1·08	·54	+·54	+100
F–G...	i.	1·77	1·81	−·04	− 2·3
	ii.	1·83	1·97	−·14	− 7·6
G–H...	i.	·94	·63	+·31	+49
	ii.	·94	·78	+·16	+20

a vertical line. The plate carrier could be moved at right angles to the line of travel of the microscope so that it is certain that the directions of travel were the same for both images. The lengths of the different sections of the images are shown in Table I. Two values have been given for every length measured. These are the results for two separate sets of measurements by different observers. One observer missed out the point B in his measurement, therefore the value for the section A–C is given instead. It will be seen that there is some discrepancy in the values obtained. This is undoubtedly due to the fact that the thickness of the image is not negligible in comparison with

the lengths measured. Thus it will be noticed that the biggest percentage variation occurs in the measurement of the short sections. Although the actual values vary, the sign of the difference, left-hand image minus right-hand image, remains the same for both determinations. The table shows that with the exception of two sections, the left-hand image is longer than the right-hand image, indicating that the flash started at the ground and travelled upwards towards the cloud. In the case of the negative values the differences are small compared with the other sections of the flash, and it may be that errors in determining the position of the points of reference have increased one length at the expense of the next. The speed of rotation of the lenses was not sufficient to produce large variations in the length of the images: thus the two negative values of small magnitude do not seriously contradict the general statement that the flash proceeded from the ground towards the cloud.

A peculiarity that will be noticed in the two images is the drawing out of certain points into long curved lines owing to the movement of the lenses. It has been suggested that this is due to certain points of the flash being raised to a higher temperature than the rest of the flash, and in consequence remaining luminous for a longer time. It has also been suggested that actually the whole flash remains luminous for a long time, but it is only at points where, owing to an end-on view of a portion of a flash at a sudden bend the intensity of illumination is a maximum, that this phenomenon becomes noticeable. It is not proposed to say more than this concerning the effect, as it is felt that the propounding of a theory with small data at hand would be premature.

Flash III., shown in fig. 4 (Pl. X.) & fig. 5, commenced as a short discharge with one end in the cloud and the other end petering out somewhere between the cloud and the ground. This was followed by a second discharge, which reached from the cloud to the ground. A third discharge followed about ·006 sec. later, but the images are not very clear owing to a large amount of general illumination, and measurements are not possible. A double series of observations on the first pair of images (called flash II. A) shows that this flash started in the cloud and extended towards the ground, as can be seen in Table II. A, where the changes of length are all negative. If the centre of rotation of the image of flash II. A is located on the figure, a circle drawn with this centre and radius so as to pass through the upper

end of the image, will also pass through the upper end of the image of the second flash, flash II. B. Thus it appears that the second flash, during part of its progress, passed along part of the ionized path left by flash II. A. The pair of images of flash II. B were divided into sections at suitable points, and Table II. B gives the results of a double series of measurements of the lengths of the sections.

TABLE II. A (see fig. 5).

Section of flash.	Observer.	Left-hand image.	Right-hand image.	L.H.I.–R.H.I.	Per cent. change of length.
		mm.	mm.	mm.	
A–B...	i.	1·57	1·89	− ·32	−20
	ii.	1·74	2·06	− ·32	−18
B–C...	i.	1·21	1·89	− ·68	−56
	ii.	1·19	1·54	− ·35	−29
C–D...	i.	2·94	4·11	−1·17	−40
	ii.	2·94	4·68	−1·74	−59

TABLE II. B (see fig. 5).

Section of flash.	Observer.	Left-hand image.	Right-hand image.	L.H.I.–R.H.I.	Per cent. change of length.
		mm.	mm.	mm.	
A–B...	i.	3·94	3·36	+·13	+ 4
	ii.	4·03	3·82	+·21	+ 5·5
B–C...	i.	1·30	1·59	−·29	−22
	ii.	1·15	1·32	−·17	−15
C–D...	i.	2·66	2·35	+·31	+13
	ii.	2·53	2·10	+·43	+20
D–E...	i.	1·25	1·38	−·13	−10
	ii.	1·68	1·88	−·20	−12

Table II. B shows that the top section of the flash suffered very little change of length as a result of the movement of the lenses. This agrees with the earlier statement that the top part of the flash travelled along the ionized path produced by flash II. A, for here the velocity of propagation would be greater and the distortion of the image would be less. Of course it is not certain that the point B selected as a point of reference coincides with the point where the

flash joined the ionized path of flash II. A, thus there is no reason to expect the change to be zero.

The changes in length in the other sections of the flash lead to the deduction that the initial break-down of the atmosphere took place near the point D. From here the flash travelled to the ground and at the same time up towards the cloud. The negative value for the Section B–C gives the unexpected indication that here the direction of propagation was towards the ground. General notions of the behaviour of electric sparks lead one to think that the most likely happening would be for the discharge, when it approached the ionized path left by the previous flash, to extend itself towards this conductor and travel towards it. As a consequence, it was thought that the indefinite nature of the bend at the point "B" had led to an error in the measuring of the flash, but a repetition of the measurements gave the same result as before. This is in line with the conclusions drawn by Prof. Boys from the photograph of a lightning flash which he obtained in 1928 with his rotating lens camera. He states: "The flash started at the ground, and almost immediately after started also in the length next the cloud. The flash then travelled from both these parts and finished in the middle upright portion about 1/7000 sec. later [7]."

In the case of flash II. B, the direction of propagation was probably from A to B to C or in the neighbourhood of C, and from D both upwards towards C and downwards towards E.

Flash III. is shown in figs. 6 and 6 *a* (Pl. XI.) and fig. 7. Here, again, is a double flash, but in this case it is difficult to say which was the initial discharge. It would seem, as will be shown later, that the two images in an approximately horizontal line are those of the second flash. Measurements had to be made on these, however, as one of the images in a vertical line was partly obscured by part of the camera apparatus. The flash was divided into sections as usual, and Table III. gives the results of the measurements.

The first deduction to be made from these measurements is that the flash apparently started somewhere about the point D, and travelled downwards to the ground and upwards towards the cloud. In sections D–F and E–F the change of length of the two images is very small, and this may indicate that for the last part of its path the discharge followed an already ionized path. If this is true it is possible that the path was provided from the level of the ground by means of point discharge.

Section C–D also shows a very low percentage change of length, indicating a high velocity of propagation. Here, again, the presence of a previously ionized path can be deduced and, as will be shown below, can be actually found.

The very high percentage changes for the Sections A–C and B–C are due to the fact that the motion of propagation was in a horizontal direction while the measurement of the distortion produced is in the vertical direction. It should be noticed that in all the measurements already considered, this phenomenon has to be reckoned with to a greater or less extent. A section of the flash may appear vertical, but may in reality be inclined to the vertical in a vertical plane passing through the flash and the camera. Therefore its

Table III. (see fig. 7).

Section of flash.	Observer.	Left-hand image.	Right-hand image.	L.H.I–R.H.I.	Per cent. change of length.
		mm.	mm.	mm.	
A–C...	i.	1·38	·59	+ ·79	+134
	ii.	1·68	·47	+1·21	+258
B–C...	i.	·82	·64	+ ·18	+ 28
	ii.	·60	·58	+ ·02	+ 3·4
C–D...	i.	4·59	4·33	+ ·26	+ 6
	ii.	4·47	4·38	+ ·09	+ 2
D–E...	i.	·26	·29	− ·03	− 11
	ii.	·23	·35	− ·12	− 52
E–F...	i.	1·17	1·21	− ·04	− 3·4
	ii.	1·20	1·18	+ ·02	+ 2

apparent change of length will be exaggerated, and this will account for the variation in the percentage change of length from section to section of a flash as shown in Table II. a.

At the same time as flash III. was photographed with the rotating lenses a photograph was obtained with a stationary camera, and this photograph is shown in fig. 6 *a* (Pl. XI.). A glance at figs. 6 and 6 *a* (Pl. XI.) will make it clear that the flash in fig. 6 *a* is a composite one, containing the two images of fig. 6 superimposed one upon the other. It can also be seen that for a short distance the two flashes traversed the same path. In fig. 7 this path, common to both flashes, is indicated as extending from the point P to the point Q. This was ascertained by superimposing the negative taken with the stationary camera upon the

upper image of the vertical pair in fig. 6 (Pl. XI.), when the coincidence of the two flashes could be clearly seen. It is therefore suggested that the history of the two flashes is as follows. A flash took place along the line QCPRS, shown in fig. 7. The direction of propagation cannot be given, as measurements could not be made on the vertical pair of images. From the point C an almost vertical branch was formed (shown dotted in fig. 7) which had forks branching *upwards,* while the lower part of the flash had forks branching *downwards.* One hundredth of a second later a second flash started at a point about 600 metres above the ground and was propagated towards the ground, and at the same time upwards towards the cloud. At the point marked P in fig. 7 it joined the ionized path left by the previous flash, and travelled along that path to the point Q. Here the energy of the flow of electricity was so great that the flash continued beyond the point Q and finished up at the point B. The proof of this statement is that in fig. 6 *a* (Pl. XI.) the path common to both flashes has produced a brighter image than the rest of the two flashes. The brighter image stops at Q and is continued as a weak image. It is not likely that the first flash started at B and that the second flash, with a conducting ionized path still existing from Q to B, yet stopped at Q. This suggestion also shows why it is probable that the horizontal pair of images show the second flash of the two. Referring to Table III. again, we see that the horizontal Section A–C shows only a 24 per cent. change. This is due to the fact that along the Section Q–C the flash was travelling along an ionized path at a high velocity, thus causing a smaller distortion than would be expected. The second flash, as well as travelling along the ionized path C–Q, also produced a flow of energy into another almost horizontal side flash, which started from the point C in the first discharge, and can be seen to the left of C in the top image in fig. 6 (Pl. XI.). This side fork was a very short one, and so the length of flash which was newly formed by the second discharge is very large, giving a large distortion of the image as already referred to above. The general impression made by a study of these two flashes is that the second discharge, having joined itself to the path formed by the first discharge, travelled along it and arrived with explosive violence at the end of the path, thus starting new ionization and propagating the discharge to a greater distance.

Conclusion.

Experiments have been described in which a camera with rotating lenses has been successfully used to obtain some indication of the manner of propagation of three lightning flashes.

It has been shown that it is possible for a lightning discharge to be propagated from the ground towards the cloud, and that a flash starting at the ground may join up with a flash starting in the cloud, as was earlier shown by Boys.

Two instances have been described in which discharges started at a point above the ground and were propagated both upwards and downwards.

The photographs have demonstrated that two flashes may, for part of the distance between cloud and ground, traverse the same path.

A flash has been photographed (Pl. XI. fig. 6) showing forking towards the cloud at the top and towards the ground at the bottom. In this case at least, the direction of the forking cannot be a criterion of the direction of propagation of the flash.

The facts cited indicate the possibilities of the method in obtaining accurate information concerning the mechanism of a lightning discharge, and it is hoped that a continuation of the experiments will help in the formulation of a reliable theory of this as well as other types of discharge of electricity through gases.

In conclusion, the author wishes to thank his wife, who spent many nights assisting in making exposures before the successful photographs were taken, Prof. H. H. Paine, at whose instance the apparatus was constructed in the workshop of the Physics Department of the Witwatersrand University, Dr. B. F. J. Schonland, of the University of Cape Town, for suggestions and encouragement, and the Research Grant Board of the Union of South Africa for a grant in aid.

References.

(1) Proc. Roy. Soc. A, iii. p. 56 (1926).
(2) Journ. Frank. Inst. cci. p. 485.
(3) Phys. Rev. xxxv. p. 396 (1930).
(4) C. T. R. Wilson, Proc. Phys. Soc. xxxvii. p. 32 (1925).
(5) 'Nature,' cxxviii. p. 794 (1931).
(6) 'Nature,' cxviii. p. 749 (1926).
(7) 'Nature,' cxxii. p. 310 (1928).

XXXVII. *The Spectrum of the Discharge through Oxygen and Hydrogen Mixtures.* *By* A. S. Roy, *B.Sc., Carnegie Research Scholar, The University, St. Andrews* *.

Introduction.

THE following experimental observations were made, at first quite accidentally, in the Physics Laboratory, St. Andrews. It is thought that these observations, along with the explanations put forward, are of sufficient interest to be noted.

In carrying out experiments on the influence of foreign gases on gaseous spectra, oxygen was about to be used ; in the initial photographs it was found that besides the oxygen line spectra other lines and bands appeared on the plates. These lines were easily identified as the Balmer lines and lines of the secondary spectrum of hydrogen. The oxygen was being generated by electrolysis of a dilute solution of sodium hydroxide, and the outer nickel electrode (cathode) was found to be slightly lower than the inner tube of the generator, so that traces of hydrogen were being generated along with the oxygen in the inner tube. An examination was made of the various spectra excited in order to ascertain if the presence of the oxygen, which was in great excess, might influence the spectra of hydrogen.

Oxygen Spectra.

Before considering the experimental observations it will be convenient to give an account of the oxygen spectra found in a discharge tube with pure oxygen.

Two different line spectra of oxygen have long been known, and the names " compound line " and " elementary line " were assigned by Schuster on the supposition that complex and simplified molecules or " molecular groupings " were respectively involved in their production. Lines belonging to other line spectra were found by later experimenters.

In accordance with present views as to the origin of spectra these spectra are attributed to neutral, singly ionized, doubly ionized, and more strongly ionized atoms of oxygen, and are usually designated O I, O II, O III,

* Communicated by Prof. H. S. Allen, M.A., D.Sc., F.R.S.

and so on. The O II lines are generally produced by condensed discharges of moderate intensity through capillary tubes ; the lines O III are added to the spectrum as the pressure is lowered and the intensity of the discharge increased. If the pressure is raised to a few mm. of Hg. in the discharge tube, the series lines, O I, make their appearance.

The best known emission band spectrum of oxygen is the negative band spectrum, with four very strong bands, at λλ 6420–6300, λλ 6070–5960, λλ 5630–5550, and λλ 5290–5200. In addition there are fainter bands with heads about λλ 5900–5840, λ 6200, λλ 6790–6700.

Oxygen-Hydrogen Mixtures.

The mixtures of oxygen and hydrogen, which contained only a minute quantity of hydrogen compared with oxygen, were excited in a Geissler tube, after having been thoroughly dried in the usual manner ; a drying tube was also in direct communication with the discharge tube. The mixture was excited by a voltage of 15,000 volts, obtained by the use of a Hilger transformer and auto-transformer along with a rotary converter working with 220 volts D.C., and giving 150 volts, 60 cycles A.C.

The spectra were examined with a Hilger E I spectrograph, and the investigations were carried out in the two regions λλ 8000–4790 and λλ 5020–3800, the discharge tube being always in the " end-on " position.

At first pressures of less than 1 mm. of Hg. were used. On these plates were present the Balmer lines, the secondary spectrum of hydrogen, and the most prominent lines of the O II spectrum, agreeing with the most intense lines given in the tables of Fowler [1] and Johnson and Cameron [2]. There was no trace of any of the bands of the negative system of oxygen, but there were bands present whose heads were about λ 4835 and λ 4500. These photographs were now compared with those taken sometime earlier with pure hydrogen, using the same apparatus. It was found that the lines of the secondary spectrum were approximately of the same intensity, but the lines of the Balmer series showed a very remarkable change on the plates when oxygen was present. Most of the Balmer lines were strongly increased in intensity, but more remarkable was the fact that they did not

show the same increase in intensity. H_α was approximately of the same intensity; H_β showed a definite increase, and H_γ a still greater increase—that is, the higher members of the Balmer series showed a greater increase in intensity than the lower members.

Photographs were also taken of the discharge, using the same mixture of oxygen and hydrogen at pressures of 3 to 4 mm. of Hg. At these pressures the lines of the secondary spectrum of hydrogen were extinguished, while the Balmer lines appeared even stronger than at the lower pressures. The more intense lines of the O I spectrum, both singlet and triplet lines, were also easily identified. A number of strong bands now appeared on the plate; these bands had heads about λ 6080, λ 5610, λ 5200, λ 4835, λ 4500, and other fainter bands were also present.

These bands were at first thought to be the negative bands of oxygen, as they appeared at about the same wave-length as the latter bands. However, their structure was not at all in accord with the structure of the bands of the negative system of oxygen; all the bands on the plate were degraded to the violet and showed an increase of intensity up to the head of the band. The oxygen bands also are degraded to the violet, but show a maximum intensity in the middle of the band. These bands were identified as the Ångström bands of CO, and their excitation was very probably due to a minute carbon impurity in the discharge tube.

Discussion.

The properties of the oxygen atom and molecule are now sufficiently well known to allow an attempt to be made to interpret the above changes. Wrede [3] has shown that in the discharge through oxygen there is considerable dissociation into atoms. The O I spectrum has been recently investigated by Hopfield [4], who considered the work of other experimenters. The first ionization potential of oxygen is 13·55 volts and the resonance potential of the oxygen atom is 9·1 volts.

Many observations have been made on the ionization potentials of the oxygen molecule, and results varying from 13·5 to 15·5 volts have been found, corresponding to the formation of the normal ion, O_2^+. Mackay [5] found two distinct ionization potentials at 12·6 and 16·1

volts. An important observation was made by Hogness and Lunn [5] ; they found that above 20 volts O^+ ions were produced by single electron impacts. Smyth and Stueckelberg [7] confirmed this result, and, in addition, verified it further by observing that neon ions (having energy of 21·6 volts) formed O^+ ions by collisions of the second kind with neutral molecules of oxygen, according to the process

$$Ne^+ + O_2 \rightarrow O + O^+ + Ne + K.E.,$$

where K. E. denotes the energy left over and available as kinetic energy of the resulting particles. Therefore the potential at which O^+ is formed from O_2 must lie between 20 and 21 volts. From the potential curves of the oxygen molecule Stueckelberg [8] applying the theory of Franck [9] concerning the most probable transition between electronic states in molecules, found that the following reactions could be expected :—

$$O_2 \rightarrow O_2^+ \text{ at } 13{\cdot}5 \text{ volts.}$$

At higher voltage, but less than 20 volts, transitions to excitation levels of O_2 take place

$$O_2 \rightarrow O_2^{+\prime},$$

and at 20·3 volts

$$O_2 \rightarrow O + O^+.$$

It is also known that the carrier of the negative bands is the normal oxygen ion, O_2^+.

In the author's experiments at the low pressures the O II spectrum is present, and therefore the oxygen molecule is being dissociated in accordance with the above process,

$$O_2 \rightarrow O + O^+.$$

Therefore at this pressure besides molecular ions there will also be atomic ions in the discharge tube.

The strong appearance of the Balmer lines can be explained by the theory of collisions of the second kind between oxygen atomic ions or molecular ions and hydrogen atoms. The ionization potential of the hydrogen atom is 13·529 volts ; since this value is very close to the values of the ionization potential of atomic and molecular oxygen, it seems very probable that the increase in intensity of the Balmer lines can be accounted for by

collisions of the second kind, according to the following processes :—

(1) Producing hydrogen ions:

$$O^+ + H \longrightarrow H^+ + O$$

13·55 volts. 13·529 volts.

$$O_2^+ + H \longrightarrow H^+ + O_2$$

13·5 volts. 13·529 volts.

(2) Producing excited hydrogen atoms:

$$O^+ + H \longrightarrow H' + O - e$$

13·55 volts.

$$O_2^+ + H \longrightarrow H' + O_2 - e$$

13·5 volts.

The probability of such collisions occurring depends on the difference of the energies involved, and, in fact, is inversely proportional to that difference. The excitation potentials of the various lines in the Balmer series are

H_α.. 12·034 volts,
H_β.. 12·692 ,,
H_γ.. 12·994 ,,
H_δ.. 13·102 ,, and so on.

Accordingly it is seen that it is more probable that the higher members will show a greater increase in intensity, and this increase will be relatively larger the higher the member concerned.

The bands of the negative system might be expected to appear when the O II spectrum was extinguished at the higher pressures, showing that the molecules were not being dissociated in the manner mentioned above. At the higher pressures the Ångström bands appeared, and these would mask the negative system if the latter appeared at all. The strong excitation of these Ångström bands is no doubt due to the fact that a number of the excited states of the oxygen atom lie very close to the initial levels of the Ångström bands ; therefore these bands can be excited by collisions of the second kind between excited oxygen atoms and normal CO molecules.

During some experimental work in Michigan University it was found that the presence of a trace of CO in excess

of nitrogen caused the strong appearance of the Ångström bands. This was due to a similar reason, the excitation levels of the N_2 molecule being in close resonance with the excited states of CO.

Deodhar and Dutt [10] investigated the oxygen spectra, especially the band spectra of oxygen, and they found bands whose heads were approximately at λ 6032, λ 5630, λ 5290, λ 4830, and λ 4500. These bands are the same bands as found in the above experiments, and are in fact the Ångström bands, which are strongly excited on account of the presence of excess of oxygen and only a trace of CO as impurity. The same workers found the Balmer lines to be also very persistent on their plates ; this is very probably due to the presence of the trace of hydrogen and the effect of the oxygen in excess, as pointed out above.

I wish to express my thanks to Professor H. S. Allen, F.R.S., for his interest and help during my work in St. Andrews.

References.

(1) Fowler, Proc. Roy. Soc. A, cx. p. 476 (1926).
(2) Johnson & Cameron, Proc. Roy. Soc. A, cvi. p. 195 (1924).
(3) Wrede, *Zeits. f. Physik*, liv. p. 53 (1929).
(4) Hopfield, Phys. Rev. xxxvii. p. 160 (1931).
(5) Mackay, Phys. Rev. xxvii. p. 732 (1926).
(6) Hogness & Lunn, Phys. Rev. xxvii. p. 732 (1926).
(7) Smyth & Stueckelberg, Phys. Rev. xxxii. p. 779 (1928).
(8) Stueckelberg, Phys. Rev. xxxiv. p. 65 (1929).
(9) Franck, Trans. Far. Soc. xxi. pt. 3 (1925).
(10) Deodhar & Dutt, Phil. Mag. viii. p. 622 (1929).

XXXVIII. *The Measurement of Temperature of a Coal-gas Flame by "α-Particle Method."* By A. Shirodkar*.

Previous Work.

THE first attempt to measure the temperature of a flame experimentally was made by Sir Humphry Davy in the beginning of the nineteenth century. Davy exploded a mixture of cyanogen and oxygen, and calculated the temperature from the increase in volume of the mixture after explosion. Bunsen followed Davy's

* Communicated by Prof. R. Whiddington, F.R.S.

method with some modifications, and calculated the temperature from the increase in pressure in the explosion vessel. Though the values of temperature arrived at by Davy and Bunsen are far from being correct, still their experiments are of great historical importance.

After Bunsen, very accurate estimates of temperatures of open flames have been made by various workers at different times following different methods, all of which find place under the following headings :—(1) the thermo-couple method, (2) the optical method, and (3) the line reversal method.

The thermo-couple method, though rough, is very simple and useful, and was therefore almost universally adopted by early workers. The method is to keep one thermo-junction immersed in the flame while the other is maintained at a known constant temperature. The thermal e.m.f. developed is measured very accurately, and the temperature of the hot junction is calculated therefrom. This value of the temperature of the hot junction is looked upon as the temperature of the flame used.

The main objections to this method are : (1) a part of the heat given by the flame is carried away by conduction and radiation, and thus the flame is slightly cooled, and (2) the insertion of the foreign body in the flame disturbs it—the larger the size of the body the greater is the disturbance. To overcome these objections bodies having similar geometrical shape but decreasing in size were immersed in the flame, and the temperatures thus obtained were extrapolated so as to extend to the case of a body of infinitely small size. Waggener, Nicholas and White, and Traver found that the temperature indicated by the hot junction is almost exactly a linear function of the thickness of the element used, and that therefore the linear extrapolation to zero thickness should lead to correct values of temperatures.

In the optical method a wire is heated electrically first *in vacuo* and then in a flame. The temperature of the wire is measured by means of an optical pyrometer. The temperature is plotted against the electric current and a curve is drawn in each case. The point where the two curves cut one another gives the temperature of the flame. The explanation as given by Griffiths and Aubery is that at this point there is equality in current as well

as equality in temperature in both the cases. The first indicates that the total heat dissipated in both the cases is the same, while the second indicates that the heat loss due to conduction and radiation together is the same. Therefore the heat loss due to convection must be the same in both cases. In the first case it is zero, as the wire is heated *in vacuo*, and so in the second case too it must be zero, *i. e.*, the wire must be at the temperature of the flame.

The reversal of lines in the spectrum is a well known phenomenon in physics, and the line reversal method is based on it. This method was first suggested by Kurlbaum to measure the temperatures of luminous flames, and was later modified and adopted by Fery and others to measure the temperatures of non-luminous flames after colouring them by alkali salts. A continuously radiating body is viewed through a spectrometer and the coloured flame is placed between the radiator and the spectrometer. If the radiator be cooler than the flame the spectral lines from the coloured flame are seen as bright lines upon the continuous spectrum from the radiator, but if the flame be cooler the bright lines appear dark on the bright background of the continuous spectrum. The temperature of the radiator when the lines are just on the point of reversal is taken to be the same as the temperature of the flame.

The following table gives the value of the maximum temperature of the coal gas flame as estimated by various workers at different times using the methods just outlined :—

Date.	Author.	Deg. C.
1887.	Rosetti.	1360
1892.	Rogers.	1230
1892.	Lewes.	1630
1895.	Waggener.	1770
1899.	Berkenbusch.	1830
1902.	White & Traver.	1780
1904.	Fery.	1871
1928.	Loomis & Perrott.	1875
1929.	Griffiths & Aubery.	1883

The results of Waggener and those who follow are in fair agreement with each other, though the methods

used by them differ radically in principle. This fact is looked upon as the best justification for taking these values as the true temperatures of the flames studied.

Recently Professor David and his colleagues of the Engineering Department of this University carried out a series of experiments in order to measure the temperatures of the flame in an exploding mixture of a combustible gas and air. They calculated the temperature of the flame not only from the pressures developed in the explosion vessel but also from the readings of a thermo-couple in the explosion chamber. It was previously known that these two values differ appreciably, but the difference had been attributed to various causes, viz. : (1) loss of heat due to conduction and radiation, (2) dissociation of the products of combustion, (3) discrepancy in the specific heat data, (4) incomplete combustion, and so on ; but this difference is probably too great to be accounted for by all these causes. It was therefore suggested that the chemical combination in the gaseous state results in the formation of molecules of abnormal molecular structure. The molecules on this view possess two kinds of energy, viz.: (1) energy due to this abnormal structure (latent energy), and (2) translational energy, which is alone responsible for the temperature of the flame. When a wire or any foreign body is inserted in a flame the molecules unload both kinds of energy on it at once, and thus the temperature given by the body is higher than the true temperature of the flame.

Principle underlying the New Method.

It was because of this "latent energy" suggestion that we proposed to determine the temperatures of flames by an altogether new method, which we call the "α-particle method."

It is a well-known fact that the range of α-particles varies directly as the absolute temperature of the absorbing gas. If, therefore, a flame of known thickness be introduced in the path of α-particles in air their range will change because of (1) the difference in the stopping power of the gas in the flame and that of air, and (2) the temperature of the flame. Knowing or determining experimentally the stopping power of the gas the change due to the first cause can be calculated,

and thus the change due to the second cause is known. Then by making use of the simple relation between the temperature and the range the temperature of the flame can be calculated.

Experiments with a Gold-leaf Electroscope.

Because of the simplicity of the apparatus a series of experiments was first carried out by using a gold-leaf electroscope. Though these experiments are not conclusive, because of reasons to be explained later, a short description is given below.

Burners used are those manufactured by Geo. Bray and Co. * of Leeds and known as "flat flame burners for coal-gas." The thickness of the flame was measured by means of a Pt. and Pt.-Rho. thermo-couple, in which case the relation between the temperature and the thermal e.m.f. developed is almost linear at least up to 1400° C. The cold junction of the couple was kept in melting ice, while the hot junction was moved through the flame gradually, and the thermal e.m.f. so developed was measured accurately. Different series of readings were taken for different heights of the flame, but all were confined to the topmost portion, where the temperature is a maximum. When these values of thermal e.m.f. were plotted against the distance through which the hot junction was moved we got a curve of the following nature :—

Fig. 1.

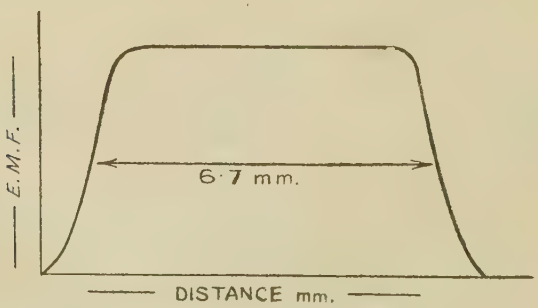

If at half of the maximum height of the curve a horizontal line be drawn then the length of this line bounded

* Through the kindness of Mr. George Bray a set of these burners was provided for the purpose of these experiments.

by the two limbs of the curve may be taken as the thickness of the flame to the first approximation. In the case of the particular burner used it was found to be 6·7 mm.

A polonium plate was the source of α-particles, and to determine the change in range the apparatus was arranged in the following way :—

Fig. 2.

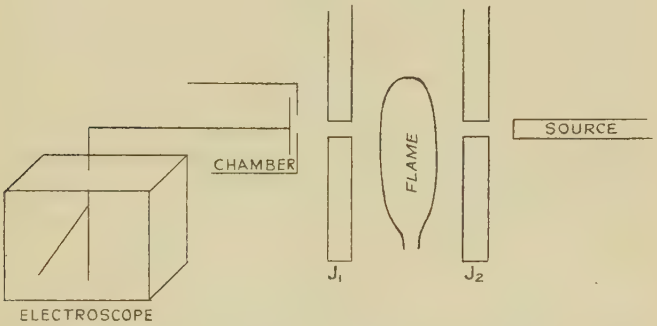

In order to prevent the path of α-particles external to the flame from getting heated the flame was enclosed by two water-jackets, J_1 and J_2, having adequately large openings in their centres and separated by twice the thickness of the flame. Two distance-ionization curves were plotted, one with the flame between the jackets and the other without it. The horizontal distance between these two curves was found to be 5·55 mm., *i. e.*, the insertion of the flame in the path of the α-particles increases their range by 5·55 mm. in air. Thus the path of 6·7 mm. in air is equivalent to a path of 6·7 mm. in flame plus 5·55 mm. in air, or the path of 6·7 mm. in flame is equivalent to 1·15 mm. in air.

The stopping power of the gas in the flame was calculated theoretically, assuming that (1) the combustion is complete in the topmost portion of the flame, (2) there is no dissociation, and (3) the gas takes air just sufficient for complete combustion. The stopping power was found to be approximately the same as that of air. This was measured experimentally too, and was found not to differ appreciably from the calculated value.

Now, since the stopping power of the gas in the flame is the same as that of air, the whole change in the path

must be due to the temperature of the flame. Thus if $t°$ C. be the temperature of the flame, then

$$\frac{6{\cdot}7}{1{\cdot}15} = \frac{273+t}{273+17} \text{ (17° C. = temp. of the room),}$$

$$t = 1417° \text{ C.}$$

From the beginning we were not sure that the electroscope method would give a correct value of the temperature, because the air outside the jackets was heated owing to the size of the openings in them being appreciable. It was not possible to overcome this difficulty using the electroscope apparatus, since any reduction in the size of the openings so reduced the amount of ionization as to make the method unworkable. A new apparatus capable of dealing with much smaller amounts of ionization was therefore set up.

Experiments with an Amplifier.

The electroscope was replaced by an amplifier * constructed on the standard resistance capacity coupling principle. With the help of this amplifier the entrance of a single α-particle in the ionization chamber could be detected by means of phones connected to it.

The following figure gives the arrangement of the apparatus :—

Fig. 3.

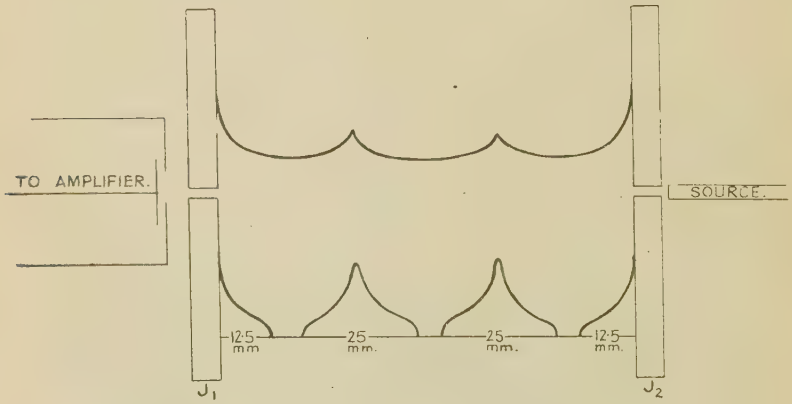

* 'Proceedings of the Royal Society,' A, vol. cxxx. pp. 464–466 (Chadwick, Constable, and Pollard).

Three flames from the same type of burners were placed one after another as shown in the figure. The distance between two successive burners in a particular experiment was 25 mm., which adjusted the flames so that they struck each other and formed one continuous flame as far as the colourless portions were concerned. This was first tested by means of a thermo-couple the hot junction of which when carried through this continuous colourless portion developed the same thermal e.m.f., and thereby ensured that there was no gap at any lower temperature even at the junctions of two flames. This continuous flame was enclosed between two water-jackets, J_1 and J_2, separated by 75 mm. Each water-jacket was 4 mm. thick and had an opening at its centre about 1 mm. in diameter. The flames, the jackets, the source, and the chamber were so arranged that the α-particles from the source could pass through the continuous colourless portion of the flame and the openings in the jackets into the ionization chamber.

As the flames were striking against the openings in the jackets a part of the gas in the flame escaped through the openings. This gas contains a large amount of water-vapour which was sufficient, when condensed, to choke up the small openings and to obstruct the path of α-particles. To prevent this condensation warm water was run through the jackets, which were, in addition, covered with thin asbestos on those sides which were not in contact with the flame. Since this did not prevent altogether the heating of the path of particles outside the jackets, the temperature of the air at different distances from one of the openings was carefully measured when the flames were burning. The following are representative observations :—

Distance, mm.....	5	8	9·5	13·5	17·5	23
Temp. deg. C.	27·2	23·0	22·4	21·7	21·1	20·8

As the graph (fig. 4) shows there is an appreciable rise in temperature just near the jacket but it falls sharply within a centimetre and a half, and after that the fall is more or less uniform and very small. A necessary correction for this is applied to the final estimate.

To get different lengths of the flame three flames were first introduced within the jackets separated

by 75 mm. Then one side-flame was stopped and the distance between the jackets reduced to 50 mm., and lastly only one flame was kept and the distance reduced to 25 mm. To measure the range of the α-particles a series of observations was taken in each

Fig. 4.

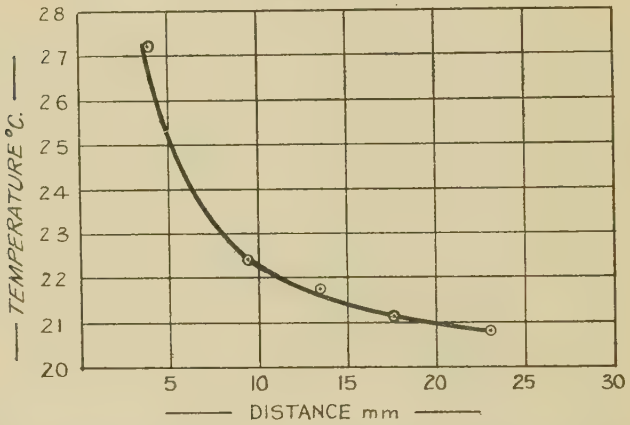

of the three cases by moving the source every time gradually away from the jacket J_2 and counting the number of α-particles entering the chamber in 10 minutes in each position of the source.

The following table gives an example of the observations :—

3 flames.		2 flames.		1 flame.	
Position of the source in mm.	α-particles in 10 minutes.	Position of the source in mm.	α-particles in 10 minutes.	Position of the source in mm.	α-particles in 10 minutes.
45·5	60	23·0	203	2·6	381
46·0	58	24·0	158	3·6	229
46·5	61	24·5	129	4·0	148
47·0	56	25·0	100	4·25	22
47·25	22	25·25	52	4·50	20
47·50	24	25·50	30	∞	22
49·00	21	25·75	20	—	—
—	22	26·00	22	—	—
—	—	∞	21	—	—

To the first approximation 47·25, 25·75, and 4·25 mm. may be taken as the positions of the source in the three cases when the range ends on the ionization chamber. Thus, when the path in flame is reduced by (75—50) 25 mm. the source is to be moved through (47·25—25·75) 21·50 mm. in order to have the end of the range on the ionization chamber, *i. e.*, to reduce the path in flame by 25 mm. is equivalent to increase the path in air by (25—21·5) 3·5 mm. We get the same result by considering the observations in the case of two flames and one flame.

In order to get a very accurate value of this equivalent path in air the experiment was repeated moving the source every time by a tenth of a millimetre. The following table gives a set of such observations :—

3 flames.		1 flame.	
Position of the source in mm.	α-particles in 15 minutes.	Position of the source in mm.	α-particles in 15 minutes.
93·50	108	50·00	348
93·65	110	50·60	345
93·75	107	50·70	322
93·85	111	50·80	277
93·95	89	50·90	223
94·00	77	51·00	121
94·10	51	51·10	56
94·20	55	51·20	52
94·30	50	51·30	55
∞	53	8	54

It is seen from the following graph (fig. 5) that the range ends on the ionization chamber when the source is at 94·10 mm. in the case of three flames and at 51·04 mm. in the case of one flame Thus the source is moved through (94·10—51·04) 43·06 mm. when the flame-path is reduced by 50 mm., or 50 mm. of flame-path are equivalent to (50·00—43·06) 6·94 mm. of air-path at the temperature of the room.

This change in range is due to (1) the difference in the stopping power of the gas in the flame and that of air, and (2) the temperature of the flame.

Fig. 5.

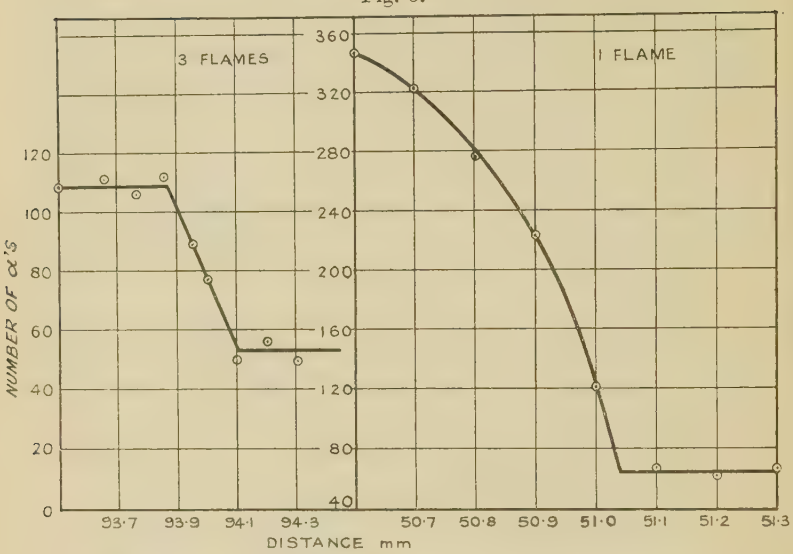

Stopping Power of the Gas in the Flame (Experimental).

To determine the stopping power of the gas in the flame it was collected from the colourless portion of the flame, cooled and passed through a tube 1 cm. in length placed between the source and the ionization chamber. The range of the α-particles was determined as before, first when the tube contained air and then when it was filled with the gas. The following table gives the observations :—

With air in the tube.		With gas in the tube.	
Position of the source in mm.	α-particles in 15 minutes.	Position of the source in mm.	α-particles in 15 minutes.
20·00	86	20·00	83
20·50	83	20·50	86
21·00	84	21·00	84
21·25	83	21·25	70
21·50	64	21·50	57
21·75	57	21·75	50
22·00	36	22·00	37
22·50	37	22·50	35
23·00	36	23·00	36
∞	37	∞	37

The two curves are separated by a little over a tenth of a millimetre the range being shorter in gas than in air. The stopping power of the gas is thus between 1·01 and 1·02, taking that of air as 1. The experiment was tried by using the gold-leaf electroscope in place of the amplifier and calculating the amount of ionization for the different positions of the source. There is a good agreement between these two results, as can be seen from the following table :—

Position of the source in mm.	Time (T) in seconds for the leaf to fall through 100 divisions of the scale in the microscope through which the leaf was observed.				100/T or relative ionization.
	(1).	(2).	(3).	(average).	
	With air in the tube.				
0·0	24·6	25·2	24·1	24·6	4·07
1·0	33·3	32·8	33·6	33·2	3·02
2·0	45·8	43·0	44·4	44·4	2·26
3·0	61·2	63·5	61·6	62·1	1·61
4·0	89·9	91·2	90·2	90·7	1·10
5·0	148·5	145·0	146·7	146·7	0·68
	With gas in the tube.				
0·0	25·4	25·1	25·6	25·4	3·93
1·0	33·5	34·5	33·0	33·7	2·97
2·0	43·0	46·5	44·2	44·4	2·26
3·0	64·5	63·5	62·5	63·5	1·58
4·0	88·5	92·5	90·5	90·5	1·11
5·0	148·0	153·0	151·0	150·5	0·67

Out of six positions of the source, in the case of four, the ionization is less when the tube contains gas than when it contains air. In one case it is equal and only in one case is it slightly higher. Thus the range ends earlier when the air in the tube is substituted by gas, *i. e.*, the stopping power of the gas is slightly higher than that of air.

The stopping power of the gas was then calculated theoretically by making use of the square root law of Bragg. The value thus arrived at is about 0·99,

i. e., slightly less than that of air. This is just the kind of difference that we should expect, because the theoretical value is for the gas in the flame with all the products of combustion while the experimental value is for the gas in the flame without water-vapour, which gets condensed when the gas is cooled. The water-vapour has its stopping power lower than that of air, and therefore

Fig. 6.

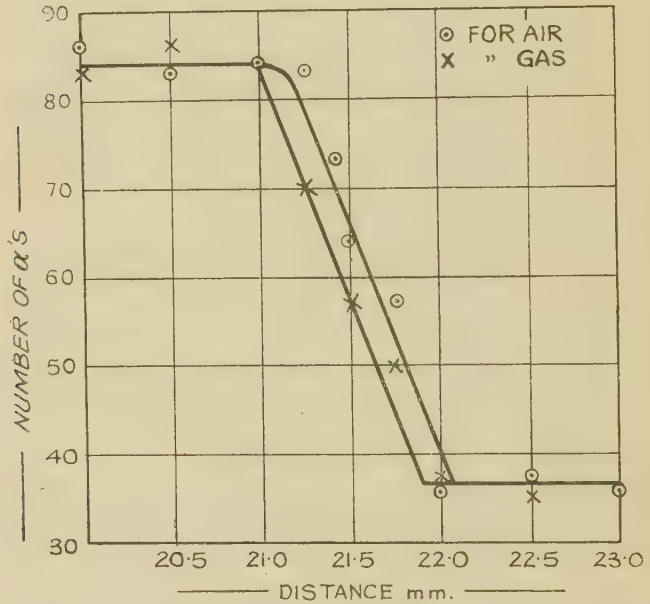

its removal increases the stopping power of the remaining mixture. The difference between the theoretical and experimental value can thus be attributed to the condensation of the water-vapour, and the stopping power of the gas in the flame can be taken to be equal to that of air within an error of 1 or 2 per cent.

Estimate of the Temperature of the Flame.

Since the stopping power of the gas in the flame is practically the same as that of air, the ratio of the path in the flame to its equivalent path in air is equal to the ratio of the absolute temperature of the flame to the absolute

temperature of the air. Thus if $t°$ C. be the temperature of the flame, then

$$\frac{50}{6{\cdot}94} = \frac{273+t}{273+17} \quad (17° \text{ C.} = \text{temp. of the air}),$$

$$t = 1816° \text{ C.}$$

It has already been pointed out that because of warm water running in the jackets the air outside them was slightly heated. The equivalent path in air, *i. e.*, the distance of 6·94 mm., was thus not at the temperature of the room. From the position of the source from the jacket J_2 this distance was found to be between 8 mm. and 15 mm. from J_2. Now from the graph (fig. 4) the temperature of this part of the path varies from 23° C. to 21·5° C., *i. e.*, from 5° C. to 3·5° C. above the temperature of the room that time. Taking the average rise to be about 4° C., the corrected value of t is given by

$$\frac{50}{6{\cdot}94} = \frac{273+t}{273+17+4},$$

$$t = 1845° \text{ C.}$$

It should be noted here that even very small experimental errors change this estimate appreciably; still it can safely be taken to be correct within an error of $\pm$ 100° C; but with a source of long range α-particles the temperature could be measured more accurately.

Summary.

A flame of length 75 mm. is placed in the path of particles from polonium, so that the path lies partly in air and partly in the flame. With the help of an amplifier and an ionization chamber the position of the source is determined when the range of α-particles ends exactly on the entrance of the ionization chamber connected with the amplifier. The flame-path is then reduced to 25 mm., and the source moved till the range ends on the entrance of the chamber. The difference between these two positions of the source is found to be 43·06 mm., *i. e.*, to decrease the flame-path by 50 mm. is equivalent to increase the air-path by (50—43·06) 6·94 mm.

The stopping power of the gas in the flame is calculated theoretically and also determined experimentally. The value arrived at in either way comes to be practically the same as that of air.

The temperature of the flame is determined by making use of the simple relation that the range varies directly as the absolute temperature of the absorbing gas. In the case of the coal-gas flame used it is estimated to be 1845° C. within an error of about $\pm$ 100° C.

Acknowledgment.

I am grateful to Professor Whiddington for suggesting this problem to me and for his continued advice and interest during my stay in Leeds. I am also indebted to Mr. E. C. Pollard for his assistance in making up the amplifier, and to Messrs. Ludbrook and Partridge in particular for workshop help.

XXXIX. *An Experiment on the Combustion of an Inflammable Gas Mixture by a Hot Wire. By* J. D. Morgan, *D.Sc.**.

IN 1914 Professor W. M Thornton drew attention to an observation made by his colleague, Mr. J. R. Thompson, that "when the source of ignition is a hot platinum wire an explosion is started at that temperature at which ions are discharged from the metal" (1). In commenting on this and another allied observation Professor Thornton remarked that "if they do not decide the ionic origin of gaseous explosions in general they prove that ionization and explosion are intimately connected." The experiment and the comment arose out of a suggestion made by Sir J. J. Thomson in a discussion of a report by Professor W. A. Bone to the British Association, the suggestion being that electrons possibly prepare the way for an explosion by ionizing the gas.

Some time afterwards the writer also noticed, without being at the time aware of Thornton's previous publication of the fact, that the temperature at which a hot wire

* Communicated by the Author.

will cause inflammation of a combustible gas mixture is about that at which it will discharge an electroscope, and, like others, he, too, thought that here was to be found reason for supposing that ignition might be due to an electrical action [2]. Believing the matter to be of sufficient interest to warrant further investigation he has recently examined it more closely, and the results of the investigation are given below.

The method of experiment involved the use of a small explosion chamber containing a short helix of platinum wire forming part of an electric circuit, the current in which could be varied by a resistance. The chamber was connected to a vacuum pump, a reservoir containing a prepared mixture of coal-gas and air, and a pressure gauge in the form of a small U-tube containing water. The gas mixture was a very weak one obtained by progressive dilution of a richer mixture, until the gas had but little effect on the wire. As is well known, a thin platinum wire becomes incandescent when exposed to a sufficiently rich coal-gas mixture. The effect does not occur with a very weak mixture. After evacuating the chamber and admitting a charge at atmospheric pressure, the temperature of the wire was increased by means of an electric current until it approached, but did not reach, the glowing temperature. There was also arranged in the chamber an insulated metal piece situated close to the wire and connected to a charged electroscope outside the chamber. At the temperature of the wire in this experiment there was no discharge of ions from the wire, and, consequently, no discharge of the electroscope, whether the latter was charged positively or negatively.

The immediate effect due to the heat given off by the wire was to cause an indication of pressure to be shown by the gauge. After a few minutes, the gauge showed a small fall of pressure. To make quite sure that the fall was a real one, the heating current was interrupted and the apparatus was allowed to cool down. It was found that the pressure was less than the original atmospheric pressure within the chamber, proving that some combination of the constituents of the gas mixture had taken place while the wire was hot. While the combination was taking place there was no discharge of the electroscope. The experiment was repeated many times, and the results were always the same.

The character of the experiment was then modified. The current was increased until the wire showed a dull red glow. It is well known that when a platinum wire is raised to a dull red heat the ions given off are positive. Consequently a positive charge was given to the electroscope so as to avoid its discharge by the emission from the wire. The combination of the constituents of the gas mixture now proceeded rapidly, though without inflammation. After the initial rise of pressure due to the heating of the gas by the wire the pressure quickly fell, showing that rapid combination was taking place. But there was no discharge of the electroscope, proving that while combination of the constituents of the gas mixture was proceeding the effect was not accompanied by any observable ionization other than the positive ionization given off by the wire.

Finally a richer mixture was used, so that the wire, which was slightly heated by an electric current, readily glowed in the presence of the gas. So long as there was no inflammation of the gas there was no discharge of the positively charged electroscope. But when the interaction of the constituents of the gas mixture proceeded with sufficient rapidity to produce flame, the electroscope was discharged instantly.

The experiments were repeated with iron and copper wires instead of the platinum wire, and a mixture of ether vapour and air was also used instead of coal-gas and air, and the results obtained were the same as those already described.

The experiments proved that ionization does not appear in the gas until flame appears, and that ionization of the gas is a consequence of inflammation—not a cause, a conclusion which agrees with what has previously been believed to be fact [3]. On the basis of these experiments it does not appear to be possible to draw any conclusion other than that the combination or combustion which occurred in the gas mixture was due to the heat given off by the wire.

References.

(1) Thornton, W. M., Proc. Roy. Soc. A, vol. xc.
(2) Morgan, J. D., Journ. Inst. Electrical Engineers, vol. liv. no. 254 (1916).
(3) Lind, S. C., Chemical Effects of Alpha Particles and Electrons (Chemical Catalogue Co.), p. 207 (1928).

XL. *Accession to Inertia of and Power radiated by a Sphere Vibrating in Various Ways; with Applications to Hornless Loud Speakers.* *By* N. W. McLachlan, *D.Sc., M.I.E.E.**

Synopsis.

1. Introduction.
2. Derivation of Formulæ for Evaluation of Accession to Inertia M_1.
3. Evaluation of M_1 for various Modes of Vibration :—
   (*a*) Sphere vibrating radially.
   (*b*) Sphere vibrating axially.
   (*c*) Two Hemispheres in opposition along Common Axis.
   (*d*) One Hemisphere quiescent the other vibrating radially.
   (*e*) One Hemisphere quiescent the other vibrating axially.
4. Reduction in Vibrational Frequency due to M_1.
5. Motion asymmetric round Polar Axis of Sphere.
   Spherical Shell with *n* Nodal Circles.
6. Power radiated for various Modes of Vibration.
   (*a*) Sphere vibrating radially.
   (*b*) Sphere vibrating radially and driven by Constant Force.
   (*c*) Sphere vibrating axially.
   (*d*) Sphere vibrating axially and driven by Constant Force.
   (*e*) Influence of Baffle on Low Frequency Power.
   (*f*) Two Hemispheres in opposition along Common Axis.
   (*g*) Hemisphere vibrating radially.
   (*h*) Hemisphere vibrating axially.
7. Power radiated by Spherical Shell with *n* Nodal Circles.
8. Comparison of Power from various Vibrators at Low Frequencies.
9. Mechanical Impedance of Massless Spherical Vibrator.
10. Extension to Vibration with Latitudinal Nodal Circles.

Abstract.

By aid of zonal spherical harmonics (Legendre's functions) formulæ are deduced for the accession to inertia of, and the power radiated from, a sphere or a hemisphere vibrating in various ways. Cases are chosen which have a direct bearing on hornless loud-speaking apparatus, and the results applied thereto.

The influence of constant driving force at all audio-frequencies is considered for several modes of vibration. It is deduced that *under certain conditions* a radially vibrating sphere gives perfect reproduction of acoustic pressures. The increase in low-frequency output due to a large baffle is calculated for disks and spheres. When two diaphragms vibrate in opposition along a common axis, it is indicated that a baffle is unessential provided the useful radiation is confined to the external surfaces of the vibrators.

* Communicated by the Author.

The accession to inertia of, and the power radiated from, a sphere having nodal circles is treated by means of sectorial harmonics. The low frequency radiation decays with amazing rapidity with increase in the number of nodal circles. This arises from interference due to oppositely vibrating segments. It follows that the L.F. interference concomitant with free-edge disks or conical diaphragms executing diametral modes is extremely large, provided the system is substantially symmetrical. By aid of formulæ given in the analysis the mechanical impedance of various types of spherical vibrator can be found.

1. *Introduction.*

THE accession to inertia M_1 of a rigid sphere moving axially in a fluid has been determined by Green [1], Poisson [7], and Lamb [2, p. 130] from the standpoint of hydrodynamics, there being no vibration. The value obtained holds for low frequencies of vibration nevertheless. When, however, the frequency increases beyond a certain value it is essential to introduce a correction factor. Accordingly, Rayleigh [8, p. 248] showed that in this particular case the introduction of frequency into the spherical harmonic analysis gave the correction factor

$$\zeta_{1r}=\frac{(2+k^2a^2)}{(4+k^4a^4)},$$

where

$$k=\frac{\omega}{c}=\frac{2\pi}{\lambda},$$

$\omega = 2\pi$ frequency,

$c =$ velocity of longitudinal waves in fluid,

$\lambda =$ wave-length of longitudinal waves in fluid.

The above factor is plotted in fig. 1 for various values of ka. It has a maximum value of 0·6 at $ka=0{\cdot}91$. For a sphere 10 cm. radius this corresponds to a frequency of 490 ~. As a first approximation this factor can be applied to rigid disks and conical shells for the same values of ka when there is no baffle. Since annularly supported loud-speaker diaphragms behave substantially as rigid structures [5] at frequencies below 200 ~, the factor can be applied when the baffling of the cone is small (4, *f*).

2. *Derivation of Formulæ for Evaluation of the Accession to Inertia.*

The velocity potential at the surface of a vibrating sphere of radius a due to the nth harmonic is

$$\phi_n = -au_n\zeta_n e^{i\omega t}, \quad \ldots\ldots \quad (1)$$

Fig. 1.

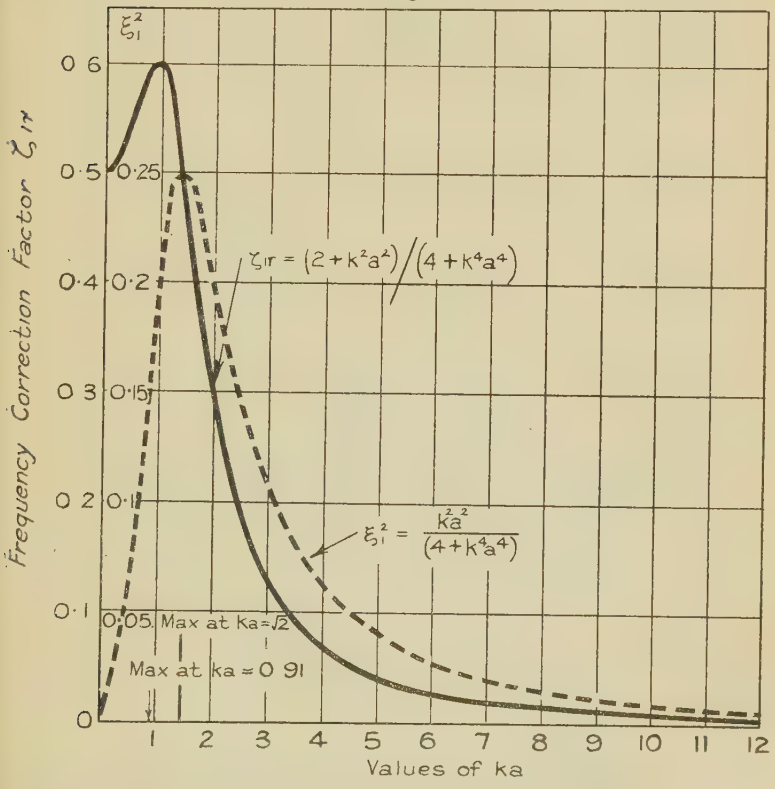

Curves showing frequency correction factors. ζ_{1r} for accession to inertia of sphere vibrating axially; ξ_1^2 for power radiated by sphere vibrating axially.

where the time-factor $e^{i\omega t}$ has been introduced, and

$$\zeta_n = \frac{f_n(ika)}{\mathrm{F}_n(ika)} \quad (8,\ \text{p. } 239).$$

Values of F_n and f_n for $n=0$ to 3 are given in Tables I. and II.

The radial pressure on the sphere per unit area due to this harmonic is

$$p_n = -\rho \frac{d\phi_n}{dt} = i\rho\omega a u_n \zeta_n, \quad . \quad . \quad . \quad . \quad (2)$$

the time-factor being omitted.

TABLE I.

$F_n(ikr) = x + iy$; $F_n^2(ikr) = x^2 + y^2 = \frac{1}{\xi_n^2}$. $z = ikr$.

n.	x.	y.
0	1	kr
1	2	$kr - \frac{2}{kr}$
2	$4 - \frac{9}{k^2r^2}$	$kr - \frac{9}{kr}$
3	$7 - \frac{60}{k^2r^2}$	$kr - \frac{27}{kr} + \frac{60}{k^3r^3}$

TABLE II.

$f_n(ikr) = x' + iy'$. When kr is very great $f_n(ikr) = 1$.

n.	x'.	y'.
0	1·0	0
1	1·0	$-\frac{1}{kr}$
2	$1 - \frac{3}{k^2r^2}$	$-\frac{1}{kr}$
3	$1 - \frac{3}{k^2r^2}$	$-\frac{1}{kr} + \frac{15}{k^3r^3}$

Since ζ_n is complex, (2) can be written in the form

$$p_n = b(iw - z), \quad . \quad . \quad . \quad . \quad . \quad . \quad (3)$$

where

$$b = \rho\omega a u_n.$$

From (3) we see that the surface-pressure consists of two components in time quadrature. The power component bz is in phase with the radial velocity, whilst the wattless or

accelerational component bw is in quadrature therewith. This latter pressure component does no useful work; it merely maintains the flow of fluid associated with the sphere, thereby introducing an inertia effect whose magnitude we desire to determine.

The kinetic energy of the fluid due to motion concomitant with the nth spherical harmonic [2, p. 51, formula 4] is given by

$$T_n = -\frac{\rho}{2}\iint \phi_{nr} u_n \, ds, \quad . \quad . \quad . \quad . \quad . \quad (4)$$

where

ρ = density of fluid medium;

u_n = radial velocity at surface of sphere due to nth harmonic;

ϕ_{nr} = velocity potential on surface, the real part of $\frac{f_n(ika)}{F_n(ika)} = \zeta_n$ being taken;

ds = element of surface where ϕ and u exist.

It is important to realize that the integration for each harmonic component in the expansion is taken over the *entire* surface of the sphere, not merely that portion of it which is in vibration. This follows from the fact that the actual motion is equivalent to the combined motions of the harmonic components, and each of these involves the whole surface.

The total kinetic energy due to all the harmonics is

$$T = -\frac{\rho}{2}\iint \phi u \, ds$$

$$= -\frac{\rho}{2}\iint (\phi_0 + \phi_1 + \ldots)(u_0 + u_1 + \ldots)\, ds. \quad . \quad . \quad (5)$$

Since ϕ_n and u_n are both directly proportional to $P_n(\mu)$, it is easy to show that the integrand in (5) involves squares and products of Legendre functions of different orders. On integration with respect to μ between the limits $+1$ and -1 only the squares remain, from which it follows that the total accession to inertia is

$$-\sum_0^n \frac{\rho}{2}\iint \phi_{nr} u_n \, ds.$$

If U is the maximum radial velocity of the sphere, the motion being sinusoidal,

$$m_n \frac{U^2}{2} = -\frac{\rho}{2} \iint \phi_{nr} u_n \, ds,$$

where m_n is the accession to inertia due to the nth harmonic. Thus

$$m_n = -\frac{\rho}{U^2} \iint \phi_{nr} u_n \, ds, \quad . \quad . \quad . \quad . \quad (6)$$

Fig. 2.

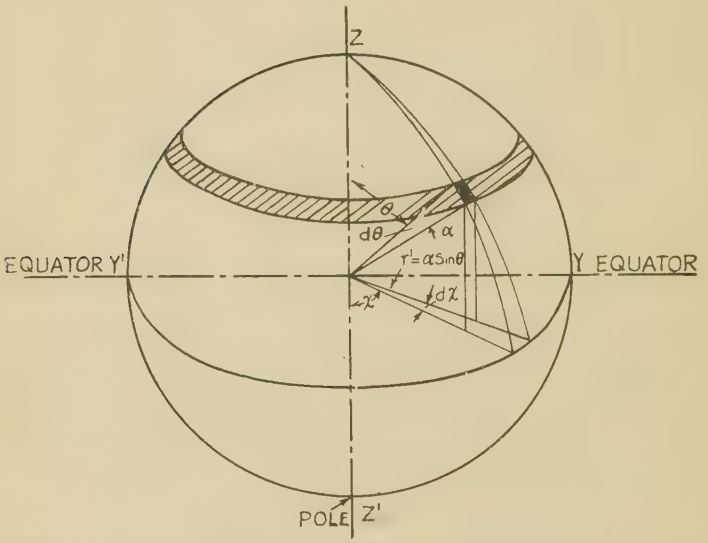

Diagram showing orientation of axes, and the angles θ and χ. The annular area is $2\pi a^2 \sin\theta \, d\theta = -2\pi a^2 d\mu$, and the rectangular area is $a^2 \sin\theta \, d\theta \, d\chi$.

and the total accession to inertia is

$$M_1 = m_0 + m_1 + m_2 + \ldots . \quad . \quad . \quad . \quad . \quad (7)$$

From (1), neglecting the time-factor, $\phi_{nr} = -a u_n \zeta_{nr}$ whilst from fig. 2 $ds = -2\pi a^2 d\mu$. Writing $u = U f(\mu)$, the nth harmonic of the radial velocity is

$$u_n = (n + \tfrac{1}{2}) P_n(\mu) U \int_{-1}^{+1} f(\mu) P_n(\mu) \, d\mu \quad (6)$$

$$= (n + \tfrac{1}{2}) P_n(\mu) U H,$$

where

U is the maximum radial velocity

and $$H = \int_{-1}^{+1} f(\mu) P_n(\mu)\, d\mu,$$

this being a numeric after integration and insertion of the limits.

Substituting these values of ϕ_n, u_n, and ds in (6), we find that the accession to inertia due to the nth harmonic is

$$m_n = 2\pi\rho a^3 (n+\tfrac{1}{2})^2 H^2 \zeta_{nr} \int_{-1}^{+1} [P_n(\mu)]^2 d\mu \quad . \quad . \quad (8)$$

$$= (2n+1)\pi\rho a^3 \zeta_{nr} \left\{ \int_{-1}^{+1} f(\mu) P_n(\mu)\, d\mu \right\}^2, \quad . \quad (9)$$

since the value of the *integral* in (8) is $\frac{1}{n+\frac{1}{2}}$.

When the motion of the two hemispheres is equal but opposite directionally (fig. 3, *c*), the integral for u_n must be split up.

We have

$$u_n = (n+\tfrac{1}{2}) P_n(\mu) U \left\{ \int_0^1 f(\mu) P_n(\mu)\, d\mu - \int_{-1}^0 f(\mu) P_n(\mu)\, d\mu \right\}$$

$$= (2n+1) P_n(\mu) U \int_0^1 f(\mu) P_n(\mu)\, d\mu,$$

or zero, according to the circumstances cited below. The symmetry of the situation entails expansion in the zeroth and even harmonics, so that $u_n = 0$ when n is odd. With this proviso we have

$$m_n = (8n+4)\pi\rho a^3 \zeta_{nr} \left\{ \int_0^1 f(\mu) P_n(\mu)\, d\mu \right\}^2 . \quad . \quad (10)$$

If the motion of the two hemispheres is identically and directionally the same as indicated in fig. 3, *a*, the expansion will contain odd harmonics only. When one-half of the sphere is at rest (fig. 3, *b*) the formula for the accession to inertia becomes

$$m_n = (2n+1)\pi\rho a^3 \zeta_{nr} \left\{ \int_0 f(\mu) P_n(\mu) d\mu \right\}^2 . \quad . \quad (11)$$

By suitable choice of the limits of integration any desired portion of the sphere, however small, can be treated, but the

number of harmonics required to attain accuracy increases with decrease in surface area.

Fig. 3.

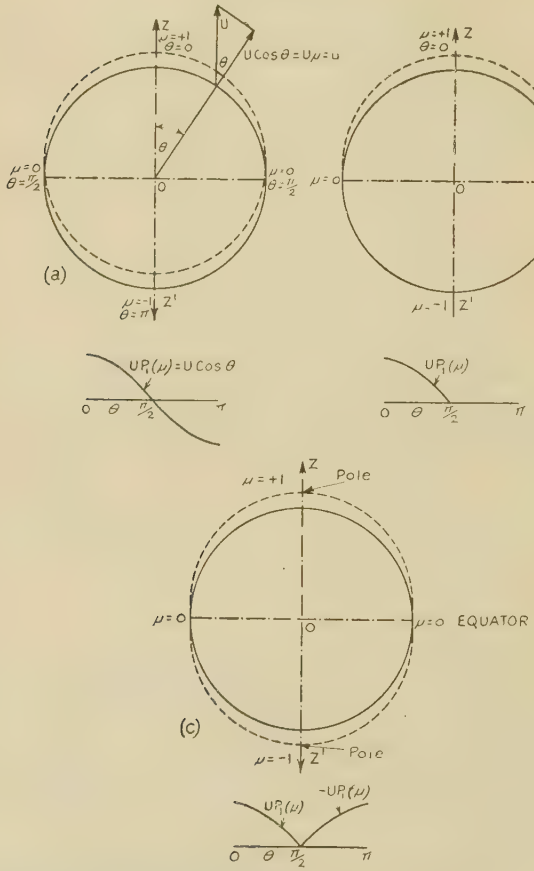

(*a*) Sphere vibrating axially as a whole. Radial velocity $u = U\mu$.

(*b*) Hemisphere vibrating axially as a whole. $u = U\mu$ from $\theta = 0$ to $\pi/2$.

(*c*) Hemispheres vibrating axially in opposition. $u = +U\mu$ from θ to $\pi/2$, $-U\mu$ from $\pi/2$ to π.

3. *Evaluation o* M_1 *for various Modes of Vibration.*

(a) *Sphere vibrating radially.*

As a preliminary illustration of formula (9) we shall evaluate M_1. By hypothesis the radial velocity is constant

for all values of θ and, therefore, of $\mu = \cos\theta$. Thus $u = \mathrm{U}f(\mu)$, so that $f(\mu) = 1$ from $\mu = +1$ to -1, and, therefore, the zeroth harmonic alone is involved.

Substituting $n = 0$, $f(\mu) = 1$, and $\mathrm{P}_0(\mu) = 1$ in (9), we obtain

$$\mathrm{M}_1 = 4\pi\rho a^3 \zeta_{0r}; \quad . \quad . \quad . \quad . \quad . \quad (12)$$

but from Tables I. and II.

$$\zeta_{0r} = \frac{1}{1+ika} = \frac{1}{1+k^2a^2} - \frac{ika}{1+k^2a^2}.$$

Taking the real part and substituting in (12) we obtain the accession to inertia of a radially pulsating sphere of radius a as

$$\mathrm{M}_1 = \frac{4\pi\rho a^3}{1+k^2a^2}. \quad . \quad . \quad . \quad . \quad . \quad (13)$$

Since $k = \frac{\omega}{c} = \frac{2\pi}{\lambda}$, the accession to inertia decreases with increase in frequency. For a small sphere, or at low frequencies when $k^2a^2 \lesssim 1$, $\mathrm{M}_1 = 4\pi\rho a^3$, which is three times the mass of fluid displaced by the sphere. It may appear remarkable that the accession to inertia of a radially vibrating shell symmetrical about any polar axis should vary. The variation is concomitant with the closer phase relationship between the total pressure and the radial velocity at the spherical surface as the frequency increases, *i. e.* the acoustic power factor increases with rise in frequency.

(b) *Sphere vibrating axially.*

The axial velocity in the two hemispheres is U, and the radial velocity is, therefore, $u = \mathrm{U}f(\mu)$, where $f(\mu) = \mu$ from $\mu = +1$ to -1. This entails the harmonic of unit order only, *i. e.*, $\mathrm{P}_1(\mu) = \mu$ (fig. 3, *a*).

To ascertain the accession to inertia we can employ either formula (9) or (10). Thus from (10) we have

$$\mathrm{M}_1 = m_1 = 12\pi\rho a^3 \zeta_{1r} \left\{ \int_0^1 \mu^2 d\mu \right\}^2.$$

Using Tables I. and II. to evaluate ζ_{1r} we obtain

$$\mathrm{M}_1 = \tfrac{4}{3}\pi\rho a^3 \left(\frac{2+k^2a^2}{4+k^4a^4} \right). \quad . \quad . \quad . \quad . \quad (14)$$

When ka is small at low frequencies we have $\mathrm{M}_1 = \tfrac{2}{3}\pi\rho a^3$,

or one-half the mass of fluid displaced by the sphere. The frequency correction factor $\frac{(2+k^2a^2)}{(4+k^4a^4)}$ is plotted in fig. 1.

This was the case treated by Rayleigh [8, p. 248], using a different method. He considered the total axial pressure on the sphere due to its motion, and showed that the accelerational component in quadrature with the energy component was

$$M_1\omega^2X=\tfrac{4}{3}\pi\rho a^3\left(\frac{2+k^2a^2}{4+k^4a^4}\right)\omega^2X.$$

The result in (14) can be applied to loud speakers as indicated in Section 1 above.

(*c*) *Two Hemispheres vibrating oppositely along Common Axis.*

The axial velocities of the two hemispheres are $+U$ and $-U$. The radial velocity is, therefore, $u=Uf(\mu)$, where $f(\mu)=+\mu$ from $\mu=1$ to 0 and $-\mu$ from 0 to -1 (fig. 3, *c*). As we showed in Section 2, the expansion of u contains even harmonics only, and with this proviso formula (10) is applicable. Thus

$$m_0=\frac{\pi\rho a^3}{(1+k^2a^2)} \quad . \quad . \quad . \quad . \quad . \quad (15)$$

and

$$m_2=\tfrac{5}{16}\pi\rho a^3\left(\frac{27+6k^2a^2+k^4a^4}{81+9k^2a^2-2k^4a^4+k^6a^6}\right). \quad . \quad (16)$$

m_4, m_6, etc., have not been evaluated since the kinetic energy associated with them is so small. From (15) and (16) it will be seen that the frequency correction factor ζ varies for each harmonic. At low frequencies, when $ka\leqq 0{\cdot}5$, the value of $\zeta_{nr}\doteqdot\frac{1}{(n+1)}$. Under this condition

$$M_1=m_0+m_2=\pi\rho a^3(1+\tfrac{5}{48})$$
$$\doteqdot 1{\cdot}1\,\pi\rho a^3, \quad . \quad . \quad . \quad . \quad (17)$$

or about $\frac{1}{4}$ that of the sphere vibrating radially throughout. This result can be applied to the external faces of the loud-speaker arrangement described in Section 6 (*f*).

(d) *One Hemisphere quiescent, the other vibrating radially.*

The radial velocity is $u=Uf(\mu)$, where $f(\mu)$ is 1 from $\mu=1$ to 0 and zero from $\mu=0$ to -1. For this case

$$u_n=(n+\tfrac{1}{2})\,\mathrm{P}_n(\mu)\,\mathrm{U}\int_0^{+1}\mathrm{P}_n(\mu)\,d\mu+0$$

$$=(-1)^{\frac{n-1}{2}}\frac{(n+\frac{1}{2})}{n(n+1)}\cdot\frac{3.5.\ldots.n}{2.4.\ldots.(n-1)}\,\mathrm{U}\,\mathrm{P}_n(\mu), \qquad (18)$$

when n is odd, but zero if n is even and >0. Thus only the terms of zeroth and odd orders occur in the harmonic expansion of the radial velocity.

From formula (11)

$$m_0=\frac{\pi\rho a^3}{(1+k^2a^2)}, \qquad (19)$$

$$m_1=\tfrac{3}{4}\pi\rho a^3\left(\frac{2+k^2a^2}{4+k^4a^4}\right), \qquad (20)$$

and

$$m_3=\tfrac{7}{64}\pi\rho a^3\zeta_{3r}. \qquad (21)$$

Higher harmonics do not contribute materially to M_1 unless a large number is taken, so that when $ka\leqq 0{\cdot}5$ we have $\zeta_{0r}=1$, $\zeta_{1r}=\frac{1}{2}$, $\zeta_{3r}=\frac{1}{4}$,

and

$$\begin{aligned}\mathrm{M}_1&=m_0+m_1+m_3\\&=\pi\rho a^3(1+\tfrac{3}{8}+\tfrac{7}{256})\\&=1{\cdot}41\pi\rho a^3, \qquad (22)\end{aligned}$$

or 0·47 that for the whole sphere vibrating radially. By taking a large number of harmonics the ratio would approach 0·5.

(e) *One Hemisphere quiescent, the other vibrating axially.*

The radial velocity is $u=\mathrm{U}f(\mu)$, where $f(\mu)=\mu$ from $\mu=+1$ to 0 and zero from 0 to -1 (fig. 3, *b*).

By trial we find that the harmonics involved are $n=0$, 1, 2, 4, 6, etc., of which only the first three are required. Thus from formula (10)

$$m_0=\frac{\pi\rho a^3}{4}\cdot\frac{1}{(1+k^2a^2)}, \qquad (23)$$

$$m_1=\frac{\pi\rho a^3}{3}\left(\frac{2+k^2a^2}{4+k^4a^4}\right), \qquad (24)$$

$$m_2=\frac{5}{64}\pi\rho a^3\left(\frac{27+6k^2a^2+k^4a^4}{81+9k^2a^2-2k^4a^4+k^6a^6}\right). \qquad (25)$$

When $ka \leqq 0{\cdot}5$ we have

$$\begin{aligned} M_1 &\doteq m_0 + m_1 + m_2 \\ &= \pi\rho a^3\left(\tfrac{1}{4} + \tfrac{1}{6} + \tfrac{5}{192}\right) \\ &= 0{\cdot}44\pi\rho a^3, \quad . \quad . \quad . \quad . \quad . \quad . \quad . \quad (26) \end{aligned}$$

or about $\frac{2}{3}$ that when the whole sphere vibrates axially. This is equivalent to $\frac{1}{3}$ the mass of fluid displaced by the sphere.

At low frequencies, when the spatial distribution is sensibly spherical, this result can be applied to loud-speaker operation. Thus in an absorbent cabinet M_1 due to the external side of the diaphragm will be $\frac{2}{3}$ that of the same diaphragm used alone or with a small baffle. The effect of an infinite baffle on a circular disk vibrating axially is to double the accession to inertia. Assuming that this also applies to the above case, M_1 of the external side of the diaphragm in the absorbent cabinet will be $\frac{2}{3}$ its value in an infinite baffle.

4. *Reduction in Vibrational Frequency due to* M_1.

When a body vibrates in a fluid medium the frequencies of the various modes are reduced due to accession to inertia. In air the reduction is slight, due to the low density thereof, but in water it is sometimes very large [4,k].

The kinetic energy of a homogeneous spherical shell of radius a, thickness t, and density ρ_1, vibrating radially *in vacuo*, is

$$\begin{aligned} \tfrac{1}{2}mv^2 &= \tfrac{1}{2}.4\pi\rho_1 a^2 t\omega^2 X^2 \\ &= 2\pi\rho_1 a^2 t\omega^2 X^2, \quad . \quad . \quad . \quad . \quad . \quad (27) \end{aligned}$$

where

X = maximum amplitude of sinusoidal motion,

and

$\omega = 2\pi$ frequency.

The kinetic energy of the fluid associated with the sphere is

$$\tfrac{1}{2}M_1\omega^2X^2 = \frac{2\pi\rho a^3\omega^2X^2}{(1+k^2a^2)}, \quad . \quad . \quad . \quad . \quad (28)$$

this being obtained by aid of formula (13).

Thus from (27) and (28) the kinetic energy of the system is

$$T = 2\pi a^2\omega^2X^2\left\{\rho_1 t + \frac{\rho a}{(1+k^2a^2)}\right\}. \quad . \quad . \quad (29)$$

The potential energy of deformation can be shown to be

$$V = \frac{4\pi t X^2 E}{(1-\sigma)}, \quad . \quad . \quad . \quad . \quad . \quad (30)$$

where

E = Young's Modulus of Elasticity

and

σ = Poisson's ratio < 1.

To ascertain the vibrational frequency we equate the potential and kinetic energies of the system.

Thus from (29) and (30) we find that

$$\omega^2 = \frac{2}{a^2} \cdot \frac{E}{\rho_1(1-\sigma)} \left\{ \frac{1}{1 + \frac{\rho}{\rho_1} \cdot \frac{a}{t(1+k^2a^2)}} \right\} . \quad . \quad (31)$$

In vacuo $\rho = 0$, and we have

$$\omega_v^2 = \frac{2}{a^2} \cdot \frac{E}{\rho_1(1-\sigma)}, \quad . \quad . \quad . \quad . \quad . \quad (32)$$

The reduction in frequency due to the fluid is determined by the bracketed quantity in formula (56), so the frequency ratio

$$\frac{\text{Fluid}}{\text{Vacuo}} = \frac{f_f}{f_v} = \left\{ \frac{1}{1 + \frac{\rho}{\rho_1} \cdot \frac{a}{t(1+k^2a^2)}} \right\} . \quad . \quad (33)$$

Expression (33) is dependent upon frequency, since $k = 2\pi f/c$. In order to determine ω it is necessary, therefore, to solve (31) as a biquadratic equation.

5. *Motion asymmetric about the Polar Axis of Sphere.*

When the dynamic deformation curve of the sphere is not symmetrical round the axis ZOZ′, the velocity potential depends upon the angle χ (fig. 2), and we require a sectorial harmonic of the nth order and nth degree, namely,

$$T_n^n(\mu) = \sin n\chi \sin^n\theta \, D^n P_n(\mu), \quad . \quad . \quad . \quad (34)$$

where $P_n(\mu)$ is Legendre's function and $n \geqslant 1$. By differentiating $P_n(\mu)$ n times (34) can be written

$$T_n^n(\mu) = 1.3.5 \ldots (2n-1) \sin n\chi \sin^n\theta$$

or

$$\sin n\chi \sin^n\theta = \frac{T_n^n(\mu)}{\lfloor 1.3.5 \ldots (2n-1) \rfloor} . \quad . \quad . \quad (35)$$

Spherical Shell with n Nodal Circles.

The deformation curve in this case is assumed to be of the type $\sin n\chi \sin^n \theta$, and the radial velocity is $u_n = \mathrm{U} \sin n\chi \sin^n \theta$. An expansion is unnecessary, since from (35) the radial velocity u_n is proportional to the nth sectorial harmonic, this being a solution of the fundamental differential equation $(\nabla^2 + k^2)\phi = 0$.

The velocity potential at any point on the surface is—choosing the real part—

$$\phi_{nr} = -a\,\mathrm{U} \sin n\chi \sin^n \theta\, \zeta_{nr}. \quad . \quad . \quad . \quad (36)$$

The area of an element on the surface is now

$$d\mathrm{s} = a^2 \sin\theta\, d\theta\, d\chi,$$

as shown in fig. 2. Thus the kinetic energy of the fluid associated with the vibrating sphere is

$$\begin{aligned} \mathrm{T} &= -\frac{\rho}{2}\iint \phi_{nr} u_n d\mathrm{s} \\ &= \rho a^3 \frac{\mathrm{U}^2}{2} \zeta_{nr} \int_0^{\pi} \sin^{2n+1}\theta \int_0^{2\pi} \sin^2 n\chi\, d\chi \\ &= \frac{2^{n+1} n!}{1.3 \ldots (2n+1)} \zeta_{nr} \pi \rho a^3 \frac{\mathrm{U}^2}{2}, \end{aligned}$$

and thence

$$\mathrm{M}_1 = \frac{2^{n+1} n!}{1.3 \ldots (2n+1)} \cdot \zeta_{nr} \pi \rho a^3. \quad . \quad . \quad . \quad (37)$$

If $n = 1$ we have

$$\mathrm{M}_1 = \tfrac{4}{3}\pi\rho a^3 \left(\frac{2 + k^2 a^2}{4 + k^4 a^4}\right), \quad . \quad . \quad . \quad . \quad (38)$$

this being identical with that of a sphere vibrating axially, and $\frac{1}{6}$ that of a sphere vibrating as a whole (see (13)). When $ka \leqq 0{\cdot}5$, $\zeta_{nr} \doteqdot 1/(n+1)$, and the accession to inertia

$$\mathrm{M}_1 = \frac{2^{n+1}}{1.3 \ldots (2n+1)} \cdot \frac{n!}{(n+1)} \cdot \pi\rho a^3. \quad . \quad (39)$$

If $n = 2$,

$$\mathrm{M}_1 = \tfrac{16}{45}\pi\rho a^3 = 0{\cdot}533, \text{ that when } n = 1.$$

If $n = 4$,

$$\mathrm{M}_1 = \tfrac{256}{1575}\pi\rho a^3 = 0{\cdot}244, \text{ that when } n = 1.$$

The values of M_1 decrease, for these values of n, approximately as $\frac{1}{n}$. This is in great contrast with the power

radiated, which decreases very rapidly with increase in n (Section 7).

6. *Power radiated.*

The power radiated as sound can be found (*a*) by integrating the in phase pressure and velocity at the surface, (*b*) by doing likewise at a great distance from the centre, where $r \gtrsim a$. The latter procedure is the simpler of the two, and will be used herein. At a great distance the pressure and particle velocity are in phase. If the pressure due to the nth harmonic is p_n and the particle velocity v_n, the power transmitted through unit area of a spherical surface of radius r is $\frac{p_n v_n}{2} = \frac{p_n^2}{2\rho c}$, since $p_n = \rho c v_n$ [8, p. 16]. The total power is the integral of $\frac{p_n^2}{2\rho c}$ over the spherical surface. Thus

$$W_n = \frac{1}{2\rho c}\iint p_n^2 \, ds,$$

where p_n is the maximum pressure whose mean square value is $\frac{1}{2}$.

Since $ds = -2\pi r^2 d\mu$, it follows that the power associated with the nth harmonic is

$$W_n = -\frac{\pi r^2}{\rho c}\int_{-1}^{+1} p_n^2 \, d\mu. \quad . \quad . \quad . \quad . \quad (40)$$

If the pressure at any point on the sphere is expressed as a series of harmonic terms, the integral of the square of this series taken over the surface is equal to that of the sum of the squares of separate terms. This follows from the fact that $\int_{-1}^{+1} P_m(\mu)\, P_n(\mu)\, d\mu$ is zero excepting when $m = n$, which is similar to the case of Fourier's series used to represent an alternating current. The electric power is independent of the phase angles of the components, and is obtained from the sum of terms of the type $\int_0^{\frac{2\pi}{\omega}} \cos^2 \omega t \, dt$. Thus, in finding the power radiated by a vibrating sphere it is merely necessary to add the contributions from each spherical harmonic.

Introducing the time-factor, the velocity potential due to the nth harmonic is

$$\phi_n = -\frac{a^2}{r} u_n \xi_n e^{i\omega t},$$

and the sound pressure

$$p_n = -\rho \frac{d\phi_n}{dt} = \frac{i\rho\omega a^2}{r} \cdot u_n \xi_n, \quad . \quad . \quad . \quad (41)$$

where $$\xi_n = \frac{f_n(ikr)}{\mathrm{F}_n(ika)} = \frac{1}{\mathrm{F}_n(ika)},$$

when r is very great. The factor $e^{i\omega t}$ has been omitted, since it is not required. The radial velocity of the surface due to the nth harmonic can be written $u_n = \mathrm{U}\mathrm{G}_n$, where $\mathrm{U} = \omega \mathrm{X}$, and

$$\mathrm{G}_n = (n+\tfrac{1}{2}) \mathrm{P}_n(\mu) \int_{-1}^{+1} f(\mu) \mathrm{P}_n(\mu)\, d\mu \quad . \quad . \quad (42)$$

$$= (2n+1) \mathrm{P}_n(\mu) \int_{0}^{1} f(\mu) \mathrm{P}_n(\mu)\, d\mu, \quad . \quad . \quad (43)$$

the field of application being defined below.

Formula (42) is applicable when the two hemispheres have identical motions in the same direction, whilst (43) applies when the motion is equal and opposite. If one hemisphere alone is operative (43) must be halved. From expressions (40), (41), and the above value of u_n we find that the power associated with the nth spherical harmonic is given by

$$\mathrm{W} = \mathrm{K}\, \xi_n^2 \int_{-1}^{+1} \mathrm{G}_n^2\, d\mu, \quad . \quad . \quad . \quad . \quad (44)$$

where $$\mathrm{K}^* = \frac{\pi \rho a^4 \omega^4 \mathrm{X}^2}{c}$$

and $$\xi_n^2 = \frac{1}{x^2 + y^2}$$

is the reciprocal of the square of the modulus of $\mathrm{F}_n(ika)$. This frequency factor is dependent upon the distribution of Spatial Radiation [4, 9]. The integration in (44) extends over the *entire* surface of the sphere, since each harmonic is concerned with the complete sphere.

(a) *Sphere vibrating radially.*

Since the harmonic of zeroth order alone is involved, the value of G_0 in (42) is unity, and

$$\mathrm{W}_0 = 2\mathrm{K}\, \xi_0^2$$

$$= \frac{2\pi \rho a^4 \omega^4 \mathrm{X}^2}{c(1 + k^2 a^2)} \cdot \quad . \quad . \quad . \quad . \quad . \quad . \quad (45)$$

* This represents four times the power radiated from one side of a rigid disk of radius a in an infinite plane when $ka < 0{\cdot}5$.

This is a well-known result, but it is usually derived and quoted in connexion with a source whose size is small compared with the wave-length. Moreover, the correction term $\frac{1}{1+k^2a^2}$ does not then appear except in the form unity, *i. e.*, when $ka=0$, or quite small.

(b) *Sphere vibrating radially and driven by Constant Force.*

In treating this problem we shall assume the effective mass [4j] of the sphere, apart from the accession to inertia due to the fluid, to be constant at all frequencies, *i. e.*, there are no resonances.

The mechanical resistance B, or in-phase acoustic force per unit radial velocity, is obtained from the relationship $W=\frac{B\omega^2X^2}{2}$. Thus, from (45)

$$B=\frac{4\pi\rho a^4\omega^2}{c(1+k^2a^2)}=4\pi a^2\rho c\left(\frac{k^2a^2}{1+k^2a^2}\right), \quad . \quad . \quad (46)$$

since $$k=\frac{\omega}{c}.$$

The effective mass $= M_1 +$ natural mass

$$= M_1 + M$$

$$= M_1(1+\beta),$$

or $$M_e=\frac{4\pi\rho a^3}{(1+k^2a^2)}\cdot(1+\beta), \quad . \quad . \quad . \quad . \quad (47)$$

where $$\beta=\frac{M}{M_1}.$$

From (46) and (47)

$$M_e=\frac{B(1+\beta)}{\omega ka}. \quad . \quad . \quad . \quad . \quad . \quad (48)$$

The driving force F = radial velocity * × impedance $= uZ$. Therefore $u=\frac{F}{Z}$, and the power radiated is

$$W=\tfrac{1}{2}Bu^2$$

$$=\tfrac{1}{2}B\left(\frac{F}{Z}\right)^2. \quad . \quad . \quad . \quad . \quad . \quad (49)$$

* $u_{max.}=\omega X$.

Since $Z=\sqrt{B^2+\omega^2M_e^2}$ and F is constant, the power W from (49) varies as $\frac{B}{(B^2+\omega^2M_e^2)}$. Substituting the value of M_e from (48) in this formula, we find that when the driving force is constant

$$W\propto\left\{\frac{1+k^2a^2}{(1+\beta)^2+k^2a^2}\right\}. \quad . \quad . \quad . \quad . \quad (50)$$

Provided $\beta=M/M_1$ is small compared with unity, *i.e.*, the accession to inertia is much greater than the natural mass of the spherical shell, the power is constant at all frequencies. Thus we have an ideal hypothetical acoustic reproducer. In general this condition will be much more readily attained in water than in air, owing to the low density of the latter. When β is not negligible in comparison with unity it follows from preceding formulæ that for constant-power output the driving force must vary as

$$\left\{\frac{(1+\beta)^2+k^2a^2}{1+k^2a^2}\right\}^{\frac{1}{2}}.$$

At low frequencies when $k^2a^2\lesssim 1$, β is constant, so also is the output for a given driving force. This conclusion applies equally to any rigid body vibrating in an infinite baffle when the sound distribution is spherical.

In our ideal reproducer the amplitude X varies as

$$\frac{1}{\omega Z}=\frac{1}{\omega\sqrt{B^2+\omega^2M_e^2}}.$$

Inserting the values of M_e and B from (47) and (49) we find that

$$X\propto\frac{1+k^2a^2}{\omega^2\sqrt{(1+\beta)^2+k^2a^2}},$$

and since $\beta\lesssim 1$, we have

$$X\propto\frac{\sqrt{1+k^2a^2}}{\omega^2}.$$

At low frequencies, when ka is small, $X\propto\frac{1}{\omega^2}$, whilst when ka is large $X\propto\frac{1}{\omega}$, which indicates the increased influence of the in-phase acoustic force at the higher frequencies.

(c) *Sphere vibrating axially.*

The radial velocity $u = \mathrm{U}f(\mu)$, where $f(\mu) = \mathrm{P}_1(\mu) = \mu$ from 1 to -1 (fig. 3,*a*). Thus, from (42) $\mathrm{G}_1 = \mu$, and from (44)

$$\mathrm{W}_1 = \mathrm{K}\xi_1^2 \int_{-1}^{+1} \mu^2 \, d\mu = \frac{2}{3} \frac{\pi\rho a^4 \omega^4 \mathrm{X}^2}{c} \xi_1^2.$$

From Table I. we find

$$\xi_1^2 = \frac{1}{x^2 + y^2} = \frac{k^2 a^2}{4 + k^4 a^4}.$$

Thus

$$\mathrm{W}_1 = \frac{2}{3} \frac{\pi\rho a^4 \omega^4 \mathrm{X}^2}{c} \left(\frac{k^2 a^2}{4 + k^4 a^4} \right). \quad . \quad . \quad . \quad (51)$$

Expression (51) represents the total power radiated by a baffleless sphere vibrating axially. When ka is small (51) becomes

$$\mathrm{W}_1 = \frac{\pi}{6} \frac{\rho a^6 k^2 \omega^4 \mathrm{X}^2}{c} = \frac{\pi}{6} \frac{\rho a^6 \omega^6 \mathrm{X}^2}{c^3}, \quad . \quad . \quad (52)$$

this being a well-known formula [3].

The relationship $\xi_1^2 = \dfrac{k^2 a^2}{(4 + k^4 a^4)}$ has been plotted in fig. 1, the maximum value occurring when $ka = \sqrt{2}$, giving the frequency correction factor $\xi_1^2 = \frac{1}{4}$. At high frequencies $\xi_1^2 \doteqdot \dfrac{1}{k^2 a^2}$, and we obtain $\mathrm{W} = \frac{2}{3}\pi\rho c a^2 \omega^2 \mathrm{X}^2$. Thus the power radiated at high frequencies is constant if the axial velocity $\omega\mathrm{X}$ is constant. The more usual condition to which we approximate in practice is that of constant driving force.

(d) *Sphere vibrating axially and driven by Constant Force.*

We shall assume the sphere to be rigid, so that its own effective mass is independent of frequency. The power radiated $\mathrm{W}_1 =$ Axial resistance $\times$ Mean square of axial velocity, or

$$\mathrm{W}_1 = \frac{\mathrm{B}\omega^2 \mathrm{X}^2}{2}. \quad . \quad . \quad . \quad . \quad . \quad (53)$$

Thus, from (51) and (53)

$$\mathrm{B} = \frac{4}{3} \frac{\pi\rho a^4 \omega^2}{c} \left(\frac{k^2 a^2}{4 + k^4 a^4} \right). \quad . \quad . \quad . \quad . \quad (54)$$

The total effective mass

$$M_e = M_1(1+\beta),$$

as before, so that we obtain

$$M_e = \tfrac{4}{3}\pi\rho a^3(1+\beta)\frac{(2+k^2a^2)}{(4+k^4a^4)}. \quad . \quad . \quad . \quad . \quad (55)$$

Using (54) and (55), we get

$$M_e = B(1+\beta)\frac{(2+k^2a^2)}{(4+k^4a^4)}. \quad . \quad . \quad . \quad . \quad . \quad (56)$$

From Section 6 (*b*) the power varies as $\frac{B}{(B^2+\omega^2 M_e^2)}$.

Using (56) in this formula we ultimately find that for constant driving force

$$W_1 \propto \frac{k^2(4+k^4a^4)}{\{(1+\beta)^2(2+k^2a^2)^2+k^6a^6\}}. \quad . \quad . \quad (57)$$

When ka is small at low frequencies the power varies as

$$\frac{k^2}{(1+\beta)^2} = \frac{\omega^2}{c^2(1+\beta)^2} \quad . \quad . \quad . \quad . \quad (58)$$

Thus the power vanishes at zero frequency—limiting motion being assumed—and increases directly with the frequency as the latter rises. This is due to the effect of lateral motion caused by the hemispheres on either side of the equatorial plane vibrating in the same direction. The great circle which joins the two halves is virtually nodal, and the sound pressure is equal and opposite at identical latitudes on either side. It is of importance to observe that, although the acoustic short-circuit phenomenon increases with falling frequency, the accession to inertia remains constant. Whereas the power is governed by spatial interference (phase), the accession to inertia depends upon the flow of fluid associated with the motion, and obviously this can never be zero. At high frequencies, when ka is large, formula (57) reduces to $\frac{1}{a^2}$, and the power is constant, provided $ka \gtrsim (1+\beta)$.

(e) *Influence of Baffle on Power radiated at Low Frequencies.*

The large increase in low-frequency power concomitant with the use of a baffle in loud-speaking apparatus of the hornless variety is extremely well known. It is of interest

to put the matter in analytical form when the *driving force is constant.*

Taking first of all the case of a rigid circular disk, the power radiated at low frequencies without a baffle [3] is

$$W_r = \frac{8}{27\pi}\frac{\rho a^6 \omega^6 X^2}{c^3}, \quad . \quad . \quad . \quad . \quad (59)$$

and *from one side* with a baffle [4, e, p. 1026],

$$W_{rb} = \frac{\pi \rho a^4 \omega^4 X^{2'}}{4c} \quad . \quad . \quad . \quad . \quad . \quad . \quad (60)$$

We have now to ascertain W_r and W_{rb} in terms of the constant force F. Assuming the acoustic load to be negligible, we can write

$$F = M_e \omega^2 X,$$

M_e being the total effective mass, from which we obtain

$$\omega X = \frac{F}{\omega M_e} = \frac{F}{\omega M_1 (1+\beta)}, \quad . \quad . \quad . \quad (61)$$

where $$\beta = \frac{M}{M_1}.$$

Thus $$\omega^2 X^2 = \frac{F^2}{\omega^2 M_1^2 (1+\beta)^2}, \quad . \quad . \quad . \quad . \quad (62)$$

without the baffle,

and $$\omega^2 X'^2 = \frac{F^2}{\omega^2 M_1'^2 (1+\beta')^2}, \quad . \quad . \quad . \quad . \quad (63)$$

with the baffle.

Inserting these (velocities)^2 in (59) and (60), taking the ratio of the two, and remembering [4, h] that $M_1' = 2M_1$, we obtain for constant driving force

$$\frac{W_{rb}}{W_r} = \frac{27\pi^2}{128} \cdot \left(\frac{1}{ka}\right)^2 \left(\frac{1+\beta}{1+\beta'}\right)^2 . \quad . \quad . \quad . \quad (64)$$

Taking $a = 10$ cm. radius, $f = 50\sim$, $\beta = 3{\cdot}4$, $\beta' = 1{\cdot}7$, and the velocity of sound in air $c = 3{\cdot}4 \times 10^4$ cm. sec.$^{-1}$, the ratio in (64) is 65/1. Thus the use of an infinite baffle at $50\sim$ would raise the intensity level on *one side* 18 decibels, which is an appreciable amount.

From (52) the low-frequency power radiated by a sphere of radius a vibrating axially without a baffle is

$$W_s = \frac{\pi}{6}\frac{\rho a^6 \omega^6 X^2}{c^3} \quad . \quad . \quad . \quad . \quad . \quad . \quad (65)$$

Proceeding on the above lines, we find that when the driving force is invariable, the ratio

$$\frac{W_{rb}}{W_s} = \frac{3\pi}{16} \cdot \left(\frac{1}{ka}\right)^2 \cdot \left(\frac{1+\beta''}{1+\beta'}\right)^2, \quad . \quad . \quad . \quad (66)$$

where $$\beta'' = \frac{\text{Mass of sphere}}{\text{Acc. to inertia of sphere}}.$$

Assuming the mass of the sphere equal to that of the disk the result in (66) is several times less than that in (64).

At high frequencies (ka large) considerable focussing occurs, the wave-propagation is sensibly plane, and the influence of a baffle is comparatively slight. This is shown very clearly by taking the ratio

$$\frac{\textit{One side} \text{ of disk in baffle}}{\text{Sphere without baffle}},$$

ka being large and a the same in both cases.

Then we have

$$\frac{W_{rb}}{W_s} = \frac{3}{4}\left(\frac{M_1''}{M_1'}\right)^2\left(\frac{1+\beta''}{1+\beta'}\right)^2 = \frac{3}{4}\left(\frac{M_1''+M_s}{M_1'+M}\right) \doteqdot \frac{3}{4}, \quad (67)$$

provided the masses of the disk and sphere are identical and $ka \gtrsim 0{\cdot}5$, since M_1'' and M_1' are then negligible and the amplitudes equal. The ratio in (67) is about 1 per cent. that when $f = \infty$.

These conclusions can readily be verified aurally or quantitatively with a moving-coil loud speaker.

(f) *Two Hemispheres vibrating oppositely along Common Axis.*

Using (43) as the integrand of (44), we obtain

$$W_0 = \frac{\pi\rho a^4\omega^4 X^2}{2c} \cdot \frac{1}{(1+k^2a^2)}, \quad . \quad . \quad . \quad (68)$$

this being $\frac{1}{4}$ the power radiated by a sphere vibrating radially throughout, and

$$W_2 = \frac{5}{32} \cdot \frac{\pi\rho a^4\omega^4 X^2}{c} \left\{\frac{k^4a^4}{81+9k^2a^2-2k^4a^4+k^6a^6}\right\}. \quad (69)$$

When $ka \leq 0{\cdot}5$ the power radiated is due almost entirely to W_0.

If the driving force is constant at all frequencies, and the acoustic component negligible in comparison with that due to inertia, the power radiated at low frequencies is

$$W_0 = \frac{F^2}{2\pi\rho c a^2(1+\beta)^2}. \quad . \quad . \quad . \quad . \quad (70)$$

The power is constant and independent of frequency, this being in striking contrast with the result in the previous section, when the two halves of the sphere moved in the *same* direction. The difference is due to the absence of interference from portions of the sphere vibrating in opposite phase [4, g].

A fact of unusual interest is the equality in radiation at low frequencies ($ka \leq 0{\cdot}5$), due to two hemispheres vibrating axially in opposition without a baffle, that of a circular disk of equal radius (both sides) with an infinite baffle, and that from a radially pulsating hemisphere (see Table III.), the amplitude being identical in each case. From this fact we deduce that if a loud speaker were situated in the centre of a room, a baffle could be avoided by actuating two diaphragms axially in opposition. It is assumed, of course, that the radiation from the inner sides of the diaphragms is dealt with suitably, *e. g.*, it could be absorbed. This problem was treated in two of the author's patent specifications [4, b, c] some years ago, from which the following quotations are taken:— "The diaphragms are attached to opposite sides of the axis of the coil (rotatable as in a M.C. ammeter), so that they cause positive or negative air-pressure waves *simultaneously* at either side of the enclosure, thus avoiding interference." Referring to the use of two or more diaphragms, the specification reads: "This poly-diaphragm system yields a much more uniform sound radiation, especially at the higher audio-frequencies, than a single diaphragm . . . . ; the principle can be extended to a polyhedron, so that the axes of the diaphragms lie in intersecting planes, thereby approximating to the action of a spherical source emitting sound equally along all its radii."

The question of uniformity of sound radiation at higher audio-frequencies mentioned in the latter quotation is of considerable interest and importance. In this connexion it is easy to show from the present and other analyses [4, d, e] that the radiation from a rigid body of customary size vibrating in an infinite baffle gradually decreases with increase in frequency. The attenuation in output is, of course, due to spatial interference when the wave-length

of sound is comparable with the diameter or other major dimension of the radiator. Consequently a rigid body vibrating—in a baffle—along an axis is not an ideal reproducer of speech and music. It so happens, however, that the reproduction on the axis of a rigid circular disk of constant effective mass at a distance of 10 or more diameters therefrom is perfect, provided the constant driving force is substantially in quadrature with the velocity, *i. e.*, inertia control[4, e]. In practice all listeners cannot be accommodated on the axis, and the reason for success in moving-coil apparatus is the occurrence of resonances which offset the power reduction due to interference, thereby making the axial pressure many times greater than it would be with a rigid disk[5]. If the vibrating area, assumed to be driven as in the case of a condenser loud speaker[4, a], by a uniformly distributed force, occupies an appreciable proportion of the wall of a room, the question of focussing does not arise. The use of such a radiator in the open would be attended with serious focussing, but in general this defect can be remedied by using a number of units suitably oriented.

(g) *Sphere with one-half quiescent, the other vibrating radially.*

The radial velocity is $u=\mathrm{U}f(\mu)$, where $f(\mu)=1$ from $\mu=1$ to 0, and zero from $\mu=0$ to -1. From (43), using the appropriate limits,

$$\mathrm{G}_0=\tfrac{1}{2}$$

and

$$\mathrm{G}_1=\tfrac{3}{4}\mu.$$

When n is even and ≥ 2,

$$\int_0^1 \mathrm{P}_n(\mu)\,d\mu=0,$$

but when n is odd we have

$$\int_0^1 \mathrm{P}_n(\mu)\,d\mu=(-1)^{\frac{n-1}{2}}\cdot\frac{1}{n(n+1)}\cdot\frac{3.5....n}{2.4...(n-1)}.$$

Thus

$$\mathrm{G}_3=-\tfrac{7}{32}(5\mu^3-3\mu),$$

and the contributions from harmonics of higher orders can be neglected.

Using formula (44), we obtain

$$\mathrm{W}_0=\frac{\pi\rho a^4\omega^4\mathrm{X}^2}{2c}\cdot\left(\frac{1}{1+k^2a^2}\right), \quad . \quad . \quad . \quad (71)$$

$$W_1 = \tfrac{3}{8}\pi\rho a^4\omega^4 X^2\left(\frac{k^2a^2}{4+k^4a^4}\right), \quad . \quad . \quad . \quad (72)$$

$$W_3 = \tfrac{7}{256}\pi\rho a^4\omega^4 X^2\left(\frac{1}{x^2+y^2}\right), \quad . \quad . \quad . \quad (73)$$

where $$x = ka - \frac{27}{ka} - \frac{60}{k^3a^3},$$

and $$y = 7 - \frac{60}{k^2a^2}.$$

The power component W_3 is small enough to be omitted. Hence for all practical purposes the power radiated by the hemisphere is

$$W = W_0 + W_1 = \frac{\pi\rho a^4\omega^4 X^2}{2}\left\{\frac{1}{(1+k^2a^2)} + \frac{3}{4}\left(\frac{k^2a^2}{4+k^4a^4}\right)\right\}. \quad . \quad . \quad . \quad (74)$$

When $ka \leqq 0{\cdot}5$, the power radiated is substantially that calculated from the first term in (74). In vibrations pertaining to harmonics of higher orders portions of the sphere move in opposition. This causes serious lateral motion at low frequencies, and the ensuing spatial interference curbs the radiation considerably. This was shown by Stokes in a famous memoir published sixty-four years ago [9].

(h) *One Hemisphere quiescent, the other vibrating axially.*

In this case $G_0 = \frac{1}{4}$, $G_1 = \frac{\mu}{2}$, so

$$W_0 = \frac{\pi\rho a^4\omega^4 X^2}{8c}\left(\frac{1}{1+k^2a^2}\right) \quad . \quad . \quad . \quad (75)$$

and

$$W_1 = \frac{\pi\rho a^4\omega^4 X^2}{6c}\cdot\left(\frac{k^2a^2}{4+k^4a^4}\right). \quad . \quad . \quad . \quad (76)$$

At low frequencies, where ka is small, the power is chiefly due to W. It is $\frac{1}{4}$ the value in (71), where the vibration is wholly radial.

7. Spherical Shell with n Nodal Circles.

The radial velocity is assumed to be of the type $u = U \sin n\chi \sin^n\theta$, this being proportional to the sectorial

harmonic of the nth order (fig. 4). Thus an expansion is unnecessary.

From (41) the pressure at a great distance r is neglecting i,

$$p_n = \frac{\rho a^2 \omega \mathrm{U} \sin n\chi \sin^n \theta}{r} \xi_n \quad . \quad . \quad . \quad (77)$$

and $$\mathrm{W}_n = \frac{1}{2\rho c} \iint p_n^2 \, ds, \quad . \quad . \quad . \quad . \quad . \quad . \quad (78)$$

where $$ds = r^2 \sin\theta \, d\theta \, d\chi.$$

Fig. 4.

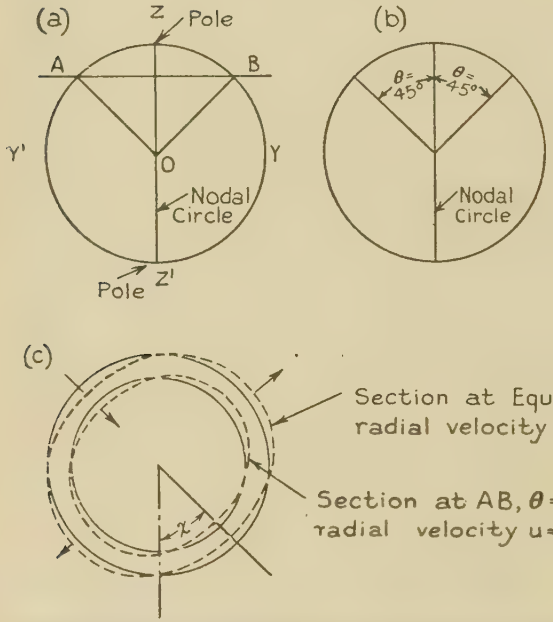

Diagrams illustrating vibration of spherical shell with two nodal circles.

Thus, substituting for p_n and ds in (78), we get

$$\mathrm{W}_n = \frac{\rho a^4 \omega^4 \mathrm{X}^2 \xi_n^2}{c} \int_0^{\frac{\pi}{2}} \sin^{2n+1}\theta \, d\theta \int_0^{2\pi} \sin^2 n\chi \, d\chi$$

$$= \frac{\pi \rho a^4 \omega^4 \mathrm{X}^2}{c} \cdot \frac{2_n . n\,!}{1.3.\ldots.(2n+1)} \cdot \xi_n^2, \quad . \quad . \quad . \quad (79)$$

where $$\xi_n^2 = \frac{1}{\mathrm{F}_n^2(ika)} = \frac{1}{x^2+y^2}.$$

By virtue of spatial interference the power at low frequencies declines with amazing rapidity as the number of nodal circles increases. This can be studied by aid of the factor [9] ξ_n^2.

At high frequencies, when the wave-length is comparable with the diameter of the sphere, there is little difference in the power radiated for various values of n (equal amplitude X). In fact, for $ka=4$ and $n=4$ the power is greater than that for a sphere vibrating radially. This is fully discussed in Stokes's memoir. His results are applied mainly to a bell with low frequency diametral modes, where that characterized by two diameters usually preponderates.

If we imagine a series of infinite rigid planes, one containing each nodal circle on the sphere, the radiation from each sector will be preserved intact, and interference eliminated. An arrangement akin to this, but with the unavoidable practical limitations, is described in Patent Specifications 270421 and 271021.

We can also use the preceding analysis to gain a rough idea of the decay in low-frequency output from a free-edge disk or a conical loud-speaker diaphragm as the nodal diameters increase[4, e]. In practical cases where asymmetry introduced due to the seam the vibrating areas are unequal, and the power radiated may be quite large, as has been shown experimentally [5].

8. *Comparison of Power from various Vibrators at Low Frequencies.*

When $ka \leqq 0{\cdot}5$ and the entire surface vibrates in phase, the radiator, whatever its shape, simulates a simple source *. Under this condition the power from a sphere and a rigid disk of like radius is comparable. The power varies as $\frac{(u\mathrm{A})^2}{\sigma}$, where u = radial velocity † (normal to surface), A = area in vibration, σ = solid angle, extending indefinitely, into which diffusion occurs. Data for various vibrators are given in Table III., the axial amplitude being identical in each case.

For a hemisphere vibrating axially the radial velocity is proportional to $\mu=\cos\theta$. To find the effective velocity-

* A sphere vibrating axially is, therefore, excluded, since the radial velocities in the two hemispheres are in opposite phase.

† When this varies with μ, it is essential to integrate the velocity-area over the surface.

TABLE III.

W_r = power radiated from both sides of a rigid disk of equal radius vibrating in an infinite baffle when $ka \geq 0{\cdot}5$. $A = \pi a^2$, a = radius, $U = r.m.s.$, radial velocity along polar axis.

Vibrational system.	Effective velocity-area (uA).	Solid angle. σ.	$(uA)^2/\sigma$.	Power ratio to rigid disk.	Actual power.
Sphere radially	4UA	4π	$4(UA)^2/\pi$	4	$4W_r$
Hemisphere radially in infinite plane	2UA	2π	$2(UA)^2/\pi$	2	$2W_r$
Hemisphere radially without infinite plane ...	2UA	4π	$(UA)^2/\pi$	1	W_r
Hemisphere axially without infinite plane ...	UA	4π	$(UA)^2/4\pi$	$\frac{1}{4}$	$W_{r/4}$
Two hemispheres axially in opposition	2UA	4π	$(UA)^2/\pi$	1	W_r
Rigid disk in infinite plane	UA (each side)	2π (each side)	$(UA)^2/\pi$	1	W_r
One side of rigid disk without plane, the other side screened	UA	4π	$(UA)^2/4\pi$	$\frac{1}{4}$	$W_{r/4}$

From a practical viewpoint it is preferable to compare the output of baffleless vibrators with that from *one* side of a rigid disk in an infinite baffle, since the baffle cuts off the other side of the disk. The output from a speaker with a large finite baffle is equal to that from one side of the rigid disk.

area it is necessary to integrate over the surface of the hemisphere. Thus

$$(u\mathrm{A})_e = 2\pi \int_0^{\frac{\pi}{2}} \mathrm{U}a^2 \sin\theta \cos\theta \, d\theta = \pi a^2 \mathrm{U} = \mathrm{UA},$$

as given in Table III. It is obviously half that of a radially pulsating hemisphere, but equal to that for one side of a rigid disk in an infinite plane.

9. *Mechanical Impedance of Massless Spherical Vibrator.*

On the assumption that the vibrator is devoid of mass, it is proposed to establish a formula for the mechanical impedance per unit area of vibrating surface. This proves useful where a "simulating" impedance is needed. For instance there is as yet no formula for the terminal impedance of a finite exponental horn. In treating reflexion at the mouth, replacement is made by some suitable impedance which can conveniently be a radially pulsating hemisphere of appropriate radius.

Electrically

$$\mathrm{Z} = \frac{\mathrm{E}}{\mathrm{I}}, \text{ so mechanically } \mathrm{Z} = \frac{\text{pressure}}{\text{radial velocity}} = \frac{p}{u}.$$

Thus

$$\mathrm{Z} = \frac{p_0 + p_1 + \ldots p_n}{u}, \quad . \quad . \quad . \quad . \quad (80)$$

where $p_0 \ldots p_n$ are the pressures due to the various harmonics. Using formula (2), (80) can be written ($z = ka$)

$$\mathrm{Z} = \frac{i\rho c z}{u} \{u_0\zeta_0 + u_1\zeta_1 + \ldots u_n\zeta_n\}, \quad . \quad . \quad . \quad (81)$$

only those harmonics which occur in the expansion of u being chosen. Since ζ_n is of the form $c + di$ as shown in section 2, the impedance occurs in the customary form $\mathrm{Z} = r_m + ix_m$ where r_m and x_m correspond respectively to mechanical resistance and reactance.

For a radially pulsating hemisphere, as in section 3*d*, we have

$$\mathrm{Z} = \frac{2\rho c z}{u} \left\{ \frac{\mathrm{U}}{2} \left[\frac{1 - iz}{1 + z^2} \right] + \frac{3}{4} \mathrm{U}\mu \left[\frac{(2 + z^2) - iz^3}{4 + z^4} \right] \right\}. \quad (82)$$

$$= \frac{\rho c}{2} \left\{ \frac{z^2}{1 + z^2} + \frac{3}{2}\mu \left(\frac{z^4}{4 + z^4} \right) + i \left[\frac{z}{1 + z^2} + \frac{3}{2}\mu \frac{(2z + z^3)}{4 + z^4} \right] \right\}, \quad (83)$$

since $u = \mathrm{U}$.

This is a fair approximation when $z=ka$ is not too large, although it entails only the harmonics of zeroth and unit orders.

10. *Extension to Vibration with Latitudinal Nodal Circles.*

The above analysis is valid for any dynamic deformation curve of the spherical surface. Nodal circles whose centres lie on the polar axis can be considered when it is desired to secure an approximate imitation of another vibrator which proves analytically intractable. The radial velocity is expressed in terms of U and μ so that M_1, W, and Z can be evaluated as shown above. If the nodal circle occurs when $\theta=\frac{\pi}{4}$ the expression $u=U(2\mu^2-1)$ might be assumed. One hemisphere is then quiescent.

References.

(1) Green, E.—Trans. R. S. Edinburgh, Dec. 16th, 1833.
(2) Lamb, H.—'Hydrodynamics' (1895).
(3) Lamb, H.—'Dynamical Theory of Sound' (1925).
(4) McLachlan, N. W.—(*a*) Patent Specification 206610 (1922); (*b*) Patent Specification 270421 (1926); (*c*) Patent Specification 271021 (1926); (*d*) 'Wireless World,' March 23rd, 30th, 1927; (*e*) Phil. Mag. vii. pp. 1011, 1026 (1929); (*f*) Phil. Mag. xi. p. 1137 (1931); (*g*) Phil. Mag. xiii. p. 747 (1932); (*h*) Journal I. E.E. lxix. p. 612 (1931); (*j*) Proc. Phys. Soc. xliv. p. 88 (1932); (*k*) Proc. Phys. Soc. xliv. p. 546 (1932); (*l*) *Ann. d. Phys.* (5) xv. p. 440 (1932).
(5) McLachlan N. W., and Sowter, G. A. V.—Phil. Mag. xii. p. 771, fig. 3 (1931).
(6) MacRobert, T. M.—'Spherical Harmonics' (1928).
(7) Poisson, E.—*Mémoires de l'Academie des Sciences*, ix. p. 521.
(8) Rayleigh, Lord.—'Sound,' ii. (1894).
(9) Stokes, G. G.—Phil. Mag. xxxvi. p. 401 (1868); Phil. Trans. c lviii. p. 447 (1868).

XLI. *Precision Measurements of Crystal Parameters.* *By* Professor E. A. Owen, *M.A., D.Sc., and* E. L. Yates, *M.Sc., University College of North Wales, Bangor* *.

IN a previous paper the crystal parameters of a number of the elements, determined by precision X-ray analysis, were recorded. The present paper gives an account of further parameter measurements which were carried out to a higher degree of accuracy ; some of the elements were also in a purer state than formerly.

* Communicated by the Authors.

The experimental technique employed has been described elsewhere *, so that no details need be given here other than the additional precautions taken to increase the degree of accuracy of the measurements.

Apparatus.

Two precision cameras were employed, one having an effective radius of 52·19 mm. (camera 1) and the other an effective radius of 69·63 mm. (camera 2). Each camera had a number of small holes drilled along the edges of the slots over which the film was placed. The actual distances between these holes were accurately known, and by measuring the distances between the imprints of the holes on the films corrections could be applied for uneven contraction or expansion of the film produced in the developing operation. Special care was taken to ensure that the film at all points was in contact with the circumference of the camera.

All measurements of the film were made with an instrument which had been calibrated by comparison with a Hilger travelling microscope, the error in any part of the scale of which did not exceed 0·02 mm. Sets of measurements of a constant distance taken with both instruments over different parts of their scales were found to agree within 0·02 per cent. This is well within the error allowed in measuring the arcs between corresponding lines in the X-ray photographs.

Corrections.

The parameter is given by the relation

$$a = \frac{\lambda\sqrt{\Sigma h^2}}{2\cos\frac{s}{8r}}, \quad \ldots\ldots\ldots \quad (1)$$

where s is the length of the arc measured on the film, r the radius of the camera, and λ the wave-length of the X-rays used. If δa is the maximum error in the parameter, then

* Owen and Iball, Phil. Mag. vol. xiii. p. 1020 (1932); Owen and Pickup, Proc. Roy. Soc. A, vol. cxxxvii. p. 397 (1932).

$$\delta a = \pm\sqrt{\left(\frac{a}{\lambda}\right)^2(\delta\lambda)^2+\left(\frac{as}{8r^2}.\tan\frac{s}{8r}\right)^2(\delta r)^2+\left(\frac{a}{8r}.\tan\frac{s}{8r}\right)^2.(\delta s)^2}, \quad . \; . \; . \quad (2)$$

where $\delta\lambda$, δr, and δs are respectively the errors in the wave-length, the radius of the camera, and the measurement of the distance between corresponding lines on the film.

The values of the wave-lengths of the X-rays employed were obtained from the International Critical Tables (vol. vi. p. 37). These differ from those given by Siegbahn (' Spectroscopy of X-rays,' p. 105) by as much as 0·0001 Å. in some cases. We shall assume $\delta\lambda = \pm$ 0·0001 Å., and that the radii of the cameras, which were measured with the Hilger travelling microscope, had a maximum error of $\pm$0·05 mm. The estimated mean error in the radius was less than this.

The accuracy with which the arcs could be measured depended entirely on the definition of the spectral lines. Lines near the ends of the film were much narrower and better defined than those near the centre ; lines near the centre need not, however, be measured to the same accuracy as those near the end to obtain the same accuracy of parameter determination. By repeated measurement of lines situated near the ends of several films it was found that these arcs could in general be measured to well within $\pm$0·1 mm. Taking the maximum value of s—that is, the length of the slot over which the photographic film was laid—and assuming that this arc length could be measured to the above accuracy, then the maximum error due to all the sources of error above mentioned, in a parameter value of 5·0 Å. measured with camera no. 1 and employing a wave-length 1·5 Å., is by (2) equal to $\pm$0·00087 Å., or about 0·02 per cent. This is the maximum error in the value of the parameter calculated from the measurement of the arc between one pair of lines situated in the most unfavourable position on the film for high accuracy of parameter determination. The error in the final value of the parameter obtained by the use of two different cameras and radiation of different wave-lengths, giving lines in various positions along the film, is, however, much smaller. An approximate estimate of the probable

error under these conditions may be obtained by the application of the theory of least squares, if not too small a number of independent determinations be made.

It was found that the accuracy of the final determination of the parameters for the materials examined was of the order of 1 in 20,000, in which case it was necessary to look into the correction to be applied on account of deviation from Bragg's Law. Darwin and Ewald have independently shown that if a be the true parameter value of a lattice, and a_1 the parameter as determined by Bragg's equation, then

$$a=a_1\left(1+\frac{5{\cdot}4a^2\rho 10^{-6}}{n^2\Sigma h^2}\right), \quad . \quad . \quad . \quad . \quad (3)$$

where ρ is the density of the reflecting material. Taking, for example, the case of iridium, for which ρ is 22·4 gm. per c.c. and a_1 is 3·831 Å., in the observation of the first order reflexion from the (311) planes when using chromium radiation, we get

$$\frac{(a-a_1)}{a_1}=+0{\cdot}00016,$$

that is, an increase of 0·016 per cent. must be made in the parameter deduced directly from Bragg's equation to obtain the true parameter. This correction is made in the last column but one in Tables I. to XI. For some of the lighter elements the correction is small and well within experimental error, but it has been included in all the tables.

Treatment of the Metals.

Fine filings were prepared of all the materials except gold, aluminium, and lead; gold was already in fine powder form, and aluminium and lead were used in the form of thin foil. The filings were in each case tested for iron; only with iridium were appreciable quantities of iron found in the powder. As a first step in the heat treatment the filings were gently heated in a pyrex glass tube, connected to a vacuum oil-pump which maintained the pressure at about 0·001 mm. of mercury. This operation was conducted to ensure that the powder, before sealing the tube for the final annealing, was free from moisture and also as far as possible from occluded gases. After sealing the evacuated tube the material was

annealed for a length of time which varied from metal to metal. Details of the heat treatment given to each metal and the results of the measurement of the photographs are given below. The mean air temperature near the camera during each exposure was recorded.

TABLE I.—Gold.

Radiation.	Camera.	Temp. (°C.).	Arc (s) (mm.).	Line.	Reflecting planes.	Parameter. Observed (Å.).	Corrected (Å.).	Calculated at 18° C. (Å.).
Copper	No. 1.	17	80·40	α_1	511	$4{\cdot}0694_7$	$4{\cdot}0698_3$	$4{\cdot}0698_9$
			74·94	α_2	333	$4{\cdot}0696_8$		
	No. 2.	17	107·44	α_1	511	$4{\cdot}0697_2$	$4{\cdot}0700_3$	$4{\cdot}0700_9$
			100·08	α_2	333	$4{\cdot}0698_2$		
Nickel	No. 1.	17	124·77	β	511 333	$4{\cdot}0697_8$	$4{\cdot}0700_4$	$4{\cdot}0700_3$
			38·36	α_1	422	$4{\cdot}0698_5$	$4{\cdot}0699_0$	
			24·96	α_2	422	$4{\cdot}0693_8$		
	No. 2.	17	50·64	α_1	422	$4{\cdot}0694_8$	$4{\cdot}0696_0$	$4{\cdot}0696_6$
			32·77	α_2	422	$4{\cdot}0691_5$		
Cobalt	No. 1.	18	124·20	α_1	331	$4{\cdot}0696_6$	$4{\cdot}0700_4$	$4{\cdot}0698_7$
			121·21	α_2	331	$4{\cdot}0697_2$		
			96·22	β	422	$4{\cdot}0694_7$	$4{\cdot}0697_7$	
			81·54	α_1	420	$4{\cdot}0693_7$	$4{\cdot}0697_9$	
			76·91	α_2	420	$4{\cdot}0695_0$		
	No. 2.	19	165·62	α_1	331	$4{\cdot}0694_9$	$4{\cdot}0697_1$	$4{\cdot}0697_3$
			161·49	α_2	331	$4{\cdot}0692_4$		
			128·34	β	422	$4{\cdot}0694_2$	$4{\cdot}0697_1$	
			109·01	α_1	420	$4{\cdot}0697_0$	$4{\cdot}0699_6$	
			102·56	α_2	420	$4{\cdot}0595_3$		
Iron	No. 1.	17	146·74	β	331	$4{\cdot}0692_6$	$4{\cdot}0696_1$	4·0697
			133·12	α_1	400	$4{\cdot}0692_2$	$4{\cdot}0696_6$	
			113·57	β	420	$4{\cdot}0694_3$	$4{\cdot}0697_8$	
	No. 2.	19	177·79	α_1	400	$4{\cdot}0596_8$	$4{\cdot}0701_2$	$4{\cdot}0700_3$
			151·70	β	420	$4{\cdot}0698_1$	$4{\cdot}0701_6$	
Chromium	No. 1.	18	98·16	α_1	222	$4{\cdot}0696_8$	$4{\cdot}0701_3$	$4{\cdot}0701_3$
			95·02	α_2	222	$4{\cdot}0694_2$		
	No. 2.	19	207·97	α_1	311	$4{\cdot}0696_6$	$4{\cdot}0701_1$	$4{\cdot}0700_8$
			205·50	α_2	311	$4{\cdot}0694_1$		
			130·82	α_1	222	$4{\cdot}0695_0$	$4{\cdot}0701_8$	
			126·93	α_2	222	$4{\cdot}0697_0$		

Mean value of the parameter of gold at 18° C $= 4{\cdot}0699 \pm 0{\cdot}0003$ Å.

Results.

1. *Gold.*

A small quantity of spectroscopically pure gold in fine powder form was available. The material was

not subjected to any heat treatment before mounting in the camera. On account of the fineness of the powder the lines in the photograph were somewhat broader than those obtained with annealed metals, but they could be measured with fair accuracy, and they give a very consistent set of results. The coefficient of linear expansion of gold at 20° C. was taken to be $14{\cdot}2\times10^{-6}$.

TABLE II.—Platinum.

Radiation.	Camera.	Temp. (°C.).	Arc (mm.).	Line.	Reflecting planes.	Parameter. Observed (Å.).	Corrected (Å.).	Calculated at 18° C. (Å.).
Copper	No. 1.	18	115·84	α_1	422	$3{\cdot}9155_5$	$3{\cdot}9158_6$	$3{\cdot}9158_6$
			112·11	α_2	422	$3{\cdot}9156_0$		
	No. 2.	18	154·70	α_1	422	$3{\cdot}9158_6$	$3{\cdot}9160_6$	$3{\cdot}9160_6$
			149·61	α_2	422	$3{\cdot}9156_9$		
Nickel	No. 1.	16	139·32	α_1	420	$3{\cdot}9155_1$	$3{\cdot}9158_9$	$3{\cdot}9159_6$
			136·51	α_2	420	$3{\cdot}9155_7$		
	No. 2.	15	185·92	α_1	420	$3{\cdot}9156_9$	$3{\cdot}9160_9$	$3{\cdot}9162_0$
			182·20	α_2	420	$3{\cdot}9157_9$		
Cobalt	No. 1.	17·5	46·25	α_1	331	$3{\cdot}9149_3$	$3{\cdot}9153_6$	$3{\cdot}9153_8$
			37·33	α_2	331	$3{\cdot}9150_8$		
	No. 2.	19	61·90	α_1	331	$3{\cdot}9150_9$	$3{\cdot}9154_0$	$3{\cdot}9153_6$
			49·68	α_2	331	$3{\cdot}9150_0$		
Iron	No. 1.	15	92·00	β	331	$3{\cdot}9152_4$	$3{\cdot}9155_9$	$3{\cdot}9157_1$
			67·40	α_1	400	$3{\cdot}9150_5$	$3{\cdot}9156_0$	
			62·12	α_2	400	$3{\cdot}9152_7$		
	No. 2.	17	122·94	β	331	$3{\cdot}9155_4$	$3{\cdot}9158_9$	$3{\cdot}9157_9$
			90·07	α_1	400	$3{\cdot}9152_3$	$3{\cdot}9156_0$	
			82·70	α_2	400	$3{\cdot}9151_0$		
Chromium	No. 1.	18	106·10	α_1	311	$3{\cdot}9150_2$	$3{\cdot}9157_4$	$3{\cdot}9157_4$
			103·42	α_2	311	$3{\cdot}9152_1$		
	No. 2.	19	141·78	α_1	311	$3{\cdot}9154_4$	$3{\cdot}9159_8$	$3{\cdot}9159_4$
			138·00	α_2	311	$3{\cdot}9152_6$		

Mean value of the parameter of platinum at 18° C. $=3{\cdot}9158\pm0{\cdot}0003$ Å.

2. *Platinum.*

Filings were prepared from a small specimen of spectroscopically pure platinum. They were annealed *in vacuo* in a pyrex glass tube for one hour at 500° C. The photographs showed that this amount of annealing was sufficient, well defined lines being obtained with each radiation. The coefficient of linear expansion of platinum at 20° C. was taken to be $8{\cdot}9\times10^{-6}$.

3. *Palladium.*

The material available was a short length of spectroscopically pure palladium wire from which filings were prepared; these were annealed *in vacuo* for six hours at 400° C. Care was taken to ensure that the metal was dry and as free as possible from occluded gases. The filings were gently heated in a container in which a low

TABLE III.—Palladium.

Radiation.	Camera.	Temp. (°C.).	Arc (mm.).	Line.	Reflecting planes.	Parameter. Observed (Å.).	Corrected (Å.).	Calculated at 18° C. (Å.).
Nickel	No. 1.	17	139·88	β	422	$3{\cdot}8828_4$	$3{\cdot}8829_8$	$3{\cdot}8829_4$
			128·70	α_1	420	$3{\cdot}8825_5$		
			125·65	α_2	420	$3{\cdot}8826_6$	$3{\cdot}8827_9$	
	No. 2.	16	211·48	α_1	331	$3{\cdot}8823_4$	$3{\cdot}8827_1$	
			208·34	α_2	331	$3{\cdot}8827_0$		
			186·28	β	422	$3{\cdot}8820_5$	$3{\cdot}8821_9$	$3{\cdot}8825_8$
			171·58	α_1	420	$3{\cdot}8822_9$	$3{\cdot}8825_6$	
			167·53	α_2	420	$3{\cdot}8824_5$		
Copper	No. 1.	17	102·60	α_1	422	$3{\cdot}8824_5$	$3{\cdot}8826_5$	$3{\cdot}8827_0$
			98·36	α_2	422	$3{\cdot}8825_3$		
	No. 2.	17	136·70	α_1	422	$3{\cdot}8821_2$	$3{\cdot}8822_6$	$3{\cdot}8823_1$
			131·00	α_2	422	$3{\cdot}8820_7$		
Iron	No. 1.	12	74·33	β	331	$3{\cdot}8819_2$	$3{\cdot}8821_1$	$3{\cdot}8823_9$
			39·75	α_1	400	$3{\cdot}8817_3$	$3{\cdot}8821_2$	
			30·00	α_2	400	$3{\cdot}8820_4$		
	No. 2.	17·5	99·26	β	331	$3{\cdot}8820_5$	$3{\cdot}8822_4$	$3{\cdot}8822_1$
			53·36	α_1	400	$3{\cdot}8819_5$	$3{\cdot}8821_2$	
			39·56	α_2	400	$3{\cdot}8818_1$		
Chromium	No. 1.	18	91·45	α_1	311	$3{\cdot}8820_7$	$3{\cdot}8824_1$	$3{\cdot}8824_1$
			88·22	α_2	311	$3{\cdot}8820_5$		
	No. 2.	19	122·11	α_1	311	$3{\cdot}8822_1$	$3{\cdot}8825_5$	$3{\cdot}8825_1$
			117·78	α_2	311	$3{\cdot}8821_9$		

Mean value of the parameter of palladium at 18° C. $=3{\cdot}8824 \pm 0{\cdot}0003$ Å.

pressure was maintained. The lines in all the photographs were very well defined. The coefficient of linear expansion of palladium at 20° C. was taken to be $11{\cdot}8 \times 10^{-6}$.

The values of the parameter obtained with nickel radiation are greater than those obtained with the other radiations. They have been omitted in calculating the mean value. The discrepancy was considered to be due to a small quantity of occluded gas still remaining in the

reflecting material. The lattice parameter measured a fortnight later with copper radiation gave the value 3·8825 Å., a decrease of 0·0002 Å. on the previous value. A measurement made a further fortnight later yielded the value 3·8823 Å. Subsequent measurements fluctuated about this value. The mean value given in Table III. is probably correct to the accuracy stated for the state of the material when under observation. Occluded gas has a marked effect on the crystal lattice of palladium,

TABLE IV.—Rhodium.

Radiation.	Camera.	Temp. (°C.).	Arc (mm.).	Line.	Reflecting planes.	Parameter. Observed (Å.).	Corrected (Å.).	Calculated at 18° C. (Å.).
Copper	No. 1.	17	52·16	α_1	422	$3{\cdot}7954_0$	$3{\cdot}7955_1$	$3{\cdot}7955_4$
			42·91	α_2	422	$3{\cdot}7953_3$		
	No. 2.	17	69·74	α_1	422	$3{\cdot}7955_3$	$3{\cdot}7956_4$	$3{\cdot}7956_7$
			57·43	α_2	422	$3{\cdot}7954_5$		
Nickel	No. 1.	17	132·64	α_1	331	$3{\cdot}7958_2$	$3{\cdot}7957_{11}$	$3{\cdot}7956_5$
			129·45	α_2	331	$3{\cdot}7952_3$		
			108·90	β	422	$3{\cdot}7953_4$	$3{\cdot}7954_9$	
			94·11	α_1	420	$3{\cdot}7955_8$	$3{\cdot}7956_8$	
			89·70	α_2	420	$3{\cdot}7954_2$		
	No. 2.	17	176·90	α_1	331	$3{\cdot}7957_0$	$3{\cdot}7960_0$	$3{\cdot}7959_9$
			173·03	α_2	331	$3{\cdot}7959_5$		
			125·64	α_1	420	$3{\cdot}7957_1$	$3{\cdot}7959_3$	
			119·91	α_2	420	$3{\cdot}7957_9$		
Cobalt	No. 1.	19	144·63	α_1	400	$3{\cdot}7951_7$	$3{\cdot}7953_9$	$3{\cdot}7953_6$
			141·80	α_2	400	$3{\cdot}7951_4$		
	No. 2.	19	211·50	β	331	$3{\cdot}7954_3$	$3{\cdot}7956_1$	$3{\cdot}7954_6$
			192·75	α_1	400	$3{\cdot}7955_2$	$3{\cdot}7955_6$	
			189·16	α_2	400	$3{\cdot}7951_1$	$3{\cdot}7953_0$	
			171·49	β	420	$3{\cdot}7951_2$		

Mean value of the parameter of rhodium at 18° C. = $3{\cdot}7956 \pm 0{\cdot}0003$ Å.

and the only satisfactory procedure is to make the measurement of the parameter when the material is *in vacuo*. A suitable camera has now been designed for this purpose.

4. *Rhodium.*

The specimen from which filings were prepared was one which had been used by Rose * for the determination of the density of this element. It was specimen "B"

* J. Inst. Metals, vol. xxxiii. p. 109 (1925).

referred to in Rose's paper, and the material was spectroscopically pure. To calculate roughly where the lines should appear in the photographs the metal was assumed to possess a face-centred cubic structure with a lattice parameter of about 3·795 Å.; the measurements recorded here prove the validity of this assumption. Jaeger and Zanstra * have recently reported evidence of a phase possessing simple cubic structure with parameter 9·21 Å. A cubic lattice of this dimension would be expected to give a large number of lines with the precision cameras used in the present investigation. None of the photographs gave any indication of this simple cubic form.

The first filings made were annealed *in vacuo* in a silica tube at 800° C. for five hours and then quenched. As the silica tube showed signs of devitrification, to avoid risk of contamination another specimen was prepared. This was annealed in an evacuated pyrex tube for one hour at 400° C. The results given in Table IV. were obtained with this specimen. It was later found that the first specimen gave, within experimental error, the same value for the parameter. The coefficient of linear expansion of rhodium at 20° C. was taken to be $8{\cdot}4\times10^{-6}$.

5. *Lead.*

A piece of lead foil (99·9 per cent. pure), the surface of which was lightly scratched with glass-paper, was used as reflecting material. The lines in the photographs were faint, but they were well defined and could be measured with accuracy. Increased exposure produced little improvement, because it increased the intensity of the background as well as that of the lines. The coefficient of linear expansion of lead at 20° C. was taken to be $29{\cdot}1\times10^{-6}$.

6. *Iridium.*

The parameter of iridium previously recorded referred to a sample the minimum degree of purity of which was 99·5 per cent. The specimen now examined was 99·8 per cent. pure.

* K. Akad. Amsterdam, Proc. vol. xxxiv. (1), p. 15 (1931).

TABLE V.—Lead.

Radiation.	Camera.	Temp. (°C.).	Arc (mm.).	Line.	Reflecting planes.	Parameter. Observed (Å.).	Corrected (Å.).	Calculated at 18° C. (Å.).
Copper	No. 1.	17	74·17	α_1	620	$4{\cdot}9393_8$	$4{\cdot}9394_2$	$4{\cdot}9395_6$
			67·93	α_2	620	$4{\cdot}9391_0$		
	No. 2.	17	203·84	α_1	600	$4{\cdot}9391_9$	$4{\cdot}9396_0$	$4{\cdot}9397_4$
			200·32	α_2	442	$4{\cdot}9396_0$		
Nickel	No. 1.	16	56·46	α_1	531	$4{\cdot}9391_6$	$4{\cdot}9393_3$	$4{\cdot}9396_2$
			48·75	α_2	531	$4{\cdot}9390_9$		
	No. 2.	18	75·22	α_1	531	$4{\cdot}9390_4$	$4{\cdot}9394_4$	$4{\cdot}9394_4$
			65·35	α_2	531	$4{\cdot}9394_2$		
Cobalt	No. 1.	19	146·51	α_1	333	$4{\cdot}9392_6$	$4{\cdot}9395_4$	$4{\cdot}9394_0$
			144·00	α_2	511	$4{\cdot}9392_8$		
	No. 2.	19	195·50	α_1	333	$4{\cdot}9393_9$	$4{\cdot}9398_4$	$4{\cdot}9397_0$
			192·27	α_2	511	$4{\cdot}9397_5$		
Iron	No. 1.	18	121·14	α_1	422	$4{\cdot}9390_3$	$4{\cdot}9394_7$	$4{\cdot}9394_7$
			118·34	α_2	422	$4{\cdot}9393_0$		
	No. 2.	15	161·55	α_1	422	$4{\cdot}9388_5$	$4{\cdot}9392_5$	$4{\cdot}9396_9$
			157·78	α_2	422	$4{\cdot}9390_5$		

Mean value of the parameter of lead at 18° C. $=4{\cdot}9396 \pm 0{\cdot}0003$ Å.

TABLE VI.—Iridium.

Radiation.	Camera.	Temp. (°C.).	Arc (mm.).	Line.	Reflecting planes.	Parameter. Observed (Å.).	Corrected (Å.).	Calculated at 18° C. (Å.).
Copper	No. 1.	16	77·15	α_1	422	$3{\cdot}8310_3$	$3{\cdot}8312_5$	$3{\cdot}8313_0$
			71·24	α_2	422	$3{\cdot}8309_2$		
	No. 2.	16	103·49	α_1	422	$3{\cdot}8318_3$	$3{\cdot}8312_7$	$3{\cdot}8313_2$
			94·38	α_2	422	$3{\cdot}8301_5$		
Nickel	No. 1.	19	122·66	β	422	$3{\cdot}8311_2$	$3{\cdot}8314_0$	$3{\cdot}8314_2$
			109·84	α_1	420	$3{\cdot}8312_0$	$3{\cdot}8314_9$	
			106·06	α_2	420	$3{\cdot}8311_1$		
	No. 2.	18	192·14	α_1	331	$3{\cdot}8313_4$	$3{\cdot}8310_6$	$3{\cdot}8310_6$
			187·88	α_2	331	$3{\cdot}8301_0$		
Cobalt	No. 2.	19	206·49	α_1	400	$3{\cdot}8307_7$	$3{\cdot}8311_4$	$3{\cdot}8310_5$
			203·30	α_2	400	$3{\cdot}8306_8$		
			187·06	β	420	$3{\cdot}8306_7$	$3{\cdot}8310_1$	

Mean value of the parameter of iridium at 18° C. $=3{\cdot}8312 \pm 0{\cdot}0005$ Å.

Owing to the extreme hardness of the metal considerable difficulty was experienced both in the filing of the

specimen and in the annealing of the powder. Iron-free iridium powder annealed *in vacuo* for one hour at 400° C. gave no lines when photographed. The powder was re-annealed under the same conditions for four hours at 500° C. An indication of a band was observed on the film. Twelve hours' more annealing at 600° C. produced broad lines which were just resolved. The material was further annealed for 240 hours at 600° C. After this treatment photographs in which the lines were well enough resolved to measure were recorded,

TABLE VII.—Iron.

Radiation.	Camera.	Temp. (°C.).	Arc (mm.).	Line.	Reflecting planes.	Parameter. Observed (Å.).	Parameter. Corrected (Å.).	Parameter. Calculated at 18° C. (Å.).
Cobalt.....	No. 1.	18	67·89	α_1	310	$2{\cdot}8605_3$	$2{\cdot}8606_3$	$2{\cdot}8606_3$
			62·10	α_2	310	$2{\cdot}8605_3$		
	No. 2.	19	90·59	α_1	310	$2{\cdot}8605_3$	$2{\cdot}8605_6$	$2{\cdot}8605_3$
			82·67	α_2	310	$2{\cdot}8603_9$		
Iron	No. 1.	15	125·53	α_1	220	$2{\cdot}8606_7$	$2{\cdot}8609_9$	$2{\cdot}8609_9$
			122·95	α_2	220	$2{\cdot}8610_7$		
			104·36	β	310	$2{\cdot}8606_8$	$2{\cdot}8607_8$	
	No. 2.	17	167·52	α_1	220	$2{\cdot}8607_6$	$2{\cdot}8609_8$	$2{\cdot}8608_7$
			163·95	α_2	220	$2{\cdot}8609_8$		
			139·20	β	310	$2{\cdot}8605_9$	$2{\cdot}8606_9$	
Chromium ..	No. 1.	18	87·15	α_1	211	$2{\cdot}8606_6$	$2{\cdot}8608_3$	$2{\cdot}8608_3$
			83·75	α_2	211	$2{\cdot}8606_7$		
	No. 2.	18	116·23	α_1	211	$2{\cdot}8606_3$	$2{\cdot}8608_1$	$2{\cdot}8608_1$
			111·71	α_2	211	$2{\cdot}8606_6$		

Mean value of the parameter of iron at 18° C. $=2{\cdot}8608 \pm 0{\cdot}0003$ Å.

but the results are not considered to be as accurate as those obtained with the other materials examined. The coefficient of linear expansion of iridium at 20° C. was taken to be $6{\cdot}5 \times 10^{-6}$.

7. *Iron.*

Filings prepared from a specimen of very pure iron (total impurities 0·018 per cent. plus traces not estimated) were annealed in an evacuated pyrex glass tube for four hours at 600° C. Poor reflexion lines were obtained. A fresh specimen was prepared and annealed *in vacuo*

for 100 hours at 600° C. Very well defined lines were now obtained. The coefficient of linear expansion of iron at 20° C. was taken to be $11{\cdot}7 \times 10^{-6}$.

A second specimen, annealed *in vacuo* for three hours and a half at 600° C., gave the results tabulated in Table VIII.

8. *Aluminium.*

Since the X-rays penetrate aluminium to an appreciable depth it is necessary to use very thin layers of material.

TABLE VIII.—Iron.

Radiation.	Camera.	Temp. (°C.).	Arc (mm.).	Line.	Reflecting planes.	Parameter. Observed (Å.).	Corrected Å.	Calculated at 18° C. (Å.).
obalt.....	No. 1.	17	67·86	α_1	310	$2{\cdot}8604_5$	$2{\cdot}8605_5$	$2{\cdot}8606_5$
			62·12	α_2	310	$2{\cdot}8605_8$	$2{\cdot}8606_8$	
	No. 2.	18	90·70	α_1	310	$2{\cdot}8606_3$	$2{\cdot}8607_3$	$2{\cdot}8606_3$
			82·67	α_2	310	$2{\cdot}8604_0$	$2{\cdot}8605_0$	
on	No. 1.	18	125·50	α_1	220	$2{\cdot}8606_2$	$2{\cdot}8607_4$	$2{\cdot}8605_9$
			122·72	α_2	220	$2{\cdot}8606_0$	$2{\cdot}8607_2$	
			104·10	β	310	$2{\cdot}8601_9$	$2{\cdot}8603_0$	
	No. 2.	17	167·42	α_1	220	$2{\cdot}8606_1$	$2{\cdot}8607_3$	$2{\cdot}8608_1$
			163·87	α_2	220	$2{\cdot}8608_3$	$2{\cdot}8609_5$	
			139·16	β	310	$2{\cdot}8605_5$	$2{\cdot}8606_5$	
romium ..	No. 1.	18	87·12	α_1	211	$2{\cdot}8606_2$	$2{\cdot}8607_8$	$2{\cdot}8608_2$
			83·75	α_2	211	$2{\cdot}8606_9$	$2{\cdot}8608_5$	
	No. 2.	18	116·28	α_1	211	$2{\cdot}8606_8$	$2{\cdot}8608_4$	$2{\cdot}8608_7$
			111·85	α_2	211	$2{\cdot}8607_5$	$2{\cdot}8609_1$	

Mean value of the parameter of iron at 18° C. $=2{\cdot}8607 \pm 0{\cdot}0003$ Å.

The final mean value of the parameter of iron at 18° C. is $2{\cdot}8607_5 \pm 0{\cdot}0002$ Å.

A piece of aluminium, 99·6 per cent. pure, obtained from a single crystal, was rolled down to a thickness of 0·02 mm. and annealed *in vacuo* for one hour at 400° C. For mounting in the camera the foil was glued to thin card in preference to copper sheet. The results of the measurements of the films are given in Table IX. The coefficient of linear expansion of aluminium at 20° C. was taken to be $23{\cdot}03 \times 10^{-6}$.

9. *Copper.*

Filings were prepared from electrolytic copper (99·9 per cent. pure) and annealed *in vacuo* for two hours at 600° C.

TABLE IX.—Aluminium.

Radiation.	Camera.	Temp. (°C.).	Arc (mm.).	Line.	Reflecting planes.	Parameter. Observed (Å.).	Corrected (Å.).	Calculated at 18° C. (Å.)
Copper	No. 1.	17·5	63·11	α_1	511	$4{\cdot}0403_6$	$4{\cdot}0404_4$	$4{\cdot}0404_9$
			55·90	α_2	333	$4{\cdot}0404_7$		
	No. 2.	17	84·09	α_1	511	$4{\cdot}0402_1$	$4{\cdot}0404_0$	$4{\cdot}0404_9$
			74·66	α_2	333	$4{\cdot}0405_2$		
Cobalt	No. 1.	17	114·00	α_1	331	$4{\cdot}0406_1$	$4{\cdot}0406_6$	$4{\cdot}0407_8$
			110·70	α_2	331	$4{\cdot}0406_1$		
			64·92	α_1	420	$4{\cdot}0407_7$	$4{\cdot}0407_2$	
			58·68	α_2	420	$4{\cdot}0405_8$		
	No. 2.	20	152·06	α_1	331	$4{\cdot}0405_6$	$4{\cdot}0406_0$	$4{\cdot}0404_3$
			147·65	α_2	331	$4{\cdot}0405_5$		
			86·45	α_1	420	$4{\cdot}0405_8$	$4{\cdot}0407_1$	
			78·41	α_2	420	$4{\cdot}0407_4$		
Iron	No. 1.	15	138·41	β	331	$4{\cdot}0405_4$	$4{\cdot}0405_9$	$4{\cdot}0410_1$
			123·93	α_1	400	$4{\cdot}0408_4$	$4{\cdot}0409_0$	
			102·38	β	420	$4{\cdot}0406_9$	$4{\cdot}0407_4$	
	No. 2.	18	184·69	β	331	$4{\cdot}0406_4$	$4{\cdot}0406_9$	$4{\cdot}0406_7$
			165·30	α_1	400	$4{\cdot}0407_6$	$4{\cdot}0408_2$	
			136·45	β	420	$4{\cdot}0404_4$	$4{\cdot}0404_9$	
Chromium	No. 1.	17	148·07	α_1	311	$4{\cdot}0407_0$	$4{\cdot}0406_6$	$4{\cdot}0407_5$
			146·07	α_2	311	$4{\cdot}0404_4$		
	No. 2.	19	197·54	α_1	311	$4{\cdot}0407_2$	$4{\cdot}0406_5$	$4{\cdot}0405_8$
			194·85	α_1	311	$4{\cdot}0403_9$		

Mean value of the parameter of aluminium at 18° C. $= 4{\cdot}0406_5 \pm 0{\cdot}0002$ Å.

TABLE X.—Copper.

Radiation.	Camera.	Temp. (°C.).	Arc (mm.).	Line.	Reflecting planes.	Parameter. Observed (Å.).	Corrected (Å.).	Calculated at 18° C. (Å.)
Copper	No. 1.	17	128·72	α_1	420	$3{\cdot}6077_8$	$3{\cdot}6078_7$	$3{\cdot}6079_{\ldots}$
			125·39	α_2	420	$3{\cdot}6077_6$		
	No. 2.	18	171·69	α_1	420	$3{\cdot}6077_3$	$3{\cdot}6078_7$	$3{\cdot}6078_7$
			167·27	α_2	420	$3{\cdot}6078_0$		
Cobalt	No. 1.	18	89·47	β	331	$3{\cdot}6076_3$	$3{\cdot}6077_4$	$3{\cdot}6077_1$
			59·83	α_1	400	$3{\cdot}6075_5$	$3{\cdot}6076_8$	
			53·13	α_2	400	$3{\cdot}6075_4$		
	No. 2.	20	119·24	β	331	$3{\cdot}6074_6$	$3{\cdot}6075_7$	$3{\cdot}6075_{\ldots}$
			79·88	α_1	400	$3{\cdot}6076_1$	$3{\cdot}6077_0$	
			70·87	α_2	400	$3{\cdot}6075_3$		

Mean value of the parameter of copper at 18° C. $= 3{\cdot}6077_5 \pm 0{\cdot}0002$ Å.

The results are tabulated in Table X. The coefficient of linear expansion of copper at 20° C. was taken to be $16{\cdot}6 \times 10^{-6}$.

TABLE XI.—Silver.

Radiation.	Camera.	Temp. (°C.).	Arc (mm.).	Line.	Reflecting planes.	Parameter. Observed (Å.).	Corrected (Å.).	Calculated at 18° C. (Å.).
Copper	No. 1.	17	84·17	α_1	511	$4{\cdot}0768_1$	$4{\cdot}0771_1$	$4{\cdot}0771_9$
			79·03	α_2	333	$4{\cdot}0771_2$		
	No. 2.	18	112·45	α_1	511	$4{\cdot}0770_5$	$4{\cdot}0772_8$	$4{\cdot}0772_8$
			105·51	α_2	333	$4{\cdot}0772_3$		
Nickel	No. 1.	19	127·20	β	511	$4{\cdot}0771_5$	$4{\cdot}0772_8$	$4{\cdot}0772_0$
					333			
			45·66	α_1	422	$4{\cdot}0770_3$	$4{\cdot}0772_8$	
			35·96	α_2	422	$4{\cdot}0772_2$		
	No. 2.	18	60·89	α_1	422	$4{\cdot}0770_2$	$4{\cdot}0772_4$	$4{\cdot}0772_4$
			47·25	α_2	422	$4{\cdot}0771_4$		
Cobalt	No. 1.	18	126·66	α_1	331	$4{\cdot}0771_0$	$4{\cdot}0771_7$	$4{\cdot}0770_7$
			123·63	α_2	331	$4{\cdot}0768_5$		
			85·32	α_1	420	$4{\cdot}0768_4$	$4{\cdot}0769_6$	
			80·73	α_2	420	$4{\cdot}0767_0$		
	No. 2.	20	168·97	α_1	331	$4{\cdot}0770_8$	$4{\cdot}0772_6$	$4{\cdot}0771_5$
			165·04	α_2	331	$4{\cdot}0770_7$		
			114·02	α_1	420	$4{\cdot}0771_4$	$4{\cdot}0773_4$	
			108·02	α_2	420	$4{\cdot}0771_6$		
Iron	No. 1.	18	135·56	α_1	400	$4{\cdot}0771_5$	$4{\cdot}0773_7$	$4{\cdot}0773_4$
			133·00	α_2	400	$4{\cdot}0771_1$	$4{\cdot}0773_1$	
			116·36	β	420	$4{\cdot}0771_2$		
	No. 2.	17	198·63	β	331	$4{\cdot}0770_4$	$4{\cdot}0772_3$	$4{\cdot}0773_7$
			180·95	α_1	400	$4{\cdot}0771_2$	$4{\cdot}0774_3$	
			177·49	α_2	400	$4{\cdot}0772_7$		
			155·18	β	420	$4{\cdot}0770_1$	$4{\cdot}0772_0$	
Chromium	No. 1.	17	101·24	α_1	222	$4{\cdot}0770_5$	$4{\cdot}0772_9$	$4{\cdot}0773_7$
			98·27	α_2	222	$4{\cdot}0768_9$		
	No. 2.	19	210·56	α_1	311	$4{\cdot}0771_2$	$4{\cdot}0772_8$	$4{\cdot}0772_3$
			208·05	α_2	311	$4{\cdot}0768_0$		
			134·89	α_1	222	$4{\cdot}0767_4$	$4{\cdot}0773_1$	
			131·31	α_2	222	$4{\cdot}0772_4$		

Mean value of the parameter of silver at 18° C. $=4{\cdot}0772_4 \pm 0{\cdot}0002$ Å.

10. *Silver.*

Silver filings (99·9 per cent. pure) were annealed *in vacuo* for three hours and a half at 500° C. The photographs showed well defined lines which yielded very consistent

results, as will be seen from Table XI. The coefficient of linear expansion of silver at 20° C. was taken to be $18{\cdot}9 \times 10^{-6}$.

The above results for aluminium, copper, and silver agree closely with the values previously recorded for these elements. Since the present results were obtained under totally different conditions—different cameras, specimens, and installations,—and there is good agreement with the old values, the parameters are given to a closer degree of accuracy than was previously possible.

A comparison of the results obtained with different radiations shows a tendency for the parameter determined with iron and chromium radiations to be somewhat greater than those determined with copper radiation. A tendency in the opposite direction is shown with cobalt radiation. It is probable that the wave-lengths of these radiations need slight adjustments.

TABLE XII.—X-ray Wave-lengths.

	Copper.	Nickel.	Cobalt.	Iron.	Chromium.
$K\alpha_1$	1·53739 Å.	1·65450	1·78529	1·93208	2·28503
$K\alpha_2$	1·54126	1·65835	1·78919	1·93601	2·28891
$K\beta$.....	1·38927	1·49705	1·61744	1·75301	2·08059

The wave-lengths of radiations used in the present investigation are collected in Table XII.

As measurements of the parameters were made at different temperatures all the values were reduced to 18° C., approximately the mean of the different temperatures of experiment. A reduction to this temperature introduces minimum error in respect of the values assumed for the coefficients of expansion.

Density.

The accuracy with which the densities can be calculated from the X-ray data depends upon the accuracy of the values of (*a*) the mass of the hydrogen atom, (*b*) the atomic weight of the element, and (*c*) the lattice parameter

of the crystal. An error of $\pm 0{\cdot}0003$ Å. in the lattice parameter or an error of $\pm 0{\cdot}05$ in the atomic weight introduces an error of $\pm 0{\cdot}005$ gm. per c.c. in the density. The uncertainty of our knowledge of the mass of the hydrogen atom considerably limits the accuracy of the densities. The most recent value of the mass of the

TABLE XIII.

Metal and degree of purity.	Parameter at 18° C. (observed).	Atomic weight (0 = 16).	Density at 20° C. (calc.).	Parameter at 0° C. (calc.).	Density at 0° C. (calc.).	Experimental density (I. C. T.).
	Å.		gm./c.c.	Å.	gm./c.c.	gm./c.c.
Gold *	4·0699 ±0·0003	197·2	$19{\cdot}29_4$ ±0·02	4·0688	$19{\cdot}30_9$	19·297 (0° C.).
Platinum *	3·9158 ±0·0003	195·23	$21{\cdot}44_7$ ±0·02	3·9151	$21{\cdot}45_9$	21·440 (20° C.).
Palladium *	3·8824 ±0·0003	106·7	$12{\cdot}02_7$ ±0·02	3·8816	$12{\cdot}03_6$	12·1 (0° C.).
Rhodium *	3·7956 ±0·0003	102·91	$12{\cdot}41_4$ ±0·02	3·7951	$12{\cdot}42_0$	12·5 (0° C.).
Lead (99·9 per cent.)	4·9396 ±0·0003	207·22	$11{\cdot}33_9$ ±0·01	4·9371	$11{\cdot}35_7$	11·347 (20°C.).
Iridium (99·8 per cent.)	3·8312 ±0·0005	193·1	$22{\cdot}65_0$ ±0·03	3·8308	$22{\cdot}65_6$	22·4 (0° C.).
Iron (99·98 per cent.)	$2{\cdot}8607_5$ ±0·0002	55·84	$7{\cdot}86_6$ ±0·01	2·8602	$7{\cdot}87_1$	7·90 (20° C.).
Aluminium (99·6 per cent.)	$4{\cdot}0406_5$ ±0·0002	26·97	$2{\cdot}69_7$ ±0·005	4·0390	$2{\cdot}70_0$	2·699 (20° C.).
Copper (99·9 per cent.)	$3{\cdot}6077_5$ ±0·0002	63·57	$8{\cdot}92_9$ ±0·01	3·6067	$8{\cdot}93_9$	8·94 (20° C.).
Silver (99·9 per cent.)	$4{\cdot}0772_4$ ±0·0002	107·88	$10{\cdot}49_3$ ±0·01	4·0758	$10{\cdot}51_1$	$10{\cdot}49_2$ (20° C.).

* Spectroscopically pure.

hydrogen atom (m_H) is $(1{\cdot}662 \pm 0{\cdot}002) \times 10^{-24}$ gm. Taking the atomic weight of hydrogen to be 1·0078 (0 = 16·00), the mass of an atom of unit atomic weight (m) is $(1{\cdot}649 \pm 0{\cdot}002) \times 10^{-24}$ gm. In the case of iridium (density 22·4) the probable error in the value of m produces an error of $\pm 0{\cdot}027$ gm. per c.c. in the density. The error in the calculated value of the density of each

element given in Table XIII. is mainly due to the error in the mass of the hydrogen atom.

The atomic weights were taken from the Thirty-sixth Annual Report of the Committee on Atomic Weights published in the 'Journal of the American Chemical Society,' March 1930.

The value of the density of rhodium (12·42 gm. per c.c.) deduced from the experimental value of the parameter does not agree with the direct determination of the density by Rose (12·47 gm. per c.c.). The difference between the two values is well beyond the limits of accuracy of our measurements. It is intended to investigate this metal further with a vacuum camera.

All the values of the parameters except that of palladium agree within experimental error with the values published previously by Owen and Iball *. Palladium was on this occasion carefully treated to remove occluded gases, and has yielded a lower parameter value. Measurements of the parameter of this metal *in vacuo* are now in progress.

We wish to take this opportunity of expressing our indebtedness and thanks to Messrs. Johnson Matthey, Ltd., of Hatton Garden, London, for supplying us with the materials.

Summary.

The lattice parameters of ten elements, each possessing cubic symmetry, were measured by a precision X-ray method. Four of the elements were spectroscopically pure and the others were of a high degree of purity. The lattice parameters at 18° C. were found to be as follows:—Au $4{\cdot}0699 \pm 0{\cdot}0003$ Å.; Pt $3{\cdot}9158 \pm 0{\cdot}0003$; Pd $3{\cdot}8824 \pm 0{\cdot}0003$; Rh $3{\cdot}7957 \pm 0{\cdot}0003$; Pb $4{\cdot}9396 \pm 0{\cdot}0003$; Ir $3{\cdot}8312 \pm 0{\cdot}0005_5$; Fe $2{\cdot}8607_5 \pm 0{\cdot}0002$; Al $4{\cdot}0406_5 \pm 0{\cdot}0002$; Cu $3{\cdot}6077_5 \pm 0{\cdot}0002$; Ag $4{\cdot}0772_4 \pm 0{\cdot}0002$. The values have been corrected for deviation from Bragg's Law. The crystal densities of the materials at 0° C. and 20° C. were calculated from the above parameters.

Bangor,
12th December, 1932.

* *Loc. cit.*

XLII. *The Diffusion of Electrolytes.* *By* R. J. Davies, *M.Sc., Simon Research Scholar, Washington Singer Laboratories, University College, Exeter* *.

1. Introduction.

THE study of diffusion is one capable of providing valuable information concerning the behaviour of particles in solution. Diffusion, the process by which intermixture of fluids takes place, occurs in all solutions provided that a concentration gradient exists within the liquid. With unionizing solutions the migratory movements of the solute are attributed to the osmotic pressure exerted by the particles, and in the case of electrolytic solutions to the combined effect of the osmotic pressures of the ions and the electrical potential gradient established in the solution on account of the generally different mobilities of the positive and negative ions. Early experimental work by Graham † established the facts that diffusion is comparatively slow in liquids and depends upon the concentration gradient existing in the solution. The process was also shown to vary with the nature of the salt used and to increase with concentration and temperature. These facts have been incorporated by Fick ‡ in his well-known Law of Diffusion, which may be stated as follows :—If the concentration gradient, measured at right angles to a plane drawn in the liquid along the direction (x) of constant density, is $\frac{dn}{dx}$, the mass of dissolved substance crossing unit area of this plane per second is $k.\frac{dn}{dx}$, where k is known as the coefficient of diffusion of the solute. Thus k_n, the diffusion coefficient at a concentration n, is the mass of solute migrating, under unit concentration gradient, across unit area situated in solution of this concentration.

* Communicated by Prof. F. H. Newman, D.Sc.

† Phil. Trans. A, cxl. pp. 1, 805 (1850); cxli. p. 483 (1851); cxliv. p. 177 (1854).

‡ Pogg. *Ann.* xciv. p. 59 (1855).

An immediate deduction from Fick's Law is the general equation of diffusion which may be written in the form

$$\frac{dn}{dt} = k_n \cdot \frac{d^2n}{dx^2}, \quad \ldots\ldots\ldots \quad (1)$$

where $\frac{dn}{dt}$ is the rate of change of concentration at a point in the solution at which the concentration gradient is $\frac{dn}{dx}$. This is the general equation governing the process of diffusion; by applying Fourier's theorem it is possible to deduce, in a form containing k_n, the concentration at a given point at any time subsequent to a given distribution of solute. Consequently equation (1) suffices to solve any problem when the initial conditions are given, and if the variation of concentration at some point is determined from time to time it will be possible to evaluate the coefficient of diffusion.

The various experimental investigations which followed the enunciation of Fick's Law show a great diversity in the methods adopted for determining the concentration at different points in the solution. It is evident that every precaution must be taken to eliminate even small disturbances of the solutions during experiment, and this condition is not realized in many of the methods of investigation commonly employed. In Kelvin's * method the concentration was determined very simply by noting the position of a series of glass beads of varying densities placed in the liquid, so that the density distribution could be observed throughout the experiment. Scheffer † and Öholm ‡ both determined the distribution of solute in the diffusing liquid by siphoning the solution into a number of separate flasks and subjecting their contents to chemical analysis. The adoption of such a method clearly makes it impossible to avoid disturbances in the liquid, which would be of quite a serious magnitude when dilute solutions are under investigation. Other methods which have been used with differing degrees of success are measurements of refractive indices §,

* See Beilstein, Lieb. *Ann.* xcix. p. 165 (1856).
† See Arrhenius, *Zeits. phys. chem.* ii. p. 390 (1880).
‡ *Ibid.* l. p. 309 (1904).
§ Wiener, Wied. *Ann.* xlix. p. 105 (1893).

rotation of polarized light for sugar solutions, and contact potential differences *. More recently Littlewood † has developed an optical method of determining concentrations to within about 0·05 gram per litre at any point and time during diffusion. On account of the changing density with depth, a ray of light, incident at grazing angle on the top surface, is bent into the form of an arc, the total deviation depending only on the refractive indices at the point of entrance into and exit from the solution. Consequently the change in deviation for a given angle of incidence depends on the difference in concentration at the various points of emergence at the side of the vessel when the incident ray is displaced laterally. Littlewood measured this difference by a tilting mirror device, capable of indicating deviations of the order of one minute of arc. From such measurements of the change in concentration with depth, made at various times, all the data necessary for a calculation of the coefficient of diffusion are obtained.

Recently Clack ‡, by a somewhat similar method, which is capable of measuring concentrations at points fairly close together, was enabled to make more detailed investigation of the change in diffusion coefficient with concentration. Clack's work marks a considerable advance in the experimental study of diffusion ; it consists of an optical examination of the "steady state" of diffusion in a diffusion cell of special design, in which a definite vertical concentration gradient from practically zero strength to saturation is produced. In common with Littlewood's experiment the method overcomes the problem which characterized the early work, viz., the determination of the concentration at various points of the solution without disturbing the diffusion process, since when steady conditions are reached the change of refractive index with depth is measured from the deviation of a ray of light, in this case initially horizontal, as it penetrates layers of increasing density. The method of measurement is different, however, and depends upon the vertical displacement of the central fringe in the interference pattern produced by two narrow horizontal

* Weber, *ibid.* vii. pp. 469, 536 (1879).
† Proc. Roy. Soc. A, xxxiv. p. 3 (1922).
‡ Proc. Phys. Soc. xxxvi. p. 331 (1924).

slits illuminated by the green line of the mercury arc spectrum (λ=5461 Å.). The Rayleigh refractometer is used to investigate the change of refractive index with concentration, and a combination of these results determines the distribution of concentration with depth. Further, since the " steady state " of diffusion is employed evaluation of the coefficient is greatly facilitated, the laborious calculations involving the Fourier series being eliminated.

In the present work the main features of Clack's method have been retained ; various modifications of the apparatus and experimental procedure have, however, been introduced, and electrolytes of a different type investigated. In Clack's work the variation of k_n with concentration for the univalent strong electrolytes, potassium chloride, sodium chloride, and potassium nitrate, was determined. In the present investigation the variation of the coefficient for the bivalent binary salts, magnesium sulphate and cadmium sulphate, has been studied. Since the principle of the former work is employed in these experiments the following account is mainly concerned with the results obtained and the experimental arrangements and procedure.

2. Experimental Arrangements.

A complete account of the theory of the method has been given by Clack *, and is briefly as follows :—

Consider a uniform vertical tube XY (fig. 1 (*a*)) initially filled with a saturated salt solution, so arranged that its upper end is kept in contact with pure water or a solution of very feeble concentration, and its lower end in contact with a saturated solution of the salt by providing it with a shallow compartment, AB, which contains crystals of the salt. After a time the mass of salt diffusing from the top of the cell will become constant and a definite concentration gradient established in the cell, *i. e.*, the " steady state " of diffusion is attained. Applying Fick's Law to the loss of solute from the cell and the gain of solvent, since solvent flows in to fill the space previously occupied by the solute, the equation

$$k_n = \frac{C}{A} \cdot \frac{dl}{dn} \cdot \frac{d-n+n\delta}{d-n} \quad . \quad . \quad . \quad . \quad . \quad . \quad (2)$$

* Proc. Phys. Soc. xxix. p. 50 (1916).

is obtained, where

n =concentration of the solution in gm. per c.c. at a point l cm. below the top of the diffusion tube ;

d =density of the solution at the same point ;

δ =ratio of the mass of water which enters the top of the diffusion tube to the mass of salt, C, leaving it per second ;

A =cross-section of the tube in sq. cm.

Thus the coefficient of diffusion, k_n, at any definite concentration, n, can be determined by means of

Fig. 1.

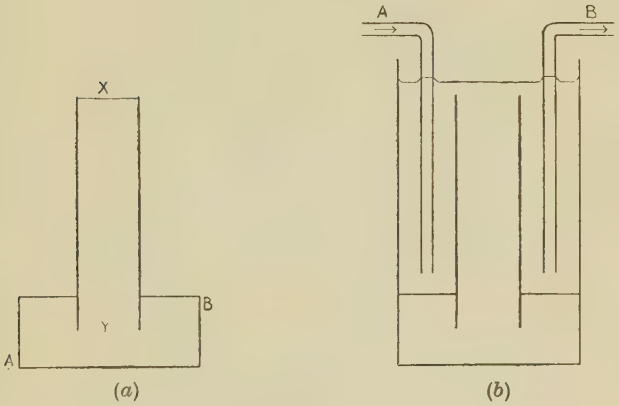

The diffusion cell.

equation (2) from a knowledge of the following quantities, when the steady state is reached :—

(*a*) C, the mass of solute leaving the cell per second ;

(*b*) $\frac{dn}{dl}$, the rate of change of concentration with depth ;

(*c*) the ratio of the mass of water entering the cell to the mass of solute leaving it per second ;

(*d*) the density, d, and the concentration, n, at any point l cm. down the tube.

For the sake of clarity the description of the experiment is subdivided into the determinations of the

quantities represented by the three fractions on the right-hand side of equation (2), viz.,

$$\frac{C}{A}, \frac{dn}{dl}, \text{ and } \frac{d-n+n\delta}{d-n}.$$

(*a*) Determination of "C."

The diffusion cell is represented in fig. 1 (*b*) ; it is made of glass plates cemented together, and is fitted at its lower end with a shallow glass box. The latter is filled with crystals of the salt under test, and the central diffusion tube with an air-free saturated solution of the salt ; the outer parts of the cell are filled with distilled water up to a level 4–5 mm. above the top of the diffusion tube, and a slow steady current of distilled water of about 35 c.c. per day is maintained through the cell, the water entering by the tube A and leaving by B. In about thirty days after the flow has commenced, the steady state is reached, in which the water current removes the salt as fast as it diffuses up the tube. The concentration of the solution at the top then reaches a value only slightly greater than zero, and the concentration at each point of the tube continues constant, remaining saturated at the bottom by reason of the salt crystals. In the optical determination of $\frac{dn}{dl}$ monochromatic light from a double-slit traverses the cell ; consequently the front and back faces of the cell are made of optically plane glass, in order that the horizontal interference fringes may not suffer distortion. The height of the complete cell is 6·8 cm. and that of the diffusion column 5·02 cm. The width of the column is 1·26 cm. and the thickness, t, 4·05 cm., giving the cross-sectional area, A, as 5·103 sq. cm.

The arrangements for producing the slow constant flow of water are shown in fig. 2 *. A number of capillary tubes of small bore are connected together by means of high-pressure rubber tubing, as shown in arrangement A. A reservoir C, containing mercury, is connected by pressure tubing to the bottom capillary tube, and may be raised or lowered, so producing a variable pressure

* See also Davies, " A Device for Producing a slow constant Flow of Liquid." Journal of Scientific Instruments, viii. p. 110 (1931).

head. By means of the upward flow of mercury through the tubes air-bubbles, which occur in the rubber tubing if a downward flow is adopted, are eliminated. From the exit-tube of the set A mercury drops into a constant-level reservoir D, which is again of variable height. In this reservoir the level is maintained constant by means of the open tube E, which also provides an outlet for the

Fig. 2.

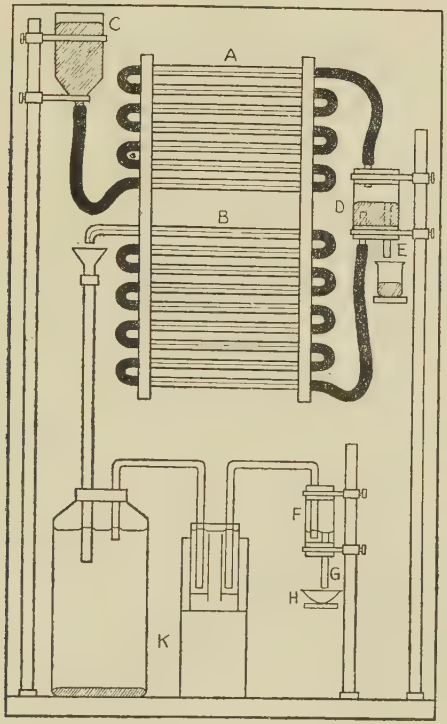

The constant water-flow arrangement.

excess of mercury. The total length of capillary tubing in the set B is greater than that of A; the tubes are connected together in exactly the same way, the flow again being upwards. Mercury from the exit-tube of B drops into a funnel-shaped tube, and thence into a large glass vessel, K, containing distilled water. The mercury displaces the water in K, which passes by means of a

siphon into the diffusion cell and is removed by a second siphon to the constant-level trap, F, from which it drops at a steady rate into the crucible H. The apparatus is rigidly mounted on a large vertical wooden panel which is firmly attached to a heavy wooden base. The latter supports the vessel K, and holds the supports for the reservoirs C and D, the diffusion cell, and the trap F. The capillary tubes are mounted 3·5 cm. apart, passing through holes in strips of wood attached to the panel. Using seven capillary tubes of 30 cm. length and 0·25 mm. bore in A, and nine of the same size in B, a steady flow of 25 c.c. to 150 c.c. a day may be obtained ; a flow of 36 c.c. a day was maintained without appreciable variation throughout the present work. The apparatus is set up on a vibration-proof bench mounted on stone pillars which extend into the foundations of the building. The whole is rigidly built, every precaution being taken to avoid any vibration of the diffusion cell.

The mass of salt, C, diffusing from the cell per second in the steady state, was determined as follows. The solution dropping from the exit-tube G per 24 hours was collected in a porcelain crucible H, and the liquid evaporated over a water-bath at 100° C. The residue was then carefully dried and weighed ; it is estimated that by taking precautions to ensure that the anhydrous salt is perfectly dry the value of C per 24 hours was obtained accurate to 0·0001 gram. The mass of salt diffusing from the cell daily was recorded, and results showed that with both of the salts investigated the mass became quite constant after the experiment had been in progress twenty-five to thirty days.

A further check on the attainment of steady conditions in the cell is provided by the optical experiments to determine $\frac{dn}{dl}$. The values obtained after continuing the experiment for thirty-two days in each case are

$MgSO_4$: C = 0·1225 gm. per day = $1{\cdot}418 \times 10^{-6}$ gm. per sec. ;
$CdSO_4$: C = 0·2252 gm. per day = $2{\cdot}604 \times 10^{-6}$ gm. per sec.

(*b*) Determination of "$\frac{dn}{dl}$."

The values of $\frac{dn}{dl}$ (which may be written in the form

$\frac{dn}{d\mu} \cdot \frac{d\mu}{dl}$) for concentrations ranging from zero to saturation, are obtained experimentally by means of independent determinations of $\frac{d\mu}{dl}$ and $\frac{d\mu}{dn}$, where μ is the refractive index of the solution of concentration n grams per c.c. In this work several departures have been made from the procedure adopted by Clack, the foremost of which is the determination of the quantities $\frac{d\mu}{dl}$ and $\frac{d\mu}{dn}$, employing monochromatic light of the same wave-length in each case. In the previous experiments, the mercury

Fig. 3.

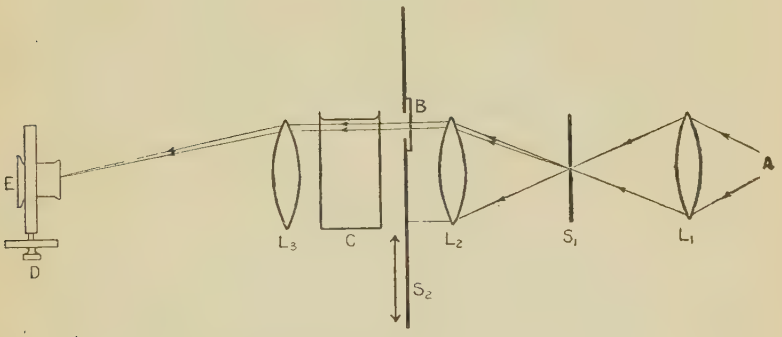

The optical arrangement.

green light ($\lambda = 5461$ Å.), obtained from the mercury arc lamp with the constant deviation spectroscope, was used in the determination of $\frac{d\mu}{dl}$, and sodium yellow light ($\lambda = 5893$ Å.) in the measurement of $\frac{d\mu}{dn}$, the two determinations being correlated by means of Cauchy's formula. Utilizing a simple device introduced by the writer, however, the sodium yellow light has now been employed in both experiments, thus achieving a greater degree of certainty in the measurements made and effecting considerable simplification of the method. Other modifications in the determination of $\frac{d\mu}{dl}$ concern

the size and method of preparation of the double-slit. the nature of the eyepiece used, the focal lengths of the lenses employed, and the experimental procedure adopted.

A section of the optical arrangement for measuring $\frac{d\mu}{dl}$ is shown in fig. 3. By means of the lens L_1 light from the sodium lamp at A is brought to a focus at a horizontal slit in a screen S_1. A second lens, L_2, of similar diameter to L_1, is situated at a distance equal to its focal length from the screen S_1; consequently L_2 gives a parallel beam of light. This beam is intercepted by an aluminium screen, S_2, which, however, has a double-slit at B, from which a pencil of light passes through the diffusion cell, C, and is brought to a focus in the eyepiece, E, by a third lens, L_3; the field of view in the eyepiece is then crossed by bright horizontal interference fringes. It has been shown by Clack that the light passing through the cell will be deviated through a small angle, α, where

$$\alpha = \frac{d\mu}{dl} . t, \quad . \quad . \quad . \quad . \quad . \quad . \quad (3)$$

t being the thickness of the cell ($=4{\cdot}05$ cm.) and $\frac{d\mu}{dl}$ the rate of change of refractive index with depth in the plane of the pencil of light. Accordingly the fringes in the eyepiece are displaced through a distance, h, given by

$$\alpha = \frac{h}{F}, \quad . \quad . \quad . \quad . \quad . \quad . \quad . \quad (4)$$

where F is the focal length of the lens L_3. Then from equations (3) and (4)

$$\frac{d\mu}{dl} = \frac{h}{F.t} . \quad . \quad . \quad . \quad . \quad . \quad . \quad . \quad (5)$$

Since F and t are known, it is only necessary to measure the displacement, h, of the fringes in the eyepiece when the light passes through the cell at various depths, to determine $\frac{d\mu}{dl}$ at these points.

The device for producing the sodium light * consists simply of a Bunsen burner inverted over a fireclay crucible containing common salt. When suitably adjusted, a yellow flame is obtained which gives a very bright band of light around the rim of the crucible ; this light, focussed on to a horizontal slit, provides an illumination which is many times more intense than that obtainable by means of the usual methods employing common salt. The latter generally demand frequent adjustment on account of the melting and spluttering away of the salt ; this device, however, overcomes these difficulties, and gives a light which continues for long periods without attention. In a preliminary series of experiments with the present apparatus the mercury green light was employed, using the mercury arc lamp and the constant deviation spectroscope ; this light was found to give fringes so faint that perfect darkness was necessary. With the sodium burner, which was subsequently introduced, the 5893 Å doublet was obtained with sufficient intensity that readings could be taken comfortably in subdued daylight.

The movable aluminium screen, S_2, was attached to the travelling stage of a cathetometer, which was capable of giving the position of the double-slit accurate to 0·1 mm. A rectangular hole, 2 cm. $\times$ 1 cm., was cut in the screen, and over this hole was cemented the photographically prepared double-slit. The method of preparation of these slits is worthy of note. In the previous experiments of Clack they were made from silvered glass plates by scraping away the deposited silver with a finely ground hacksaw blade. In the present case they consisted of the negative obtained by photographing two thick black lines drawn on a large sheet of drawing paper. A number of negatives containing slits of varying widths and distances of separation were prepared, the most satisfactory of which was one with slits 0·3 mm. wide and 0·8 mm. between corresponding points. This was found to give three bright interference fringes in the eyepiece. The negatives were made on "Imperial" Process Plates, and were developed in solutions prepared according to the Imperial Hydro-

* See also Davies, "A Source of Sodium Radiation," Journal of Scientific Instruments, ix. p. 297 (1932).

quinone formula, which gave dense black negatives with very clear slits.

The micrometer eyepiece, E, used for measuring the deflexion, h, of the fringes, contains a cross-wire capable of travelling over an aperture of about 1·2 cm. The milled screw, D, which controls the cross-wire, moves the latter 0·025 cm. for each revolution of the screw-head ; the circumference of D is divided into 100 equal parts, and it is estimated that the position of the central fringe in the eyepiece, and therefore the value of h, is determined with an accuracy of 0·005 mm. In order to accommodate deflexions greater than 1 cm., the eyepiece is attached to the moving stage of a travelling microscope, all vertical movements of the eyepiece being calibrated against the corresponding movement of the fringes within the eyepiece. In this way deflexions of any magnitude may be measured ; actually the maximum deflexion observed was 1·9235 cm. with cadmium sulphate.

The lenses L_1, L_2, and L_3 are all corrected optical-lantern objectives having a diameter slightly greater than 5 cm. L_1 possesses a very short focal length in order that it may receive a wide-angled beam of light from the source A ; L_2 has a greater focal length (approximately 12 cm.), the whole arrangement being adjusted so that the light from L_1 completely covers the surface of L_2. In the experiment with cadmium sulphate a lens L_3 of focal length 28·01 cm. was used, while with magnesium sulphate a different lens of 30·83 cm. focal length was employed. In making the measurements the screen S_2 is moved down from $l=0$ to $l=5$ in intervals of 2 mm., the position of the central fringe being recorded at each step. In a preliminary calibration experiment the cell was securely cemented into position and filled with distilled water ; readings were then taken of the position of the central fringe for different values of l. The value of h for any given position of the double-slit is then given by the distance between the position of the central fringe when the cell contains pure water and that when the steady state of diffusion has been attained. With distilled water very little movement of the fringes was found to occur over the range $l=0{\cdot}2$ cm. to $l=4{\cdot}8$ cm. ; when the light was passing through the extreme edges of the lens system, however, as it is between $l=0$ and

$l=0{\cdot}2$, and $l=4{\cdot}8$ and $l=5{\cdot}0$, the fringes showed a greater movement and were slightly distorted. In order that the measurements made in the region of dilute solution, *i. e.*, at the top of the diffusion tube, may be subject to a minimum of uncertainty, the whole lens system was raised through 0·2 cm., so that reliable values of h were obtained from $l=0$ to $l=4{\cdot}6$; the l/h curves were then extrapolated beyond $l=4{\cdot}6$ to $l=5{\cdot}0$. Results showed that the curves are perfectly smooth from $l=2$ to $l=4{\cdot}6$, and since it is improbable that these solutions will exhibit any irregularity of behaviour in the region of saturation this extrapolation would appear to be fully justified.

From these results the values of h $\left(\text{or } \frac{d\mu}{dl}\right)$ for different values of l were determined; it is necessary, however, to know the relation between $\frac{d\mu}{dl}$ and n, or between l and n. This is obtained by a graphical determination, using these curves, of the relation between l and μ, and a further determination of the refractive index of the solutions at different concentrations, by means of the Rayleigh refractometer. If the function $\frac{d\mu}{dl}$ is plotted against l as abscissa, and the total area of the curve between the ordinates at the origin and at L is measured, where L denotes the total length of the diffusion tube, then

$$\int_0^{\mathrm{L}} \left(\frac{d\mu}{dl}\right) dl = \mu_{\mathrm{N}} - \mu_{\mathrm{N}_0}, \quad . \quad . \quad . \quad . \quad . \quad (6)$$

where μ_{N} is the refractive index of the saturated solution at the bottom of the tube where $l=\mathrm{L}$, and μ_{N_0} that of the very dilute solution at the top of the tube where $l=0$. Similarly, if μ_n is the refractive index of the solution of concentration n at a point l cm. below the top of the tube,

$$\int_0^{l} \left(\frac{d\mu}{dl}\right) dl = \mu_n - \mu_{\mathrm{N}_0}. \quad . \quad . \quad . \quad . \quad . \quad (7)$$

The value of the integral was determined graphically for various values of l, and so the relation between μ and l obtained. Considerable uncertainty exists as to the concentration of the dilute solution at the top of the

diffusion tube ; in this work the value of μ_{N_0} was taken as that for pure water. Since pure water flows into the cell we might take, as an approximation, the concentration of the solution to be one-half of that of the solution flowing from the cell ; this would give 0·003 gram per c.c. in the case of cadmium sulphate and 0·002 gram per c.c. for magnesium sulphate. Consequently it is evident that the error introduced by taking μ_{N_0} as the refractive index of pure water will be extremely small.

Values of μ and $\frac{d\mu}{dn}$ for solutions of different concentrations were next determined with the Rayleigh refractometer, using the yellow sodium light as in the preceding work. Samples of solution, ranging in concentration from zero to saturation, were prepared in pairs, the concentrations of the members of each pair differing only very slightly ; the refractive index of each sample was then determined. By plotting μ against n the general relationship between refractive index and concentration is obtained. Further, by evaluating $\frac{d\mu}{dn}$ for each pair of samples and plotting the value against the average concentration of the pair the second relationship is obtained.

The numerical relations between concentration, refractive index, and $\frac{dl}{dn}$, obtained as the result of the optical experiments, are summarized in Table I.

(*c*) Determination of "$\frac{d-n+n\delta}{d-n}$."

The third factor necessary for the calculation of the coefficient of diffusion is, from equation (2), the quantity $\frac{d-n+n\delta}{d-n}$; its evaluation involves the determination of δ, the ratio of the mass of water entering the top of the diffusion tube to the mass of salt leaving it per second in the steady state, and the variation of the density of the solution with concentration. Clack * has shown that δ is given by the relationship

$$\delta = \frac{D-N}{Z-N}, \quad . \quad . \quad . \quad . \quad . \quad . \quad . \quad . \quad (8)$$

* Proc. Phys. Soc. xxxiii. p. 259 (1921).

where

N = concentration of saturated solution in gm. per c.c.,
D = density of saturated solution in gm. per c.c., and
Z = density of the salt crystals.

The quantities D and Z were both determined by the simple density-bottle method, while N was obtained by

TABLE I.

Magnesium Sulphate.

Position in tube (l cm.).	Refractive index (μ).	Concentration (n gm. per c.c.).	$\frac{dl}{dn}$.
0	1·334(1)	(0·002)	19·66(0)
0·5	1·339(0)	0·028	18·77(6)
1·0	1·3441	0·058	18·122
1·5	1·3494	0·088	17·819
2·0	1.3546	0·120	18·034
2·5	1·3599	0·152	18·357
3·0	1·3649	0·181	18·960
3·5	1·3698	0·210	19·714
4·0	1·3745	0·237	20·669
4·5	1·3789	0·265	21·969
5·0	1·383(2)	0·286	23·70(1)
	Cadmium Sulphate.		
0	1·334(1)	(0·003)	6·89(9)
0·5	1·341(0)	0·073	6·318
1·0	1·3485	0·151	5·897
1·5	1·3574	0·245	5·694
2·0	1·3645	0·318	5·688
2·5	1·3725	0·401	5·822
3·0	1·3802	0·480	6·015
3·5	1·3876	0·556	6·257
4·0	1·3948	0·631	6·507
4·5	1·4016	0·700	6·886
5·0	1·408(0)	0·768	7·28(2)

evaporation of the solvent as in the foregoing work. The resulting values of δ are :

Magnesium sulphate ..... $\delta = 0{\cdot}6809$;
Cadmium sulphate ..... $\delta = 0{\cdot}3826$.

The variation of density with concentration was determined in a similar manner, d being obtained by the density-bottle method and n by the evaporation of a known volume of solution. The values of $\frac{d-n+n\delta}{d-n}$

from zero concentration to saturation, calculated from these results, are given in Table II.

TABLE II.

Magnesium sulphate.			Cadmium sulphate.		
Concentration (gm. per c.c.).	Density (gm. per c.c.).	$\frac{d-n+n\delta}{d-n}$.	Concentration (gm. per c.c.).	Density (gm. per c.c.).	$\frac{d-n+n\delta}{d-n}$.
0	1·000	1·000	0	1·000	1·000
0·028	1·023	1·019	0·073	1·061	1·028
0·058	1·048	1·040	0·151	1·125	1·059
0·088	1·072	1·061	0·245	1·204	1·097
0·120	1·098	1·083	0·318	1·265	1·128
0·152	1·125	1·107	0·401	1·335	1·164
0·181	1·148	1·127	0·480	1·401	1·195
0·210	1·171	1·148	0·556	1·464	1·234
0·237	1·195	1·169	0·631	1·527	1·270
0·265	1·218	1·190	0·700	1·586	1·302
0·286	1·236	1·211	0·768	1·641	1·336

TABLE III.

Coefficient of Diffusion of Aqueous Electrolytic Solutions.

Magnesium Sulphate (T=15·5° C.).
Cadmium Sulphate (T=16·8° C.).

Normality.	$k_n \times 10^6$ C.G.S.	Normality.	$k_n \times 10^6$ C.G.S.
0	5·45(2)	0	3·52(0)
0·5	5·30(9)	0·5	3·37(0)
1·0	5·228	1·0	3·254
1·5	5·233	1·5	3·181
2·0	5·406	2·0	3·166
2·5	5·621	2·5	3·203
3·0	5·898	3·0	3·271
3·5	6·240	3·5	3·377
4·0	6·701	4·0	3·499
4·5	7·22(6)	4·5	3·634
		5·0	3·803
		5·5	3·998
		6·0	4·205
		6·5	4·45(8)
		7·0	4·73(5)

(*d*) Results for k_n.

The values of the coefficient of diffusion, k_n, calculated by means of equation (2), for solutions of the salts magnesium sulphate and cadmium sulphate, are given in Table III. The concentrations of the solutions are

given in terms of the normality (gram equivalents per litre of solution). All measurements were made at room temperature, which varied from 15° to 17° C.

It was noted, when considering the optical experiments, that uncertainty exists as to the concentration of the solution at the top of the diffusion tube when the steady state of diffusion has been established. It is evident, however, that any error introduced into the quantity $\frac{dn}{dl}$, and therefore into the value of k_n, by reason of the assumption that the solution at this point is infinitely dilute, *i. e.*, pure solvent, will be greatest when the measurements refer to dilute solutions and of decreasing importance as solutions of greater concentration are dealt with. If the concentration of the solution in the plane containing the top edges of the diffusion tube is regarded as that of the solution flowing from the cell in the steady state—an improbable assumption—the maximum error introduced into the value of $\frac{dn}{dl}$ for very dilute solutions would be of the order of 0·05 per cent. for the salts employed in the present experiments. The exact magnitude of the importance of the assumption is at present unknown ; the existence of the uncertainty, however, is indicated in Tables I. and III. by noting in parenthesis the digits which may be influenced by the possible error. The curves, constructed from Table III., showing the variation of k_n with concentration, are given in fig. 4.

A further point of uncertainty, involving an error which is possibly of more serious magnitude, concerns the temperature variations throughout the experiment. Nernst * evaluated the diffusion temperature coefficient at ordinary temperatures for a number of neutral salts as 0·026, while Öholm † found that its value for different electrolytes increased as the value of the coefficient of diffusion decreased. In view of the experimental difficulties which characterized the early work on diffusion it is not possible to assess the accuracy of Nernst's value of the temperature coefficient ; but, assuming it to be of the

* *Zeits. phys. chem.* ii. p. 613 (1888).
† *Loc. cit.*

correct order, it is evident that a temperature variation during experiment of only one degree will introduce a serious error. It is thus apparent that all measurements of diffusion should be made under strict thermostatic control. In the present work the temperature variations throughout were very gradual, and for the four or five days following the establishment of steady conditions in the cell it was extremely small. Consequently the temperatures given in Table III. are those which obtained in the cell when the measurements of h were made, viz., 15·5

Fig. 4.

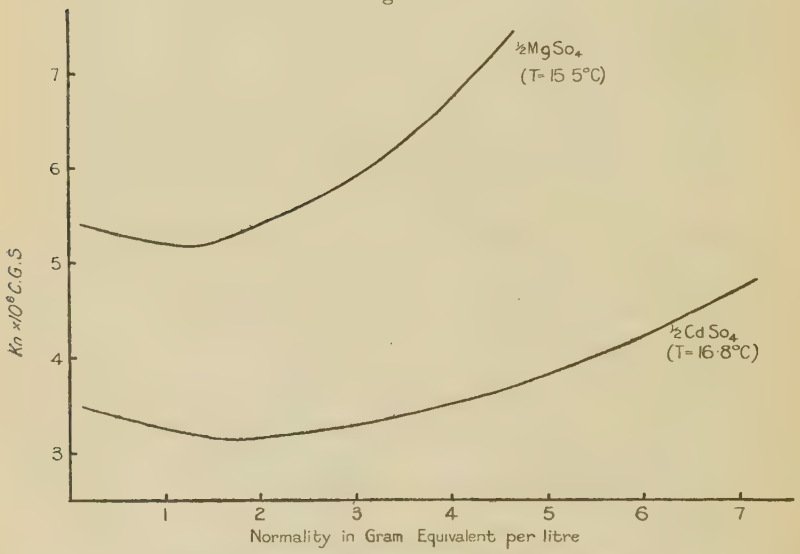

Variation of diffusion coefficient with concentration.

$\pm 0{\cdot}1^\circ$ C. for magnesium sulphate, and $16{\cdot}8 \pm 0{\cdot}1^\circ$ C. for cadmium sulphate. On account of the slight temperature variation, however, it is very doubtful if the values of k_n can be relied upon to more than 0·1 per cent.; in the absence of reliable data of the temperature effect obtained by the more accurate methods which have been developed in recent years no account of the possible error is taken in the numerical results of Table III. The possibility of such error must nevertheless be borne in mind in the employment of these results until the acquisition of accurate data of the temperature coefficient makes

possible a satisfactory estimation of the importance of the temperature variations.

3. Discussion of Experimental Results.

It will be observed that the curves given in fig. 4 are of approximately the same form as those obtained by Clack for potassium chloride, sodium chloride, and potassium nitrate; these curves pass through a minimum value of the diffusion coefficient, after which the coefficient increases with concentration. In the case of potassium and sodium chlorides the minimum is associated with dilute solutions, occurring at 0·3 N. for the former and 0·4 N. for the latter. With potassium nitrate, magnesium sulphate, and cadmium sulphate, however, the minimum value is associated with concentrations in the vicinity of 1·5–2·0 N. The same discrepancy in the situation of the minimum value of the diffusion coefficient is found in the results of early workers on the diffusion of electrolytes; for example, Scheffer * observed the minimum in the region of small concentration, while Öholm's † work suggests a minimum in solution of considerable concentration. In the earlier work the minimum was not so clearly established as in the more recent experiments, its existence being inferred from the general character of the curves obtained; the discrepancies between the positions of the supposed minima of different workers were attributed to uncertainties associated with their various methods of investigation. In most of the early experiments the essential condition demanded of all measurements of diffusion, viz., the avoidance of disturbances of the solution, was denied by the experimental methods.

Arrhenius ‡, by his conception of the principle of ionic dissociation, enabled Nernst § to apply his theory to the diffusion of dilute solutions of electrolytes, with the result that he deduced the well-known expression by means of which the coefficient of diffusion of such solutions was given in terms of the specific ionic velocities. Later Arrhenius ‖ himself attempted to apply these methods to more concentrated solutions, and concluded that the

* *Loc. cit.*
† *Loc. cit.*
‡ *Zeits phys. chem.* i. p. 631 (1887).
§ *Loc. cit.*
‖ *Zeits. phys. chem.* x. p. 51 (1892).

coefficient of diffusion, with increasing concentration, should first fall from its value at infinite dilution on account of decreasing dissociation, and later, in more concentrated solutions, should increase on account of intermolecular attraction. The theory of Arrhenius, however, takes no account of ionic solvation or the existence of complex ions and neutral molecules in solution. A great deal of evidence has accumulated along various lines in favour of the view that ions are, more or less, solvated. An atmosphere of solvent is supposed to move about every ion, the dimensions of this atmosphere, and therefore the frictional resistance to motion of the ion, being determined by the individual characteristics of the ion *. The variation of the diffusion coefficient with concentration may be partly explained on the solvation theory, since, as the concentration is raised, the number of solvent molecules attached to an ion decreases, so that the ionic velocity is increased. Fajans † has deduced from optical measurements that neutral molecules and complex ions are present in solutions of most strong electrolytes. Recently Jacobs & King ‡, from work on the optical properties of strong electrolytes, consider that their observations undoubtedly indicate the existence of some small percentage of undissociated molecules, or ion-pairs or groups, in even the best examples of highly dissociated electrolytes. These conclusions are also supported by the experiments of Kinsey §, Rao ‖, and Woodward ¶ on the Raman absorption spectra of solutions of strong electrolytes.

It is probable that potassium chloride and sodium chloride, and other simple univalent binary salts of the same type, most nearly conform to the conditions assumed by Arrhenius in his simple theory. The theory assumes

* See, for example, Buchböck, *Zeits. phys. chem.* lv. p. 563 (1906); Washburn, *ibid.* lxvi. p. 513 (1909); Riesenfeld, *ibid.* lxvi. p. 672 (1909); Hevesy, *Jahrb. f. Radioakt und Elektromek,* xi. p. 419 (1914); xiii. p. 271 (1916); Ulich, Trans. Farad. Soc. xxiii. p. 392 (1927); Remy, *ibid.* xxiii. p. 387 (1927); Remy & Reisener, *Zeits. phys. chem.* cxxvi. p. 161 (1927); Baborovsky, *ibid.* cxxix. p. 129 (1927); and Baborovsky & Wagner, *ibid.* cxxxi. p. 129 (1928).

† Trans. Farad. Soc. xxiii. p. 357 (1927).

‡ Journ.Phys. Chem. xxxv. p. 480 (1931).

§ Phys. Rev. xxxv. p. 284 (1930).

‖ 'Nature,' cxxiv. p. 762 (1929); Proc. Roy. Soc. A, cxxvii. p. 279 (1930).

¶ *Phys. Zeits.* xxxi. p. 192 (1930); xxxii. pp. 212, 261 (1931).

that the only forms in which the substance exists in solution are the ultimate simple ions into which the molecules dissociate, and the unionized molecules themselves. This assumption is certainly fulfilled in the case of most uni-univalent electrolytes, and it is not surprising that the theory of Arrhenius is supported by measurements made with these simple salts. Bjerrum *, however, has come to the conclusion that certain electrolytes, among them potassium nitrate, cannot be completely dissociated. His argument is that a certain proportion of the ions will form pairs which will act osmotically as single molecules if one or both of these ions has a radius smaller than a critical value. These views find strong support in the computations of MacInnes & Cowperthwaite †. In addition Onsager ‡ has shown that bivalent binary electrolytes in water, in particular magnesium and cadmium sulphates, do not support his formula for the relationship between conductivity and concentration. This lack of coordination is attributed to the presence of complex ions. Later McBain & Rysselberge § found that most bivalent salts contained complex ions to some extent.

It is thus evident that the behaviour of the bivalent group of salts will not comply with the simple theory of Arrhenius, as is the case with the univalent chlorides. From measurements of the electrical conductance of aqueous electrolytic solutions it is seen that there is a surprisingly close agreement between the behaviour of salts of the same valency type. The same correspondence is apparent with respect to the diffusivity ; the curves for magnesium and cadmium sulphates are of distinctly the same form, as are Clack's curves for potassium and sodium chlorides. In Table IV. are given the values of the coefficient of diffusion, k, and the equivalent conductance, Λ, for a number of salts ; all values refer to infinite dilution.

The values of Λ are taken from a table compiled by Noyes & Falk ||, the values of k for potassium chloride, sodium chloride, and potassium nitrate are those of Clack ¶,

* *Kgl. Danske. Viden. Sels.* vii. 9, p. 2 (1926).
† Trans. Farad. Soc. xxiii. p. 400 (1927).
‡ *Phys. Zeits.* xxviii. p. 277 (1927).
§ Journ. Amer. Chem. Soc. l. p. 3009 (1928).
|| *Ibid.* xxxiv. p. 454 (1912).
¶ Proc. Phys. Soc. xxxvi. p. 331 (1924).

that for lithium chloride is due to Öholm *, and those for magnesium sulphate and cadmium sulphate from the present investigation. The results show that the electrolytes which have the greater equivalent conductances also possess the higher diffusion coefficients, in agreement with present views of the nature of these solutions. It will be noted that the diffusion coefficients of the bivalent sulphates are considerably less than those for the univalent salts. This is regarded as partly due to the existence of complex ions and to the fact that the degree of dissociation at great dilution, as given by the "conductance ratio" and freezing-point depression methods, is much smaller—of the order of 0·7—for these

TABLE IV.

Equivalent Conductance and Coefficient of Diffusion at Infinite Dilution.

Electrolyte.	Λ.	$k \times 10^5$.	Temp.
Potassium chloride	122·37	1·55	18° C. approx.
Potassium nitrate	118·10	1·45	,, ,,
Sodium chloride	101·88	1·26	,, ,,
Lithium chloride.....	91·97	1·12	,, ,,
Magnesium sulphate	76·21	0·54	15·5±0·1° C.
Cadmium sulphate	70·34	0·35	16·8±0·1° C.

solutions, *i. e.*, they contain a greater proportion of neutral molecules. These molecules will also diffuse, but at a rate which is, in general, different from that of the ions; usually their diffusion coefficient is less. For instance, Haskell †, working with 0·1 normal solutions of thallium sulphate and barium nitrate, found that the rate of diffusion of the undissociated molecules was only one half that of the ions. The presence of these molecules in the solutions of magnesium and cadmium sulphates will naturally reduce the observed value of k below that which would be obtained from a solution of the ions alone.

As a result of the investigation described in the foregoing pages a number of suggestions for the improvement of the experimental method have been forthcoming. The writer intends to construct a diffusion cell of slightly

* *Loc. cit.*

† Phys. Rev. xxvii. p. 145 (1908).

different design in an attempt to eliminate the present uncertainty as to the concentration of the solution at the top of the diffusion tube, and to effect such modifications in the examination of the steady state of diffusion as will permit an increase in the length of the diffusion tube, so that more detailed information may be obtained of the behaviour of ions at high dilutions. In view of the extreme importance of even small temperature variations, alterations in the form of the apparatus are anticipated, so that it may be more suitable than the present arrangement for the introduction of thermostatic control. It is proposed to pursue investigations of the diffusion of further electrolytes, employing the present method subjected to modifications along these lines. At present very little reliable data of the diffusion of electrolytes is available; the subject is one which is capable of throwing a great deal of light on the nature of these solutions. The present state of the study of electrolytic solutions is due in large measure to the very valuable work which has been done on the conductance of these solutions. Data of equal importance is obtainable from the study of diffusion, in particular that of the inter-diffusion and the diffusion temperature effect of electrolytes in both aqueous and non-aqueous solution. It is to be hoped that, with the recent advances that have been made in the experimental methods, this long-awaited data will shortly be forthcoming in adequate volume.

Summary.

An account is given of an investigation, employing a modified form of the method developed by Clack, of the diffusion of the bivalent binary salts, magnesium sulphate and cadmium sulphate, in aqueous solution. Contrary to Arrhenius's theory, which is supported by Clack's work with the univalent chlorides, the results show a definite minimum value of the coefficient of diffusion in solutions of concentration 1·4 N. and 1·8 N. respectively. Considerations are put forward in support of the view that the discrepancies in the behaviour of the two groups of electrolytes are due to the presence of complex ions and a larger proportion of unionized molecules in solutions of the latter. The theory of ionic solvation is supported by the form of the curves obtained.

XLIII. *A Direct Determination of the Indices and Locations of the Spots in a Laue Pattern of Calcite.* By G. F. Herrenden Harker, *M.A., University College, Cardiff**.

[Plate XII.]

Abstract.

The indices of the spots of a Laue pattern for calcite are deduced from first principles, assuming the lattice type and lattice constants known. The location of the spots as calculated and observed is compared.

Introductory.

It appears to be customary, in English texts treating of the application of X-rays to crystal analysis, to restrict the discussion of the Laue diagram to crystals possessing a cubic lattice. It may, therefore, be of interest to indicate how the indices corresponding to the Laue spots obtained, using an important particular crystal (calcite), can be deduced from first principles, and without recourse to the various types of projection, provided its lattice type and lattice constants are known.

I. *The Space Lattice.*

1. Consider any two line lattices intersecting in a node and defining a lattice plane. Then the family of line lattices drawn parallel to one of these line lattices will form, with the family of line lattices drawn parallel to the other line lattice, a network of parallelograms. If all the nodes located in the plane are situated at the angular points of these parallelograms, the line lattices are said to be conjugate.

Consider any three line lattices which are not coplanar and which intersect in a node. They will define three lattice planes. The families of lattice planes drawn respectively parallel to each of these three lattice planes will partition space by their intersections into a system of parallelepipeds. If all the nodes distributed throughout space are situated at the corners of these parallelepipeds the three line lattices are said to be conjugate, and the three planes determined by them are termed conjugate lattice planes.

2. Let us take as axes Ox, Oy, Oz of oblique coordinates any three conjugate line lattices and let the face-angles

* Communicated by the Author.

yOz, zOx, and xOy be respectively α, β, and γ. Then, if the distances separating consecutive nodes along the axes Ox, Oy, Oz, i. e., the axial parameters, are a, b, and c respectively, the volume of the simple unit cell which is a parallelepiped of edges a, b, and c will be

$$V_p = abc\{1-\cos^2\alpha-\cos^2\beta-\cos^2\gamma+2\cos\alpha\cos\beta\cos\gamma\}^{\frac{1}{2}}.$$

3. The equation to any plane referred to oblique coordinate axes as above will be

$$Ax+By+Cz=D.$$

Putting $$D=AA_1=BB_1=CC_1,$$

this equation becomes

$$x/A_1+y/B_1+z/C_1=1,$$

where the constants A_1, B_1, C_1 represent the intercepts of the plane upon the three coordinate axes.

If these axial intercepts A_1, B_1, and C_1 are respectively equal to a, b, and c, the plane will represent a lattice plane, since it will pass through three nodes, and its equation will be

$$x/a+y/b+z/c=1.$$

In general any lattice plane can be represented by an equation of the form

$$px/a+qy/b+rz/c=K,$$

where p, q, r, and K are integers.

If p, q, and r are prime to one another they define the indices of the lattice plane in the notation of Miller.

If K is given in succession the values 0, ±1, ±2, . . . the corresponding equations will define a parallel family of adjacent lattice planes, *i. e.*, a parallel family of lattice planes specified by the symbol (p, q, r), between the consecutive members of which no nodes are located.

4. The member of this family of adjacent planes whose equation is $px/a+qy/b+rz/c=0$ will clearly pass through the origin.

The equation to the adjacent parallel plane will be

$$px/a+qy/b+rz/c=1.$$

Now the perpendicular distance from the origin on the plane $Ax+By+Cz=D$ will be

$$h_n = \frac{V_p}{abc\,[(A/D)^2\sin^2\alpha+(B/D)^2\sin^2\beta+(C/D)^2\sin^2\gamma \\ -2\{(A/D)(B/D)(\cos\gamma-\cos\alpha\cos\beta) \\ +(B/D)(C/D)(\cos\alpha-\cos\beta\cos\gamma) \\ +(C/D)(A/D)(\cos\beta-\cos\gamma\cos\alpha)\}]^{\frac{1}{2}}}$$

Hence, writing $A/D=p/a$, $B/D=q/b$, $C/D=r/c$, the perpendicular distance from the origin on the plane

$$px/a+qy/b+rz/c=1$$

will be

$$\Delta_{pqr}=\frac{V_p}{[p^2b^2c^2\sin^2\alpha+q^2c^2a^2\sin^2\beta+r^2a^2b^2\sin^2\gamma \\ -2\{pq\,bc.ca\,(\cos\gamma-\cos\alpha\cos\beta) \\ +qr\,ca.ab\,(\cos\alpha-\cos\beta\cos\gamma) \\ +rp\,ab.bc\,(\cos\beta-\cos\gamma\cos\alpha)\}]^{\frac{1}{2}}},$$

and this represents the equidistant interval measured along the normal separating two adjacent members of the family of planes (p, q, r).

II. *Application of the Preceding Results to Calcite.*

1. Take as oblique axes Ox, Oy, Oz three conjugate line lattices directed along the edges of the simple unit cell as indicated in fig. 1. In this figure the simple unit cell (continuous line and Greek letters) is shown inscribed in the unit cleavage cell (broken line edges and capital letters).

The constants of this simple unit cell, which contains nodes, *i. e.*, calcium atoms, only at its corners, are, in the case of calcite,

$$\left.\begin{matrix}a=b=c=4{\cdot}04\times10^{-8}\text{ cm.}\\ \alpha=\beta=\gamma=76^\circ\ 8'\end{matrix}\right\}*.$$

Hence from I., 2,

$$V_p=(4{\cdot}04)^3\{1-3\cos^2 76^\circ\ 8'+2\cos^3 76^\circ\ 8'\}^{\frac{1}{2}}\times10^{-24}\text{ cm.}^3$$
$$=60{\cdot}98\times10^{-24}\text{ cm.}^3$$

Since in the calcite molecule the atom of calcium is more than twice as massive as either of the others, the pattern revealed in the Laue diagram will correspond to the lattice formed by the calcium atoms alone.

2. The general expression for the equidistant normal interval between adjacent members of the parallel family of p, q, r planes obtained in I., 4, reduces, in the case of calcite, to

$$\Delta_{pqr}=\frac{60{\cdot}98\times10^{-24}}{(4{\cdot}04\times10^{-8})^2\sin 76^\circ\ 8'\left[p^2+q^2+r^2 \right. \\ \left. -2\dfrac{\cos 76^\circ\ 8'-\cos^2 76^\circ\ 8'}{\sin^2 76^\circ\ 8'}(pq+qr+rp)\right]^{\frac{1}{2}}}$$
$$=\frac{3{\cdot}848\times10^{-8}}{\{p^2+q^2+r^2-0{\cdot}3867(pq+qr+rp)\}}\text{ cm.}$$

* Ch. Mauguin, 'La structure des cristaux,' p. 109.

3. For practical purposes it is more convenient to use rectangular axes OX, OY, and OZ. These will be taken in directions indicated in fig. 2. OZ represents the direction along which the X-rays are incident normal to the cleavage

Fig. 1.

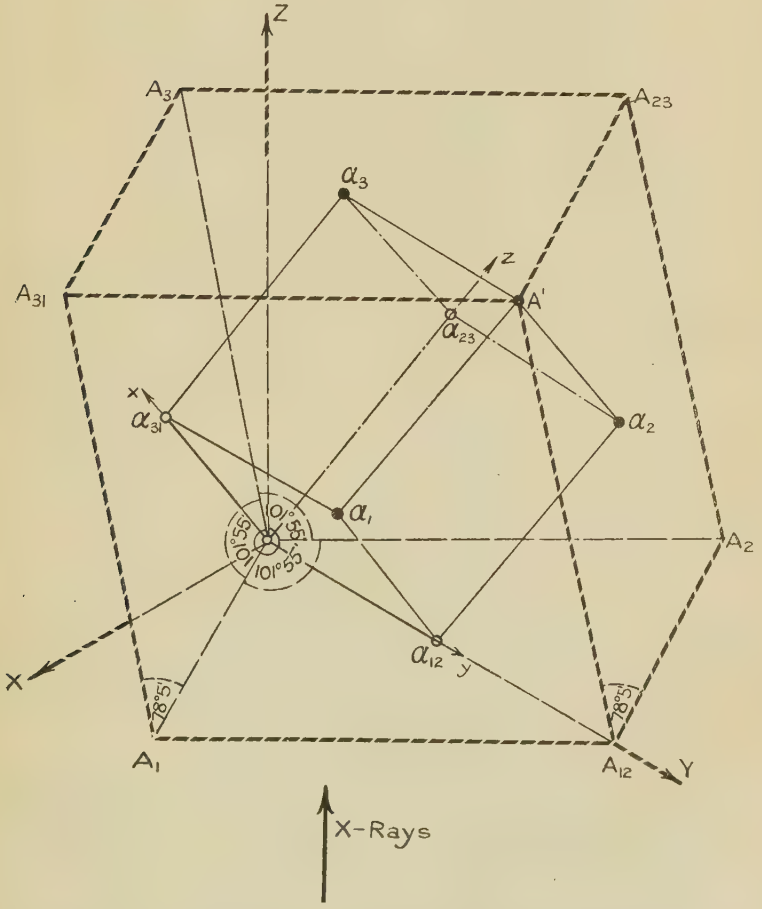

face XOY of the crystal. In fig. 2 OA, OB, and OC represent three edges of the unit cleavage cell of calcite meeting at a blunt corner.

We have

$$OA = OB = OC = 6{\cdot}414 \times 10^{-8} \text{ cm.},$$

while $$A\hat{O}B = B\hat{O}C = C\hat{O}A = 101^\circ\ 55'.$$

Fig. 2.

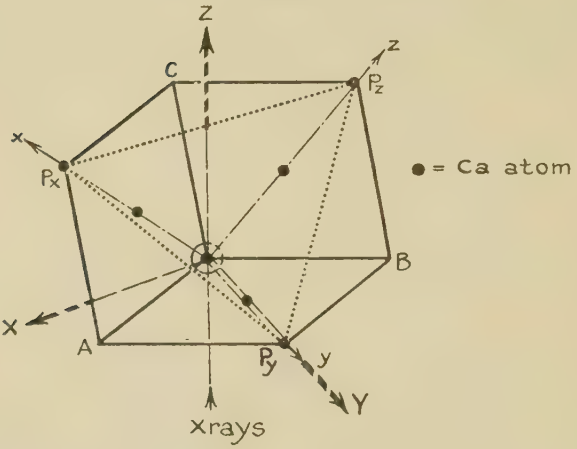

Hence (fig. 3)

Fig. 3.

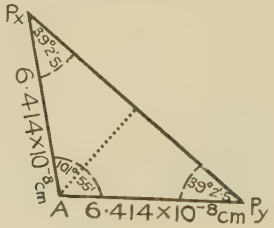

$$P_xP_y = P_yP_z = P_zP_x$$
$$= 2.6{\cdot}414 \times 10^{-8}.\cos 39^\circ\, 2'{\cdot}5$$
$$= 9{\cdot}963 \times 10^{-8} \text{ cm.}$$

Let $l_x m_x n_x$, $l_y m_y n_y$, $l_z m_z n_z$ be the direction cosines of Ox, Oy, Oz with respect to OX, OY, and OZ. Then we have at once, since $y\hat{O}X = y\hat{O}Z = 90^\circ$ and $y\hat{O}Y = 0^\circ$,

$$l_y = 0, \quad m_y = 1, \quad n_y = 0.$$

Again, since Ox, Oy, and Oz are directed along the edges of the simple unit cell,

$$x\hat{O}Y = z\hat{O}Y = 76^\circ\, 8',$$

so that

$$m_x = m = \cos 76^\circ\, 8' = 0{\cdot}2397.$$

Further, since the diagonals of a rhombus bisect one another

at right angles, OX will be parallel to P_zP_x. Hence from fig. 4,

Fig. 4.

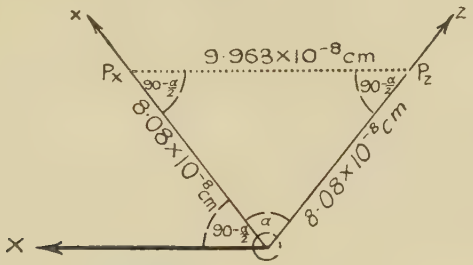

$$P_x\hat{O}P_z = \alpha = 76^\circ\ 8'.$$

$$\therefore \quad x\hat{O}X = \hat{O}P_xP_z = 90^\circ - 38^\circ\ 4' = 51^\circ\ 56'$$

and $$z\hat{O}X = 180^\circ - 51^\circ\ 56';$$

$$\therefore \quad l_x = \cos 51^\circ\ 56' = 0{\cdot}6166$$

and $$l_z = \cos(180^\circ - 51^\circ\ 56') = -0{\cdot}6166.$$

Hence $n_x = \{1 - (0{\cdot}6166)^2 - (0{\cdot}2397)^2\}^{\frac{1}{2}} = 0{\cdot}7499$,

and, by symmetry,

$$n_z = n_x = 0{\cdot}7499.$$

Collecting the results, we have

$$\left.\begin{aligned} l_x &= 0{\cdot}6166, \\ m_x &= 0{\cdot}2397, \\ n_x &= 0{\cdot}7499. \end{aligned}\right\} \qquad \left.\begin{aligned} l_y &= 0, \\ m_y &= 1, \\ n_y &= 0. \end{aligned}\right\} \qquad \left.\begin{aligned} l_z &= -0\ 6166, \\ m_z &= \ \ 0{\cdot}2397, \\ n_z &= \ \ 0{\cdot}7499. \end{aligned}\right\}$$

The equations connecting the coordinates of a point in the rectangular system of axes with the corresponding coordinates in the oblique system of axes are

$$\left.\begin{aligned} \mathrm{X} &= l_x x + l_y y + l_z z, \\ \mathrm{Y} &= m_x x + m_y y + m_z z, \\ \mathrm{Z} &= n_x x + n_y y + n_z z, \end{aligned}\right\}$$

from which

$$x = \frac{\begin{vmatrix} \mathrm{X} & l_y & l_z \\ \mathrm{Y} & m_y & m_z \\ \mathrm{Z} & n_y & n_z \end{vmatrix}}{\begin{vmatrix} l_x & l_y & l_z \\ m_x & m_y & m_z \\ n_x & n_y & n_z \end{vmatrix}}, \qquad y = \frac{\begin{vmatrix} l_x & \mathrm{X} & l_z \\ m_x & \mathrm{Y} & m_z \\ n_x & \mathrm{Z} & n_z \end{vmatrix}}{\begin{vmatrix} l_x & l_y & l \\ m_x & m_y & m_z \\ n & n_y & n \end{vmatrix}}, \qquad z = \frac{\begin{vmatrix} l_x & l_y & \mathrm{X} \\ m_x & m_y & \mathrm{Y} \\ n_x & n_y & \mathrm{Z} \end{vmatrix}}{\begin{vmatrix} l^x & l_y & l_z \\ m_x & m_y & m_z \\ n_x & n_y & n_z \end{vmatrix}}.$$

In the present case

$$\left.\begin{aligned} X &= 0{\cdot}6166(x-z), \\ Y &= 0{\cdot}2397(x+z)+y, \\ Z &= 0{\cdot}7499(x+z). \end{aligned}\right\}$$

Further, since

$$\begin{vmatrix} l_x & l_y & l_z \\ m_x & m_y & m_z \\ n_x & n_y & n_z \end{vmatrix} = 2(0{\cdot}6166)(0{\cdot}7499),$$

$$\therefore \quad x = (0{\cdot}7499\,X + 0{\cdot}6166\,Z)/2(0{\cdot}6166)(0{\cdot}7499),$$

$$\left.\begin{aligned} i.e., \quad & x = 0{\cdot}8109\,X + 0{\cdot}6667\,Z. \\ \text{Similarly,} \quad & y = Y - 0{\cdot}3196\,Z, \\ & z = 0{\cdot}6667\,Z - 0{\cdot}8109\,X. \end{aligned}\right\}$$

4. The plane of the family (p, q, r) adjacent to the origin has as equation referred to oblique axes Ox, Oy, Oz (I., 4)

$$px/a + qy/b + rz/c = 1,$$

where, in the case of calcite,

$$a = 4{\cdot}04 \times 10^{-8} \text{ cm.}$$

Hence, referred to rectangular axes OX, OY, OZ, the equation to this plane will be

$$0{\cdot}8109(p-r)X/a + qY/a + \{0{\cdot}6667(p+r) - 0{\cdot}3196q\}Z/a = 1.$$

Its intercepts on these axes will be

$$\left.\begin{aligned} X_a &= a/0{\cdot}8109(p-r), \\ Y_a &= a/q, \\ Z_a &= a/\{0{\cdot}6667(p+r) - 0{\cdot}3196q\}, \end{aligned}\right\}$$

and if l, m, and n are the direction cosines of the normal to this plane and Δ_{pqr} the perpendicular distance from the origin on it, we have

$$\left.\begin{aligned} l &= \Delta_{pqr}/X_a = 0{\cdot}8109(p-r)\Delta_{pqr}/a, \\ m &= \Delta_{pqr}/Y_a = q\Delta_{pqr}/a, \\ n &= \Delta_{pqr}/Z_a = \{0{\cdot}6667(p+r) - 0{\cdot}3196q\}\Delta_{pqr}/a. \end{aligned}\right\}$$

5. Consider now a quasi-cylindrical beam IO of X-rays of small aperture incident along the direction of the Z-axis and normal to the cleavage plane XOY of the crystal of calcite (fig. 5). At a distance D from the plane XOY and parallel

to it is placed the photographic film $X_0I_0Y_0$. The undeviated beam strikes the photographic film at I_0 and furnishes the central spot of the Laue diagram.

Fig. 5.

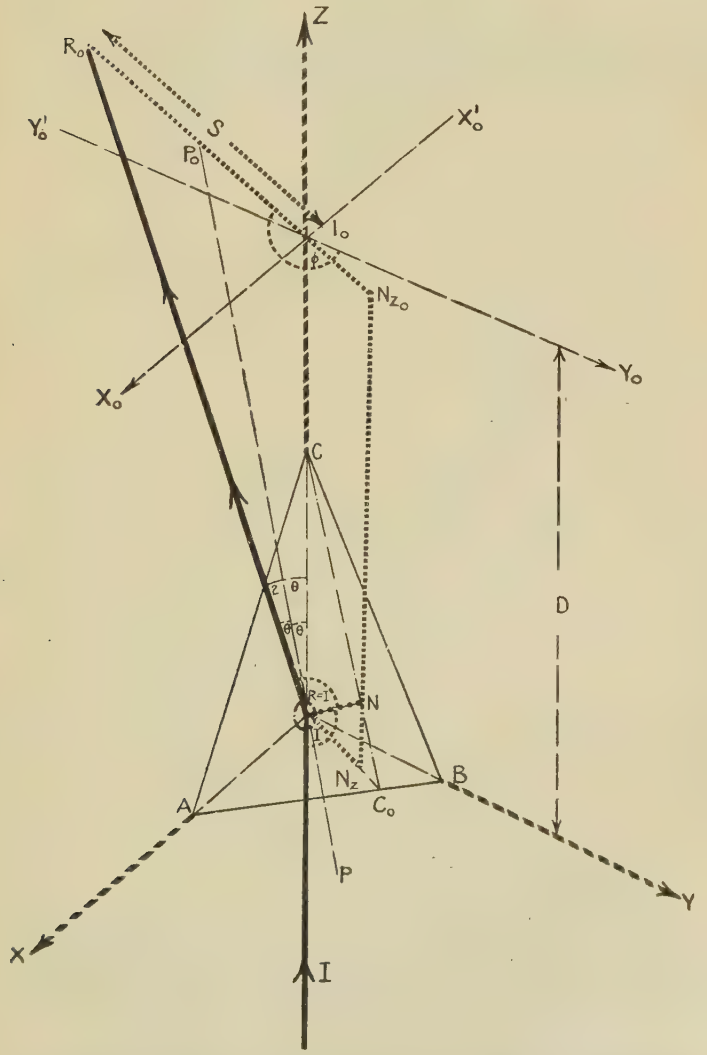

Let ABC represent one of the (p, q, r) family of adjacent lattice planes and ON the normal from O on this plane.

Then the plane ION containing the incident ray and the normal at the point of incidence will likewise contain the reflected ray. This plane will intersect the plane $X_0I_0Y_0$ in the line $N_{z_0}I_0$, and the reflected ray will meet the photographic film in a point R_0 along $N_{z_0}I_0$ produced at a distance s from I_0. The beam reflected in the direction OR_0 imprints on the photographic film the spot corresponding to reflexion from the (p, q, r) family of adjacent lattice planes.

In fig. 5 the angle of incidence

$$\mathrm{ION} = \mathrm{I},$$

Fig. 6.

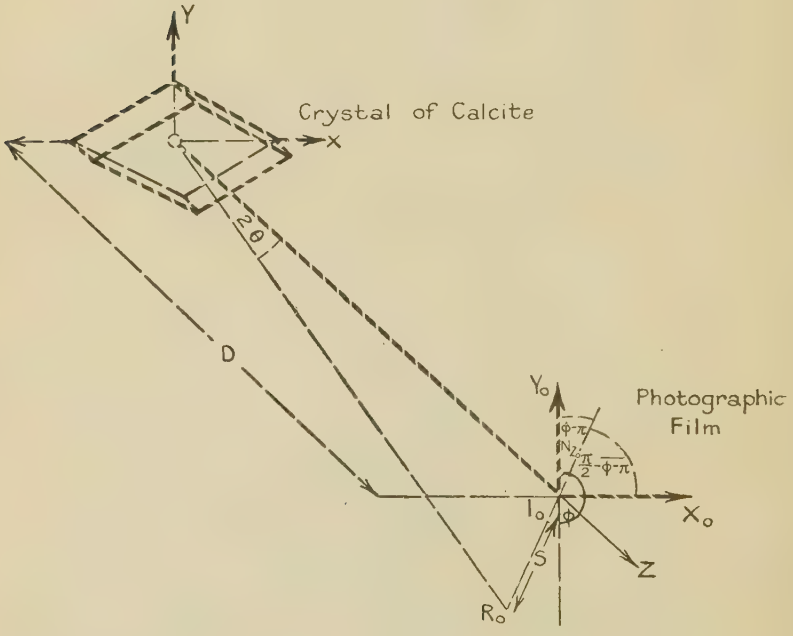

and the angle of reflexion

$$\mathrm{R_0ON} = \mathrm{R} = \mathrm{I}.$$

Now the member of the (p, q, r) family of adjacent lattice planes which passes through the origin O will intersect the plane OI_0R_0 in the line POP_0, where POP_0 is parallel to C_0NC and perpendicular to ON.

Hence, if the glancing angle $\mathrm{IOP} = \theta$, $\mathrm{R_0\hat{O}I_0} = 2\theta$.

Now, if l, m, and n are the direction cosines of ON,

$$n = \cos \mathrm{N\hat{O}Z} = \cos(\mathrm{R} - 2\theta) = \cos(\mathrm{I} - 2\theta),$$

and since $$I = \frac{\pi}{2} + \theta,$$

$$\therefore \qquad n = \sin\theta.$$

Also from this figure

$$s = D \operatorname{tg} 2\theta.$$

The crystal of calcite is mounted as indicated in fig. 6 in such a way that the vertical axis of symmetry of the Laue diagram coincides with the axis I_0Y_0. Accordingly we may specify the position of the spot R_0 relative to the central spot I_0 in terms of its polar coordinates,

$$I_0R_0 = s \quad \text{and} \quad Y_0\hat{I}_0R_0 = \phi.$$

Now the projection of ON on $OX = l.ON$.

Further, from fig. 5, the projection of ON on the plane $XOY = ON_z = I_0N_{z_0} = ON\cos\theta$, and the projection of ON_z on OX

$$= \text{the projection of } I_0N_{z_0} \text{ on } I_0X_0$$

$$= I_0N_{z_0}\cos\left(\frac{\pi}{2} - \overline{\phi - \pi}\right)$$

$$= -I_0N_{z_0}\sin\phi = -ON\cos\theta\sin\phi.$$

Hence $$l = -\cos\theta\sin\phi.$$

Again, the projection of ON on $OY = m.ON$, and the projection of $I_0N_{z_0}$ on I_0Y_0

$$= I_0N_{z_0}\cos(\phi - \pi)$$

$$= -ON\cos\theta\cos\phi.$$

Hence $$m = -\cos\theta\cos\phi.$$

Making use of these values of l, m, and n in the results of II., 4, we have

$$\left.\begin{aligned} l &= -\cos\theta\sin\phi = 0{\cdot}8109(p-r)\Delta_{pqr}/a, \\ m &= -\cos\theta\cos\phi = q\Delta_{pqr}/a, \\ n &= \sin\theta \qquad\qquad = \{0{\cdot}6667(p+r) - 0{\cdot}3196q\}\Delta_{pqr}/a. \end{aligned}\right\}$$

Hence, substituting the value of Δ_{pqr} from II., 2, and the value of a given in II., 4, we obtain finally

$$\left.\begin{aligned} \sin\theta &= \frac{0{\cdot}6350(p+r) - 0{\cdot}3044q}{\{p^2+q^2+r^2-0{\cdot}3867(pq+qr+rp)\}^{\frac{1}{2}}}, \\ s &= D \operatorname{tg} 2\theta, \\ \operatorname{tg}\phi &= \frac{0{\cdot}8109(p-r)}{q}. \end{aligned}\right\}$$

III. *Experimental Details and Tabulated Data.*

1. The accompanying plate (Pl. XII.) represents an enlargement of the Laue pattern for calcite taken at the Physiology Institute, University College, Cardiff in the laboratory directed by Dr. J. H. Shaxby.

The specimen was flaked off a large mass of calcite picked up locally. The distance D was 4·85 cm. An exposure of 140 minutes was given and the current traversing the

Fig. 7.

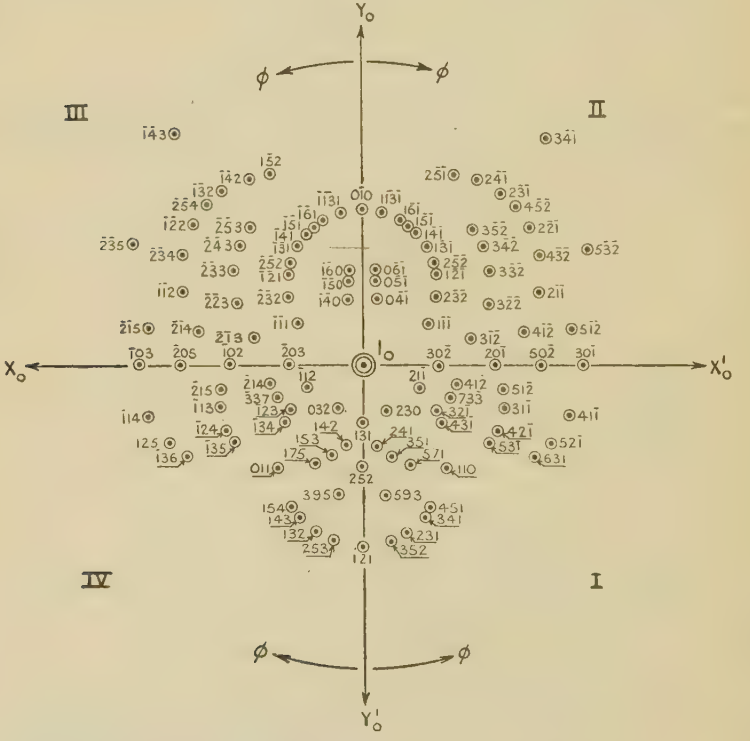

Coolidge tube was kept between 4 and 5 milliamperes. The indices corresponding to each spot are marked on fig. 7.

2. On pp. 523–526 are tabulated, for the appropriate values of the indices p, q, and r, the following six functions:

$$A = 0{\cdot}6350(p+r) - 0{\cdot}3044q,$$

$$B = p^2 + q^2 + r^2 - 0{\cdot}3867(pq + qr + rp),$$

$$\sin\theta = A/\sqrt{B},$$

$$s = 4{\cdot}85 \operatorname{tg} 2\theta \text{ cm.},$$

p.	q.	r.	Location of spot.	A.	B.	Sin θ.	tg 2θ.	s (cm.).	Measured s (cm.).	tg ϕ.	ϕ.	Measured ϕ.
0	$\bar{1}$	0	1_0Y_0	0·3044	1·000	0·3044	0·7115	3·45	3·45	0·0000	0°·00	0°·0
$\bar{1}$	$\bar{1}\bar{3}$	1	III.	3·957	171·39	0·3023	0·7054	3·42	3·40	0·1248	7°·12	7°·3
1	$\bar{1}\bar{3}$	$\bar{1}$	II.						3·40			7°·1
$\bar{1}$	$\bar{6}$	$\bar{1}$	III.	1·191	34·68	0·2023	0·4320	2·10	2·09	0·1352	7°·70	6°·8
0	$\bar{6}$	1	II.						2·13			8°·2
$\bar{1}$	$\bar{5}$	0	III.	0·8870	24·07	0·1808	0·3805	1·85	1·85	0·1622	9°·22	9°·1
0	$\bar{5}$	$\bar{1}$	II.						1·89			9°·2
$\bar{1}$	$\bar{4}$	0	III.	0·5826	15·45	0·1482	0·3064	1·49	1·49	0·2027	11°·47	11°·5
0	$\bar{4}$	$\bar{1}$	II.						1·52			11°·6
$\bar{1}$	$\bar{6}$	1	III.	1·826	38·39	0·2948	0·6822	3·31	3·30	0·2703	15°·13	14°·4
1	$\bar{6}$	$\bar{1}$	II.						3·30			15°·0
$\bar{1}$	$\bar{5}$	1	III.	1·522	27·39	0·2908	0·6694	3·25	3·22	0·3244	17°·97	17°·9
1	$\bar{5}$	$\bar{1}$	II.						3·23			18°·2
$\bar{1}$	$\bar{4}$	1	III.	1·218	18·39	0·2839	0·6494	3·15	3·12	0·4054	22°·07	22°·0
1	$\bar{4}$	$\bar{1}$	II.						3·19			22°·4
$\bar{1}$	$\bar{5}$	2	III.	2·157	32·71	0·3772	0·9759	4·73	4·56	0·4865	25°·95	25°·9
2	$\bar{5}$	$\bar{1}$	II.						4·69			25° 8
$\bar{1}$	$\bar{3}$	1	III.	0·9132	11·39	0·2706	0·6104	2·96	2·97	0·5406	28°·40	28°·1
1	$\bar{3}$	$\bar{1}$	II.						2·98			28°·7
$\bar{1}$	$\bar{4}$	2	III.	1·853	23·32	0·3836	1·004	4·87	4·77	0·6082	31°·30	31°·1
2	$\bar{4}$	$\bar{1}$	II.						4·80			31°·3
$\bar{2}$	$\bar{5}$	2	III.	1·522	34·55	0·2590	0·5777	2·80	2·72	0·6487	32°·97	34°·7
2	$\bar{5}$	$\bar{2}$	II.						2·78			35°·0
$\bar{1}$	$\bar{2}$	1	III.	0·6088	6·387	0·2409	0·5287	2·56	2·57	0·8109	39°·03	39°·0
1	$\bar{2}$	$\bar{1}$	II.						2·59			39°·2
$\bar{2}$	$\bar{5}$	3	III.	2·157	42·25	0·3318	0·8030	3·89	3·86	0·8109	39°·03	39°·3
3	$\bar{5}$	$\bar{2}$	II.						3·88			39°·0

p.	q.	r.	Location of spot.	A.	B.	Sin θ.	tg 2θ.	s (cm.).	Measured s (cm.).	tg ϕ.	ϕ.	Measured ϕ.
$\bar{1}$	$\bar{3}$	2	III.	1·548	15·93	0·3879	1·022	4·96	4·91	0·8109	39°·03	38°·8
2	$\bar{3}$	$\bar{1}$	II.						4·91			39°·0
$\bar{1}$	$\bar{4}$	3	III.	2·488	30·25	0·4523	1·365	6·62	6·52	0·8109	39°·03	39°·1
3	$\bar{4}$	$\bar{1}$	II.						6·42			39°·0
$\bar{2}$	$\bar{5}$	4	III.	2·792	51·96	0·3873	1·020	4·95	4·91	0·9731	44°·22	44°·2
4	$\bar{5}$	$\bar{2}$	II.						4·89			44°·3
$\bar{2}$	$\bar{4}$	3	III.	1·853	32·87	0·3231	0·7729	3·75	3·72	1·014	45°·38	45°·4
3	$\bar{4}$	$\bar{2}$	II.						3·72			45°·5
$\bar{2}$	$\bar{3}$	2	III.	0·9132	18·55	0·2120	0·4557	2·21	2·21	1·081	47°·23	47°·6
2	$\bar{3}$	$\bar{2}$	II.						2·25			47°·3
$\bar{1}$	$\bar{2}$	2	III.	1·244	10·55	0·3830	1·001	4·85	4·83	1·216	50°·58	50°·5
2	$\bar{2}$	$\bar{1}$	II.						4·78			50°·5
$\bar{2}$	$\bar{3}$	3	III.	1·548	25·48	0·3067	0·7194	3·49	3·50	1·352	53°·50	53°·5
3	$\bar{3}$	$\bar{2}$	II.						3·49			53°·7
$\bar{1}$	$\bar{1}$	1	III.	0·3044	3·387	0·1654	0·3450	1·67	1·66	1·622	58°·35	58°·2
1	$\bar{1}$	$\bar{1}$	II.						1·71			58°·5
$\bar{2}$	$\bar{3}$	4	III.	2·183	34·41	0·3722	0·9556	4·63	4·61	1·622	58°·35	58°·3
4	$\bar{3}$	$\bar{2}$	II.						4·59			58°·4
$\bar{2}$	$\bar{3}$	5	III.	2·818	45·35	0·4185	1·170	5·67	5·69	1·892	62°·15	62°·2
5	$\bar{3}$	$\bar{2}$	II.						5·54			62°·6
$\bar{2}$	$\bar{2}$	3	III.	1·244	20·09	0·2775	0·6306	3·06	3·06	2·027	63°·73	63°·3
3	$\bar{2}$	$\bar{2}$	II.						3·08			63°·8
$\bar{1}$	$\bar{1}$	2	III.	0·9394	7·160	0·3511	0·8724	4·23	4·29	2·433	67°·65	67°·6
2	$\bar{1}$	$\bar{1}$	II.						4·20			67°·8
$\bar{2}$	$\bar{1}$	3	III.	0·9394	16·71	0·2299	0·5000	2·43	2·44	4·054	76°·10	76°·1
3	$\bar{1}$	$\bar{2}$	II.						2·49			76°·1
$\bar{2}$	$\bar{1}$	4	III.	1·574	24·87	0·3157	0·7481	3·63	3·66	4·865	78°·40	78°·6
4	$\bar{1}$	$\bar{2}$	II.						3·63			78°·4
$\bar{2}$	$\bar{1}$	5	III.	2·209	35·03	0·3733	0·9601	4·66	4·76	5·676	80°·00	80°·1
5	$\bar{1}$	$\bar{2}$	II.						4·66			80°·2

p.	q.	r.	Location of spot.	A.	B.	Sin θ.	tg 2θ.	s (cm.).	Measured s (cm.).	tg ϕ.	ϕ.	Measured ϕ.
$\bar{2}$	0	3	I_0X_0	0·6350	15·32	0·1622	0·3378	1·64	1·62	∞	90°·00	90°·0
3	0	$\bar{2}$	I_0X_0'						1·69			90°·0
$\bar{1}$	0	2	I_0X_0	0·6350	5·773	0·2643	0·5930	2·88	2·91	∞	90°·00	90°·0
2	0	$\bar{1}$	I_0X_0'						2·93			90°·0
$\bar{2}$	0	5	I_0X_0	1·905	32·87	0·3323	0·8040	3·90	4·00	∞	90°·00	90°·0
5	0	$\bar{2}$	I_0X_0'						3·93			90°·0
$\bar{1}$	0	3	I_0X_0	1·270	11·16	0·3802	0·9895	4·80	4·94	∞	90°·00	90°·0
3	0	$\bar{1}$	I_0X_0'						4·84			90°·0
$\bar{2}$	1	5	IV.	1·601	32·71	0·2799	0·6371	3·09	3·16	5·676	80°·00	80°·1
5	1	$\bar{2}$	I.						3·14			80°·0
$\bar{2}$	1	4	IV.	0·9656	23·32	0·2000	0·4245	2·06	2·07	4·865	78°·40	78°·7
4	1	$\bar{2}$	I.						2·12			78°·7
$\bar{1}$	1	4	IV.	1·601	18·39	0·3733	0·9601	4·66	4·84	4·054	76°·10	76°·1
4	1	$\bar{1}$	I.						4·67			76°·1
$\bar{1}$	1	3	IV.	0·9656	11·39	0·2862	0·6560	3·18	3·27	3·244	72°·83	73°·1
3	1	$\bar{1}$	I.						3·26			73°·0
$\bar{3}$	3	7	IV.	1·627	70·48	0·1938	0·4108	1·99	2·02	2·703	69°·70	70°·0
7	3	$\bar{3}$	I.						2·05			69°·9
$\bar{1}$	1	2	IV.	0·3306	6·387	0·1308	0·2686	1·30	1·28	2·433	67°·65	67°·8
2	1	$\bar{1}$	I.						1·34			68°·1
$\bar{1}$	2	5	IV.	1·931	28·84	0·3596	0·9057	4·39	4·59	2·433	67°·65	67°·7
5	2	$\bar{1}$	I.						4·49			67°·4
$\bar{1}$	2	4	IV.	1·296	20·23	0·2882	0·6619	3·21	3·30	2·027	63°·75	64°·0
4	2	$\bar{1}$	I.						3·29			63°·8
$\bar{1}$	3	6	IV.	2·262	42·52	0·3469	0·8571	4·16	4·31	1·892	62°·15	62°·1
6	3	$\bar{1}$	I.						4·29			61°·9
$\bar{1}$	2	3	IV.	0·6612	13·61	0·1792	0·3772	1·83	1·82	1·622	58°·35	58°·3
3	2	$\bar{1}$	I.						1·88			58°·8

p.	q.	r.	Location of spot.	A.	B.	Sin θ.	tg 2θ.	s (cm.).	Measured s (cm.).	tg ϕ.	ϕ.	Measured ϕ.
$\bar{1}$	3	5	IV.	1·627	32·29	0·2863	0·6560	3·18	3·27	1·622	58°·35	58°·4
5	3	$\bar{1}$	I.						3·26			58°·6
$\bar{1}$	3	4	IV.	0·9918	24·07	0·2022	0·4314	2·09	2·12	1·352	53°·83	53°·8
4	3	$\bar{1}$	I.						2·14			53°·8
0	1	1	IV.	0·3306	1·613	0·2603	0·5812	2·82	2·91	0·8109	39°·03	39°·4
1	1	0	I.						2·91			39°·4
0	3	2	IV.	0·3568	10·68	0·1092	0·2223	1·08	1·09	0·5406	28°·40	28°·1
2	3	0	I.						1·09			28°·1
1	5	4	IV.	1·653	30·79	0·2979	0·6916	3·35	3·50	0·4865	25°·95	26°·1
4	5	1	I.						3·45			26°·0
1	7	5	IV.	1·679	56·82	0·2228	0·4820	2·34	2·41	0·4634	24°·87	24°·9
5	7	1	I.						2·40			25°·2
1	4	3	IV.	1·322	18·65	0·3062	0·7177	3·48	3·62	0·4054	22°·07	22°·1
3	4	1	I.						3·61			22°·0
1	5	3	IV.	1·018	26·11	0·1992	0·4245	2·06	2·11	0·3244	17°·97	18°·0
3	5	1	I.						2·10			17°·9
1	3	2	IV.	0·9918	9·746	0·3177	0·7545	3·66	3·79	0·2703	15°·13	15°·3
2	3	1	I.						3·79			15°·0
1	4	2	IV.	0·6874	15·59	0·1741	0·3653	1·77	1·80	0·2027	11°·47	11°·5
2	4	1	I.						1·79			11°·0
3	9	5	IV.	2·340	81·36	0·2595	0·5789	2·81	2·89	0·1802	10°·22	10°·1
5	9	3	I.						2·90			10°·3
2	5	3	IV.	1·653	26·01	0·3241	0·7766	3·77	3·91	0·1622	9°·22	9°·2
3	5	2	I.						3·91			9°·1
1	3	1	I_0Y_0'	0·3568	8·293	0·1239	0·2537	1·23	1·23	0	0°·00	0°·0
2	5	2	I_0Y_0'	1·018	23·72	0·2090	0·4480	2·17	2·21	0	0°·00	0°·0
1	2	1	I_0Y_0'	0·6612	4·066	0·3279	0·7888	3·83	3·99	0	0°·00	0°·0

s as measured from the original photograph,

$$\text{tg}\,\phi = 0{\cdot}8109(p-r)/q,$$

ϕ deduced from this, ϕ measured directly.

Measurements are expeditiously made by means of a plotting protractor which carries an arm graduated in mm.

The location of each spot is given in the table and the corresponding axes and quadrants indicated in fig. 7.

I desire to express my thanks to Dr. J. H. Shaxby for the experimental facilities he placed at my disposal, and for the benefit of his advice throughout.

XLIV. *Notices respecting New Books.*

The Structure of Molecules. Edited by P. Debye. Authorized Translation by Winifred M. Deans. [Pp. xii+190.] (London: Blackie, 1932.) Price 15*s*.

THIS translation will make available to a wider circle a series of lectures on molecular structure given at a conference organized by Debye at Leipzig in 1931. It is made up of eight separate papers dealing with the following topics: Problems of rotation about carbon bands (Wolf), results of spectroscopy of polyatomic molecules (Mecke), the Raman effect and the structure of molecules and crystals (Rasetti and Placzek), band spectra and dissociation (Sponer), predissociation from the experimental (Henri) and theoretical side (Kronig), and the electronic structure of molecules (Herzberg). The individual papers are of a high standard—it would be invidious to pick out any for special comment—and collectively they give a remarkably complete and fascinating account of the lines of investigation now being followed up on a subject which makes the highest demands both on physicists and chemists.

For the most part the authors present their subject-matter from the rather specialized standpoint inspired by their own particular lines of research. For this reason the book will be found particularly stimulating to those actively engaged in investigation in the same field, but a considerable background is necessary before the papers can be fully appreciated. The book suffers from the usual drawbacks of such collections of papers by different authors, and for many physicists and chemists its value would have been greatly enhanced had it included a more general survey of the whole field. Debye's

preface does indicate the interconnexion between the different papers, but it is all too brief.

The book is well produced. It contains five excellent plates, a considerable number of diagrams and useful tables, and a good index.

Kleiner Leitfaden der praktischen Physik. By Friedrich Kohlrausch. Fifth edition, revised by Friedrich Krüger. Pp. xxviii+498. (Leipzig: Teubner, 1932. RM. 14.80.)

In recent editions the "small Kohlrausch" has become much more than a reference manual for instruction in practical physics. It is now designed to give an account of physical apparatus and methods (leaving aside only methods of very specialized interest, and measurements of high precision) such as will serve as an adequate guide in making physical measurements in such fields as chemistry, medicine, general and electro-technology, as well as in physics in the narrower sense. In the range covered the new edition has been thoroughly revised and brought up to date.

The book is divided into sixteen main sections (*e. g.*, elasticity, acoustics, heat), and these are further subdivided. As an indication of the scope, the largest section, on electricity and magnetism, comprising some 190 pages, has fifteen subsections dealing not only with resistance, alternating currents, etc., but also with such topics as the photoelectric effect, cathode rays, X-rays, and radioactivity.

Each subsection opens with a succinct account of the concepts and laws involved in the measurements described. Instruments are briefly described, and practical details and corrections required are indicated. Where necessary, references are given, and in some special cases, firms, not exclusively German, are mentioned, from which the apparatus may be obtained. There are 379 clear diagrams well placed with reference to the relevant text, and at the end of the book is a most useful series of tables of physical constants.

Although the range is so comprehensive, and the presentation is condensed, the primary purpose of a reference book is well fulfilled in that reference to it is made easy by the perspicuous arrangement, the analytical table of contents, and the satisfactory index.

The cheapness of a book of over 500 pages of by no means straightforward printing is worthy of more than favourable comment. The book should prove of great value in all laboratories where physical measurements are made.

[*The Editors do not hold themselves responsible for the views expressed by their correspondents.*]

Fig. 1.

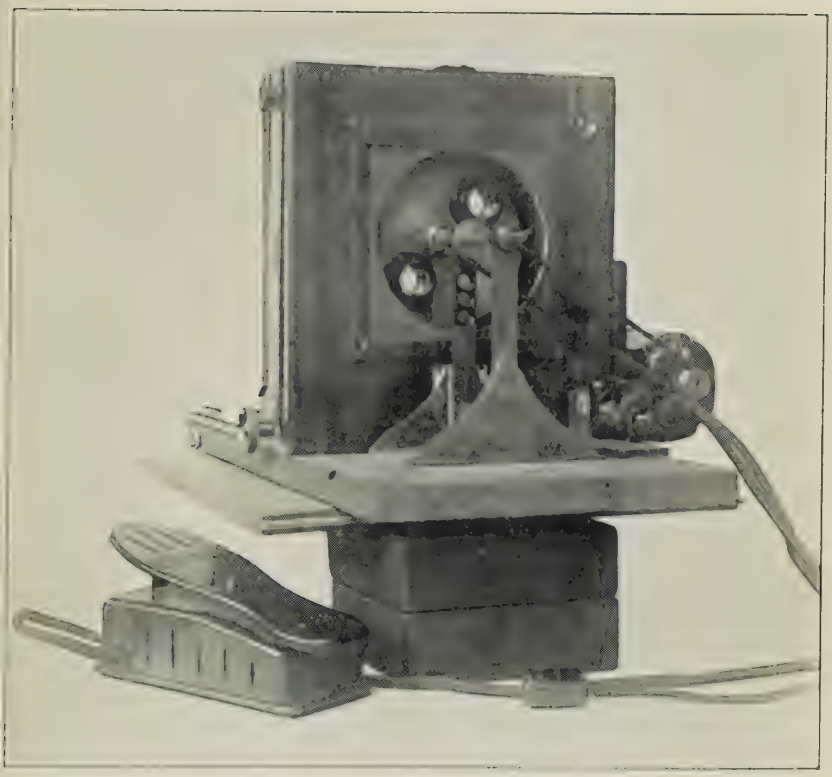

Fig. 2.

Fig. 4.

Fig. 6.

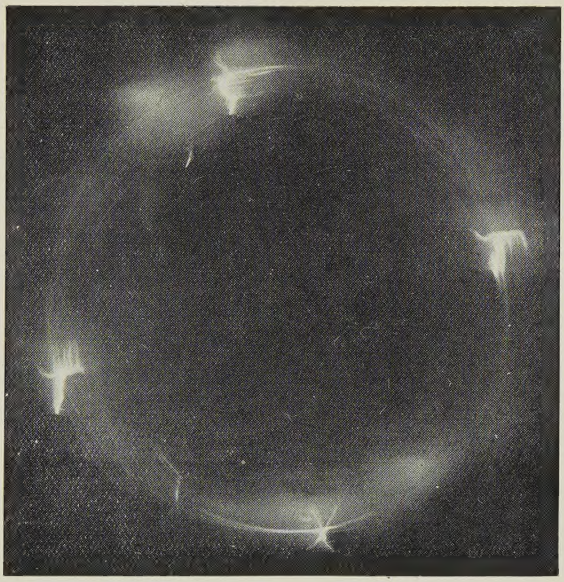

Fig. 6 *a*.